



University
of Glasgow

Montgomery, Jennifer (2013) Interrogation and modulation of the myeloid aspect of the inflammatory immune response in spinal cord injury. PhD thesis

<http://theses.gla.ac.uk/4820/>

Copyright and moral rights for this thesis are retained by the author

A copy can be downloaded for personal non-commercial research or study, without prior permission or charge

This thesis cannot be reproduced or quoted extensively from without first obtaining permission in writing from the Author

The content must not be changed in any way or sold commercially in any format or medium without the formal permission of the Author

When referring to this work, full bibliographic details including the author, title, awarding institution and date of the thesis must be given.

**Interrogation and modulation of the myeloid aspect
of the inflammatory immune response in spinal
cord injury.**

Jennifer Montgomery

BSc (Hons)

Submitted in fulfilment of the requirements for the Degree of Doctor
of Philosophy

College of Medical, Veterinary and Life Sciences

Institute of Infection, Inflammation and Immunity

University of Glasgow

2013

Abstract

Spinal cord injury (SCI) affects approximately 40,000 people in the UK; the most common type of SCI is a contusion injury and the majority of these cases are male and aged between 16 and 30 years old. The initial physical trauma to the spinal cord during injury leads to substantial damage and loss of neurones. After the primary traumatic insult has occurred a sequence of events is initiated that sets off a cascade of biochemical, cellular and inflammatory events that are massively destructive and continue for weeks to months after the initial SCI. This phenomenon is known as “secondary death” and leads to an increase in the size of the damaged area. Infiltrating monocytes and monocyte-derived macrophage have been implicated as a crucial component in the perpetration of secondary death.

It was demonstrated in this thesis that staphylococcus protein A (SpA), when in complex with IgG forms homogeneous small immune complexes (SIC) that can polarize macrophages *in vitro* to an anti-inflammatory phenotype, resulting in increased production of the immune-suppressive cytokine IL-10 and reduced ability to produce the pro-inflammatory cytokine IL-12. SIC treatment of IFN γ -primed macrophages in conjunction with LPS also induces a down-regulation of MHC II surface expression; however, the macrophages still exhibit normal levels of co-stimulatory molecule CD86 compared to a classically-activated macrophage.

In an *in vivo* setting it was demonstrated that SpA binds to monocytes and preferentially to the “inflammatory” Ly6C^{hi} monocyte sub-set. The binding of SpA to this monocyte population induced the maturation of the Ly6C^{hi} “inflammatory” monocyte into Ly6C^{low} “anti-inflammatory” monocytes within the steady state and in the sterile inflammatory setting of SCI. In the inflammatory environment of the damaged spinal cord, SpA treatment induced a higher percentage of Ly6C^{low} monocytes to produce the immune-modulatory cytokine IL-10 compared to the control treated group. These observations indicate when SpA and IgG form SIC they interact with macrophages and monocytes *in vitro* or *in vivo* polarizing them to an anti-inflammatory phenotype.

In conclusion, it has been shown in this thesis that SIC has the potential to be used as a method of polarizing monocytes and macrophages to an anti-inflammatory phenotype, which in turn has the potential to modify the overt inflammatory response that is responsible for the death of neurons days to weeks after the initial injury and is responsible for reduced functional recovery in SCI patients.

2.2.1	Isolation of bone marrow cells	63
2.2.2	Generation of L929 supernatant.....	63
2.2.3	Harvesting macrophages.....	64
2.3	Conditioning and activation of BMDM.....	64
2.3.1	Complex formation	65
2.4	ELISA	65
2.5	Flow cytometry.....	66
2.6	T cell activation assay	66
2.6.1	Pulsing of BMDM.....	66
2.6.2	Isolation of CD4 ⁺ T cells	66
2.6.3	Culturing BMDM and T cells	67
2.7	SpA labelling and binding assays	68
2.7.1	Labelling SpA and OVA with Alexa-488	68
2.7.2	In vitro binding of SpA-488	68
2.7.3	In vivo binding of SpA-488 in C57BL/6.....	69
2.7.4	In vivo binding of SpA-488 in μ MT mice	70
2.8	SpA treatment <i>in vivo</i>	70
2.9	Adoptive transfer of Ly6C ^{hi} monocytes	70
2.9.1	Isolation of GFP ⁺ Ly6C ^{hi} monocytes from BM.....	70
2.9.2	Adoptive transfer of Ly6C ^{hi} cells in C57BL/6 mice	71
2.10	SCI model	71
2.11	Basso Mouse Scale (BMS).	72
2.12	DigiGait - measurement of gait change after SCI	72
2.13	Grip strength	73
2.14	Tract tracing of the cortico spinal tract.....	73
2.14.1	Perfusion of mice.....	73
2.14.2	Tissue processing	74
2.14.3	Microscopy.....	74
2.15	Statistical analysis.....	74
3	The ability of SIC to polarize macrophages to an anti-inflammatory phenotype via CD64	76
3.1	Introduction	76
3.1.1	Classical macrophage activation	76
3.1.2	The broad category of regulatory macrophage	78
3.1.3	SpA and its potential to interact with macrophages	82

3.1.4	Aims of this experiment	84
3.2	Results	85
3.2.1	SpA can bind to BMDM but only when in complex with IgG	85
3.2.2	BMDM polarization by SIC	87
3.2.3	SIC does not alter the ability of macrophages to secrete IL-6 and Nitric oxide (NO)	89
3.2.4	SIC induced MHC II down-regulation	89
3.2.5	T cell activation is not affected by SIC-conditioned macrophages ..	93
3.2.6	SIC binding in WT, CD64 ^{-/-} , CD32 ^{-/-} and common γ chain ^{-/-}	95
3.2.7	SIC has the ability to polarize macrophages to a regulatory phenotype in WT and CD32 ^{-/-} BMDM but not CD64 ^{-/-} or common γ chain ^{-/-} BMDM	97
3.2.8	The ability of SIC to induce the down-regulation of MHC II is not affected when IL-10R is blocked in WT and CD32 ^{-/-} macrophages	99
3.2.9	SpA can engage cell-bound IgG to interact with cells	101
3.2.10	Complex formation with SpA and IgG2a induces IL-10 production in macrophages in the presence of LPS	102
3.2.11	SIC generated with IgG2a induces down-regulation of MHC II but not to the same extent as SIC made with polyclonal IgG	105
3.2.12	Mixed IgG sub-classes down-regulate MHC II to the same extent as polyclonal IgG	105
3.3	Discussion	109
4	SPA has the ability to induce maturation of Ly6C ^{hi} monocytes into Ly6C ^{low} monocytes under steady-state or inflammatory conditions	115
4.1	Introduction	115
4.2	Results	120
4.2.1	SpA binding to Monocytes and Neutrophils	120
4.2.2	SpA requires IgG to interact with myeloid cells in vivo.....	124
4.2.3	SpA treatment for 24hrs under non-inflammatory conditions leads to a shift in the blood monocyte population.....	126
4.2.4	Fc γ RIII and SpA.....	128
4.2.5	SpA-488 cannot penetrate the blood-brain barrier and interact with cells in the undamaged spinal cord	130
4.2.6	SpA-488 interactions in the damaged spinal cord	132

4.2.7	24hr treatment with SpA has an effect on the infiltrating monocyte populations after SCI.....	136
4.2.8	IL-10, SCI and SpA	137
4.2.9	SpA is inducing Ly6C ^{hi} monocytes to differentiate into Ly6C ^{low} monocytes	144
4.3	Discussion	155
5	Optimisation of behavioural testing for murine spinal cord injury.....	163
5.1	Introduction	163
5.1.1	Experimental methods for SCI induction.....	163
5.1.2	Behavioural testing methods for SCI assessment	164
5.2	Aims.....	171
5.3	Results	172
5.3.1	BMS.....	172
5.3.2	Grip Strength	173
5.3.3	DigiGait.....	178
5.3.4	BDA tract tracing	188
5.4	Discussion Conclusion	191
6	Discussion, conclusion and future experiments	196
6.1	Discussion	196
6.2	Conclusion	201
7	Appendix 1	203
1.	Buffer and solutions:	203
2.	Immunohistochemistry antibodies	203
	Primary antibody:	203
	Secondary antibody:	203
	Streptavidin:.....	203
3.	Flow Cytometry Antibodies.....	204
	APC.....	204
	APC cy7.....	204
	FITC/Alexa-488.....	204
	PE cy7	204
	PE	205
	PerCP-cy5.5/PE cy 5.5	205
	Purified.....	205
	AF700	205

8	Appendix 2	206
9	Appendix 3	217
	List of references	218

List of figures

Figure 1.1. Ontogeny of monocytes, macrophages and DCs	27
Figure 1.2. Fc γ receptors and their associated signalling molecules, in the murine system.....	53
Figure 1.3. SpA bound to IgG through interaction in the constant region.....	61
Figure 3.1. Different fates of macrophage activation	83
Figure 3.2. SpA has the ability to bind to BMDM only when it is in complex with IgG.....	86
Figure 3.3. SIC has the ability to polarize macrophages to an anti-inflammatory cytokine profile.....	88
Figure 3.4. SIC does not have the ability to change BMDM production of Nitric oxide and IL-6 when stimulated with LPS.....	91
Figure 3.5. SIC treatment leads to the down-regulation of MHC II levels but has no effect on CD86 up-regulation.....	92
Figure 3.6. SIC did not effect the ability of macrophages to activate T cells.....	94
Figure 3.7. SIC has the ability to bind to BMDM only when CD64 and the common γ chain is present.....	96
Figure 3.8. SIC has the ability to polarize macrophages to an anti-inflammatory cytokine profile in WT and CD32 ^{-/-} macrophages but not CD64 ^{-/-} and common γ chain ^{-/-} macrophages.....	98
Figure 3.9. SIC has the ability to down-regulate MHC II expression in WT and CD32 ^{-/-} macrophages.....	100
Figure 3.10. SpA has the ability to bind to WT and CD32 ^{-/-} BMDM when the cells have been pre-coated with IgG.....	103

Figure 3.11. SIC that has been preformed with purified IgG2a but not IgG1 can induce macrophages to a regulatory phenotype.....	104
Figure 3.12. SIC that has been preformed with purified IgG2a but not IgG1 or IgG2b can induce the down-regulation of MHC II levels on BMDM	107
Figure 3.13. SIC that has been preformed with a mixture of purified IgG2a and IgG1 can induce macrophages to a regulatory phenotype.....	108
Figure 4.1. Time course of innate immune cell infiltration into the damaged spinal cord after injury.....	119
Figure 4.2. SpA-488 binding in monocytes and neutrophils in blood.....	121
Figure 4.3. SpA-488 binding in monocytes and neutrophils in bone marrow	123
Figure 4.4. SpA requires IgG to interact with monocytes in vivo.....	125
Figure 4.5. SpA treatment for 24h under non-inflammatory conditions leads to a shift in the blood monocyte population.....	127
Figure 4.6. FcγRIII is not involved in SpAs ability to induce Ly6C ^{hi} monocytes maturation to Ly6C ^{low} monocytes in the blood.....	129
Figure 4.7. SpA cannot cross the intact blood brain barrier to interact with cell within the spinal cord.....	131
Figure 4.8. SpA-488 can bind to cells within a damaged spinal cord.....	134
Figure 4.9. SpA-488 binding profile in blood monocytes and neutrophils after SCI	135
Figure 4.10. 24h treatment with SpA alters the infiltrating monocyte populations after SCI	139

Figure 4.11. 24h treatment with SpA alters the blood monocyte populations after SCI	140
Figure 4.12. Does SpA treatment induce monocytes to become polarized to an IL-10 producing phenotype in the context of SCI.....	142
Figure 4.13. Does SIC have the ability to induce BMDM from vertex mice to produce IL-10 in vitro	143
Figure 4.14. Gating strategy for isolation of Ly6C ^{hi} GFP ^{int} monocytes from the bone marrow cells of CX ₃ CR1 mice.....	145
Figure 4.15. GFP ⁺ monocytes were present 22h after adoptive transfer.....	147
Figure 4.16. SpA treated mice have a higher number of GFP+ cells present 22h after adoptive transfer.....	148
Figure 4.17. SpA treatment for 22h leads Ly6C ^{hi} monocyte's to differentiate into Ly6C ^{low} monocytes in the blood.....	150
Figure 4.18. SpA treatment for 22h leads Ly6C ^{hi} monocyte's to differentiate into Ly6C ^{low} monocytes in the spleen.....	153
Figure 4.19. SpA treatment for 22h leads Ly6C ^{hi} monocyte's to differentiate into Ly6C ^{low} monocytes in the bone marrow.....	154
Figure 5.1. Healthy paw placement on the DigiGait in a healthy rodent and the different phases of walking they go through.....	170
Figure 5.2. BMS hind limb motor assessment for 6 weeks post operatively after SCI.....	174
Figure 5.3. Assessment of grip strength in the fore paws pre-operatively and for 6 weeks post operatively, following SCI surgery.....	177
Figure 5.4. DigiGait apparatus.....	178

Figure 5.5. Assessment of swing stride percentage in the fore and hind limbs pre-operatively and 6 weeks post operatively, following SCI surgery.....	181
Figure 5.6. Assessment of percentage brake stance in the fore and hind limbs pre-operatively and 6 weeks post operatively, following SCI surgery.....	182
Figure 5.7. Assessment of stride frequency per second in the fore and hind limbs pre-operatively and 6 weeks post operatively, following SCI surgery.....	184
Figure 5.8. Assessment of the number of steps taken with in a second in the fore and hind limbs pre-operatively and 6 weeks post operatively, following SCI surgery.....	185
Figure 5.9. Assessment of stride length in the fore and hind limbs pre-operatively and 6 weeks post operatively, following SCI surgery.....	186
Figure 5.10. Assessment of paw angle in the fore and hind limbs pre-operatively and 6 weeks post operatively, following SCI surgery.....	187
Figure 5.11. BDA staining of the corticospinal track in a 100KD SCI mouse.....	190
Table 5.1. BMS scoring definitions.....	167
Table 5.2. Parameters measured by DigiGait Imaging System.....	169
Table 9.1. Comparison of SpA-488 ability to bind cells of the myeloid lineage in the blood, damaged spinal cord and bone marrow after SCI	217

Acknowledgements

Firstly I would like to thank all my supervisors, Dr Carl Goodyear, Dr John Riddell and Professor Sue Barnett, for all their help and guidance throughout my PhD. Special thanks has to go to my primary supervisor Dr Carl Goodyear as without his encouragement and belief in me, this thesis would not have come to fruition. I have to also thank him for taking the time and having the patience to teach me flow cytometry (believe me this was not an easy task!) and to interpret my data accurately and without bias. I am also very appreciative of the support and guidance he has offered me over the last 4 years.

The Goodyear lab has been a great place to carry out my PhD and I have seen many brilliant people come and go in the time I have spent here and I would like to thank you all for making my PhD as good as it was. There are a few people who have made a big impact in my science life over the last 4 years: Lindsay, who has also taught me too many things to mention and helped out with the “donkey work” on the vast majority of my big experiments, without her amazing help I would have had so many more late night finishes. She has also managed to drum into me a basic ability to do calculations, which I didn’t think was possible 4 years ago. Susan has also been a massive help in anything that involves chemistry or technology. Jamie and Felix, thank you for dragging yourselves in at 6.45am on more than 1 occasion to help “squirt” bone marrow and I think more importantly for all the numerous crazy drunken nights out, which helped take my mind off science for a while.

A massive thank you also has to go out to Andrew Toft for all of his help in all things neuroscience and behavioural testing. Also for some excellent banter and listening to me moaning about the Digigait. Another thanks is due to Diane in the FACS facility for the use of the machines and for her help and advice, especially with cell sorting. I also owe a massive debt of gratitude to the people at the CRF for all their assistance, especially Tony and Craig.

Josie Fullerton, the very first student I have ever supervised, you left an unforgettable impression on me after our first meeting in the CRF, three years ago, you will know exactly what time I’m talking about! Your soap opera stories and insatiable appetite made all those hours spent with our furry little friends

more than bearable and your continued friendship to this day has especially helped me through the later stages of writing this up. Good luck to you in your PhD!

The eternal optimist and master signature forger that is Alison, who was only around for the writing up phase of this thesis but you have always put a positive spin on every situation, even if I couldn't see it, has helped me to stay (mostly) positive though the horrible writing up phase, thank you! Greg, your continued friendship, scientific advice and support though out my PhD, even though you are no longer in Glasgow, was and is irreplaceable. To all my other non-science friend's thank you for all your support, shoulders to cry on and all the fun times we have had over the last 4 years.

Last but most definitely not least, I have to take this opportunity to thank my family and especially my parents for all their support, encouragement and understanding not only in my PhD but all through out my academic life, if you had not convinced me that it was a good idea to take biology over "spooney science" all those year ago, I would definitely not be sitting here writing this so thank you! To my wonderful boyfriend, Graeme, you have put up with a lot over the last year (ok, maybe two) with me not being able to make social things due to work commitments or turning up late as an experiment ran on later than I thought it would, but I promise I will be around a lot more now. Thank you for putting up with it all and not giving up on me.

Author's declaration

I declare that, except where explicate reference is made to the contribution of others, that this thesis is the result of my own work and has not been submitted for any other degree at the University of Glasgow or to any other institution.

Signature:

Printed name: Jennifer Montgomery

Abbreviations

ALS - Amyotrophic lateral sclerosis

APC - Antigen presenting cell

BBB - Basso Beattie Bresnahan locomotor scale

BBB - Blood brain barrier

BCR - B cell receptor

BM - bone marrow

BMS - Basso mouse scale

BSA - Bovine serum albumin

CDP - Common DC progenitors

CMP - Common myeloid progenitor

CNS - Central nervous system

CSPG - Chondroitin sulphate proteoglycan

DC - Dendritic cell

DRG - Dorsal root ganglion

ELISA - Enzyme-linked immunosorbant assay

FACS - Fluoresce associated cell sorting

FcR - Fc receptor

FCS - Foetal calf serum

FDA - Food and Drug Administration

GM-CSF - Granulocyte macrophage colony stimulating factor

GMP - Granulocyte macrophage progenitor

HSC - Haematopoietic stem cells

IFN - Interferon

Ig - Immunoglobulin

IGF - Insulin like growth factor

IgSF - Immunoglobulin superfamily

IH - Infinite horizon

IL - Interleukin

iNOS - Inducible nitric oxide synthetase

ITAM - Immunoreceptor tyrosine-based activation motif

ITAMi - Inhibitory ITAM

ITIM - Immunoreceptor tyrosine-based inhibitory motif

IVIg - Intravenous Immunoglobulin

K/O - Knock out

LPS - Lipopolysaccharide

MCP-1 - Monocyte chemoattractant protein-1

M-CSF - Macrophage colony stimulating factor

MDP - macrophage dendritic cell precursor

MHC - Major histocompatibility complex

MIF - Macrophage inhibitory factor

ml - Millilitre

MMP - Matrix metalloproteinase

MR - mannose receptor

ng - nanograms

NLR - NOD-like receptors

NO - Nitric oxide

NYU_i - New York University impactor

OSU_d - Ohio State University device

OVA - Ovalbumin

PBMC - Peripheral blood mononuclear cells

PBS - Phosphate saline buffer

pg - Picograms

PNS - Peripheral nervous system

ROS - Reactive oxygen species

SC - Spinal cord

SCI - Spinal cord injury

SIC - Small immune complex

SpA - Staphylococcus protein A

TCR - T cell receptor

TGF - Transforming growth factor

TLR - Toll-like receptor

TNF - Tumor necrosis factor

WT - Wild type

ZAM - Zymosan activated macrophages

1 Introduction

1.1 An overview

Spinal Cord Injury (SCI) is a condition that affects thousands of people annually, and can lead to mild or severe paralysis depending on where and how severely the spinal cord is damaged.

It has been recently theorised that the initial injury is not the only contributing factor to the overall damage. In fact, it is the inflammatory immune response that magnifies the initial trauma and perpetuates damage to neurons weeks after the initial trauma.

One of the main components of the inflammatory immune response after SCI is the massive infiltration of monocytes from the peripheral circulation, which differentiate into macrophages; these can be detected 12h post injury. Macrophages are a component of the innate immune system that are bimodal in their activation phenotypes and can either be anti-inflammatory or pro-inflammatory in nature depending on their mode of activation.

This thesis tries to address the hypothesis: that it is possible to skew the infiltrating monocyte/macrophage population to anti-inflammatory phenotype after contusive SCI with the use of *Staphylococcus aureus* protein A (SpA).

This introduction will explore monocyte and macrophages development, phenotypes and functions. It will then focus on SCI and what is known of the ensuing inflammatory immune response and the phenomenon of secondary death. It will finish with a review of some strategies that have been used in inflammatory conditions to suppress an overt inflammatory response.

1.2 Immune system in brief

The immune system is entrusted with protecting the body from harmful pathogens and regulating tolerance to harmless antigens such as food and “self antigens”. However, when a breakdown in tolerance to self-antigens occurs auto-immunity ensues, leading to conditions such as Systemic Lupus Erythematosus - a condition where the immune system produces auto-antibodies to DNA resulting in inflammation and tissue damage. Rheumatoid Arthritis is another common auto-immune disease where the immune system produces an aberrant antibody response to immunoglobulin (i.e. rheumatoid factor), and the immune complexes that are formed as a consequence contribute to massive inflammation and joint destruction. Auto-immunity is a poignant example of the destruction the immune system can cause if it is not properly regulated ¹.

The immune system can be divided into two distinct branches: the innate and the adaptive responses. Innate immunity is highly conserved across time and species; it is involved in the immediate response to pathogens, and consists of monocytes, neutrophils, macrophages, dendritic cells and complement to mention only a few. The innate immune system must activate the adaptive immune system and is often entrusted with regulating its activation. The adaptive immune system is only found in more highly evolved species and its onset comes later than that of the innate immune system. It is more precise in its killing and, in addition, the adaptive immune system possesses the ability to generate “memory” to pathogens. The adaptive immune system consists of T cells and B cells, which both have many subsets and a diverse array of functions ².

1.3 Innate immune system

The innate immune system can be further sub-divided into granulocytes (also referred to as polymorphonuclear leukocytes) and the mononuclear phagocyte system (MPS) ^{3 4}. Granulocytes are made up predominantly of neutrophils (as well as basophils and eosinophils). These cells can be recognised by their unique multi-lobed nucleus and their granular cytoplasm. Granulocytes are early responders to pathogen and do not possess the ability to activate the adaptive immune system. The other major cellular component of the innate immune is

the MPS. The MPS is composed of monocytes, macrophages (as well as specialist tissue macrophages such as Kupffer cells of the liver, microglia of the brain/spinal cord and osteoclasts of bone) and dendritic cells. The scope of this review will only focus on macrophages and their precursor monocytes of the MPS and not dendritic cells or granulocytes.

1.3.1.1 Monocyte derived macrophage Ontogeny

Monocytes in an adult originate from self-renewing hematopoietic stem cells (HSC), which are located in specialized niches of the bone marrow⁵. HSC are thought to go through successive and irreversible developmental checkpoints, which lead to the generation of intermediate precursor populations that increasingly lose self-renewal capacity and become restricted to one lineage⁶. HSC, which are defined as Lin⁻, c-Kit⁺, Sca1⁺, can differentiate into either the common lymphoid progenitor (CLP)⁷ or the common myeloid progenitor (CMP)⁸. IL-7R α is used to define these two populations: CLP are IL-7R α ⁺, as IL-7 is an essential developmental cytokine in both B and T cell ontogeny, acting as a survival factor for thymocytes (T cell precursors) through the maintenance of Bcl-2⁹. In B cells, it leads to the rearrangement of the heavy chain V segment in BCR development through the activation of the Pax5 gene¹⁰.

CMP are IL-7R α ⁻ and can be identified as Fc γ RII/III^{low}, CD34⁺, c-Kit⁺, Sca1⁻. The CMP fraction of the bone marrow can then give rise to two subsequent populations; these populations can be sub-divided on the expression of Fc γ RII/III and CD34. Fc γ RII/III^{low}CD34⁻ are megakaryocyte-erythrocyte progenitors (MEPs), and Fc γ RII/III^{hi}CD34⁺ are granulocyte-macrophage progenitors (GMPs)¹¹. By this stage of the developmental pathway these previously pluripotent HSC have now lost their ability to self-renew. MEPs will go through further subsequent precursor steps to eventually give rise to either megakaryocytes or erythrocytes. GMPs have the potential to differentiate into either monocytes or the common dendritic cell progenitor (CDP), which will give rise to pre-DCs or plasmacytoid DCs.¹² (figure 1.1).

Unsurprisingly, there is a complex interplay of transcription factors that are vital in controlling the process of myelopoiesis. GATA-1, GATA-2 and PLZF are expressed at high levels in HSC. However, PLZF decreases as HSC commit to any

hematopoietic lineage. GATA1/2 is elevated in the further differentiated CMP fraction of the bone marrow but is then selectively repressed when the CMP enters the monocyte lineage - but stays at an elevated level if the CMP commits to other myeloid lineages such as erythrocytes, mast cells and megakaryocytes¹³.

PU.1 is the transcription factor that controls the commitment of HCS to CMPs and is therefore indispensable in the formation of monocytes/macrophages. PU.1 is the product of the Spi-1/Sfp-1 gene, a member of the ets proto-oncogene family^{14 15}. PU.1 is not only expressed by mature monocyte/macrophages but is also expressed by other cell types such as B cells and neutrophils^{16 17}. When PU.1 is knocked out in mice the embryo dies at a late stage of gestation and has severe defects in its hematopoietic cell compartments, which include defects in T cells and B cells as well as monocytes and granulocytes¹⁸. When PU.1 is knocked out in embryonic stem cells (embryonic stem cells have the ability to be induced to differentiate, *in vitro*, into monocyte/macrophages under the appropriate culture conditions) they then lack the ability to differentiate into mature monocyte/macrophages *in vitro* that express Csf-1R, CD11b and FcγRI. However, the embryonic stem cells can differentiate into monocyte precursors, which express GM-CSFR, which is another early myeloid marker and is usually expressed in conjunction with CSF-1R. This discovery led to the revelation that PU.1 is dispensable for the commitment to the myeloid lineage but is essential for the maturation of precursors into mature monocytes^{19 20}. The ability of stem cells to complete myelopoiesis is due to PU.1's vital role in cleaving the Csf-1R gene, which allows its expression on the surface of monocytic precursors.

The expression of Csf-1R (also known as c-fms, M-CSFR or CD115) is an essential developmental check point in monocyte maturation and cannot be dispensed with. The Csf-1R was thought to have only one cognate ligand Csf-1/M-CSF²¹. However, when Csf-1R^{-/-} mice were generated and phenotyped, they possessed virtually all of the reported defects of Csf1^{op/op} or Csf-1^{-/-} mice, hence all of the effects of Csf-1 appear to be mediated by the Csf-1R. However, it was noticed that Csf-1R^{-/-} mice display a more exaggerated phenotype than the Csf1^{op/op} or Csf-1^{-/-} mice with more severe osteopetrosis, fewer tissue macrophages and shortened life-spans²². For this reason it was theorized that there may have been another ligand for Csf-1R which can also play a part in the orchestration of

monocyte development; IL-34, was recently discovered as an alternative ligand for the Csf-1R²³.

C/EBP is another transcription factor that is limited to the myeloid lineage and is essential for its maturation. C/EBP α is expressed in immature myeloid precursors but decreases steadily as monocytes mature as it is essential for granulocytic development. However, C/EBP β and C/EBP δ increase as macrophages mature into terminally differentiated cells²⁴. C/EBP α is antagonized by PU.1 at the GMP stage to drive the cells to the monocytic pathway at the expense of the granulocytic pathway²⁵. This leads to the up-regulation of the GM-CSFR and Csf-1R²⁶. C/EBP α activates Gfi-1 to stably confirm the myeloid precursor to the granulocyte lineage, whereas PU.1 must activate Egr-1 and its cofactor Nab to commit the cells to a monocyte/macrophage fate. Egr-1 is solely expressed in monocyte/macrophages, although Egr-1^{-/-} mice have macrophage populations and therefore it is not essential for macrophage maturation. When bone marrow was taken from Egr-1^{-/-} and WT and then treated with M-CSF or GM-CSF, these cells were also able to be differentiated into normal macrophages and produce the same level of nitric oxide as the WT bone marrow derived macrophages²⁷. However, Egr-1^{-/-}Egr-2^{-/-} mice show a defect in Csf-1 dependent macrophage differentiation leading to speculation that Egr-1 and Egr-2 have the ability to compensate for the loss of each other and still allow the monocyte/macrophage to terminally differentiate when one of these molecules is lost - but not when both are knocked out²⁸.

c-Myc is highly expressed in proliferating myeloblastic cells and is repressed once the cells are terminally differentiated into monocytes; it is also present in a large number of other undifferentiated proliferating cells, acting to down-regulate the C/EBP α during monocyte maturation²⁴. c-Myc suppression is then necessary for the induction of C/EBP β and C/EBP δ , which occurs later in the monocyte maturation process²⁹. IL-6 induction through stat 3 signalling is responsible for the repression of c-Myc and therefore can suppress monocyte differentiation in favour of granulocyte development³⁰.

It is only very recently that the two transcription factors controlling the differentiation of the two-monocyte subsets have been discovered. Nurr77^{-/-}

mice show a deficiency in the patrolling / anti-inflammatory Ly6C^{low} monocyte subset. However, these mice exhibit normal levels of the inflammatory Ly6C^{hi} monocyte subset³¹. The converse was noted in KLF4^{-/-} mice, where they exhibited reduced levels of Ly6C^{low} monocyte but were completely deficient in the Ly6C^{hi} population³².

There is still much controversy and mystery over the relationship that the MDP have with the two-monocyte subsets and the developmental relationship they share with each other, however, this will be explored in more detail in section 1.3.3

1.3.2 Microglial ontogeny and function

Microglia are a separate arm of the macrophage family found solely in the CNS. They patrol the central nervous system hunting for damaged neurons and infectious agents, and are also associated with the pathogenesis of severe neurodegenerative diseases³³. In contrast to many other macrophage populations, it has been discovered recently that microglia do not in fact derive from monocyte precursors (figure 1.1) but are thought to renew independently from the HSC in the bone marrow under steady-state conditions³⁴. However, under inflammatory insult, Ly6C^{hi} monocytes have been shown to infiltrate into the CNS and differentiate into activated microglia^{35 36}.

Fate mapping studies indicate that microglia in the adult brain derive essentially from primitive macrophage progenitors that arise before embryonic day 8 independent of the fetal liver and HSC³⁷. Recently, it was discovered that these primitive progenitor cells originate in the embryonic yolk sack. The yolk sack produces progenitor cells, which likely migrate to the brain via newly formed blood vessels from embryonic day 8. Myb is an essential transcription factor in the development of HSC while PU.1 is an essential transcription factor for generation of macrophages. Studies in Myb^{-/-} knockout mice embryos have demonstrated that CD11b^{high} CD45⁺ F4/80⁻ monocytes are absent from the blood while the number of CD11b^{low} CD45⁺ F4/80^{bright} macrophage (microglia) in the embryonic brain are normal. In comparison, the CD11b^{low} CD45⁺ F4/80^{bright} microglial population along with the CD11b^{high} CD45⁺ F4/80⁻ blood monocytes are missing from PU.1 knockout embryos, demonstrating that CD11b^{low} CD45⁺

F4/80^{bright} microglial population are of the macrophage lineage. Thus, the data suggests that microglia do not develop from HSC and originate from the yolk sac during foetal development. The authors also suggest that microglia are replaced in adult life via a combination of proliferation and local self-renewal. How this local self-renewal occurs has not been explained as yet and requires further investigation^{38 39}.

1.3.3 Murine monocyte heterogeneity

Monocytes make up roughly 2-5% of the total white blood cells in the murine system. Morphologically, monocytes are irregular shaped cells that possess kidney shaped nucleus, cytoplasmic vesicles and have a high cytoplasm to nucleus ratio. Over the last 20 years, research has hinted at the possibility of different subsets of monocytes and it is now accepted that monocytes do in fact form at least two distinct subsets. Both subsets express CD115, CD11b and F4/80^{int} but can be divided based on their expression of Ly6C and the fractalkine receptor CX₃CR1⁴⁰.

The antigens used to distinguish monocytes, Ly6C, CD11b, CD115 and CX₃CR1, from other effector cells of the immune response are not solely expressed on the monocyte population, but it is the unique pattern of expression that allows their use in the identification of the monocytes. Ly6C (Lymphocyte antigen 6 complex, locus C) is a 14-17KD glycosylphosphatidylinositol-anchored cell surface protein that is rich in cysteine residues. It is part of the Ly6 protein 'superfamily'⁴². The Ly6 protein domain is 80 amino acids long and is characterized by a conserved pattern of 8 to 10 cysteine residues that have a defined disulphide-bonding pattern⁴³. The Ly6 protein domain is rare as it is thought that only 2% of all surface molecules on leukocytes contain this domain. The Ly6 locus is located on murine chromosome 15⁴⁴. Ly6C was first described as having a function in endothelial cell adhesion and homing of T cells by activating integrin dependent pathways⁴⁵. However, no function has been described for it in the context of monocytes. Ly6C is the most widely used marker to identify monocytes and one of two markers that are currently used to define the two subsets within the monocyte population. That said, it is not known what regulates its expression or why the two subsets differentially express Ly6C.

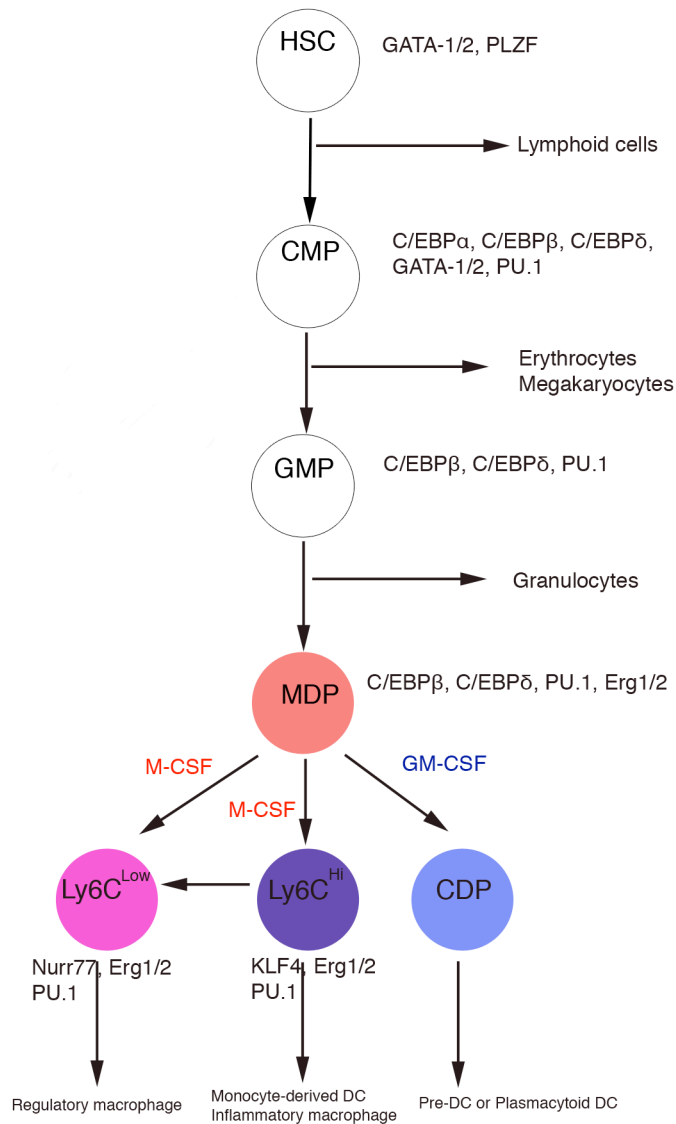


Figure 1.1. Ontogeny of monocytes, macrophages and DCs.

Commitment to differentiation into a monocyte or dendritic cell occurs at the MDP stage. MDP can give rise to CDP, which in turn can give rise to pre-DC or plasmacytoid DC. MDP also give rise to Ly6C^{hi} and Ly6C^{low} monocytes; Ly6C^{hi} monocyte have also been shown to have the ability to differentiate into Ly6C^{low} monocytes if they do not encounter inflammation. Adapted from ⁴¹

Ly6C^{hi} monocytes express CX₃CR1 at a low to intermediate level and are thought to be the inflammatory subset of the monocytes population as they are released from the bone marrow in a CCR2-dependent manner⁴⁶. Ly6C^{low} CX₃CR1^{hi} monocytes are the other subset identified in mice. These monocytes are thought to be the patrolling/anti-inflammatory monocytes as they were found to circulate in the blood for 2-3 weeks seeking out damage in blood vessels and are said to continually migrate into tissues in the steady state to replace some resident macrophage and DC populations. Ly6C^{hi} CX₃CR1^{low} and Ly6C^{low} CX₃CR1^{hi} monocytes are seen in the blood at a 1:1 ratio. However, in the bone marrow this is not the case, Ly6C^{hi} monocytes far outnumber the Ly6C^{low} monocytes.

There is some controversy over the origins and the relationship between the two-monocyte sub-populations. It has been frequently proposed that Ly6C^{low} cells derive from Ly6C^{hi} monocytes. Evidence that has been put forward to support this theory shows that in cell depletion or cell transfer studies not only can MDP produce both Ly6C^{hi} and Ly6C^{low} monocytes *in vivo* but also that Ly6C^{hi} cells home back to the bone marrow where they can mature into Ly6C^{low} cells⁴⁷. However, the signals that induce Ly6C^{hi} monocytes to mature into Ly6C^{low} monocyte are still largely unknown. In juxtaposition, it has been proposed that Ly6C^{low} monocytes can be generated independently of their Ly6C^{hi} counterparts based on observations that the numbers of circulating Ly6C^{low} monocytes were not affected after prolonged antibody depletion (2 weeks) of the Ly6C^{hi} monocytes⁴⁸. Nevertheless, the existence of a direct precursor relationship between MDP and Ly6C^{low} monocytes without the intermediate Ly6C^{hi} monocyte has not been irrefutably demonstrated yet and is a highly debated subject in the field of monocyte biology (figure 1.1).

1.3.3.1 The different role monocyte subsets play

There are many examples of the role that monocytes or specifically the Ly6C^{hi} monocyte subpopulation play in clearing infections. One of these examples is illustrated by work done in *M. tuberculosis* infection studies. CCR2^{-/-} mice have significantly reduced circulating levels of Ly6C^{hi} monocytes as they cannot egress from the bone marrow; however, the Ly6C^{low} population remains unaffected (this is discussed in more detail in section 1.3.5). When the CCR2^{-/-} mice are challenged with *M. tuberculosis*, they show reduced ability to fight the

infection: they have higher mortality rates within the early stages of infection compared to WT controls. This outcome was shown to be due to reduced production of IFN γ , nitric oxide and effective CD4 T cell priming as the Ly6C^{hi} monocyte population cannot infiltrate the lung and differentiate into inflammatory macrophages and DCs^{49 50}. *T. gondii* is an example of a protozoan infection that is reliant on the recruitment of Ly6C^{hi} monocytes for clearance⁵¹. The recruited Ly6C^{hi} monocytes play a similar role to that described above in clearing the bacteria *M. tuberculosis*. The authors also used CCR2^{-/-} mice to show that with reduced Ly6C^{hi} monocyte recruitment there was a significantly decreased ability to clear the infection. The reduced ability to clear the pathogen was demonstrated to be due to reduced inflammatory macrophages and DCs at the sight of infection and therefore decreased production of IL-12, IFN γ and NO, which are essential for clearance^{51 52}.

Transcriptional analysis studies examining monocyte presence in the early and late phase of *L. monocytogenes* infection were some of the first to define the separate role of Ly6C^{hi} and Ly6C^{low} monocytes in inflammation; before this, little was known about the interplay of the two monocyte subsets with each other and the part Ly6C^{low} monocytes played in the progression of an immune response to an infection. All that was previously known about Ly6C^{low} cells, was that they had been shown to have “crawled” along the lumen wall of blood vessels in the steady state.

These seminal studies with *L. monocytogenes* revealed that the early stages of infection (1h post infection) were associated with the presence of TNF α and IL-1 producing Ly6C^{low} monocytes⁵³. These early-responding Ly6C^{low} monocytes show up-regulation of genes encoding lysozymes, defensins and complement, which are associated with pro-inflammatory macrophages. Ly6C^{low} monocytes are ideally placed to rapidly respond to infection as they patrol along the blood vessels and express an array of adhesion molecules, which allow them to rapidly extravasate into inflamed tissues. By comparison, Ly6C^{hi} monocytes are recruited to the site of infection at a later phase - as they must traffic from the bone marrow^{47 54}. The transcriptional profile of Ly6C^{hi} monocytes at the site of infection was consistent with that of classically-activated macrophages, which are typically thought of as highly inflammatory. In contrast, in the final stages of infection (12h post infection), the second wave of Ly6C^{low} monocytes that are

now recruited exhibit an altered differentiation pathway congruent with regulatory macrophages with an up-regulation of arginase 1, Fizz 1 and the mannose receptor; a population which are thought to be involved in the resolution of inflammation and tissue repair⁵³.

After the *L. monocytogenes* seminal work was completed, other groups started to examine the different roles monocytes play in other diseases and conditions, and not just focus on what the Ly6C^{hi} monocytes were contributing; examples of this is in cardiovascular disease where it was demonstrated that the splenic reservoir of monocytes is mobilized after myocardial infarction and this is thought to be important in the healing process. Ly6C^{hi} monocytes dominate the first phase of inflammation at day 1 post infarct and secrete high levels of proteases and TNF α , which contribute to clearance of apoptotic debris. Through days 5-10 the second phase of infiltration occurs, which is predominated by Ly6C^{low} monocytes secreting VEGF and encouraging myofibroblast accumulation and angiogenesis, vital for the start of the tissue repair process^{55 56}.

Atherosclerosis and hypercholesterolemia are two other conditions that have recently been shown to preferentially increase the production and circulation of Ly6C^{hi} monocytes^{57 58}. The most common model for atherosclerosis research is the ApoE^{-/-} knockout mouse, which when fed on a high fat and cholesterol rich diet develops atherosclerosis. Ly6C^{hi} monocytes infiltrate in large numbers into aortic plaques via a CCR2 dependent mechanism. When in the plaques they have been shown to produce IL-1 β , reactive oxygen species and numerous proteases that all contribute to lesion exacerbation⁵⁹. Ly6C^{low} monocytes are evident at a far lower level in the lesional plaque, trafficking into it in a CCR5 dependent manner. Unlike the Ly6C^{hi} monocyte subset, emerging evidence suggests that Ly6C^{low} monocytes may play a role in providing added protection from atherosclerosis. This was demonstrated when double knock-out mice were produced to make the mice susceptible to atherosclerosis and deficient in Ly6C^{low} monocytes (ApoE^{-/-} Nurr77^{-/-}). These mice were shown to have lesions with significantly higher lipid burdens than the normal atherosclerosis susceptible mice (ApoE^{-/-}) - along with higher level of CD36+ macrophages that produce high levels of TNF α . This implies that the Ly6C^{low} monocyte must play a protective role in this model of atherosclerosis^{60 61}. However, more work needs

to be done in this area to elucidate the mechanism behind this potentially protective role Ly6C^{low} monocytes play in the disease.

Monocyte phenotypes have been a controversial issue in recent years; when the original discovery of the two subsets of monocytes was made, the Ly6C^{hi} monocytes were described as the pro-inflammatory subset and Ly6C^{low} monocytes were the patrolling/anti-inflammatory sub-set⁴⁰. However, it has been demonstrated that these roles can become reversed under certain environmental conditions⁶². It is, however, accepted that the original classification of “inflammatory” and “patrolling/anti-inflammatory” is the evolutionary conserved function of the two subsets. Moreover, there is now an acceptance that monocyte and macrophage activation phenotypes and functions are not constrained and can be affected by the environment they are activated within and can over-write the cells default phenotype⁶³. This dichotomy is exemplified in the gut; newly arrived Ly6C^{hi} inflammatory monocytes differentiate *in situ* into IL-10-producing anti-inflammatory CX₃CR1^{hi} resident macrophages in homeostasis. However, intestinal inflammation induces the Ly6C^{hi} monocytes to differentiate into pro-inflammatory macrophages, which are Toll-like receptor (TLR) responsive and produce vast quantities of inflammatory mediators. Thus, resident and inflammatory macrophages in the gut represent divergent differentiation outcomes of the same Ly6C^{hi} monocyte precursor⁶⁴.

1.3.4 Human monocyte heterogeneity

The two distinct monocyte subsets are evolutionarily conserved across species and can be defined not only in mice but also in humans where the Ly6C^{hi} population has been shown to correspond to the “classical” CD14⁺⁺ CD16⁻ population and Ly6C^{low} murine monocytes correspond to the “non-classical” CD16⁺⁺ CD14⁺ population⁶⁵. Monocytes make up 10% of the total number of white blood cells present in the circulation and unlike in the murine system where there is a 1:1 ratio of the two subsets, there is a 9:1 ratio of CD14⁺⁺CD16⁻ to CD14⁺CD16⁺⁺ in the blood⁶⁶.

1.3.5 Monocyte trafficking under homeostatic conditions and inflammation

In steady-state, monocytes that are produced in the bone marrow are released into the circulation and can extravasate into distant lymphoid and non-lymphoid tissues. The process of extravasation typically associates with an irreversible program of differentiation, resulting in the generation of tissue resident macrophage and DC populations with specialized functions⁶⁷. Ly6C^{hi} and Ly6C^{low} monocytes have different tropisms and fates in steady-state. Ly6C^{low} monocytes patrol non-inflamed blood vessels and have the potential to enter non-inflamed tissue, contributing to the replacement of resident macrophage and dendritic cells in conjunction with local cell renewal^{38 40}. Ly6C^{hi} cells selectively migrate to sites of inflammation, but in the absence of this they return to the bone marrow and differentiate into Ly6C^{low} monocytes⁴⁷.

The reason monocytes have this ability to migrate into tissue or patrol blood vessels, is that they are equipped with multiple chemokine and integrins that mediate these processes. The chemokine receptor CCR2 has been shown to play a vital role in the recruitment of Ly6C^{hi} monocytes. Within the bone marrow, inflammatory monocytes (CCR2⁺) are evenly distributed throughout the bone marrow, however, upon LPS stimulation the CCR2⁺ monocytes rapidly (2h) associate with cadherin-positive vascular endothelial cells. Ly6C^{hi} monocytes are also seen in increased frequency within the lumen of blood vessels. Interestingly, CCR2^{-/-} mice have significantly reduced numbers of inflammatory monocytes in the blood vessels when stimulated with LPS compared to WT mice⁶⁸. Two of the ligands for CCR2, CCL2 and CCL7, have been shown to play a role in the migration of inflammatory monocytes out of the bone marrow. Although expression of CCR2 is restricted to only a few cell types, most cells, with the exception of red blood cells, express CCL2 in response to activation by pro-inflammatory cytokines or stimulation of innate immune receptors by a range of microbial molecules⁶⁹. CCL7 is generally induced during bacterial infection. If CCL2 or CCL7 is deleted it reduces the recruitment of Ly6C^{hi} monocytes from the bone marrow in *L. Monocytogenes* infection by up to 40-50%⁷⁰. The exact mechanism that CCL2 and CCL7 play in the recruitment of monocytes is not yet known. It has been suggested that by interacting with CCR2 they guide monocytes through different niches within the bone marrow and out into the

circulation. Interestingly, CCR2 also binds CCL8 and CCL12, though deletion of these two markers has no noticeable effect on monocyte recruitment ⁶⁹.

CX₃CL1 (Fractalkine) is a membrane bound chemokine, which specifically binds to CX₃CR1 and is expressed in a variety of tissues, including the marginal zone of the spleen, and is essential for Ly6C^{low} monocytes effector functions. If the CX₃CR1 gene is deleted then there is diminished patrolling of Ly6C^{low} monocytes ⁵³. CX₃CR1 and CX₃CL1 not only play a pivotal role in monocyte patrolling/trafficking, they also provide a survival signal for Ly6C^{low} monocytes. When a Bcl-2 transgene is introduced into CX₃CR1^{-/-} or CX₃CL1^{-/-} mice, which show reduced numbers of Ly6C^{low} monocytes in the blood, it rescues the knockout phenotype back to the normal wild type phenotype in inflammation and steady-state conditions ⁷¹.

1.4 Macrophage phenotype, heterogeneity and polarization

Under homeostatic conditions macrophages provide various housekeeping functions that require no special activating stimuli or are activated during development. Macrophages are phagocytic cells that constitutively express a variety of scavenger receptors that facilitate the removal of aged red blood cells, necrotic tissues and toxic molecules from the circulation ⁷². However, many things can affect the phenotypic and functional characterization of macrophages ⁷³. Macrophage activation has been described as a spectrum of functionally diverse phenotypes. Hence, the plasticity that is associated with macrophages allows them to contribute to inflammation or, conversely, contribute to the resolution of inflammation ⁷⁴. The type of macrophage that matures is a direct consequence of its specific environment ⁷⁵. The micro-environmental stimuli and the resulting functional phenotypes are varied and there is a diverse spectrum of phenotypes; two main macrophage phenotypes have been suggested, mirroring the Th1/Th2 polarization concept of T cell activation. These two functional extremes are the “regulatory” macrophages and the pro-inflammatory “classically” activated macrophages ⁷⁶. The functional diversity of macrophages can be attributed to their ability to respond to different microenvironments, such as the cytokine profile of the tissue it is

inhabiting when the macrophage is activated in and at what stage of the immune response the macrophage is recruited into.

The classically-activated macrophages are known as being pro-inflammatory due to their production of vast quantities of pro-inflammatory cytokine such as IL-1 β , IL-6, IL-12 and IFN γ . These pro-inflammatory macrophages are sometimes referred to as M1 macrophages. The classically-activated macrophage was the first activation phenotype to be characterized in macrophages, mediating host defense to a variety of bacteria, protozoa and viruses. Classically-activated macrophages also have a role in anti-tumor properties⁷³. Regulatory-macrophages, which are also known as M2 macrophages, are characterized by increased expression of IL-10, which is an immune-modulatory cytokine, and decreased expression of IL-12⁷⁷. These macrophages participate in the resolution of inflammation and therefore are seen at the end of an immune response to a pathogen. Regulatory-macrophages can be sub-divided into two further broad categories depending on how they are activated: wound-healing and anti-inflammatory⁷⁸. A more detailed account of macrophage phenotypes, polarization and activation is given in section 3.1.

1.5 Spinal Cord: A brief overview

The spinal cord is a crucial part of the central nervous system (CNS). Its main function being to relay neural impulses between the brain and periphery, as it is the link between the CNS and the peripheral nervous system (PNS)⁷⁹. If a trans-section of the spinal cord is taken, it can be seen that it is made up of two types of matter: the white matter is the outer most and inside this is the grey matter, which has a butterfly appearance in shape. The grey matter is made up of neuronal cell bodies, and the white matter is made up of axons that have been myelinated, hence their white appearance. Cell bodies generate electrical signals, which are relayed up and down the myelinated axon that carry them out to the PNS through the dorsal root ganglia⁸⁰. Due to the fundamental role played by the spinal cord in the body, it is encased in a bony process known as the vertebral column, which protects it from damage. It is further protected by the spinal meninges, which are three specialized membranes that enclose the spinal cord. These membranes protect it from the bony vertebrae of the vertebral column and help with shock absorption. The three layers are called the

dura, arachnoid and pia ⁸¹. The spinal cord also has an intrinsic layer of protection against the constantly fluctuating conditions in the blood and to unwanted cellular infiltration, and this is known as the blood brain barrier.

1.5.1 Blood brain barrier (BBB)

The BBB was first proposed by Paul Ehrlich, when he injected dyes into the circulation of animals, which would lead to all tissues, with the exception of the brain and spinal cord, becoming stained ⁸². When these dyes were injected directly into the cerebral spinal fluid, by Edwin E. Goldman, an associate of Ehrlich, the animal's brain and spinal cord would become stained but no other tissue would. This research led to the theory that there must be a barrier of some sort stopping molecules passing from the blood stream to the CNS. It was later shown that the barrier was due to special properties of the epithelial cells of the capillaries in the CNS, which are joined together by tight junctions and have astrocytes interacting with them ⁸³. One of the crucial roles of the BBB is to restrict immune cells migrating into the CNS under normal physiological conditions ⁸⁴. When there is an infection in the CNS, which is usually very rare, the BBB becomes leaky for a short period of time and allows the immune cells to extravasate through the BBB. However, if there has been trauma to the CNS, this can cause damage to the BBB, allowing immune cells to migrate in an unregulated fashion and cause massive inflammation ^{85 86}.

1.6 SCI

Even though the spinal cord is well protected, its soft tissue can still become damaged. This happens when there is such trauma that causes the vertebrae to become crushed or broken. SCI affects approximately 40,000 people in the UK annually. There are many types of injury that can occur to the spinal cord some of which are lacerations, contusions and compression injuries; the most common of these is a contusion injury. This form of injury occurs when a substantial force impacts the spinal cord causing movement of the vertebra, injuring the normally protected spinal cord, leading to haemorrhaging and bruising. There are in excess of 1200 new cases of paralysis annually attributed to SCI, costing the UK more than £500 million per annum. The majority of these cases are male and 55% of those are aged between 16 and 30 years old. Almost half of all spinal cord

injuries occur at the cervical level in humans, the part of the spinal cord that controls both the upper and lower extremities. As a result, severe injuries to this area can leave patients as quadriplegics^{87 88}.

1.6.1 What happens when the spinal cord is injured?

Damage begins straight after the trauma, with bits of bone fragment and disc material damaging the fragile spinal cord and bruising the surrounding ligaments. This leads to shearing of axons, disruption of neuronal cell membranes and disruption of blood vessels, leading to heavy bleeding into the grey matter⁸⁹. When this happens, the site of injury will swell up, filling the spinal canal and thus compressing the capillaries that supply blood and oxygen to the spinal cord. The dramatic reduction in blood pressure can lead to a loss in the ability to self-regulate autonomic functions - as very low blood pressure interferes with neurons ability to generate electrical impulses. Evidence suggests that in cases of human SCI, residual neural connections normally persist after this stage, indicating the potential for some level of recovery⁹⁰.

Once the initial physical trauma has occurred, a cascade of biochemical, cellular and inflammatory events are set in motion that are massively destructive and continue for weeks to months after the initial SCI⁹¹. This cascade leads to an increase in the size of the damaged area⁸⁹. The phenomenon is known as secondary death, which will be looked at in closer detail in section 1.7.1.2.

1.7 An overview of the “sterile” immune response to SCI

Immune cells play a critical role in the resolution of inflammation and pathologies that occur in peripheral organs. However, in the CNS, which is considered an immune-privileged site, after SCI the contribution of these cells to the healing and regeneration of the damaged cord remains a subject of controversy. Early reports indicated that when the infiltration of monocytes/macrophages into the damaged spinal cord was blocked, this resulted in neuro-protection due to a reduction in the release of inflammatory mediators^{92 93 94 95}. An example of one macrophage-specific factor that promotes damage in the spinal cord is Leukemia Inhibitory Factor (LIF). LIF induces the proliferation of microglia and the infiltration of neutrophils and

macrophages owing to its own chemo-attractant properties and its ability to induce CCL2 expression ⁹⁶. IL-6 is another cytokine that is released by infiltrating monocyte/macrophages and promotes astrogliosis, a stereotypical response to CNS injury that inhibits axon regeneration - in part through the transcriptional activation of genes associated with chondroitin sulphate proteoglycan (CSPG) formation, which is a major component of the glial scar ^{97 98}. On the other hand, more recent studies have suggested that there are potentially beneficial roles for monocytes/macrophages in SCI regeneration and recovery: leukocytes were demonstrated to promote removal of tissue debris, secrete neurotrophic factors, and support axonal regeneration ⁹⁹. However, this beneficial role may only be transient.

1.7.1 Time course of the immune response to SCI

The immune response that ensues after SCI can be broken up into phases. The acute phase is dominated by the infiltration of neutrophils at 4-8 hours after injury and these peak 3 days post-injury ¹⁰⁰. Neutrophils are cells of the innate immune system that become activated when they enter tissue. They are highly phagocytic cells and produce chemicals such as reactive oxygen species, chemokines and cytokines, which are highly destructive to the fragile spinal cord ¹⁰¹. However, it is hypothesised that in the early stages of injury, to decrease the likelihood of auto-reactive responses, their highly phagocytic activity is essential for the clearance of neural cellular debris. Next is the sub-acute phase, from 12h on, and is characterized by activated resident microglia and infiltrating monocyte/macrophages ⁹¹. These cells are also phagocytic and release a vast array of chemokines and cytokines ^{102 103}. From day 7 post-injury, T and B cells start to migrate into the CNS and the glial scar forms from 7-14 days post injury.

1.7.1.1 Glial scar

The glial scar forms around the injured site after SCI when astrocytes become activated by inflammation caused by immune cell infiltration. This is not only a physical barrier to axonal regeneration but also an environment awash with soluble factors such as CSPG, slit proteins and ephrin-B2 that inhibit axonal regeneration ¹⁰⁴. Various therapeutic approaches have attempted to eliminate and reorganize the chemical components of the glial scar or to regulate its

negative effects. These include degrading enzymes to eliminate scar components (especially CSPGs) ^{105 106}, blocking the activity of the growth inhibitors using specific antibodies, blocking the receptors that recognize the growth-inhibitory factors, regulating intracellular signals induced by the growth-inhibitory compounds ¹⁰⁷, inhibiting astrocyte proliferation to attenuate scar formation, and applying growth-inducing agents and growth factors to form bridges across the injury site ¹⁰⁸. Obviously, all of these approaches have been based on the perception that the glial scar is an obstacle to recovery that should be modified, eliminated, suppressed or circumvented.

However, accumulating evidence indicates that scar tissue and its components might have an important role in the immediate response to CNS injury. Reactive astrocytes, which are the main cellular component of the glial scar, have an important role in scavenging, which regulates the levels of potassium, glutamate and other ions. The abolition of astrocytes leads to a vast decrease in the presence of glutamate transporters ¹⁰⁹. Recently, it has been implied that the glial scar contributes to immuno-modulation within the injury site.

Two weeks after SCI, microglia and blood monocyte/macrophages were discovered to associate with each other at the margins of the glial scar, where vast quantities of CSPG are produced. The localization of the monocyte/macrophages and microglia at this location was shown to result in the production of high levels of neuronal survival factor, IGF-1 ¹¹⁰. When the production of CSPG is inhibited via Xyloside, a knock-on effect of this is that the reduction in the production of IGF-1, which leads to an increased production of TNF α from the monocytes/macrophages and microglial that had co-localized at the margins of the lesion. The consequence of this is an increase in lesion size and decrease in functional recovery ¹¹¹. It should also be appreciated that the infiltrating immune cells can have an impact on the size of the glial scar too. At 7 days post-SCI, IL-10-producing monocyte/macrophages are present at the CSPG-rich region of the lesion. These macrophages produce increased levels of metalloproteinase-13 (MMP), which in turn lead to the degradation of the glial scar, demonstrating a unique balance between regulation of the myeloid response and size of the glial scar ¹¹².

1.7.1.2 Monocyte/macrophages and microglia in secondary death after SCI

As discussed above a robust innate immune response occurs following SCI. One-week post injury, the lesion has been abundantly infiltrated by macrophages and microglia. Many groups have previously published data to suggest macrophage and or microglial depletion or inhibition has a neuro-protective consequence^{95,100}. It has also been shown that the injection of zymosan (a potent inducer of inflammation that has been used to replicate the inflammation seen after SCI) into the CNS parenchyma activates resident microglia and leads to an influx of monocyte/macrophages from the periphery. This infiltration sets off a chain of negative events, which leads to the withdrawal of astrocytes, axonal damage, fluid- or matrix-filled cysts and cavities, and deposition of growth inhibitors such as CSPGs¹¹³. These toxic effects appear to be mediated by soluble factors derived from macrophages, i.e. IL-1, TNF α and reactive oxygen species, as well as direct physical interactions between macrophages and dystrophic axons¹¹⁴. Deletion of macrophages through clodronate liposomes diminishes astrocyte withdrawal, cavitation and axon dieback after zymosan injection or at the post SCI stage^{94 115}.

Macrophages and microglia express a variety of TLR such as TLR2 and 4 in the injured CNS. When TLRs are engaged by their ligand this sets off a signalling cascade that involves NF κ B and leads to the production of pro-inflammatory cytokines¹¹⁶. TLR activation has been implicated in the propagation of pathology in certain models of SCI and CNS auto-immune conditions such as demyelination. It was shown by in-situ hybridisation that TLR2 and CD14 (an accessory molecule for TLR2 and 4) expression is increased after SCI. There was also an increase in NF κ B- α expression in conjunction with TLR2 and CD14 expression leading to the proposal that there is an increased signalling by these molecules after injury, and the resulting production of large amounts of pro-inflammatory products¹¹⁷. TLRs recognise pathogen-associated molecules as well as also recognising some self-molecules, which are known as “danger signals”. Danger signals are released from cells when they become stressed; this can happen when they are being attacked by pathogens or are injured due to trauma¹¹⁸. An example of some of these danger signals are heat shock proteins, extracellular matrix proteins, certain proteolytically-cleaved products, oxidized lipids and necrotic cells. The

concept of “sterile inflammation” is now widely accepted in SCI, in that TLR activation of macrophages and microglia after SCI is linked to the production of self-danger signals rather than pathogen-associated molecules^{119 120}.

1.7.1.3 Apoptosis versus necrosis after SCI

The process of apoptosis is how cells commit suicide; this process is biologically advantageous, as it effectively clears away old or damaged cells without exposing the cellular contents to the rest of the system. This programmed cell death is characterized by cell membrane blebbing and formation of apoptotic bodies, which contain the toxic components of the cell and are then quickly cleared by phagocytosis. Necrosis occurs when cells rupture and their toxic components are released, potentially causing damage to the surrounding environment. Necrosis is the primary form of cell death immediately after SCI by virtue of the traumatic event suffered. However, a short time after the initial trauma neuronal death is no longer predominated by necrotic death, in fact neurons start to die by apoptosis at the lesion margins. Oligodendrocytes also start to die by apoptosis at the site of degenerating axons after the initiation of neuronal apoptotic death. Neurons and glial cells can die by apoptosis even weeks after the initial trauma¹²¹. CD95, CD95L and TNF α are all seen to be up-regulated by neurons and glial cells after SCI.

Neutralizing antibodies was used against these molecules to assess the impact of apoptosis on SCI recovery. After blockade, animals showed better functional recovery in behavioural testing than untreated controls¹²², thus showing that in this situation excessive apoptosis leads to the death of healthy cells that would otherwise participate in regeneration after SCI. Another contributing factor to secondary death, is the release of excess neuro-transmitters such as glutamate, which can also lead to the perpetuation of apoptotic-induced cell death. At the site of SCI, dying neurons flood the area with glutamate, which in excess kills healthy neurons and oligodendrocytes, and also leads to the activation of microglia. Interestingly, when microglia become activated they release more TNF α and CD95L. Infiltrating immune cells, such as macrophages, also contribute to this initiation as they can also release TNF α , CD95L and cause oxidation of proteins, lipids and nucleic acid¹⁰⁰.

1.7.2 When the immune system works towards repair and regeneration of the damaged spinal cord

Contrary to the above evidence - that the immune response plays only a sinister role in SCI - it has been shown in numerous studies that this is not the case¹²³. Despite having the ability to damage neurons and glia, microglia and macrophages can be intrinsically neuro-protective; both have the ability to produce neuro-protective cytokines and growth factors. An example of this is TGF β , which is a potent anti-inflammatory cytokine, displaying beneficial effects on neuronal survival, including limiting oligodendrocyte toxicity¹²⁴. Macrophages and microglia also possess the ability to produce neurotrophic factors including insulin-like growth factor, platelet derived growth factor and brain-derived neurotrophic factor^{125 126}, which are all beneficial to neuronal survival and growth. Macrophages can even play a role in modulating glutamate excitotoxicity and promoting the growth of injured axons via increasing their Na⁺-dependent transporters that are able to take up extracellular glutamate and clear it away from neurons¹²⁷.

Within the first few hours after injury to the brain or spinal cord, concentrations of IL-6 increase in the CNS. Neurons, glia and infiltrating leukocytes all produce and respond to IL-6, signifying that it is a pivotal mediator of the acute CNS injury response; for example, injecting anti-IL-6 antibodies early after SCI confers neuro-protection. This response is mediated through the reduced monocyte infiltration and increased efficiency of microglia phagocytosis¹²⁸. However, IL-6 that is produced by macrophages and microglia can also be of benefit to neuronal growth. Transection of axons in a hippocampal slice culture increases IL-6 levels, which in turn leads to spontaneous recovery of synaptic activity and regenerative sprouting. If this is done in the presence of an anti-IL-6 antibody, the expression of regeneration-associated genes (GAP43) and recovery of synaptic activity are abolished¹²⁹.

During postnatal development, iron is an essential component in the normal process of myelination. Microglia are thought to be the source of iron for the oligodendrocytes during this process of myelination as their levels are high before myelination, and then decrease when oligodendrocytes iron levels increase (at the point at which myelination starts)¹³⁰. After SCI, there is a build

up of free iron at the sight of trauma, and this can become toxic to oligodendrocytes when it is at too high a concentration through a processes of oxidative damage. Macrophages and microglia have been shown to sequester iron after trauma and then shuttle it back to oligodendrocytes at lower concentrations, which is essential and therefore beneficial to the process of remyelination after injury ¹³¹.

1.7.3 Attempts at modulating the immune response to be more conducive to recovery and regeneration

Immediately after SCI, the immune system plays an essential role in clearing away debris and initiating the wound-healing cascade as well as being able to produce neurotropic and neuro-protective factors. Nevertheless, it has been exhibited in many studies that the potential for regeneration in the CNS after SCI is far increased when the overt inflammatory immune response is down-regulated after the initial acute phase ¹³². Normally, inflammatory cascades are self-limiting and typically resolve quickly after the initial “danger” has been contained outside the immune privileged site of the CNS. However, within the injured spinal cord, neuro-inflammatory cascades persist for extended periods of time. Activated macrophages and microglia are found in the injured spinal cord of rats up to 6 months after injury due to limited mechanisms for extinguishing the inflammation ¹⁰¹. This is why there has been so much research done to develop therapies that can harness the initial beneficial effects of the immune response and then “turn it off” before it becomes destructive; some of these strategies are discussed below.

1.7.3.1 Macrophage polarization as a method of reducing inflammation after SCI

Macrophage/monocyte infiltration is a major component of the inflammatory immune response after SCI; it is also known that macrophages and monocytes can exhibit not only a pro-inflammatory state of activation but also an anti-inflammatory one. Taking into consideration the beneficial roles macrophages can play in neuro-protection and neuro-regeneration, studies have started to try and exploit the different states of activation macrophages adopt and question if anti-inflammatory macrophages could play a beneficial role in SCI.

Supernatants taken from cultures of inflammatory macrophages or anti-inflammatory macrophages have already been shown to induce quite different phenotypes on the regrowth of axons *in vitro*. When treated with toxic pro-inflammatory macrophage supernatants, cortico-spinal tract neuronal cultures experience vast amounts of apoptotic death, whereas cultures treated with anti-inflammatory macrophage supernatants did not ¹³³. In addition, DRG neurones were shown to have significantly increased growth after treatment with anti-inflammatory macrophages supernatants compared to pro-inflammatory macrophage supernatants. Neurons were also shown to be far less branched and were longer when conditioned with the anti-inflammatory macrophage media ¹³³. Interestingly, IL-10, which is produced by anti-inflammatory macrophages, helps with the resolution of the redundant inflammatory immune response seen in peripheral tissue. Local infusions of IL-10 or insertion of a viral vector that expresses IL-10 have been shown to be neuro-protective after SCI due to its ability to resolve inflammation through antagonizing pro-inflammatory signaling (NF- κ B) at the site of injury ¹³⁴. The neuro-protective effect of IL-10 after SCI is not only via down-regulation of the inflammatory immune response, it also has direct neuro-protective effects on neurons with the inhibition of apoptotic mediators cytochrome C and caspase 3 activation, along with inducing an increase in expression of pro-survival factors Bcl-2 and Bcl-x_L ¹³⁵.

A major problem for SCI patients, months to decades after their initial injury, is the formation of fluid-filled cyst/cavities. In rats, treated with the autologous skin or peripheral nerve-activated macrophages, cyst/cavity formation was significantly decreased ^{136 137}. Macrophages that are incubated with autologous skin displayed increased expression of CD86 and MHC II, which is associated with an anti-inflammatory macrophage phenotype ¹³⁸. Examination of the macrophage secretory profile demonstrated that they had decreased expression of TNF α , increased expression of IL-1 β but showed no change in IL-6 production. Importantly, macrophages also increased their production of brain-derived neurotrophic factor, which stimulates axonal sprouting ¹³⁹. For optimum beneficial results, the autologously-activated macrophages must be injected into the lesion margins during the sub-acute phase of injury, which is from day 3, and no later than two weeks after SCI. It is noteworthy to mention that injection of the skin-activated macrophages into the non-injured spinal cord had no adverse

clinical or histological effects. Due to these findings, this experimental treatment for SCI was taken into phase I clinical trials and was named Pro-cord.

The Pro-cord phase I clinical trial was carried out on 16 patients with complete SCI. This was done after the hyper-acute phase and once their American Spinal Injury Association score was confirmed as A (the most severe grading of injury). After treatment, 5 patients showed marked recovery, two patients increased their score to B and three patients improved their scores to level C¹⁴⁰. After the success of the phase I clinical trial, phase II clinical trials were initiated but were later cancelled. There were two reasons for the cancellation: 1, macrophages were not injected until day 14, instead of administration in the hyper-acute phase. 2, in the phase I clinical trials macrophages were implanted at the same time as the patient received their spinal fusion operation¹³². This did not happen in the phase II study, meaning patients had to go through a secondary operation. Although Pro-cord was terminated in its phase II trial, it nevertheless demonstrated the beneficial effect macrophages can have on SCI when they are not activated in a pro-inflammatory setting.

1.7.3.2 Dendritic cell-based therapy

Dendritic cells are an alternative differentiation state of cell within the myeloid compartment. They can also be activated to pro-inflammatory and anti-inflammatory phenotypes. Dendritic cells have received little attention in SCI research, as they are not seen in the damaged cord to any great extent. However, dendritic cells may be beneficial after SCI, especially if they are prepared *ex vivo* where they can be polarized to an anti-inflammatory phenotype before implantation into the injury site. Dendritic cell transplantation was shown to activate neuronal stem cells, leading to the regeneration of neurons and significantly increased functional recovery in a murine model of SCI¹⁴¹. Dendritic cell implantation was also shown to be beneficial in a non-human primate (common marmoset) model of SCI where reduced levels of axonal demyelination in close proximity to the injury site and increased functional recovery after injury was observed¹⁴².

1.7.3.3 Adaptive immune system targeting

Inflammation induced by auto-immunity has been viewed as an important mediator of CNS secondary damage that occurs following the initial trauma of SCI, including neuronal and glial cell death, axon fracture or demyelination, as well as the formation of cavities and glial scar¹⁴³. However, in animal models of SCI, active or passive immunization with CNS myelin-associated self-antigens reduced neuronal loss and exerted immune neuro-protection^{144 145}. Recently it was demonstrated that neonatally-thymectomized rats that were reconstituted with myelin basic protein-activated T cells had increased levels of neuro-protection and a decreased level of neuronal Wallerian degeneration after SCI¹⁴⁶. However, the mechanism for this neuro-protective effect has not been elucidated yet.

1.7.3.4 IgG administration as a treatment of SCI

Preparations of human immunoglobulin G (IgG), usually referred to as IVIg, are well known immune-modulators that suppress some of the destructive pathways of the inflammatory cascade and promote recovery in many auto-immune and inflammatory conditions such as ITP¹⁴⁷. Intra-peritoneal injection of a single dose of IgG at the time of SCI was associated with significantly increased neurologic function in rats¹⁴⁸. Interestingly, histological and biochemical markers of neuronal injury were significantly reduced in the treated group compared to controls. The IgG treatment group had relatively well-preserved neuronal ultrastructure and reduced cavity and cyst formation. Additionally, it was demonstrated that there was a decrease in neuronal infiltration in the IgG-treated group compared to the untreated group¹⁴⁹. This is an interesting and novel treatment that can modulate the immune response after SCI. Nevertheless, the authors have no theory on the mode of action of this treatment or even what cell types it works though. This is potentially very dangerous, as many inflammatory and auto-immune conditions, such as Rheumatoid Arthritis and type III hypersensitivity, have implicated immune complex deposition as a cause of destructive pathology and perpetuation of the inflammatory immune response¹⁵⁰. However, immune complexes, if utilized in an appropriate manner, can induce anti-inflammatory immune responses in cells like macrophages¹⁵¹.

1.8 Immunoglobulin G (IgG) and its interactions with Fc receptors

In 1890 Von Behring and Kitasato demonstrated that serum taken from a previously immunized animal with diphtheria could confer protection to another unimmunized animal ¹⁵². Over many years, researchers investigated the active component(s) of serum that could neutralize toxins, precipitate toxins and cause agglutination of bacteria. It was initially thought that a different component of the immune serum caused each of these effects. However, it was not until the late 1930s that Elvin Kabat discovered a fraction of the immune serum that contained all of these functional activities. The active component of the fraction that he purified is known today as immunoglobulin or antibody ¹⁵³.

There are five classes of antibodies: IgG, IgA, IgM, IgD and IgE. Each of the subclasses is specialised for a different function and located to different compartments of the body. Antibodies have an approximate molecular weight of 150KD and consist of two heavy chains of 50KD and two light chains of 25KD. The light chains can either be κ or λ ¹⁵⁴. Each component chain is made up of one NH₂-terminal variable and a COOH-terminal constant immunoglobulin superfamily domain (IgSF). The IgSF domains are made up of two β -pleated sheets pinned together by disulfide bridges between two conserved cysteine residues. Each of the variable and constant domains consists of 110-130 amino acids; the light chains only consist of one constant domain whereas the heavy chains can consist of three or four. The variable region is the region in which antigen binding is mediated. It contains three complementarity-determining regions, which are embedded in framework regions. When folded correctly, all three of the complementarity regions are brought together to form the antigen-binding site ¹⁵⁵. The constant regions of the antibody molecule confer the class of immunoglobulin and mediate other functions like binding to effector cells and participation in the complement cascade.

IgG is the most common of all the immunoglobulins in the circulation; 75% of immunoglobulin in murine and human serum is IgG, and it is a vital component of the immune system. This is exemplified in the early days of a foetus, as it and IgA are the only isotypes that are transported by the Fc neonatal receptor across the placenta and so continues to protect the infant until its own immune system

matures. This is partly due to the long half-life in serum of IgG and the supplementation via breast milk ^{156 157}. IgG is made up of a number of subclasses in humans: these are IgG1, IgG2, IgG3 and IgG4; mice do not have the IgG4 subclass but instead possess IgG2a and IgG2b ¹⁵⁴. The constant region of an antibody does not only confer the isotype of the antibody, it also plays an integral role in antibody function for binding receptors such as Fc receptors and complement proteins.

1.8.1 Glycosylation of the Fc domain in Immunoglobulin

Antibodies are glycoproteins, and the glycans that are associated with the Fc portion of the immunoglobulin molecule are very important for the antibodies' function. The particular immunoglobulin isotype determines the amount of glycosylation; for IgG there is an N-linked glycosylation site on Asparagine 297 on each of the C_H2 domains ^{158 159}. Variation in glycosylation can be seen between IgG molecules - as well as within 3 sites on the same molecule because of differences in terminal sialic acid, galactose, N-acetylglucosamine, and fucosylation of the core sugars. These differences can lead to as many as 32 possible glycosylation patterns ^{160 161}. These glycans interact with a hydrophobic pocket on the Fc domain that stabilizes the immunoglobulin structure. It has been shown by mutagenesis studies that glycosylation is very important in allowing IgG to bind to FcγR as, if glycosylation does not occur due to mutations in the IgG amino acid sequence, this abrogates bind to FcγR. This is in contrast to IgA and IgE who do not lose their ability to bind to FcRs if they are not glycosylated ^{162 163}.

1.8.2 Fc Receptors and their interaction with IgG molecules

FcγR are a well-characterized part of the Ig superfamily: Ig superfamily molecules are characterized by having sequences similar to the variable or constant domains of antibodies. FcR are highly conserved through numerous species including humans, mice, rats, dogs and monkeys; the genes that encode FcR in humans, mice and monkeys are clustered on chromosome 1; rats' and dogs' FcR genes are located on chromosome 13 and chromosome 38 respectively ¹⁶⁴. FcγR are widely expressed on cells of the immune system; however, the exception to this is in T cells, which do not express any FcγR. In humans, there

are three types of FcγRs (FcγRI, FcγRII and FcγRIII), however, there are various isoforms of each receptor. In mice there are four FcγR (FcγRI, FcγRIIb, FcγRIII and FcγRIV). All FcγRs are type I trans-membrane proteins comprising an extracellular region containing two or more IgG-like domains and either a polypeptide or lipid anchor in the membrane ¹⁶⁵. Until a co-crystalline structure of the human FcγRIIIA and IgG1 was produced it was uncertain if one IgG molecule could bind to two FcγR as the IgG molecule is composed of two identical constant heavy chains. Theoretically, one IgG molecule could bind two FcγRs and therefore cross-link two receptors ¹⁶⁶. However, this seemed unlikely, as the biological consequence could be the permanent triggering of unnecessary inflammatory cascades. When the co-crystalline structure of IgG1 and FcγRIIIA was produced, it showed a 1:1 stoichiometry for the IgG and FcγR. It also demonstrated that the FcγR interacts with both of the two-polypeptide chains of the IgG1 molecule at their lower hinge region. It is now accepted that this is the relationship all IgG and FcγR molecules share with each other ^{167 168}.

1.8.2.1 FcγRI

FcγRI is the high affinity IgG receptor that only binds monomeric IgG. Murine FcγRI has high-binding affinity for IgG2a and lower affinity for IgG2b but does not bind IgG1 or IgG3. IgG2a and IgG2b have been shown to be the most pro-inflammatory IgG isotopes in the murine system. FcγRI contains three extracellular immunoglobulin-like domains unlike FcγRII and FcγRIII, which are the low affinity receptors and contain two extracellular domains ¹⁶⁹. The first two extracellular domains of FcγRI have high sequence similarities to the two extracellular immunoglobulin-like domains of FcγRII and FcγRIII. This has led to the conclusion that the third domain must confer the high affinity binding properties. Mutagenic and chimeric studies have shown that the removal of the third Fc domain leads to the loss of high affinity binding of monomeric IgG, although the mutant FcγRI molecules can still bind IgG with low affinity ¹⁶⁹. However, if FcγRI's domain 3 is linked to FcγRII it does not confer high affinity binding properties to the low affinity receptor. It has also been proposed that the Cγ2 domain of IgG is important for the interaction of FcγRI with IgG in particular residues 234-237 of the lower hinge region and residue 331 in the Cγ2 domain ¹⁷⁰. The binding domains for the lower affinity receptors binding sites to IgG have been mapped to similar regions.

FcγRI is expressed primarily on monocyte, macrophages and dendritic cells. Due to its ability to bind monomeric IgG, which is constantly present in serum, the FcγRI receptor is always saturated; however, cells are not activated until the occupied receptors are cross-linked by multi-valiant antigen ensuring against false activation - which can lead to excess inflammation and auto-immunity ¹⁷¹.

1.8.2.2 FcγRII

FcγRIIB binds monomeric IgG with very low affinity in comparison to FcγRI. This ensures FcγRIIB only binds IgG that has been previously aggregated by a multivalent antigen. FcγRIIB only binds immune complexes that contain the IgG subclasses IgG1, IgG2a and IgG2b. FcγRIIB is the only negative inhibitory FcγR, transmitting a negative signal through an immunoreceptor tyrosine-based inhibitory motif (ITIM) ¹⁷². The main area of FcγRIIB binding is confined to the second extracellular domain of the receptor, specifically residues 154-161, 109-116 and 130-135. FcγRIIB along with FcγRIII and FcγRIV have been recently shown to be the low affinity receptors for IgE, interestingly, FcγRI does not share this property and is strictly an IgG receptor, showing no binding potential for IgE ¹⁷³. In the murine system this inhibitory receptor is the only Fc receptor found on B cells, it is also found on other cell types too such as monocytes, macrophages, neutrophils and mast cells. On B cells, cross-linking of the receptor by IgG in complex with antigen sends a negative modulation signal to the B cell ¹⁷⁴. In the instance of the mouse, there are two forms of the FcγRII gene, giving a B1 and B2 transcript. The B1 transcript has an insertion of 46 amino acids in its cytoplasmic tail, which renders it unable to endocytose immune complexes, though it can still transmit a negative activation signal. B cells preferentially express the B1 isoform of the receptor - unlike all other cell types ¹⁷². FcγRIIB has also been shown to be a negative regulator of mast cells that can override the activatory signal, received when their high affinity FcεRI is triggered by IgE ¹⁵⁴. FcγRIIB^{-/-} mice spontaneously develop lupus, which can be ameliorated when bone marrow from WT mice is engrafted, showing this receptor is vital in maintaining tolerance in mice ^{175 176}. FcγRIIB has also been shown to help with the resolution of inflammation in the murine model for atherosclerosis (Apoe^{-/-} mice develop atherosclerosis when fed on a high fat diet). When mice were double knock outs for FcγRIIB and Apoe they experienced

an increase in pro-inflammatory cytokine production, such as IL-17 and IL-23, in the aortas which correlated with exacerbated disease progression ¹⁷⁷.

1.8.2.3 FcγRIII

FcγRIII is another low affinity FcR that only binds IgG when it is in immune complexes. FcγRIII binds to the same subclasses of IgG as the inhibitory receptor FcγRIIB, IgG1, IgG2a and IgG2b. FcγRIII is the only Fc receptor that is found on natural killer cells; it is also expressed on all myeloid cell population in mice ¹⁷¹. In vitro experiments have demonstrated that FcγRIII is involved in the process of endocytosis and phagocytosis. Murine FcγRIII mediates the fast internalization of antigen-antibody complexes, which leads to increased antigen presentation on the cell surface. FcγRIII has also been shown to be involved in antibody-dependent cell-mediated cytotoxicity (ADCC), which is the process where immune cells lyse target cells that are opsonised by antibody. Mice that are deficient in the common γ chain are unable to mediate ADCC ¹⁷⁸. FcγRIII on mast cells has been linked with the involvement of the propagation of the murine model of auto-antibody mediated arthritis (K/BxN serum transfer model) as when mice are deficient in FcγRIII they are protected from disease ¹⁷⁹. The cause of this protection was later demonstrated to be through mast cells' inability to become activated and produce IL-1 early in the initial phase of disease ¹⁸⁰.

1.8.2.4 FcγRIV

FcγRIV is the newest Fc receptor to be discovered and is the only one that is found in mice and not in humans. It is a medium affinity receptor, that interacts with IgG2a and IgG2b; it is expressed on neutrophils, macrophages and the Ly6C^{low} monocyte subset ¹⁸¹. IgG2b has been shown to preferentially bind to FcγRIV in murine models of idiopathic thrombocytopenia purpura (ITP) and nephrotoxicity. In circumstances where FcγRIV was knocked out, mice were protected from ITP and nephrotoxicity. IgG2b's ability to fix complement was shown to be very important in the pathogenesis of these disease models ^{171 182}. FcγRIV^{-/-} deficient mice and mice that have had cell-specific deletion of FcγRIV in their osteoclast population were protected from the K/BxN serum transfer arthritis. In the passive serum transfer model of inflammatory arthritis it was

shown that Ly6C^{hi} monocytes, when stimulated with RANKL, differentiate into mature osteoclasts and simultaneously up-regulation FcγRIV. These cells are thought to represent the precursor cell population of osteoclasts in the inflamed tissue. Cross-linking of FcγRIV enhanced osteoclast differentiation, demonstrating that immune complex binding to osteoclasts via the FcγRIV is directly involved in the maturation process under inflammatory circumstances¹⁸³.

1.8.2.5 FcRn

The neonatal FcR is the only FcR that has specificity for all IgG isotypes at a pH of 6.5 or below. Interestingly, unlike the other Fc receptors, FcRn does not play a role in the activation or inhibition of any cell type and its primary function is to conserve IgG and protect it from destruction within cells by recycling it back out into the circulation¹⁸⁴. This is the reason why IgG has a far longer half-life (roughly 28 days) than the other antibody classes. When IgG is non-specifically taken up by endothelial and epithelia cells, it is shuttled to acidic lysosomes; if IgG binds to the FcRn in the lysosome it will be returned to the surface of the cell and back into the circulation. However, if it does not bind, the IgG will be degraded. FcRn is unrelated to classical FcRs and binds to a different region in the antibody Fc fragment as structurally it is related to the MHC class I molecule¹⁸⁵.

1.8.3 Signalling molecules associated with the Fcγ receptors

The three activatory FcγR in the murine system are FcγRI, FcγRIII and FcγRIV: these receptors are not able to signal themselves as they have very short cytoplasmic tails. Therefore they must associate with the common γ chain sub-unit. The common γ chain has a long cytoplasmic tail, which contains an immunoreceptor tyrosine-based activation motif (ITAM). ITAMs are motifs that are found in the cytoplasmic tails of TCRs and BCRs as well as being associated with activatory FcγRs. ITAM motifs are defined by a twice-repeated YxxL sequence separated by 6-12 variable residues¹⁸⁶.

The activation of FcγR is not just down to being bound by its ligand, it also requires the cross-linking of multiple Fcγ receptors by the same multi-valiant

antigen or immune complex¹⁸⁷. Notably, high and low-affinity FcγR trigger cell responses with equal efficiency. The difference between the activation of the signaling cascade is based on the order in which FcγR aggregation occurs. The high affinity FcγRI receptor is constantly engaged by monomeric immunoglobulin prior to aggregation by multivalent antigens, whereas low affinity receptors only bind immunoglobulin that has complexed with antigen prior to binding¹⁸⁸. Whether the FcγR is high or low affinity the first intracellular event following aggregation of FcγR is the phosphorylation of the tyrosine residues in the ITAM motifs on the common γ chains. Phosphorylation of ITAMs is correlated with the activation of several sets of cytoplasmic protein tyrosine kinases. The first sets are the Src family kinases, followed by the recruitment and activation of the Syk family kinases. Syk then activates a signaling cascade leading to downstream activation of MAP kinases and the transcription factor NF-κB, which are important signaling effectors and inducers of gene expression that lead to the activation of the cell¹⁸⁹.

FcγRIIB is the only inhibitory Fcγ receptor, which is present on all immune cells except T cells¹⁷⁴. FcγRIIB does not associate with an accessory molecule as it can signal through its cytoplasmic tail, whose intra-cytoplasmic domain possesses a and ITIM motif that inhibits cell activation¹⁹⁰. This motif contains a single YxxL sequence that was designated as an ITIM¹⁹¹. Engagement of ITIM-containing receptor FcγRIIB results in Src family kinase-mediated phosphorylation of the ITIM's tyrosine residues and recruitment of inhibitory signaling molecules such as the tyrosine phosphatases SHP-1 and SHP-2 and the inositol phosphatase SHIP that attenuate ITAM-induced signaling by dephosphorylating the tyrosine residues on the ITAMs and thereby inactivating their ability to send a positive activatory signal to the cell¹⁹².

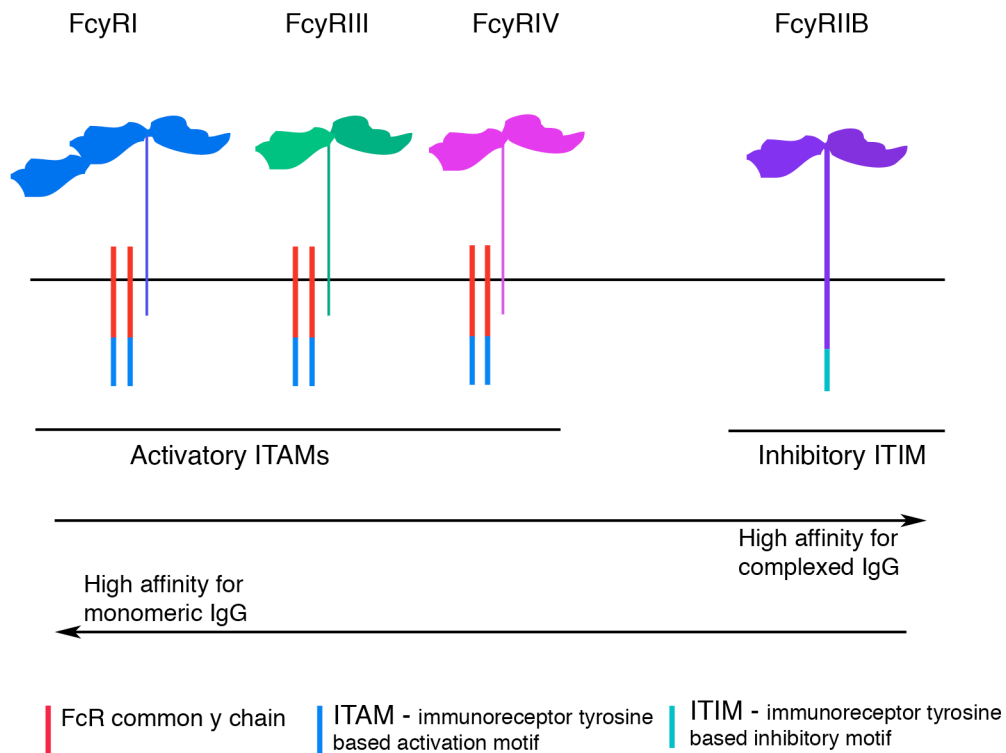


Figure 1.2, Fc γ receptors and their associated signalling molecules in the murine system. The Fc γ receptor family in mice are made up of three activatory receptors (Fc γ RI, Fc γ RIII and Fc γ RIV), which associate with the FcR common γ chain containing two ITAMS that are used by the receptor to send an activatory signal to the cell. Fc γ RIIB is the inhibitory receptor of the Fc γ receptor family; unlike the three activatory receptors it does not associate with two FcR common γ chain molecules as it contains an ITIM in its cytoplasmic tail, which delivers an inhibitory signal to the cell once it is activated. Adapted from ¹⁷⁴.

1.9 Therapies involving IgG as a modulator of inflammation

1.9.1 IVIg's anti-inflammatory properties and mechanisms

Since IgG and Fc receptors have been shown to be vital to the initiation and resolution of autoimmune/inflammatory-mediated diseases it is not surprising that they play a vital role in their treatment. One such treatment that takes advantage of this essential regulatory role is IVIg, which is the pooled product of highly purified polyclonal IgG from multiple donors. In the 1950s, IVIg was initially administered intramuscularly to patients suffering from hypogammaglobulinemia, particularly those with X-linked agammaglobulinemia, Bruton disease and common variable immunodeficiency, as an antibody replacement therapy¹⁹³. It was noted that the IgG preparation had many beneficial properties and was adapted over the next 20 years so it could be given intravenously in the early 1980s. A physician named Imbach was treating his patients, who had B cell deficiency disorders, with the new preparation of IgG and noticed that it also relieved and in some cases resolved the patients' ITP. ITP is a condition in which the sufferer has low platelet levels usually caused by the production of auto-antibodies, which attack the platelets. Along with this and other discoveries, IVIg is now primarily used to treat autoimmune and inflammatory conditions rather than as a replacement therapy¹⁴⁷.

There has been much speculation over the mechanism by which IVIg elicits its immuno-modulatory effect, but no unified mechanism has been agreed on how to explain IVIg's effect. Some of the mechanisms that have been proposed are discussed in the following paragraphs.

1.9.1.1 Glycosylation pattern of IVIg as a mode of action

Recent studies have proposed that the sialylation pattern of the N-linked glycan of IgG plays an important role in the mode of action of IVIg's anti-inflammatory properties^{163,194}. If the terminal sialic acid is removed from IVIg this abrogates its anti-inflammatory effects in animal models of serum-induced arthritis, EAE and nephrotoxic nephritis. Consistent with this, if the sialylated fraction of IVIg is enriched, its anti-inflammatory activity is greatly increased¹⁹⁵. When this was investigated further it was shown that not only is the sialic acid crucial, but a

specific type of sialic acid was critical. Sialic acid can be found in either a 2,3 or a 2,6-linkage to the final galactose on the complex glycan found at the Asparagine 297 position on the IgG molecule. When mass spectrometry was performed on IVIg preparations it was discovered there was a preferential sialylation pattern of the 2,6-linkage. The importance of this linkage was confirmed by treating IVIg with either a 2,3 or 2,6 sialidase. The 2,3 and 2,6 purified preparations were then used to treat K/BxN, which is a serum-transfer arthritis model. This action revealed that when IVIG was treated with the 2,6 sialidase, which removes all of the 2,6-linked sialic acid, the IVIg anti-inflammatory effect was abrogated, but it was unaffected with the 2,3 sialidase treatment. The authors indicate that the sialiated Fc of IVIg binds to a specific receptor, DC-SIGN, inducing the production of IL-33, which leads to the expansion of an IL-4-producing basophil population. The IL-4 induces the up-regulation of the inhibitory FcγRIIb on monocytes and macrophages, increasing the threshold level of activation on these pro-inflammatory effector cells ¹⁹⁶.

1.9.1.2 Anti-idiotypic antibodies in IVIg

Another concept that has been proposed for the mechanism by which IVIg mediates its anti-inflammatory effect is the discovery of anti-idiotypes in IVIg. Antibodies have been purified from IVIg that had the ability to bind auto-antibodies against DNA, Factor VIII and thyroglobulin ¹⁹⁷. Other studies have shown that auto-antibodies to GM1 ganglioside in patients with Guillain-Barre can be neutralized by antibodies present in IVIg ¹⁹⁸. It has been suggested that this may be the mechanism by which IVIg works. Essentially the anti-idiotypes bind to auto-antibodies and inhibit their destructive effect on the body. Critics of this proposed mechanism say that idiotypic antibodies make up too small a proportion of the IVIg for this to be the sole mechanism it mediates its effect though ¹⁹⁹. This has turned the focus of research from the Fab portion of the IgG to the Fc portion and its interaction with Fc receptors on many different cell types.

1.9.1.3 Neonatal Fc receptor saturation by IgG

Saturation of the neonatal Fc receptors has also been proposed as a potential mechanism for IVIg. Neonatal Fc receptors bind serum IgG in the lysosome and

protect them from degradation by recycling them back to the plasma circulation. This is the reason why IgG has such a long half-life (FcRn is also discussed in section 1.8.2.5). It was theorised that IVIg saturates the neonatal Fc receptor leading to an increase in the degradation of pathogenic autoantibodies. This has been shown in mouse models of arthritis where IVIg has reduced pathogenic antibody levels (below disease-causing levels) and this effect is ablated in neonatal Fc receptor knock-out mice²⁰⁰. However, recently it has been shown in a murine model of ITP that the neonatal Fc receptor was not required or necessary for IVIg to be protective in this setting²⁰¹. This result has left confusion over the part the neonatal Fc receptor plays in the anti-inflammatory role exerted by IVIg.

1.9.1.4 ITAMi induction by IVIg

ITAMi signalling through FcγRIII might be another mechanism by which IVIg works. The classical concept of ITIM and ITAM, where ITIM is the inhibitory signalling motif and ITAM is the activatory signalling motif, which has been explained in greater detail in section 1.8.3 and figure 1.2, has been challenged recently with the concept of ITAMi. In this concept, FcγRIII associates with two Fc common γ chains, which contain ITAMs in their cytoplasmic tail. Each common γ chain contains two ITAMs each. In general, when the receptor is activated, via crosslinking induced by a multivalent antigen in complex with IgG molecules, all four of the tyrosines are phosphorylated by Syk (kinase of the Src family), which subsequently initiates an activatory signalling cascade. However, when the receptor is bound in a low affinity manner with a monovalent ligand that does not aggregate the receptor, this leads to hypo-phosphorylation of the tyrosine molecules (only 2 phosphorylated) in the Fc common γ chains. This results in the transient recruitment of Syk kinase (but the stable recruitment of SHP-1), which induces an inhibitory signalling cascade²⁰².

An example of this type of signalling has been demonstrated using various FcγR knock-out mice in studies of antibody-independent obstructive nephropathy. It was shown that IgG1 or IVIg could reduce MARCO-dependent endocytosis, reduce production of ROS in macrophages and reduce transcript levels of TNFα and MCP-1 through an FcγRIII ITAMi-dependent mechanism. Furthermore, when mice deficient in SHP-1 were used, the inhibitory effect of IVIg was ablated. This

mechanism proposes a very interesting novel pathway, outlining the pleiotropic properties of FcγR and IgG as mediators of inflammation and also the crucial role they also play in the resolution of inflammation²⁰³.

1.9.1.5 Modulation of cytokine production by IVIg

IVIg has been seen to have an effect on adhesion molecules. For example, it causes the down regulation of ICAM-1 and VCAM-1 mRNA transcripts in endothelial cells *in vitro*. Endothelial cells were also shown to down-regulate their production of a number of pro-inflammatory mediators such as GM-CSF and TNFα, IL-1β and IL-6 in response to IVIg; it is of note that the authors do not speculate on the mechanism by which this effect is mediated²⁰⁴. However, if this phenotype could be demonstrated in an inflammatory *in vivo* setting the down-regulation of adhesion molecules on endothelial cells would have a massive effect on cell infiltration into inflamed tissue.

IVIg has been shown to induce immature dendritic cells (DC) refractory to LPS stimulation, with a significant decrease in the levels of co-stimulatory CD40, CD80 and CD86; however there was no effect on MHC II expression. The DCs were induced to produce IL-10 but did not produce IL-12 in comparison to LPS only-treated counterparts. IVIg did not only change the cytokine and co-stimulatory profile of these DC, it also rendered autologous cells inactive and non-proliferative. The author demonstrated that in this setting both the Fc and Fab regions of the IVIg were important for the modulation of DC phenotype²⁰⁵.

IVIg has also been shown to drive monocytes and macrophages to an anti-inflammatory phenotype. When monocytes from human blood were treated in the presence of LPS and IVIg, it induced inhibition of IL-1, TNF-α and IFNγ release; furthermore, an up-regulation of IL-1 receptor antagonist was also seen. Additionally, it has been shown that IVIg makes murine and human macrophages refractory to phagocytosis by IFNγ, by down-regulation of the IFNγ receptor 2 sub-unit²⁰⁶.

1.9.1.6 Fcγ blockade or FcγR binding on phagocytes

Finally, studies have suggested that IVIg exerts its effect via a simple blockade of the FcγRs on phagocytes, therefore slowing down their ability to phagocytose

opsonized antigen such as platelets in the case of ITP. However, it has been demonstrated that in some cases the effects of IVIg are long-lasting after the initial treatment, implying that a simple block of receptors is not the mode of action. It was demonstrated in a mouse model of ITP, where platelets are coated with an anti-platelet antibody, that platelet numbers could only be rescued when IVIg was given that had dimers of IgG - and non-dimeric IgG containing IVIg showed little effect. It was also demonstrated that FcγRIII played a role in the mechanism as no ITP was exhibited when FcγRIII^{-/-} mice were used in the model²⁰⁷. There seem to be many modes of action that IVIg can work by, but the recurring theme is that Fc receptors play a major role in the mediation.

1.9.2 The downside of un-optimized IVIg treatment

As demonstrated by the vast array of potential modes of action of IVIg, it has been revealed to be a very non-specific treatment option for the modulation of an overt inflammatory immune response. IVIg has also been shown to have side effects, which are not only due to the impurities of the preparation method. The most common side effects of IVIg specifically associated with the IgG component are headaches, fever, nausea, back pain, cardiovascular malfunctions (such as tachycardia) and changes in blood pressure. These mostly start within 30-60 minutes of infusion and are generally associated with the formation of large aggregates of IgG, which leads to the activation of the complement system²⁰⁸. Another issue with IVIg as a therapeutic, is the use of human IgG in rodent models of disease to define its therapeutic abilities. An example of this was the use of IVIg treatment in adjuvant arthritis in a rat model (an animal model of Rheumatoid Arthritis), which showed amelioration of disease but which had little clinical benefit^{209,210}. This dichotomy could be attributed to the non-optimized nature of IVIg treatment. Another potential issue with the use of IVIg as a general therapeutic is that the immune complex component of the preparation is not of a defined conformation in every preparation and though immune complexes have been shown to modulate macrophages to an anti-inflammatory phenotype (section 3.1.2.2 and figure 3.1), immune complexes also have reported roles in the destructive pathogenesis of Rheumatoid Arthritis and type II hypersensitivity.

1.9.3 Staphylococcal protein A and its immune-modulatory effects

A well-known protein that can harness IgG is SpA (Staphylococcus protein A). It is a 42KD bacterial protein, which is a key virulence factor of *Staphylococcus aureus*, a gram-positive bacterium²¹¹. SpA has the ability to bind IgG on B cells through the Fab region, but unlike conventional antigens it does not bind using the complementarity determining region of the IgG molecule's Fab portion but binds through interactions with the framework region of the variable domain²¹². This interaction is restricted to V_H3-encoded BCR, a subset of B cells that accounts for 30-50% of the B cell repertoire of humans²¹³. However, this is not the only mechanism by which SpA can interact with immunoglobulin. The "classical" binding interaction is via the Fc portion of the IgG molecule. SpA binds a wide variety of IgG subclasses from different species; in the murine system it binds IgG2a, IgG2b and IgG1, whereas in the human system SpA binds IgG1, IgG2 and IgG4²¹⁴. Due to SpA's IgG binding ability it has been used as a tool for the detection and purification of IgG in the past²¹⁵. The ability of SpA to bind IgG was further exploited when it was used as the active component of a discontinued US Food and Drug Administration (FDA)-approved apheresis therapy (ProSORBA column) for inflammatory and autoimmune diseases, which included Rheumatoid Arthritis. It was noted that the ProSORBA column has the ability to remove IgG from 60 litres of plasma which, compared to traditional plasmapheresis techniques, was a very small amount. However, the ProSORBA column was used when the traditional apheresis techniques did not work and the ProSORBA column showed long lasting effects after treatments. Interestingly, it was discovered that during each treatment, SpA could be proteolytically cleaved and enter the patient's circulation²¹⁶. The quantity of SpA entering was significantly less than the amount of circulating immunoglobulin, and it had been demonstrated that, when immunoglobulin is present in excess, SpA will form only one type of immunoglobulin complex with 2 molecules of SpA binding 4 molecules of IgG (figure 1.3)²¹⁷.

Interestingly, immune complexes have been used for sometime now to induce macrophages to an anti-inflammatory phenotype (see section 3.1.2.2 and figure 3.1); however, the majority of previous studies have depended on the use of rat or rabbit IgG to generate immune complexes^{218 219}. The interaction of rabbit IgG

with murine Fc receptors has never been specifically examined, though results suggest that rabbit IgG has an order-of-magnitude lower affinity for mouse Fc receptors compared to mouse IgG^{220 221}. As SpA can co-opt endogenous IgG, it would therefore be of interest to investigate the effect SpA-IgG complexes have on macrophages in an inflammatory setting and to determine how macrophages are induced to exhibit anti-inflammatory properties. SpA has another major advantage to its use as a potential therapeutic: as well as being able to co-opt with endogenous IgG, it also forms specific homogeneous immune complexes, unlike IVIg and many other antibodies/protein complexes²²². It is also proposed that the small size of the SpA:IgG complex will have other potential benefits over complexes which are formed in non-specific ways. Their small size would decrease the risk of immune complex mediated pathology (section 1.9.2) and may have less likelihood of activating complement, which is an issue with standard IVIg treatment.

SpA is also known for its immune-modulating properties as a B cell super-antigen as it induces massive clonal expansion^{223 224}, which subsequently leads to apoptosis of the B cell via an IgG-dependent but complement-independent mechanism (unpublished data, Goodyear). SpA treatment was used in a murine model of Rheumatoid Arthritis, Collagen-Induced Arthritis (CIA), which showed protection from the disease²²⁵ (Appendix 2). This phenotype could not be attributed totally to B cell depletion, as murine B cells only have 5-10% of B cells with the specific V_H3 portion, and may indicate that SpA treatment could have an anti-inflammatory effect which is mediated by the formation of immune complexes leading to the polarization of macrophages to an anti-inflammatory phenotype.

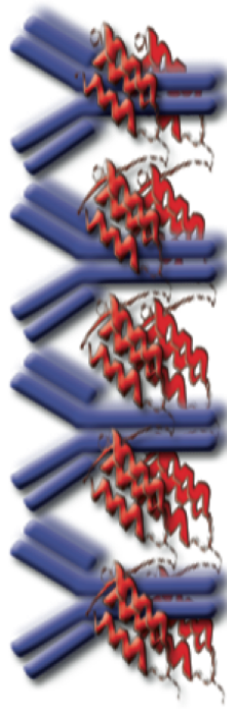


Figure 1.3, SpA bound to IgG through interaction in the constant region.

When SpA is in the presence of excess IgG, it will form homogeneous complexes. These complexes will contain 4 IgG molecules (Blue) and 2 SpA molecules (Red); they are small immune complexes.

1.10 Research Aims

Immune complexes have been used previously to induce macrophages to an anti-inflammatory phenotype; however, the immune complexes used in previous studies were not homogenous in conformation and were not species-specific to the model of disease used to show their anti-inflammatory effects. Given that SpA can form small immune complexes with IgG of relevant and assay complementary species, it is plausible that it can be used to evaluate species-specific homogenous complexes on macrophage phenotype.

- Can SpA generated immune complexes polarize macrophages and monocytes to an anti-inflammatory phenotype?

A large volume of research has already been published demonstrating that classically activated (pro-inflammatory) macrophage and their precursors, monocytes, are detrimental to recovery in SCI. Conversely, it has also been noted that macrophages can produce neurotropic and neuro-protective factors that contribute to regeneration if they are polarized to an anti-inflammatory phenotype. Therefore, it was hypothesized that if macrophages could be successfully polarized to an anti-inflammatory phenotype, via immune complexes formed with endogenous IgG and SpA, they would contribute to the recovery of SCI in a more protective and productive role.

- Is SpA a potential therapeutic for SCI through its potential ability to polarize macrophages and monocytes to an anti-inflammatory phenotype?

Evaluation of SCI is generally through behavioural testing, however, to date the vast majority of research has been on rats. The final aim of this thesis was to determine whether in a mouse model of SIC there was an appropriate behavioural test that was both sensitive enough to detect subtle changes and reliable enough that it could be repeated without large variations within the data collected

- Can a mouse model of SCI and suitable behavioural tests be used to demonstrate SpAs potential as a therapeutic for SCI?

2 Material and Methods

2.1 Mice

C57BL/6 mice (7-10 weeks) were purchased from Charles River (Massachusetts, USA). μ MT, CX₃CR1-GFP and OTII mice were bred and maintained at the University of Glasgow. FcR γ ^{-/-}, Fc γ RI^{-/-} and Fc γ RII^{-/-} (C57BL/6 background) mice were bred and maintained at the University of Southampton. The Ethical Review Process Committee and the UK Home Office approved all experimental procedures.

2.2 Generation of bone marrow-derived macrophages (BMDM)

2.2.1 Isolation of bone marrow cells

Skin and muscle were cleared from the hind legs of schedule 1, CO₂-asphyxiated mice. Bone marrow was flushed out by inserting the tip of a 21g needle into the marrow space and flushing with 3ml of RPMI 1640 (Gibco, Invitrogen, Paisley, UK) from a 5ml syringe (Becton-Dickinson, New Jersey USA). The marrow was flushed into a 90mm petri dish (Sterilin, UK) and dissociated by passing up and down the syringe multiple times. Cells were subsequently filtered through sterile Nitex mesh (Cadisch and Sons, London UK) into a 50ml conical falcon (Corning, Massachusetts, USA). The single cell suspension was centrifuged at 450g for 5 minutes, counted and resuspended at 5x10⁶ cells/ml. 1ml of the single cell suspension was seeded into a non-tissue culture-treated 90mm petri dish containing 9ml of complete medium (see appendix 1) containing 20% (v/v) supernatant from the L929 cell line (refer to 2.2.2 for further information). The petri dishes were cultured at 37^oC in 5% CO₂. On day 3 or 4 of culture, 5ml of fresh complete media containing 20% (v/v) L929 supernatant was added to the petri dishes.

2.2.2 Generation of L929 supernatant

L929 cell line is a murine fibrosarcoma cell line that secretes M-CSF (macrophage colony stimulating factor) into its supernatant. When the supernatant is used as a 20% (v/v) supplemented in bone marrow cell cultures it induces macrophage

differentiation after 6- 7 days²²⁶. To generate the supernatant, L929 cells were grown to 70% confluence in 10ml of complete media in a T75 flask (Corning, Massachusetts, USA). They were then split equally into 5 T150 flasks and 98ml of complete media was added to each. The cells were grown to confluence and then left a further 3-4 days before the supernatant was removed and centrifuged at 450g for 5 minutes. Aliquots were made and frozen at -20°C. Upon use, aliquots were doubly sterile filtered with 0.2µm minisart filters (Sartorius, Epsom Surry, UK).

2.2.3 Harvesting macrophages

Differentiated macrophages were harvested on day 6 or 7 of culturing. Culture media was removed and 9ml of ice-cold phosphate saline buffer (PBS) (refer to appendix 1) was added. Adherent cells were gently disassociated with cell scrapers (Corning, Massachusetts, USA) and transferred into 50ml conical tubes. Cells were centrifuged at 450g for 5 minutes, counted, and resuspended at the desired concentration for flow cytometry or cytokine assays (see sections 2.3) in complete medium. Routine purity checks were carried out by staining cells with antibodies to CD11b and F4/80 and determining their cellular expression via flow cytometry (see section 2.5).

2.3 Conditioning and activation of BMDM

Harvested BMDM were resuspended at a final concentration of 5×10^5 /ml in complete medium. For flow cytometric analysis, 1×10^6 cells per well were cultured in 6 well tissue culture plates (Costar Corning, Massachusetts, USA) along with 100U/ml of IFN γ (Sigma-Aldrich, Missouri, USA) overnight. For determination of cytokine secretion via ELISA, 1×10^5 cells per well were cultured in 96 well tissue culture plates (Costar Corning, Massachusetts, USA) overnight at 37°C in 5% CO $_2$.

The next day, cells were stimulated with 10µl of either media, SpA (Repligen, Massachusetts, USA) (1.56µg/ml), IgG (chrome pure, Jackson ImmunoResearch, Philadelphia, USA) (25µg/ml), SpA:IgG complexes (see section 2.3.1) (IgG at 25µg/ml and SpA at 1.56µg/ml), OVA (Sigma-Aldrich, Missouri, USA), anti-OVA antibody (2B scientific, Oxfordshire, UK), or OVA:anti-OVA antibody complex

(see section 2.3.1) that had been left to form for an hour at 37°C. In addition, the wells received either media or LPS (100ng/ml E.coli 0127:B8, Sigma-Aldrich, Missouri, USA) and were cultured for 6h at 37°C in 5% CO₂. After stimulation, media was removed and BMDM were dissociated for flow cytometric analysis or 180µl of supernatants were harvested from the 96 well plates and stored at -20°C until required.

2.3.1 Complex formation

SpA immunoglobulin complexes (SIC) were generated by incubating 25µg/ml of IgG and 1.56µg/ml of SpA (1:4 molecular weight ratio) for 1h at 37°C, allowing them to form a complex containing 2 SpA molecules for every 4 IgG molecules. OVA immune complexes (OIC) were formed by the generation of a 10-fold excess of anti-OVA antibody to OVA protein. This was left for 30min at room temperature and used at 150µg/ml.

2.4 ELISA

To determine the levels of IL-10 (BD pharmingen, New Jersey USA) and IL-12p40 (ebioscience, California, USA), ELISAs were performed as per the manufacturers instructions. In brief, 96 well half-area plates (Costar Corning, Massachusetts, USA) were coated overnight at 4°C with anti-IL-10 or anti-IL-12 capture antibody. The plate was washed 3 times with PBS/0.05% Tween (v/v) (Sigma-Aldrich, Missouri, USA), blocked with 150µl of PBS/10% FCS (v/v) for 1h at room temperature and then washed a further 3 times. 50µl of supernatant was added per well, either neat or diluted as required. The standards were serially diluted 1:2 and applied at 50µl per well. The top standard for IL-10 was used at 2µg/ml and IL-12p40 at 300pg/ml. After 2h incubation at room temperature, the plates were washed 5 times before 50µl of biotinylated detection antibody and streptavidin-HRP were added for 1h at room temperature. After a final 7 washes, 50µl of tetramethylbenzidine (TMB) substrate was added per well and left to develop. Stop solution (3M sulphuric acid) was added to the plate, which was then read using a MRX II micro plate reader (Dynex, Virginia, USA) at 450nm wavelength.

2.5 Flow cytometry

Cells were pre-incubated with or without Fc Block (BD pharmingen, New Jersey, USA) or rat serum for 20 minutes in the dark at 4⁰C to block any non-specific antibody binding. Cells were stained with specific antibodies or isotype controls for 20 minutes in the dark at 4⁰C (see appendix 1 for a list of antibodies and isotypes used). Cells were washed with 400µl of FACS buffer (please refer to appendix 1) and resuspended in 300µl of FACS buffer. Cells were filtered through nitex mesh to remove cellular aggregates. DAPI (Sigma-Aldrich, Missouri, USA) was added at a 1:10000 dilution to cells immediately prior to acquisition to allow for dead cell exclusion. Data were acquired on a FACSCalibur, LSRII, FACSAia cell sorter (Becton-Dickinson, New Jersey, USA) or MACSQuant (Miltenyi, Bergisch Gladbach, Germany) and analysed using FlowJo software (Treestar Inc, Oregon, USA).

2.6 T cell activation assay

2.6.1 Pulsing of BMDM

BMDM were harvested from petri dishes on day 6, resuspended at 1x10⁶ cells in 2ml of complete media and aliquoted into wells of a 6 well tissue culture plate. Cells were treated with various conditions (as described in section 2.3) for 6h. Three hours into the incubation, BMDM were pulsed with 10µg/ml OVA 323-339 peptide (Sigma-Aldrich, Missouri, USA). After the total 6h incubation, BMDM were dissociated and transferred to 15ml conical tubes (Corning, Massachusetts, USA) before being centrifuged at 450g for 5 minutes. To remove any residual peptide, pelleted cells were resuspended in fresh complete media and centrifuged as described. This washing step was repeated once. Cells were finally resuspended in complete media and transferred back to fresh 6 well plates.

2.6.2 Isolation of CD4+ T cells

OTII mice, which have a transgenic TcR for the OVA 323-339 peptide, were killed by schedule 1 CO₂ asphyxiation and spleen and lymph nodes were removed. The tissues were dissociated and pooled to make a single cell suspension. In brief, tissue was passed through a 70µm nitex cell strainer (BD falcon, New Jersey,

USA) into 2ml of media. The single cell suspension was transferred to a 15ml conical tube and centrifuged at 450g for 5 minutes. Cell pellets were resuspended in 1ml of Ammonium-Chloride-Potassium (Ack) lysis buffer (Gibco, Invitrogen, Paisley, UK) for 1 minute to lyse red blood cells. Cells were then washed with 10ml of complete media to remove residual lysis buffer, counted and resuspended at a final concentration of 1×10^7 /ml in complete media.

An Easy-Sep (Stemcell technologies, Grenoble, France) mouse CD4⁺ T cell enrichment kit was used to isolate CD4⁺ T cells from the single cell suspension according to the manufacturer instructions. In brief, cells were resuspended as stated above at 1×10^7 /ml in separation media (refer to appendix 1) and transferred into a 5ml polystyrene (BD Falcon, New Jersey, USA) tube. 50 μ l/ml of CD4⁺ T cell enrichment cocktail was added to the cell suspension and incubated at 4^oC for 15 minutes. Biotin selection (100 μ l/ml) was subsequently added and incubated at 4^oC for a further 15 minutes. After this incubation the magnetic nanoparticles were added (50 μ l/ml) and incubated for a further 15 minutes at 4^oC. The cell suspension was increased to a final volume of 2.5ml with separation media without rat serum. The 5ml tube containing the cells was placed into a kit-specific magnet (Stemcell technologies, Grenoble, France) minus the cap for 5 minutes. To obtain the enriched T cells the magnet and tube were inverted in one swift motion so that the enriched T cells were poured into a fresh 5ml polystyrene tube. The magnetically labelled, unwanted cells remained in the tube contained within the magnet. Unlabelled T cells were then counted and resuspended at 1×10^6 /ml in complete media.

2.6.3 Culturing BMDM and T cells

T cells were added at a 1:1 ratio with macrophages for 18h. After incubation, macrophages and T cells were removed from the 6 well tissue culture plates and transferred to 5ml polypropylene FACS tubes where they were stained as previously described in section 2.5. Macrophages were distinguished with the use of CD11b and F4/80 antibodies and T cells with an anti-CD4 antibody. Activation of T cells was assessed with CD25 and CD69 surface expression, whereas surface expression of MHC II was indicative of macrophage activation.

2.7 SpA labelling and binding assays

2.7.1 Labelling SpA and OVA with Alexa-488

To visualise the binding of SpA to cells both *in vitro* and *in vivo*, SpA was labelled using an Alexa-488 kit (Invitrogen, Paisley, UK) and OVA was used as a control protein. Labelling was carried out in accordance with manufacturer's instructions. In brief, this involved taking 2mg of recombinant SpA or OVA and adding 50 μ l of sodium bicarbonate (1M, pH 9) to the provided Alexa-488 vial, which was left to stir for 1h to allow chemical conjugation to Alexa488-N-hydroxyl succimide. A column was used to exclude non-conjugated dye and non-labelled protein from labelled protein using Bio-Rad BioGel P-30 fine exclusion purification resin. The resin is contained in PBS with 2mM sodium azide. Labelled protein runs quicker through the resin and is collected at the bottom of the column in a vial leaving the unlabelled protein and excess dye in the column matrix. The labelled protein was analysed on a nano drop (Thermo scientific, Massachusetts, USA) to examine protein concentration at wavelength of 280nm and the fluoresce intensity of the conjugation at 494nm. The labelling efficiency was determined using the following calculation-

$$\text{Moles dye per mole protein} = A_{494} / 71,00 \times \text{protein concentration (M)}$$

(Where 71,000cm⁻¹M⁻¹ is the molar extinction coefficient of the Alexa-488 dye at 494nm)

2.7.2 *In vitro* binding of SpA-488

BMDM were dissociated from petri dishes as described in section 2.2.3 on day 7 and 1X10⁶ cells were transferred to 5ml polypropylene FACS tube. Complexes were formed as stated previously in section 2.3.1 with the substitution of non-labelled SpA or OVA for Alexa-488 labelled protein. BMDM were incubated with complexes for 30mins at 4⁰C. Cells were washed in 400 μ l of FACS buffer before 5% (v/v) of rat serum was added to block non-specific binding. Cells were stained with anti-CD11b and anti-F4/80 fluorochrome-labelled antibodies for 30mins at 4⁰C. Further to this cells were washed for the penultimate time in 400 μ l of FACS buffer and resuspended in 300 μ l of FACS buffer after the wash step. Tubes were analysed by flow cytometry.

2.7.3 *In vivo* binding of SpA-488 in C57BL/6

C57BL/6 mice that had or had not received SCI (described in section 2.10) were injected intraperitoneally with labelled protein (500µg) and 2h later blood, bone marrow (BM), spinal cord and spleen were harvested.

2.7.3.1 Isolation of blood, spleen, BM and spinal cord.

Mice that had or had not received SCI were euthanised using asphyxiation with CO₂. Cardiac puncture was then immediately performed with a 1ml syringe and 21g needle that had been flushed with 5mM EDTA, to prevent the blood clotting.

Spleens were removed and transferred to a 35mm petri dish containing 1ml of complete medium. Cells were dissociated from the tissue by disrupting the spleen with the blunt end of a 5ml syringe plunger through nitex.

Bone marrow was extracted as previously described in section 2.2.1. In brief, fur was cleared from hind legs and bones were cut off at the hip joint before being placed in 1ml of complete media in a 35mm petri dish. Cells were dissociated from the bones using hydrostatic pressure.

For the spinal cord, a scalpel was used to make an incision between the ears of the mouse to half way down the back. The muscle layer was bluntly dissected so the vertebral column was visible. The spinal column between segments cervical 4 (C4) and thoracic 2 (T2), which contained the damaged portion of the spinal cord, between C5-C6 and a corresponding undamaged portion of spinal cord from uninjured mice, were cut free and hydrostatic pressure was applied to release the spinal cord from the column.

2.7.3.2 Preparing freshly isolated cells for FACS analysis

As described previously (Section 2.7.3.1), cells were isolated from spleen and bone marrow and red blood cell lysis were performed (1ml of ACK lysis buffer per sample for 1 minute at room temperature). Red cell lysis was also carried out on blood samples using a 1:10 dilution of blood to ammonium chloride solution (Stemcell technologies, Grenoble, France). Blood samples were left on ice for 20 minutes and vortexed every few minutes throughout the incubation.

Freshly lysed cells were subsequently washed twice with 10ml of complete media before being resuspended in FACS buffer at 20×10^6 /ml. 50 μ l of cells were transferred to each 5ml polypropylene FACS tube.

The spinal cord was passed through a 25g needle and then a 21g needle to macerate the tissue into smaller sections. The solution was then centrifuged at 450g for 5 minutes and excess liquid was removed carefully. The tissue was resuspended in a 1ml solution of DNase (1mg/ml) and Collagenase D (1mg/ml) (Roche, Bavaria, Germany). Tissue was left to digest for 30mins at 37⁰C. After the incubation, cells were washed twice in complete media and all cells were transferred into 5ml polypropylene FACS tubes.

All cells were then FACS stained as described in section 2.5.

2.7.4 In vivo binding of SpA in μ MT mice

As μ MT mice lack functional B cells and have no endogenous IgG, mice were preconditioned with intravenous injections of either PBS or 6mg of mouse IgG (Europa, Cambridge, UK) in PBS. This was followed by an intraperitoneal injection of 300-500 μ g of labelled protein (Section 2.7.1). 2h later, the blood and spleens were harvested after the mice had been asphyxiated with CO₂ and cells were prepared as stated in the above sections.

2.8 SpA treatment *in vivo*

600 μ g of SpA or OVA was administered intraperitoneally to mice 24h after they received SCI. SpA or OVA was also administered to uninjured mice in the same manner. 24h later, mice were asphyxiated with CO₂ and blood, bone marrow and spinal cord was harvested as detailed in section 2.8.3.1/2. Cells were stained and flow cytometric analysis was performed as described in section 2.5.

2.9 Adoptive transfer of Ly6C^{hi} monocytes

2.9.1 Isolation of GFP⁺ Ly6C^{hi} monocytes from BM

Twenty CX₃CR1-GFP⁺ mice were euthanised by CO₂ asphyxiation. Bone marrow was recovered from the hind legs of the mice as described in section 2.8.3.1 and

2.8.3.2. In brief, the fur and muscle was cleared from the hind legs, which were then removed from the torso by cutting the femur at the hip joint. Paws were also removed by cutting the tibia at the ankle joint. Bone marrow was flushed out by hydrostatic pressure. Cells isolated from the bone marrow were then subjected to passage through 70µm cell strainers into 50ml conical tubes and red cells were lysed with ACK buffer. Cells were then washed and resuspended at $10 \times 10^6 / 50 \mu\text{l}$ for FACS staining, whereby the cells were incubated for 20min at 4°C with Fc block, CD11b, CD117, Ly6C and Ly6G. Cells were washed in 25ml of FACS buffer and centrifuged at 400g for 5 minutes before being resuspended at a concentration of $10 \times 10^6 / \text{ml}$ and transferred to 5ml polypropylene tubes. Cells were passed through 70µm nitex cell strainers immediately before being loaded onto a Flow cytometric cell sorter (FACSAria). CD11b^+ , CD117^- , Ly6C^- , Ly6C^{hi} cells were sorted into 15ml conical tubes, which had previously been filled a third full with complete medium. Once cell sorting was finished, the proportion of dead cells in the sorted population was tested using DAPI.

2.9.2 Adoptive transfer of Ly6C^{hi} cells in C57BL/6 mice

Cells were washed with PBS at 400g for 5 minutes and resuspended at a concentration of $1.5 \times 10^6 / 200 \mu\text{l}$. Ly6C^{hi} cells were then injected intravenously into the tail vein of male C57BL/6 mice. Along with the cells, mice were given intraperitoneal injections of 600µg SpA or OVA. After 22h, mice were scheduled to be killed by asphyxiation and blood, spleen and bone marrow were removed, as described in section 2.8.3.1. Cells were prepared for FACS as described in section 2.8.3.2 with one modification; instead of 2×10^6 cells per FACS tube for spleen and bone marrow, 10×10^6 cells were used per tube. Total cell counts of live leukocytes were acquired using the MACSQuant as a cell counter and cells were analysed on the LSR II.

2.10 SCI model

Mice were treated with Buprenorphine (Baxter Healthcare, Berkshire, UK) (vetergesic 0.05mg/kg) for pain relief via subcutaneous injection. Mice were anaesthetised with Isoflurane (Baxter Healthcare, Berkshire, UK) before hair was removed, via shaving, from the area above the C2 to T2 vertebrae. The animals were placed in a restraining device and anaesthesia was supplied through a mask

that was secured over the animals' mouth and nose throughout the surgery. The skin was disinfected with ethanol and an incision was made at the shaved area. The layers of muscle overlying the vertebral column were bluntly dissected. A dorsal laminectomy was performed above the C5 and C6 vertebrae. Contusion injuries were induced using the Infinite Horizons (IH) Impactor (Precision Systems & Instrumentation, Ohio, USA). The impactor tip, the diameter of which was 1.25mm, was centered over the exposed C5 C6 border of the spinal cord and a measured force (50, 80, 100 or 120 Kilodynes (Kdyn)) was delivered. The wound was closed in layers, muscle was sutured together with 3-0 vicryl (Ethicon, New Jersey, USA) and skin was closed using skin clips. Mice were moved to heated recovery boxes and their bladders were palpated 3 times a day for the first 24h or 48h depending on the survival term.

2.11 Basso Mouse Scale (BMS).

BMS is an adaptation of the Basso, Beattie, Bresnahan locomotor rating scale (BBB), which quantifies recovery of hind limb function after SCI in rats. One week prior to surgery, mice were acclimatised to the equipment used for the BMS, which is a large circular pen 1m in diameter. Baseline data were recorded at the end of this week. Mice were individually placed into the pen for 4 minutes and the mouse's hind limbs were observed by two people and scored according to categories outlined in table 5.1. Mice were in recovery for one week post-surgery prior to being retested. Testing continued for a total of 6 weeks post-injury.

2.12 DigiGait – measurement of gait change after SCI

In order to quantify changes in the mouse gait after SCI, commercial equipment (DigiGait) was used. DigiGait (Mouse Specifics Inc, Massachusetts, USA) apparatus consists of a digital camera placed under a clear plastic belted treadmill. Mice were acclimatised for 1 week prior to acquiring baseline data. Baseline data, prior to SCI surgery, were acquired for three 4 second runs at two speeds; 15 and 20 meters/second. Mice received injuries of 50Kdyn, 80Kdyn, 100Kdyn and 120Kdyn severity. Data for week 1 post injury were gathered in the same way as baseline data and collection continued for a further 6 weeks post operation. Data were analyzed using the DigiGait system software, which plots the

footprints of the mice and gives a readout of over 20 different parameters of the mouse's gait (refer to table 5.2).

2.13 Grip strength

In order to assess the changes in forelimb function in mice after SCI, the grip strength test was employed. This consists of a force meter (Andilog, Vitrolles, France) with a protruding bar for the mice to grasp onto while they are being pulled back. Mice were allowed to adjust to the force meter for a week prior to surgery. At the end of this week baseline data were taken, which consists of allowing the mouse to grab the bar and then pulling the mouse back by its tail until it releases the bar and a value will be registered on the force meter. This was done three times per session with each mouse. Mice received either 80Kdyn, 100Kdyn or no injury. One week post-surgery data were collected as described for the acquisition of baseline data. Data were collected once per week from the animals for 6 weeks post-surgery.

2.14 Tract tracing of the cortico spinal tract

The scalp was incised and a small window drilled into the skull over the left sensorimotor cortex. Using the bregma as an anatomical reference point, injections of Biotinylated Dextran Amine (BDA) (Invitrogen, 20% solution in 0.3% (w/v) triton-x-100 in 0.1M Phosphate Buffer, pH 7.4) were made at four sites. Approximately 300 - 400 μ l of BDA was delivered at each location using pressure injection through a fine glass pipette (tip diameter 30 - 40 μ m). Injections were made at depths of between 0.5 mm and 1 mm from the surface along each injection track. The pipettes were left at the top of each injection track for 1 - 2 minutes before removal from the cortex. The scalp incision was sutured closed with 3-0 vicryl and the mice were allowed to recover for 14 days.

2.14.1 *Perfusion of mice*

Mice were transcardially perfused with freshly depolymerised 4% (w/v) paraformaldehyde solution in 0.1M phosphate buffer, pH 7.4, using the following method. Each animal was first deeply anaesthetised with intraperitoneal sodium pentobarbital solution (0.15ml of 200mg/ml Euthatal, Vericore Ltd, New York, USA). Animals were then fixed onto a corkboard with pins through each paw

while in a supine position. The thoracic cavity was opened with scissors, a 25G needle inserted into the left ventricle and the right atrium opened. Approximately 10ml of mammalian Ringer's solution was gravity-fed through the 25G needle followed by 25ml of 4% (w/v) paraformaldehyde fixative solution.

2.14.2 Tissue processing

Immediately after perfusion, a block of cervical spinal cord containing the injury site was removed and post-fixed overnight in sucrose-fix (see appendix 1 buffers and solutions) before being stored at 4⁰C in sucrose-buffer (see appendix 1 buffers and solutions). The blocks were subsequently cut into 70µm sagittal sections on a freezing microtome, incubated for 30min in 50% ethanol and washed for 10min in 0.3 M PBS. Sections were then incubated for 72h in Streptavidin-488 and primary antibodies to NF200 and GFAP (see appendix 1). Sections were subsequently incubated for 3-4h in fluorophore-conjugated species-specific donkey IgG secondary antibodies (see appendix 1), then washed for 10 min in 0.3ml PBS. All antibodies were diluted in PBS with 0.3 % (w/v) triton X-100. Sections were mounted in Vectashield (Vector Labs, California, USA) and stored at -20⁰C. Slides were then imaged at a later date.

2.14.3 Microscopy

Sections were initially examined at low power under the epi-fluorescence microscope (Nikon Eclipse E600). Selected sections were further looked at by serially scanning the tissue at 2 µm intervals using a Bio-Rad Radiance 2100 confocal system (Spectra-Physics, California, USA). Z-series' of these confocal image stacks were put together using ImageJ software (Rasband) and projections of multiple fields of view were pulled together into single images using Adobe Photoshop CS3 (Adobe Systems, California, USA). Images selected for use were processed with minor changes in brightness and contrast for presentation.

2.15 Statistical analysis

Prism (GraphPad software, California, USA) was used for all statistical analyses. T-test was performed when comparing two sets of normally distributed data. One-way ANOVA was employed when comparisons of more than two groups of data were required. Two-way ANOVA with repeated measure was performed

when tracking multiple groups of animals through various time points. Post hoc Bonferroni test was used to test for significance in with groups after the use of one or two-way ANOVA's. The specific statistical test for each experiment will be identified in the figure legend.

3 The ability of SIC to polarize macrophages to an anti-inflammatory phenotype via CD64

3.1 Introduction

It was Ilya Ilyich Metchnikov who first defined macrophages over a century ago, pioneering work which was to win him a Noble prize in 'Physiology and Medicine' in 1908 ²²⁷.

Macrophages, in the murine system, can be detected at embryonic day 9. These cells have their origins within the foetal yolk sac and are precursors for the long-lived tissue-resident macrophages of the skin, brain and kidneys. Interestingly, it is not until embryonic day 16 that macrophages originating from haematopoietic stem cells (HSC) of the foetal liver can be detected. These macrophages are constantly replaced throughout life by blood monocytes that have previously differentiated from the HSC in the bone marrow ³⁸.

3.1.1 Classical macrophage activation

Macrophages are an integral cog in the finely tuned machine that is the immune system. They are at the forefront of innate immune defence and are gatekeepers to the adaptive immune system. Deficiencies in human macrophage functioning lead to conditions such as chronic granulomatous disease (CGD) and leukocyte adhesion deficiency (LAD), which are caused by a deficiency in mac-1 ^{228,229}. Macrophage deficiencies can also lead to high susceptibility to *Neisseria meningitides* and *Salmonella* infections. This gives us a small insight into the essential role macrophages play in host defence. Macrophages are equipped with a variety of receptors to sense invaders; these include Toll-like receptors (TLR), Nod-like receptors (NLR), many scavenger receptors such as CD206 (mannose receptor), MARCO and Dectin-1 ²³⁰.

Classically activated macrophages (also referred to as M1 macrophages) are some of the first cell types, after neutrophils, to become activated at the site of pathogen invasion. Classical macrophages adapt well to this role as they are highly phagocytic and produce large volumes of pro-inflammatory cytokines. Thus these cells are highly specialised at containing and fighting the pathogen at

the primary site of infection. Other immune cells are also attracted into the battle site by the inflammatory milieu macrophages create. An example of how macrophages become activated in a classical inflammatory manner, via one of their most highly studied and utilised receptors in both *in vivo* and *in vitro* laboratory settings, is the interaction of TLR4 with lipopolysaccharide (LPS)²³¹, a gram-negative bacterial product. This interaction activates macrophages to a pro-inflammatory “classical” activation state via a MyD88-dependent signalling pathway in conjunction with IFN γ ²³². The induction of the MyD88 signalling pathway induces a cascade of pro-inflammatory transcripts such as IL-1 β , IL-6, IL-12 and TNF α ²³³. When macrophages become activated in this setting they not only produce pro-inflammatory cytokines but they also become highly phagocytic to eliminate the invading pathogen and produce reactive oxygen species and nitric oxide²³⁴.

Both innate and adaptive immune cells can produce the essential IFN γ signal that is required for macrophage polarization to a classical phenotype. Natural killer cells are an important, innate, early source of this cytokine, as natural killer cells respond to stress and infections by producing IFN γ ²³⁵. However, the IFN γ produced initially by the natural killer cells is usually only transient. Consequently, an adaptive immune response is usually necessary to maintain classically-activated macrophages and confer stable host defense. Th1 cells can produce IFN γ , which has been demonstrated to require IL-12 production from classically-activated macrophages leading to a positive feedback loop as IFN γ then stimulates additional macrophage activation²³⁶.

3.1.1.1 Macrophages as antigen presenting cells (APCs)

An essential function of the classically activated macrophages, shared only with DC and B cells, is their ability to present antigen to CD4⁺ T cells. When macrophages become activated in a classical manner in the presence of IFN γ , they increase their phagocytic activity and up-regulate their MHC II expression. This is done in conjunction with an increased expression of co-stimulatory molecules; CD40, CD80 and CD86²³⁷. The MHC II complex presents antigen from the extracellular microenvironment to the antigen’s cognate T cell. The upsurge in phagocytic activity by classically activated macrophages allows an intensification of the take up of an invading pathogen into its endosomes. Once

the pathogen has been secured in an endosome, the endosome moves further into the cell, becoming increasingly acidic as it approaches the cell's interior. The endosomes then fuse with lysosomes, which contain proteinases that become activated at low pH and in turn degrade the antigen in the lysosome. Pre-formed MHC II molecules are exported from the endoplasmic reticulum in a vesicle where an invariant chain occupies their binding sites. The vesicles bind and fuse with the low pH lysosome containing the degraded pathogen. The invariant chain is degraded by proteases in the lysosome and peptide can then bind to the MHC II molecule. The complex is then trafficked to the cell surface

238 239

The up-regulation of MHC II loaded with pathogen-derived peptides on macrophages can lead to the initiation of the adaptive immune response in secondary lymphoid tissue, though this is very rare and usually the job of a DC. Therefore, it is more likely that macrophages contribute to the continual priming of an already initiated humoral immune response in the tissue by re-stimulating T cells with their cognate antigen. This induces the clonal expansion of Ag-specific T cells that recognise the invading pathogen - which leads to stimulation of B cells (by these T cells) inducing antibody production and class-switching.

3.1.2 The broad category of regulatory macrophage

In steady-state, tissue macrophages have intrinsic anti-inflammatory functions; for example, colonic macrophages spend their life languishing in IL-10 and extinguish any inflammatory response to the gut flora and their products. Therefore, disruption to the normal sources or quantities of IL-10 or IL-10 signaling in immune cells leads to massive inflammation in the gut²⁴⁰. Another example of how macrophages in homeostasis exhibit anti-inflammatory functions is in the marginal sinus of the spleen, where macrophages interact with apoptotic cells and consequently contribute to decreased self-reactivity within the T and B cell repertoire. In support of this, depletion of marginal zone macrophages leads to the formation of DNA-specific antibodies and a systemic lupus erythematosus-like auto-immune syndrome in mice²⁴¹.

It should also be appreciated that, even in an activated state, macrophages can have anti-inflammatory functions. Macrophage activation has been described as a spectrum of functionally diverse phenotypes. The functional extremes of the spectrum are the “regulatory” anti-inflammatory macrophages (also referred to as M2 macrophages in some literature) and the “classical” pro-inflammatory activated macrophages ⁷⁶, described in section 3.1.1. The regulatory macrophage phenotype is characterized by increased production of the immune-suppressive cytokine IL-10 and decreased production of the pro-inflammatory cytokine IL-12. The regulatory macrophage category can be sub-divided into two further broad categories, wound-healing/alternative (also referred to as M2a) or anti-inflammatory (also referred to as M2b) macrophages ⁷⁸. The pliability of macrophage activation allows them to contribute to both inflammation and the resolution of inflammation over the course of the same immune response (figure 3.1) ⁷⁴, and the phenotype that the macrophage adopts is dependent in the manner of its activation ⁷⁵.

3.1.2.1 Wound-healing/alternative macrophages

In contrast to pro-inflammatory macrophage responses, macrophages, as mentioned above, can also exhibit potent anti-inflammatory activity and hold important roles in wound-healing and fibrosis. Macrophages that exhibit this wound-healing phenotype antagonize the established pro-inflammatory macrophage responses, and this is crucial for the activation of the wound-healing cascade (and also for tissue homeostasis to be restored). Recent studies have shown that pro-inflammatory macrophages can ‘transform’ into regulatory macrophages that have wound-healing phenotype ⁶².

Macrophages are polarized to the wound-healing phenotype after IL-4 and IL-13 stimulation. When tissue damage is incurred, one of the most significant soluble mediators produced is IL-4, which can be secreted by mast cells, neutrophils and basophils after injury ²⁴². When macrophages are exposed to IL-4 after tissue injury they are induced to produce extracellular matrix proteins such as fibronectin ²⁴³. Wound-healing macrophages also up-regulate the production of arginase, which allows the conversion of arginine to ornithine, a precursor of polyamines and collagen. The production of these extracellular matrix proteins allows the macrophage to play a major role in the repair of damaged tissue ²⁴⁴.

Wound-healing macrophages also produce growth factors that stimulate epithelial cells and fibroblasts, including TGF β and platelet-derived growth factor. TGF β produced by the wound-healing macrophages contributes to tissue regeneration and wound repair by promoting fibroblast differentiation into myofibroblasts. This is done by enhancing expression of tissue inhibitors of metalloproteinase that block the degradation of extracellular matrix, and by directly stimulating the synthesis of interstitial fibrillar collagens in myofibroblasts^{245 246}. Wound-healing macrophages can also be induced as a consequence of helminths and parasite infections, as Th2 cells produce copious amounts of IL-4 and IL-13⁷⁵. IL-33 is another cytokine that is produced in a Th2-driven immune response and leads to an expansion of IL-13 induced wound-healing alveolar macrophages. The expansion of these alveolar macrophages is not always beneficial to the host as they can contribute to airway inflammation and have detrimental effects if expansion is not tightly regulated²⁴⁷. IL-33 is not the only other Th2 cytokine linked with the alternative-activated macrophage; IL-21 can also play a role in polarizing and expanding Kupper cells, which are macrophages of the liver, to the alternatively activated/wound-healing phenotype and has also been linked to the cause of liver fibrosis after clearance of pathogens in this organ²⁴⁸. Markers that are specifically used to identify the wound-healing macrophages subset are CD206 (mannose receptor), transcription factor FIZZ1 and the chitinase family protein Ym1^{249 250}.

3.1.2.2 Anti-inflammatory macrophage

As mentioned earlier, the other category of regulatory macrophage that is often referred to in literature is the anti-inflammatory macrophage. Anti-inflammatory macrophages can arise during the later stages of adaptive immune responses and the primary role of these cells seems to be to dampen the immune response and limit additional cellular and tissue damage due to aberrant inflammation. There are many different ways in which regulatory macrophages are generated, but a single molecular mechanism that mediates this phenotypic switch has yet to be identified.

Phagocytosis of apoptotic bodies in the presence of pro-inflammatory stimuli can induce macrophages to an anti-inflammatory phenotype by the induction of TGF β and prostaglandin E2. These can both function in an autocrine and a

paracrine mechanism to inhibit the production of pro-inflammatory cytokines such as IL-1B²⁵¹. Macrophages can be polarized to an anti-inflammatory phenotype, high IL-10 and low IL-12 production, via an immune complex-mediated FcγR-dependent mechanism when given in conjunction with inflammatory stimuli such as LPS^{252 222}. Anti-inflammatory macrophages that have been induced via immune complexes have been shown to reduce inflammation and disease progression in an *in vivo* murine model of multiple sclerosis and in experimental autoimmune encephalomyelitis (EAE). In this setting, the administration of macrophages that have been stimulated with immune complexes in the presence of IFNγ and LPS can protect mice from disease²⁵³. Another physiological mechanism for generating anti-inflammatory macrophages is with the treatment of glucocorticoids. These are produced by the hypothalamic-pituitary-adrenal (HPA) axis, as a response to stress-induced inflammation and can inhibit the transcription of pro-inflammatory cytokine genes such as IL-12, IFNγ and TNFα in macrophages after exposure²⁵⁴. A few other stimuli that have been noted to induce anti-inflammatory macrophages are adenosine, dopamine, histamine and vasoactive intestinal peptide^{255 256 257}.

Each mechanism for generating an anti-inflammatory macrophage has a slightly different phenotype, but all possess a common mechanism of polarization, such that they must be activated in a two-signal process with one signal being non-inflammatory and the other being an inflammatory signal. When these signals are combined they induce the macrophage to produce high levels of IL-10 and/or TGFβ. This can set up a positive feedback loop as anti-inflammatory macrophages can be induced by exposure to IL-10 when in the presence of an inflammatory stimuli. And in so doing, IL-10 exposure has the ability to stop the induction of pro-inflammatory cytokines such as IL-1α, IL-6, IL-8 and TNFα, as well as down-regulating MHC II expression on the macrophages' surface - compared to macrophages that received LPS and IFNγ without IL-10²⁵⁸. IL-10 and TGFβ have also been shown to be an essential mechanism for the generation of inducible Tregs that are generated in the tissue (and not the thymus)²⁵⁹, which help to resolve inflammation.

In conjunction with the up-regulation of anti-inflammatory cytokines, anti-inflammatory macrophages have been recognised to reduce production of IL-12.

This phenotype is the most reliable way of characterising a macrophage as an anti-inflammatory phenotype ²³⁴. Some anti-inflammatory macrophages still possess the ability to produce some other pro-inflammatory cytokines such as IL-6. Interestingly, IL-6 has a dual role in the CNS where it can also play a protective role in neuronal survival during injury and inflammation ²⁶⁰. Anti-inflammatory macrophages may also express co-stimulatory molecules including CD80 and CD86 on their surface and can present antigen/interact with T cells ²¹⁹.

3.1.3 SpA and its potential to interact with macrophages

SpA is a key virulence factor of *Staphylococcus aureus* (discussed further in section 1.9.3) that has the ability to bind to the Fc portion of immunoglobulin. Using a separate non-overlapping area of the SpA, it can also bind to V_H3-encoded BCR. When SpA binds to B cells via their BCR it induce massive clonal expansion ^{223 224}, which consequently leads to apoptosis of the B cell via an IgG dependent mechanism (unpublished data, Goodyear). In collagen-induced arthritis (CIA), a murine model of rheumatoid arthritis, SpA treatment inhibits disease ²²⁵. The protective effect of SpA could not be attributed to B cell depletion as the murine B cell repertoire is only composed of 2-5% V_H3-encoded B cells. It has been shown previously that SpA can complex with IgG to form immune complexes and that they can interact with macrophages via an Fc dependent binding ²⁶¹. Macrophages can be polarized to an anti-inflammatory phenotype (high IL-10, low IL-12) via an immune complexes and FcγR dependent mechanism when given in conjunction with inflammatory stimuli such as LPS *in vitro* ^{252 222}. These macrophages are particularly important in controlling inflammatory-mediated disease as demonstrated in an *in vivo* model of EAE ²⁵³. It has therefore been hypothesised that SpA generated immune complexes may be interacting with macrophages through their various Fc receptors, polarizing the macrophages to a regulatory phenotype that leads to the amelioration of inflammation in the CIA model - and not the previous assumption that this was dependent on deletion of auto-reactive B cell clones.

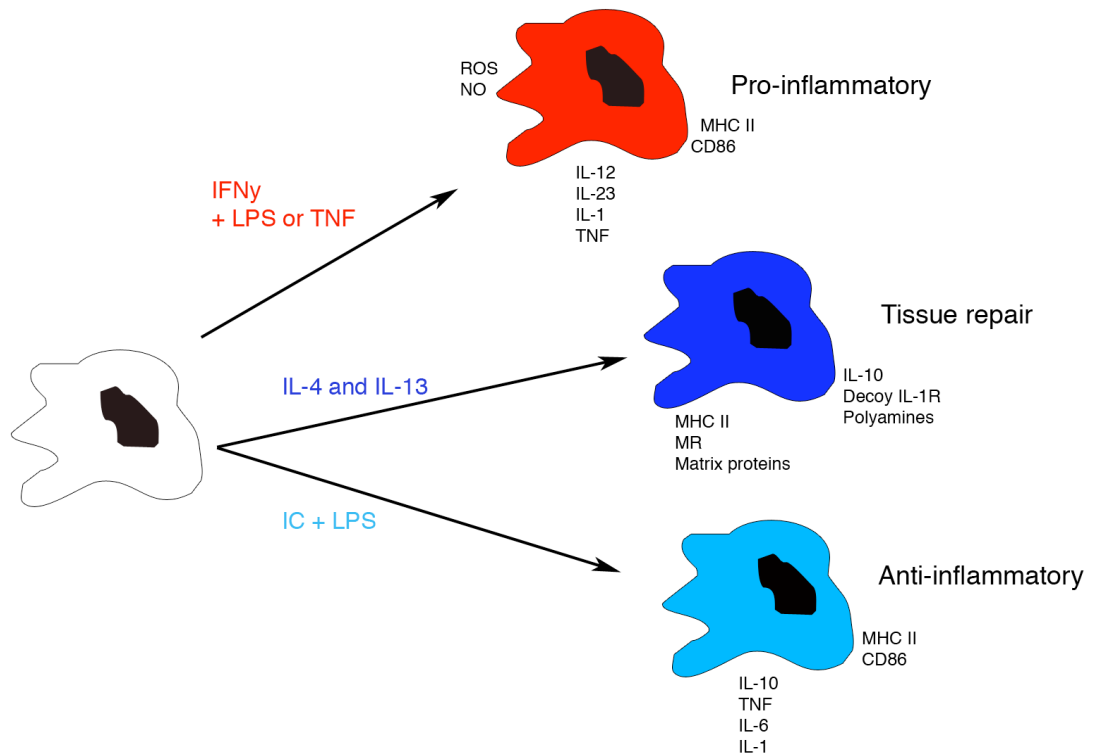


Figure 3.1. Different fates of macrophage activation

Macrophages are heterogeneous in their phenotype. This is dependent on how they have become activated. If monocytes are recruited to a site of inflammation where they encounter IFN γ and TNF or IFN γ and LPS, the monocyte will differentiate and become activated to a classically activated pro-inflammatory macrophage. Whereas, regulatory macrophages, which can be broadly subdivided into tissue repair and anti-inflammatory macrophages, are generated when macrophages are activated in the presence of IL-4 + IL-13 and immune complex (IC) + LPS respectively. However, it must be noted that these are not the only ways to generate macrophages of the phenotypes described above.

3.1.4 Aims of this experiment

The aim of the research undertaken in this chapter was to examine the ability of SIC to modulate macrophage phenotype to an immune-regulatory state. This was achieved by:

- Assessing the ability of SpA to bind to bone marrow-derived macrophages in the presence and absence of IgG and examining what receptor this is mediated through.
- Examining the potential of SpA in-conjunction with IgG to polarize BMDM to a regulatory phenotype.

3.2 Results

3.2.1 *SpA can bind to BMDM but only when in complex with IgG*

To examine the binding potential of SpA to macrophages when in complex with IgG (SIC), BMDM were generated as stated in the 'materials and methods' section 2.2. On day 7, BMDM were harvested and stained for purity using two phenotypic antigens, F4/80 and CD11b (figure 3.2A). The macrophages generated via this method of culture were a highly pure homogeneous population. The complexes of interest were formed with Alexa-488-labelled SpA and polyclonal IgG (in excess), (known as SIC from here on in). Alexa-488-labelled OVA was incubated with excess polyclonal IgG to demonstrate that SpA exhibited a specialised ability to form complexes with IgG and that it was not a non-specific protein interaction. OVA was specifically chosen as the control protein as it has the same molecular weight as SpA. Alexa-488-labelled OVA was also incubated with excess anti-OVA IgG to form immune complexes (known as OIC from here in) that had been previously used in the literature to polarize macrophages to a regulatory phenotype.

Macrophages were incubated with SIC-488, SpA-488, OVA-488, OVA-488+IgG or OIC-488 for 40min at 4° before being assessed by flow cytometry. SpA, OVA and OVA+IgG were unable to bind to BMDM; however, SIC and OIC showed substantial binding (figure 3.2B). Furthermore, it is interesting to note that SIC has a higher affinity for binding to BMDM than the OIC, which are used in established protocols to generate regulatory macrophages. Since it has now been shown that SIC can bind to macrophages, the next logical step was to examine if there was any functional/phenotypic changes to the macrophages after SIC binding.

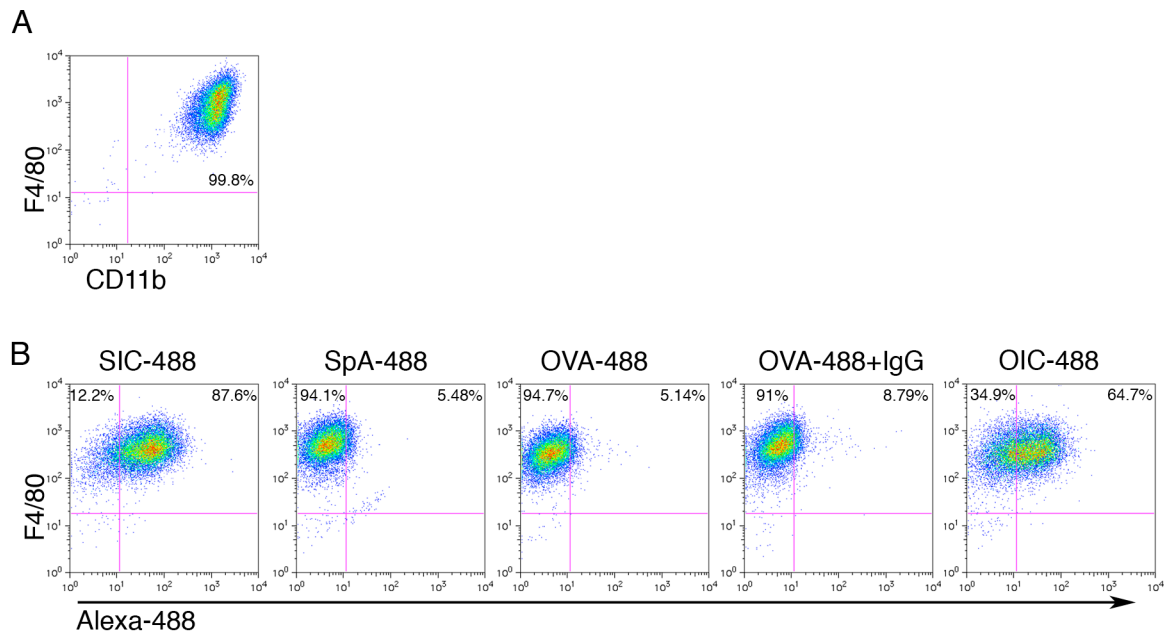


Figure 3.2. SpA has the ability to bind to BMDM only when it is in complex with IgG.

(A) Cells were stained with macrophage phenotypic markers F4/80 and CD11b to check purity. (B) Representative FACS plots of different binding profiles of SpA and OVA when alone or in the presence of IgG. This experiment was carried out in duplicate and is representative of two separate experiments.

3.2.2 BMDM polarization by SIC

It was established in section 3.2.1 that SpA can form complexes with IgG and can only bind to macrophages when in complex. Studies have already demonstrated that when macrophages interact with immune complexes in the presence of inflammatory stimuli they are polarized to a regulatory phenotype, which is characterised by high IL-10 production and reduced IL-12 production²⁵².

To assess the potential of SIC to induce the polarization of macrophages to a regulatory phenotype, BMDM were generated as described in section 2.2. On day 6 macrophages were seeded into 96 well tissue culture plates at a concentration of 1×10^5 /200 μ l per well. Cells were left overnight to equilibrate. On day 7, pre-formed complexes were added to the macrophages in the presence or absence of LPS (100ng/ml) and incubated for 6h before removal of supernatants. The supernatants were screened via IL-10 and IL-12p40 ELISAs. In the absence of LPS, SIC had the ability to induce IL-10 production in macrophages (Figure 3.3A) but did not alter the production of IL-12 (Figure 3.3B). The addition of LPS substantially increased the production of IL-10 in all culture conditions but was highest in the SIC-treated cultures (figure 3.3A). In parallel, there was a significant reduction in IL-12 production in cultures treat with SIC and LPS compared to control cultures (figure 3.3B). Thus, when SIC is given in conjunction with an inflammatory stimulus such as LPS, macrophages are induced to produce high levels of IL-10 and reduced production of IL-12p40, which is the classical cytokine signature of a regulatory macrophage.

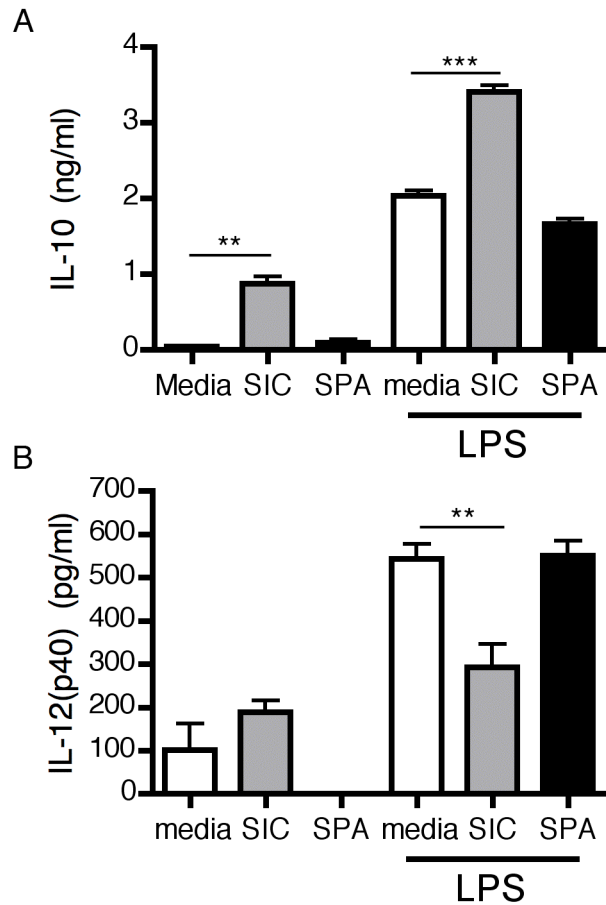


Figure 3.3. SIC has the ability to polarize macrophages to an anti-inflammatory cytokine profile.

BMDM were seeded on day 6 at $1 \times 10^5/200 \mu\text{l}$ per well. On day 7, macrophages were stimulated with or without LPS in the presence or absence of SIC or SpA for 6h before supernatants were removed. This experiment was carried out in quadruplicate and graphs are representative of two separate experiments that showed the same pattern of results. Statistical analysis was conducted using one-way ANOVA for either with or without LPS stimulation. Significant differences between groups were identified using a post-hoc Bonferroni test, which compared all controls to SIC, ** = $P < 0.01$; *** = $P < 0.001$ (A) The mean \pm SD ng/ml for IL-10 production after macrophages have been stimulated for 6h (IL-10 LPS group, $F_{2,11} = 189.2$, $P < 0.0001$. IL-10 non-stimulated group, $F_{2,11} = 70.96$, $P < 0.0001$). (B) The mean \pm SD pg/ml for IL-12p40 production after macrophage stimulation for 6h (IL-12p40 LPS group, $F_{2,11} = 16.89$, $P < 0.0009$).

3.2.3 SIC does not alter the ability of macrophages to secrete IL-6 and Nitric oxide (NO)

To assess further the phenotype of macrophages that SIC treatment induces, supernatants from the previously described experiment (section 3.2.2) were probed for IL-6 and NO as they are both known to be produced by macrophages when they become classically activated. NO is a free radical that is produced by inducible nitric oxide synthase (iNOS) when macrophages are activated. It is toxic to bacteria and one mode of action for the killing of pathogens is the induction of DNA damage. To evaluate NO production in BMDM cultures stimulated with LPS and/or SIC, a Griess assay was performed. The data showed that LPS induced the production of NO in macrophages and SIC did not reduce this (figure 3.4A). The same result was seen with an IL-6 ELISA (figure 3.4B). LPS conditioning induced macrophages to produce IL-6, and addition of SIC does not have the ability to inhibit the production of IL-6 when given in the presence of LPS. Although IL-6 is thought of as a pro-inflammatory mediator, regulatory macrophages that have been generated with immune complexes and an inflammatory stimulus still retain their ability to produce IL-6 when they lose their ability to produce IL-12 and acquire the ability to produce IL-10^{78,138}.

3.2.4 SIC induced MHC II down-regulation

The phenotype of the macrophages that have been polarized by SIC have so far fallen neatly into the stereotypical definition of a regulatory macrophage that has the ability to produce high levels of IL-10 and IL-6, but low levels of IL-12. However, SIC-treated macrophages also have the ability to produce NO, which is not normally seen in regulatory macrophages; this indicates that SIC may not be inducing the stereotypical regulatory macrophage and further phenotypic classification is therefore still needed. Another classical marker of a regulatory macrophage is that they express MHC II and CD86 on their surface and retain the ability to interact with T cells.

BMDM were harvested on day 6 and seeded at a concentration of 5×10^5 /ml in 24 well plates before being stimulated with 100U/ml of IFN γ overnight. The next day, SIC was added with or without LPS for 6h before media was discarded and macrophages were dissociated from the plates and flow cytometric analysis

performed to examine MHC II and CD86 expression (figure 3.5). To compare SIC to previously validated immune complexes that generate a regulatory phenotype²⁵³, macrophages were also treated with OIC (immune complexes generated with OVA and anti-OVA antibodies). As previously stated, OIC immune complexes and LPS have been used in the past to generate regulatory macrophages, which produce high IL-10 and reduced IL-12 production²¹⁹.

Under non-inflammatory conditions BMDM express minimal levels of MHC II, but when they are treated with LPS and IFN γ they increase their expression of MHC II significantly. When the macrophages were treated with SIC in conjunction with LPS and IFN γ they show a significant reduction in the level of MHC II expressed compared to the classically-activated macrophages (figure 3.5A). Macrophages activated with OIC do not show reduced MHC II expression compared to the classically activated counterparts, which is similar to previous observations²⁵³. Unlike MHC II levels, CD86 was unchanged by the treatment of SIC compared to the classically-activated and OIC activated-macrophages (figure 3.5B). The observation that SIC macrophage polarization, in terms of MHC II expression, differs from OIC, highlights the heterogeneity of macrophage activation and confirms the concept of macrophage activation being a spectrum, and not simply three steadfast phenotypes.

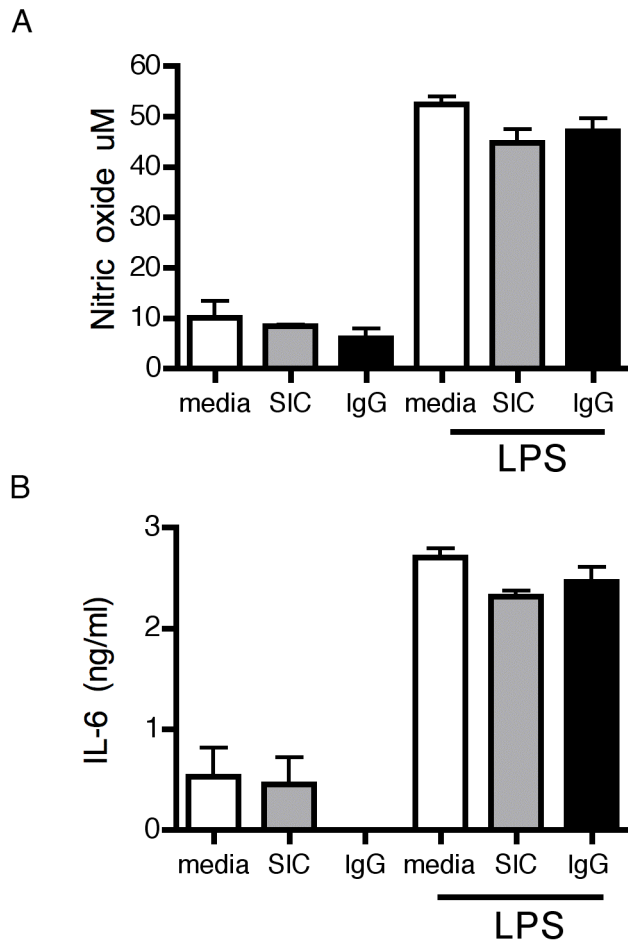


Figure 3.4. SIC does not have the ability to change BMDM production of Nitric oxide or IL-6 when stimulated with LPS.

BMDM were seeded on day 6 at $1 \times 10^5/200\mu\text{l}$ per well. On day 7, macrophages were stimulated with or without LPS in the presence or absence of SIC or IgG for 6h before supernatants were removed. (A) The mean \pm SD for Nitric oxide (μM) production after macrophages have been stimulated for 6h. (B) The mean \pm SD for IL-6 (ng/ml) production after macrophage stimulation for 6h. This experiment was carried out in quadruplicate once.

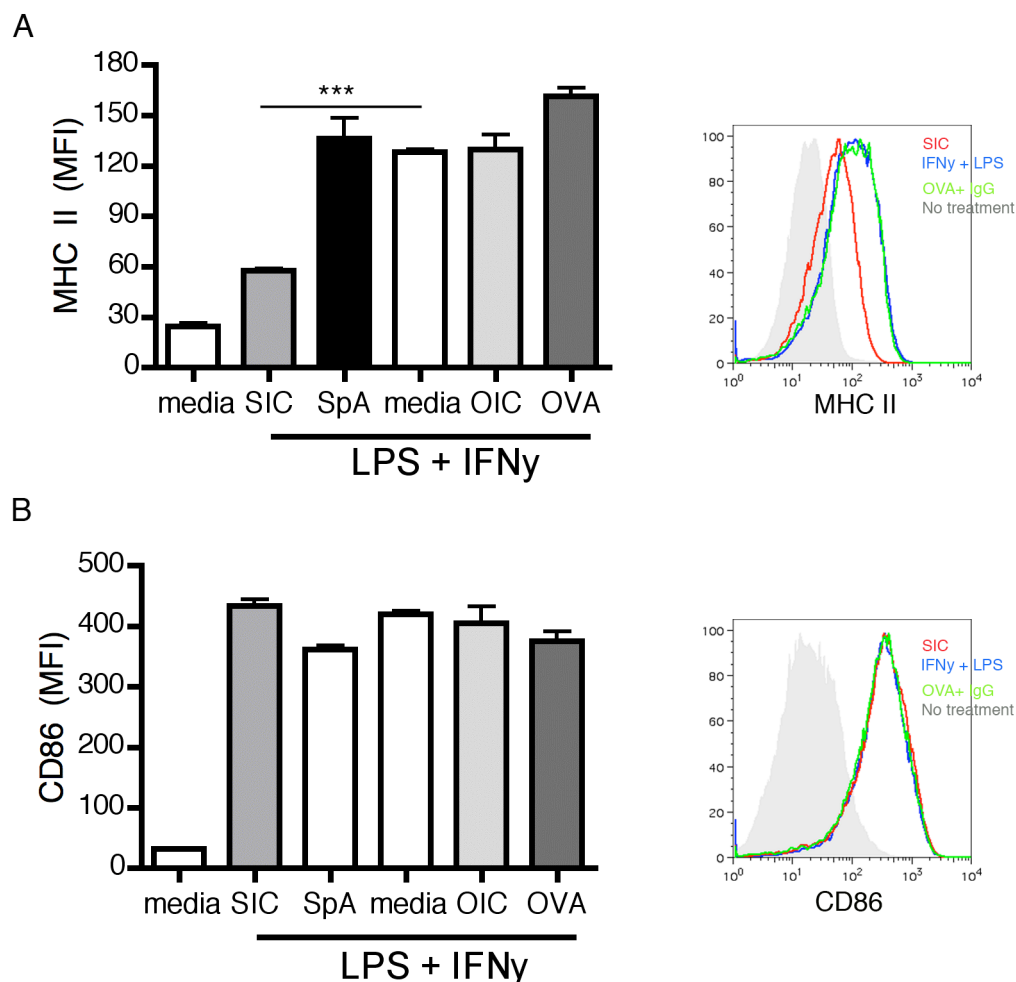


Figure 3.5. SIC treatment leads to the down-regulation of MHC II levels but has no effect on CD86 up-regulation.

BMDM were seeded on day 6 at 5×10^5 /ml per well and treated with 100U/ml of IFN γ overnight. On day 7, macrophages were stimulated with or without LPS in the presence or absence of SIC, SpA, OVA or OIC for 6h before supernatants were removed and cells stained for flow cytometric analysis. This experiment was carried out on three separate occasions and results have been pooled together for statistical analysis purposes. Statistical analysis was conducted using one-way ANOVA for LPS + IFN γ stimulation. Significant differences between groups were identified using a post-hoc Bonferroni test, which compared all controls to SIC, *** = $P < 0.001$. (A) The mean \pm SD MFI values for MHC II ($F_{4,14} = 29.29$, $P < 0.0001$), along with a histogram of MHC II levels to the right (media alone grey, SIC+LPS+IFN γ - red, LPS+IFN γ - blue, OIC+LPS+IFN γ - green). (B) The mean \pm SD MFI values for CD86, histogram of CD86 to the right (media alone grey, SIC+LPS+IFN γ - red, LPS+IFN γ - blue, OIC+LPS+IFN γ - green).

3.2.5 T cell activation is not affected by SIC-conditioned macrophages

MHC II expression is a vital part of T cell activation, and therefore it was hypothesised that the ability of SIC to reduce the level of MHC II may be linked to their ability to activate T cells. To examine this, a co-culture system was set up with T cells from OTII mice that have T cell receptors (TCRs) transgenically engineered to be specific for an OVA peptide sequence 323-339. Macrophages were incubated for 16h with or without IFN γ and then for a further 6h with or without LPS, plus SIC or appropriate controls and TCR-specific OVA peptide. Macrophages were washed and were incubated with the CD4 OTII T cells for a further 20h. Cells were harvested, stained and analysed by flow cytometry to examine T cell activation state via CD69 expression (figure 3.6).

Macrophages that were treated with SIC, IFN γ , LPS and co-cultured with T cells had far lower levels of MHC II on their surface compared to macrophages treated exactly the same way but with the omission of SIC (figure 3.6A). T cells that were cultured with the stimulated SIC-treated macrophages that had low MHC II on their surface showed the same level of CD69 expression as T cells cultured with the classically-activated macrophages, which had high MHC II levels on their surface (figure 3.6B). Thus the regulatory phenotype induced by SIC does not have an effect on subsequent T cell activation. However, under normal physiological conditions, macrophages do not migrate to draining lymph nodes with antigen and no evidence exists for macrophage participation in the activation of naïve CD4 T cells²⁶². In that respect, macrophages are thought to be involved in the expansion of primary or secondary responses already initiated by dendritic cells in the tissue.

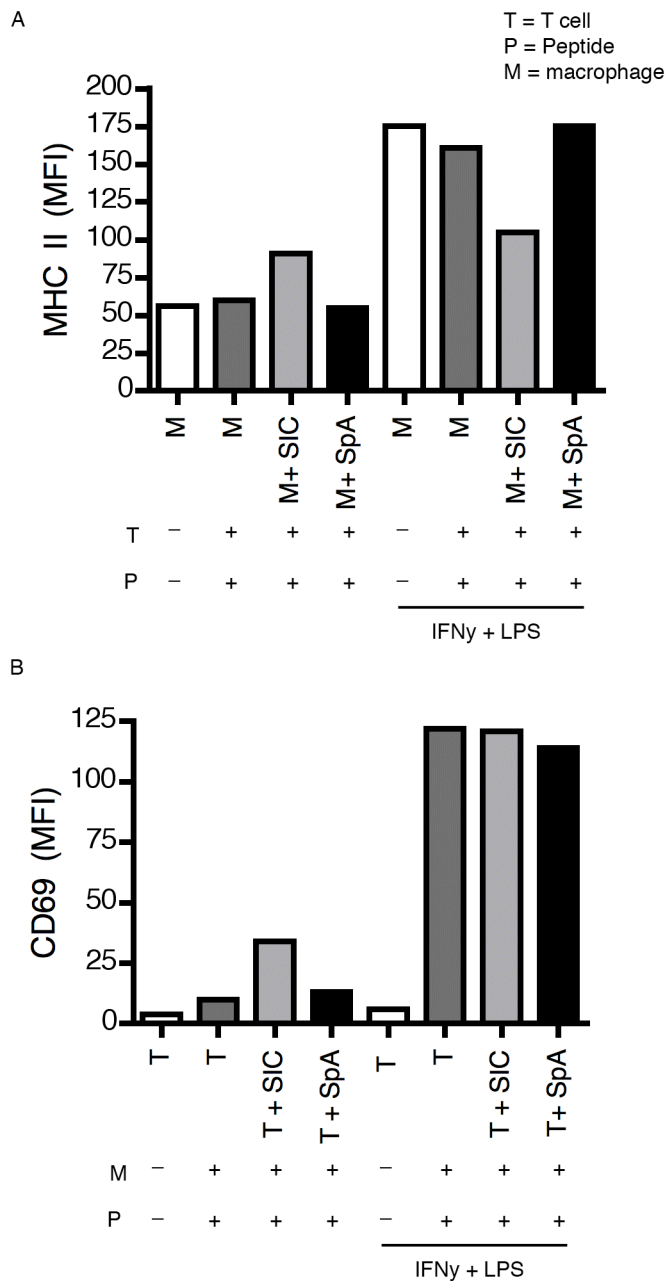


Figure 3.6. SIC did not affect the ability of macrophages to activate T cells.

BMDM were stimulated overnight with or without IFN γ . 16h later, BMDC were pulsed with OVA in the presence or absence of SIC, SpA and or LPS for 6h. BMDM were then cultured with OTII CD4⁺ T cells at 1:1 ratio for 20h. (A) The mean \pm SD MFI values for MHC II expression on CD11b⁺ macrophages. (B) The mean \pm SD MFI values for CD69 on T cells co-cultured with macrophages. This experiment was carried out once.

3.2.6 SIC binding in WT, CD64^{-/-}, CD32^{-/-} and common γ chain^{-/-}

Having established that SIC can polarise macrophages to a regulatory phenotype, it was important to investigate the mechanism by which SIC could induce this regulatory phenotype. Thus we sought to identify the specific receptor(s) that enable SIC to interact with macrophages. In previous work with SpA, which looked into its ability to induce proliferation and then apoptosis in B cells with V_H3 specific BCR, studies demonstrated that this process was dependent on the presence of Fc γ RIII in conjunction with IgG (unpublished data). Taking these studies into account and those which have previously shown that immune-complexes work via Fc γ R²⁵², the logical next step was to examine the role of Fc γ R receptors in the SIC-mediated production of regulatory macrophages. To investigate whether Fc γ receptors are required for SIC binding and function, bone marrow was acquired from Fc γ RI^{-/-} (CD64), Fc γ RIIb^{-/-} (CD32) and the common γ chain^{-/-} mice and BMDM were generated.

As in previous experiments, Alexa-488 labelled SpA was incubated with IgG to form SIC, then incubated with the macrophages for 40min at 4°C. Macrophages were stained with F4/80 and analysed by flow cytometry (Figure 3.7). The common γ chain deficient macrophages were unable to interact with SIC. The analysis of BMDM from CD64^{-/-} mice demonstrated that they were also unable to interact with SIC (figure 7B); proving that the presence of Fc γ RI, which is knocked out on both the common γ chain^{-/-} BMDM and the CD64^{-/-}, is essential for SIC binding. In juxtaposition, CD32^{-/-} (Fc γ RIIb) macrophages did show significant increased binding to SIC compared to CD64^{-/-} and common γ chain^{-/-} BMDM; nevertheless, this was at a decreased level compared to the WT control BMDM (figure 3.7B).

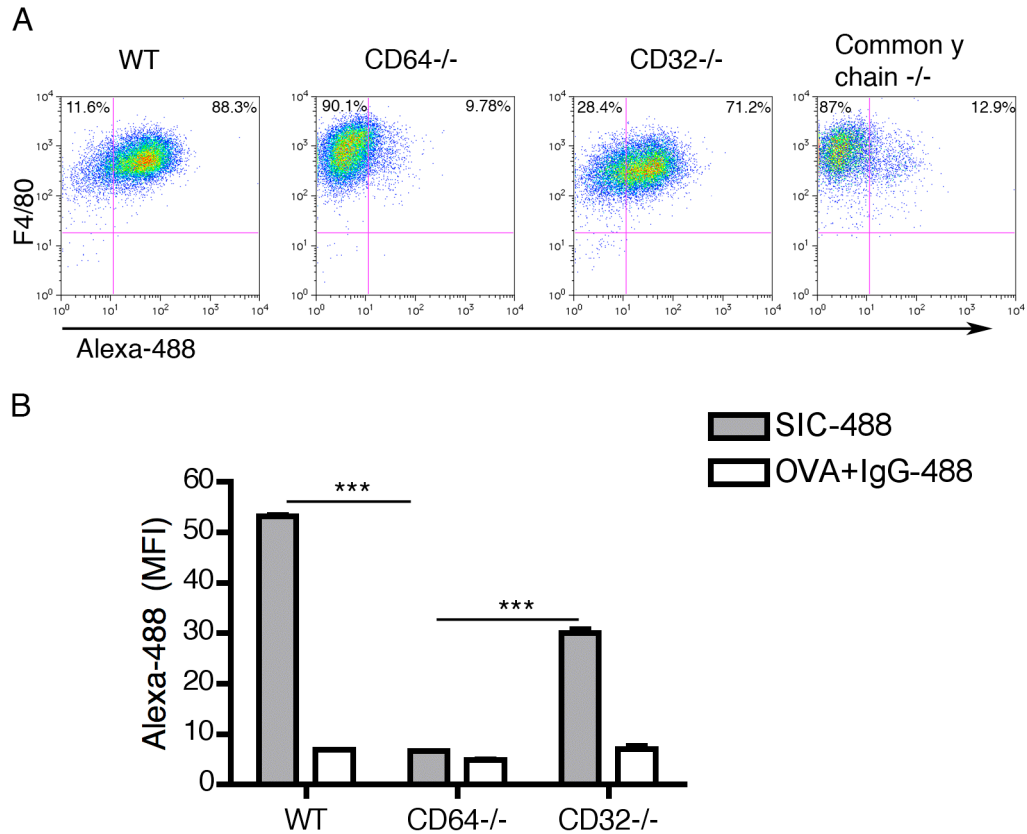


Figure 3.7. SIC has the ability to bind to BMDM only when CD64 and the common γ chain is present.

BMDM were generated with the use of M-CSF from the cell line L929. Cells were harvested on day 7 and incubated with preformed SIC, SpA, OVA+IgG or OVA. SpA and OVA were fluorescently labelled with alexa-488. This experiment was carried out on three separate occasions and data pooled together for statistical analysis purposes. Statistical analysis was conducted using a one-way ANOVA to compare the differences in SIC-488 binding. Significant differences between groups were identified using a post-hoc Bonferroni test, which compared all groups to each other, *** = $P < 0.001$ (A) Representative image of the binding potential of SIC-488 to WT, CD64^{-/-}, CD32^{-/-} and common γ chain^{-/-} BMDM. (B) The mean \pm SD MFI values for SIC-488 ($F_{2,8} = 1564$, $P < 0.0001$) and OVA+IgG-488 binding to WT, CD64^{-/-}, CD32^{-/-} and common γ chain^{-/-} BMDM.

3.2.7 SIC has the ability to polarize macrophages to a regulatory phenotype in WT and CD32^{-/-} BMDM but not CD64^{-/-} or common γ chain^{-/-} BMDM

To validate that CD64 was not only essential for binding of SIC, but was also essential for the polarization of macrophages to a high IL-10 and low IL-12 producing regulatory state (figure 3.3), macrophages were generated from WT, CD64^{-/-}, CD32^{-/-} and the common γ chain^{-/-} bone marrow and seeded at $1 \times 10^5/200$ per well and cultured overnight. The following day, the macrophages were treated with SIC, SpA or media in the presence or absence of LPS. Supernatants were removed from the culture 6h later and ELISAs for IL-10 and IL-12p40 were performed (figure 3.8).

WT macrophages behaved as characterised before (figure 3.3) with significantly higher IL-10 production and significantly reduced production of IL-12p40 in SIC and LPS-treated macrophages compared to LPS alone or LPS in the presence of SpA (figure 3.8A). Interestingly, CD64^{-/-} and common γ chain^{-/-} macrophages when treated with SIC and LPS showed no change in their production of IL-10 and IL-12p40 when compared to the LPS alone control, demonstrating that SIC cannot induce the polarization of macrophages to a regulatory phenotype in the absence of CD64 (figure 3.8B&C). Examination of the cytokine profile of CD32^{-/-} macrophages showed that when SIC is given in conjunction with LPS it induces the same regulatory phenotype seen in the WT cells, i.e. a significant increase in IL-10 and a significant decrease in IL-12p40 (figure 3.8D). It should be appreciated, however, that CD32^{-/-} macrophages produce reduced levels of cytokine compared to the WT macrophages (figure 3.8A). Furthermore, SIC binding to the CD32^{-/-} macrophages was slightly reduced, leading to the assumption that this receptor may still play a small role in how SIC manipulates macrophage activation states.

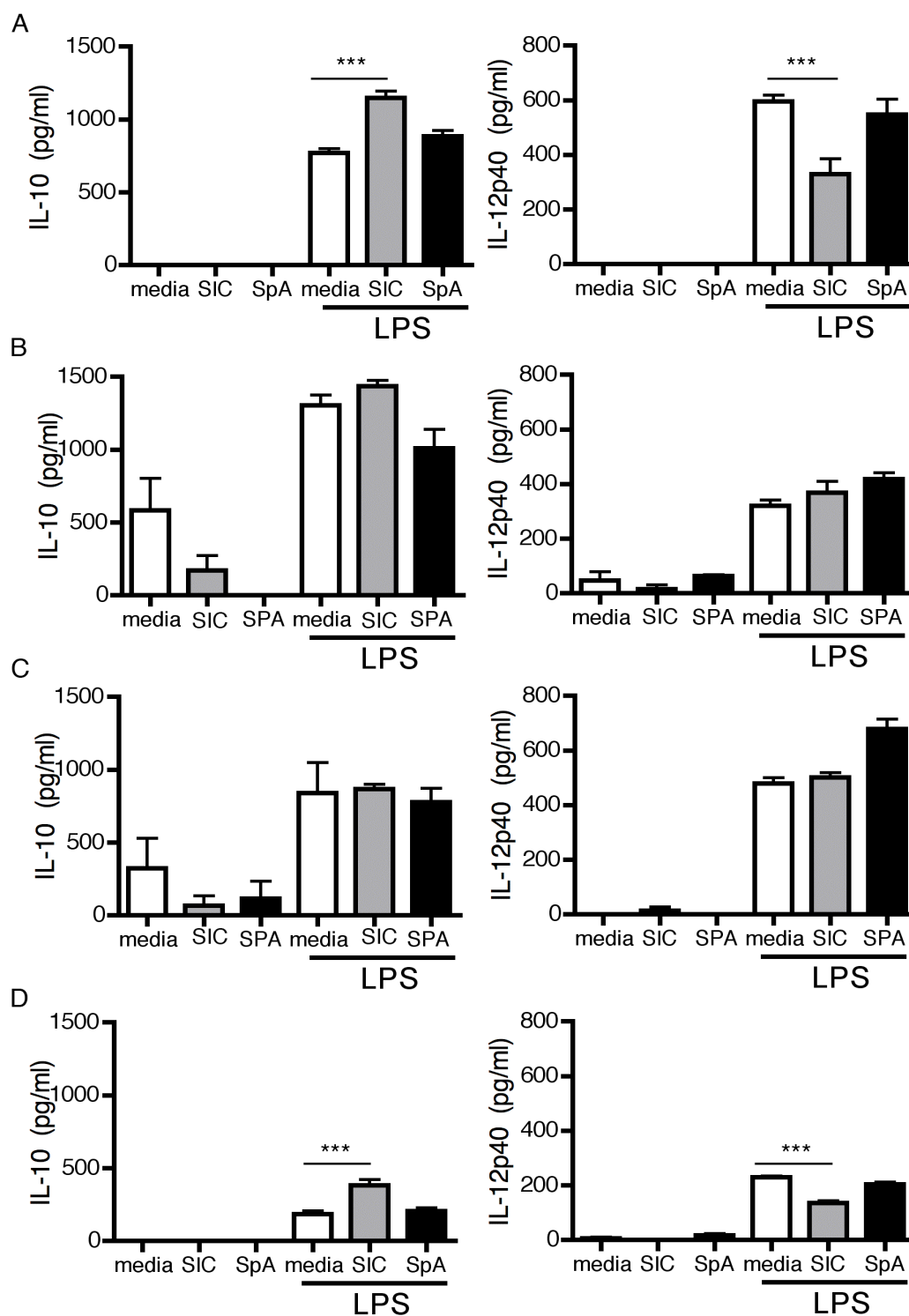


Figure 3.8. SIC has the ability to polarize macrophages to an anti-inflammatory cytokine profile in WT and CD32^{-/-} macrophages but not CD64^{-/-} and common γ chain^{-/-} macrophages. BMDM were seeded on day 6 at $1 \times 10^5/200\mu\text{l}$ per well. On day 7, macrophages were stimulated with or without LPS in the presence or absence of SIC or SpA for 6h before supernatants were removed. This experiment was carried out in quadruplicate and graphs are representative of two separate experiments that showed the same pattern of results. Statistical analysis was conducted using one-way ANOVA for LPS stimulation. Significant differences between groups were identified using a post-hoc Bonferroni test, which compared all controls to SIC, *** = $P < 0.001$. The mean \pm SD for IL-10 (pg/ml) and IL-12p40 (pg/ml) production after macrophages have been stimulated for 6h. (A) Wild type macrophages (IL-12p40 LPS group, $F_{2,11} = 16.92$, $P < 0.0009$) (IL-10 LPS group, $F_{2,11} = 28.28$, $P < 0.0009$). (B) CD64^{-/-} macrophages. (C) Common γ chain^{-/-} macrophages. (D) CD32^{-/-} macrophages (IL-12p40 LPS group, $F_{2,11} = 58.18$, $P < 0.0001$) (IL-10 LPS group, $F_{2,11} = 16.54$, $P < 0.001$).

3.2.8 The ability of SIC to induce the down-regulation of MHC II is not affected when IL-10R is blocked in WT and CD32^{-/-} macrophages

It was shown that CD64^{-/-} macrophages cannot bind SIC or become polarized to a regulatory phenotype in the presence of SIC and LPS (Figures 3.7 & 3.8). To prove further that SIC imparts this regulatory phenotype through CD64, the ability of SIC to down-regulate MHC II expression was examined in CD64^{-/-} and CD32^{-/-} cells. The experiment was carried out as described previously (section 3.2.5). In brief, on day 6 BMDMs were harvested and stimulated with IFN γ (100U/ml) overnight. SIC, SpA and media were added in the presence and absence of LPS for 6h before cells were examined by flow cytometry. A slight modification to this experiment involved the addition of an IL-10R blocking antibody in conjunction with SIC to examine if the autocrine production of IL-10 was the mechanism that led to the down-regulation of MHC II (figure 3.9). It was important to examine this as it had previously been demonstrated that if macrophages are polarized to a regulatory phenotype via IL-10 they have reduced MHC II on their surface²⁵⁸.

In WT BMDM, SIC induces the down-regulation of MHC II in the presence or absence of the IL-10R blocking antibody (figure 3.9A). This finding demonstrates that IL-10 is not the factor that elicits the down-regulation of MHC II expressed on macrophages that have been polarized with SIC and LPS. Moreover, the absence of CD32 on macrophages did not affect the ability of SIC to induce the suppression of MHC II after IFN γ and LPS stimulation, and this was also IL-10 independent (figure 3.9B). Macrophages deficient in CD64 did not show any increase in their surface expression of MHC II when stimulated with IFN γ and LPS. Therefore, we were unable to investigate the effect of loss of this receptor on SIC-induced down-regulation of MHC II expression (figure 3.9C).

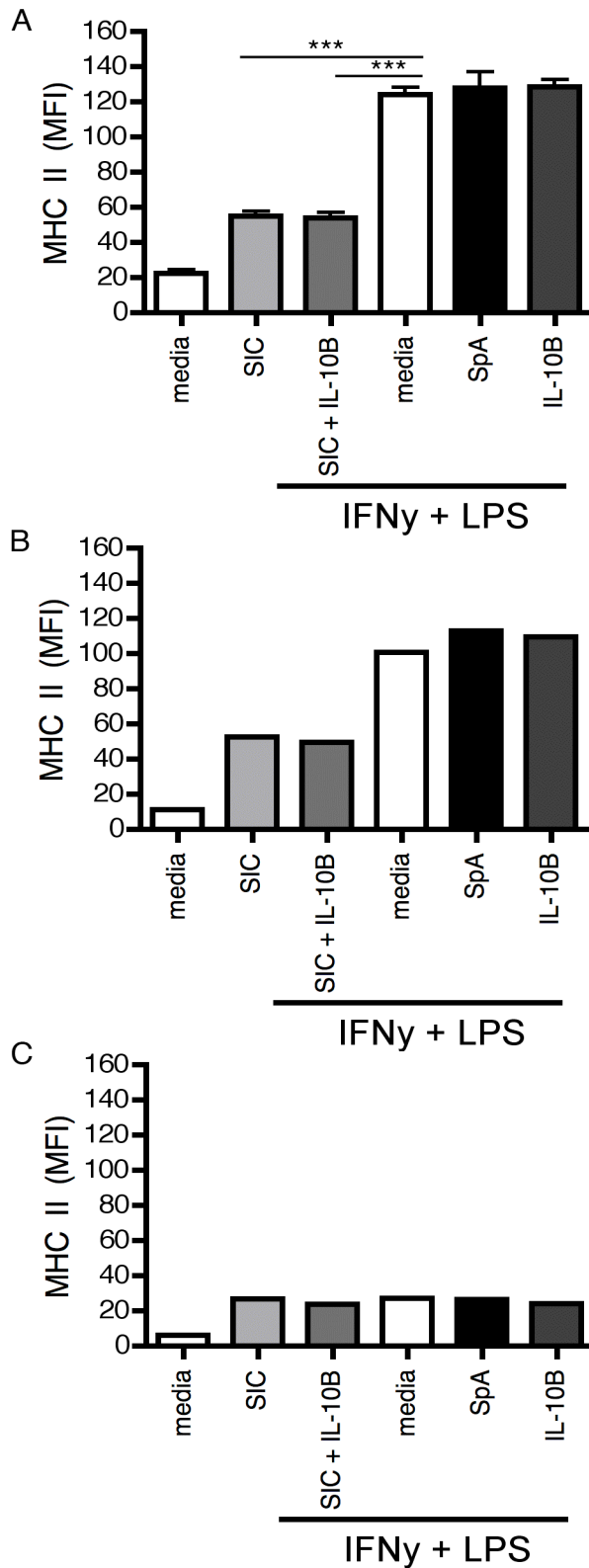


Figure 3.9. SIC has the ability to down-regulate MHC II expression in WT and CD32^{-/-} macrophages.

BMDM were seeded on day 6 at 5×10^5 /ml per well and treated with 100U/ml IFN γ overnight. On day 7, macrophages were stimulated with or without LPS in the presence or absence of SIC, SpA or IL-10R blocker (annotated as IL-10B on graphs) for 6h before supernatants were removed and cells stained for flow cytometric analysis. The WT experiment was carried out on three separate occasions and data pooled together for statistical analysis purposes. CD64^{-/-} and CD32^{-/-} experiments were carried out only once and therefore no statistical analysis was performed. Statistical analysis was conducted using one-way ANOVA for LPS + IFN γ stimulation. Significant differences between groups were identified using a post-hoc Bonferroni test, which compared all groups to media, *** = $P < 0.001$. The mean \pm SD MFI values for MHC II. (A) Wild type macrophages ($F_{5,22} = 92.55$, $P < 0.0001$). (B) CD32^{-/-} macrophages. (C) CD64^{-/-} macrophages.

3.2.9 SpA can engage cell-bound IgG to interact with cells

In an *in vivo* setting, the high affinity Fc γ RI (CD64) receptor is always occupied with IgG. To examine whether or not SIC and/or SpA can interact with cells when CD64 is occupied with IgG macrophages from WT, Fc γ RI^{-/-} (CD64), Fc γ RIIb^{-/-} (CD32) and the common γ chain^{-/-} were coated with or without IgG for 20mins before incubation with fluorochrome-labelled SIC or SpA and assessed via flow cytometry (figure 3.10).

Initially, cells were probed with an anti-IgG antibody to show that the cells were coated with IgG (Figure 3.10A). The level of IgG on WT and CD32^{-/-} cells was comparable. Conversely, CD64^{-/-} macrophages show a reduced ability to bind to IgG compared to WT and CD32^{-/-}, most likely because CD64 is the high affinity receptor for monomeric IgG. IgG binding to the CD64^{-/-} macrophages might be explained by the IgG having formed aggregates and then binding via one of the low affinity Fc γ Rs the macrophages still express. However, this is not likely as the IgG was centrifuged prior to their use to exclude aggregates that might have formed. The other possibility is that Fc γ RIV, which has intermediate binding affinity for IgG²⁶³ is compensating for CD64^{-/-}. The common γ chain^{-/-} cells showed no binding of IgG, and Fc γ RIV does associate with the common γ chain^{-/-} and would be knocked out in these cells too, explaining why no binding of IgG was observed (figure 3.10A).

As expected when SpA-488 is administered to cells that have not been pre-incubated with IgG or do not bind IgG, SpA-488 was unable to bind to these macrophages (figure 3.10B). However, when macrophages are pre-incubated with IgG, WT and CD32^{-/-} cells still show binding of SpA-488 as they can interact with the IgG on the macrophage surface. This binding is at a slightly reduced level compared to binding levels of preformed SIC in both WT and CD32^{-/-}. Even though CD64^{-/-} macrophages could bind IgG, it may be at too low a level for them to interact with the SpA and therefore no binding of SpA-488 or SIC-488 was exhibited in these cells. These results demonstrate the role that CD64 plays in SIC's ability to bind to macrophages. Furthermore, complexes do not have to be preformed as SpA can interact with IgG already present on the macrophage's surface-bound receptor.

3.2.10 *Complex formation with SpA and IgG2a induces IL-10 production in macrophages in the presence of LPS*

So far, it has been proven that SpA must be in complex with IgG for it to bind to macrophages and to impart a regulatory phenotype on them. However, it is not known what sub-classes of IgG are required in the complex to induce polarization to a regulatory phenotype.

To address this issue, purified IgG1 and IgG2a were used to form complexes with SpA in the same manner as previously stated (section 2.3.1). Macrophages were stimulated for 6h with or without LPS in the presence of SIC made from polyclonal IgG, IgG1 or IgG2a. Supernatants were removed and assessed via IL-10 ELISA to characterize the macrophage phenotype (figure 3.11).

Macrophages that were treated with SIC formed with polyclonal IgG in the presence of LPS, as before, exhibited the same significant up-regulation of IL-10 production (figure 3.11A). Complexes formed with purified IgG2a showed the same up-regulation of IL-10 as the complexes formed with polyclonal IgG, though IL-10 production was at a slightly reduced level (figure 3.11B). However, complexes formed with IgG1 alone did not induce the regulatory phenotype (figure 3.11C). This data indicates that IgG2a must be a component of the SIC complex. This is consistent with the idea that IgG2a binds preferentially to Fc γ RI, which is required for SIC complex binding (Figure 3.7).

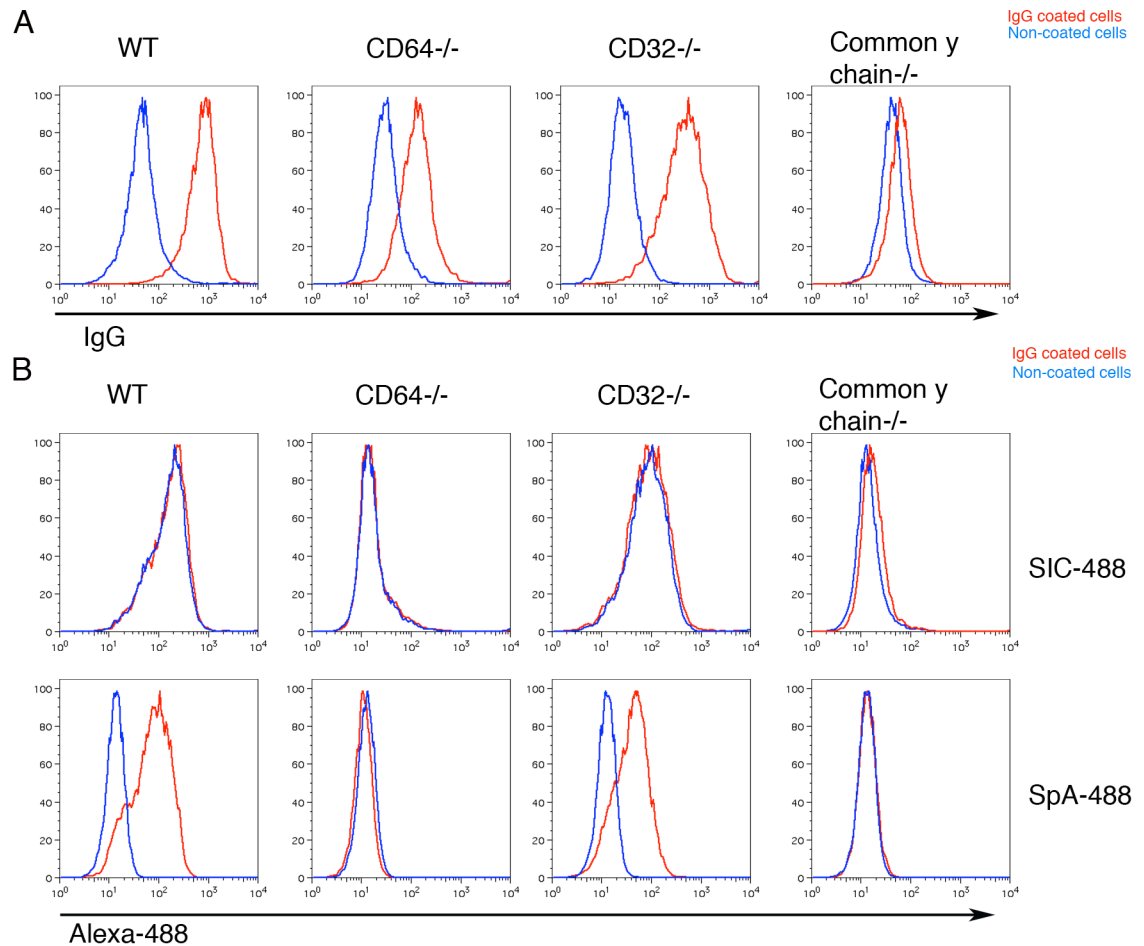
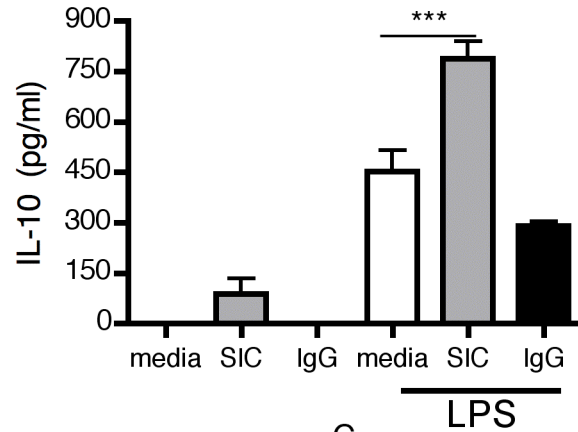


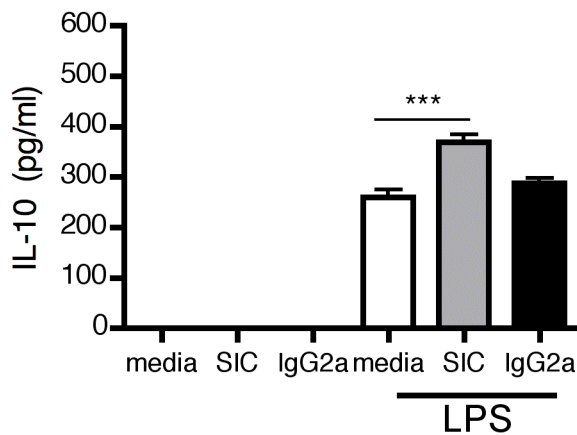
Figure 3.10. SpA has the ability to bind to WT and CD32^{-/-} BMDM when the cells have been pre-coated with IgG.

BMDM were generated with the use of M-CSF from the cell line L929. Cells were harvested on day 7 and incubated with or without IgG for 20mins, cells were then washed to remove unbound IgG. Macrophages were then incubated with preformed SIC-488 or SpA-488. SpA was fluorescently labelled with alexa-488. (A) Cells were stained with anti-IgG to show IgG binding. (B) Representative histograms of different binding affinities of SpA when alone or in complex with IgG coated cells. This experiment was conducted on two separate occasions; the data shown is a representative image of the two experiments.

A



B



C

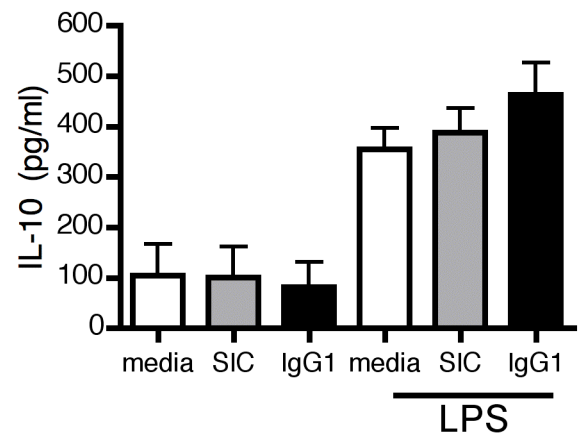


Figure 3.11. SIC that has been preformed with purified IgG2a but not IgG1 can induce macrophages to a regulatory phenotype.

BMDM were seeded on day 6 at $10^5/200\mu\text{l}$ per well. On day 7, macrophages were stimulated with or without LPS in the presence or absence of SIC that had been pre-formed with polyclonal IgG, purified IgG2a or IgG1 for 6h before supernatants were removed and assessed for IL-10 (ng/ml) production via ELISA. This experiment was carried out in quadruplicate and graphs are representative of two separate experiments that showed the same pattern of results. Statistical analysis was conducted using one-way ANOVA for LPS stimulation subset only. Significant differences between groups were identified using a post-hoc Bonferroni test, which compared all controls to SIC, *** = $P < 0.001$. (A) SIC that had been preformed with polyclonal IgG ($F_{2,11} = 18$, $P < 0.0007$). (B) SIC that had been preformed with purified IgG2a ($F_{2,11} = 35.31$, $P < 0.0001$). (C) SIC that had been preformed with purified IgG1.

3.2.11 SIC generated with IgG2a induces down-regulation of MHC II but not to the same extent as SIC made with polyclonal IgG

When SIC were generated with IgG2a, they could induce macrophages to significantly up-regulate their IL-10 production and become polarized to a regulatory phenotype; however this was not seen with complexes formed with IgG1. To investigate further if IgG2a is a required component of SIC to induce macrophages to a regulatory phenotype, IgG2a complexes were examined to determine their ability to down-regulate MHCII expression. Complexes were formed with alexa-488-labelled SpA and either polyclonal IgG, purified IgG1, IgG2a or IgG2b. The ability of these complexes to interact with cells and inhibit the surface expression of MHC II was studied via flow cytometric analysis.

Flow cytometric binding studies demonstrated that polyclonal IgG has the highest level of macrophage binding (figure 3.12A). This correlated with the ability of these polyclonal SIC complexes to substantially down-regulate MHC II expression (figure 3.12B). In comparison, complexes formed with IgG1 or IgG2b were unable to interact with macrophages and hence could not down-regulate MHC II expression. Interestingly, SIC formed with IgG2a was able to interact with macrophages and to some degree down-regulate MHC II expression. However, in both instances this was not as substantial as the polyclonal SIC complexes, confirming what was demonstrated via IL-10 ELISA (figure 3.11), that IgG2a formed SIC is the only purified sub-set that has the ability to bind to macrophages and cause functional and phenotypic alteration. However, it has also been shown that the effect exerted by SIC formed with IgG2a, in comparison to SIC formed with polyclonal complexes, was not as pronounced.

3.2.12 Mixed IgG sub-classes down-regulate MHC II to the same extent as polyclonal IgG

SIC made with purified IgG2a can induce significant reduction of MHC II expression and can significantly increase the production of IL-10 by macrophages when treated with LPS. However, the effect that was wielded by SIC formed with IgG2a was not observed to the same degree as SIC formed with polyclonal IgG. This led to the speculation that the complexes formed with polyclonal IgG contain multiple subclasses of IgG and that they must therefore be more potent.

To address this, SIC were generated using two subclasses of IgG and macrophages were treated with the complexes in the presence and absence of LPS and IFN γ as previously described (section 3.2.4). Macrophages were examined for their potential to bind the complexes and for altered surface MHC II levels (figure 3.13).

When complexes containing IgG2a with either IgG1 or IgG2b are formed with alexa-488-labelled SpA they show increased binding compared to complexes formed without IgG2a which showed only background levels of binding (figure 3.13A). It is important to note that none of the combinations of IgG subclass SIC induced the same level of binding as the polyclonal SIC. Upon examination of the ability of these combinatorial SIC complexes to down-regulate MHC II, it was found that IgG1/2a SIC had the same capacity to down-regulate MHC II expression as polyclonal IgG derived SIC (figure 3.13B). The complexes formed with IgG1/2b showed no ability to down-regulate the expression of MHC II and complexes formed with IgG2a/2b showed the same reduction in the level of MHC II expression as IgG2a alone, leading to the assumption that the down-regulated expression is an effect of IgG2a and not an effect of the mixed complex of IgG2a/2b.

SIC that were generated with the subclasses IgG1/2a show the same ability as SIC formed with polyclonal IgG to induce macrophages to a regulatory phenotype; however, they do not show the same intensity of binding as polyclonal SIC. This may be due to the ability of SpA to bind to IgG3, though these complexes have no functional effects in the polarization of macrophages to a regulatory phenotype (data not shown). When IgG3 was combined with any other sub-class, complexes interacting with macrophages was exhibited, but there was no functional effect of macrophage polarization (data not shown). Elucidating the subclasses of IgG that bind to SpA to form SIC - that have the ability to polarize macrophages to a regulatory phenotype - is vitally important if a therapeutic is ever to be designed.

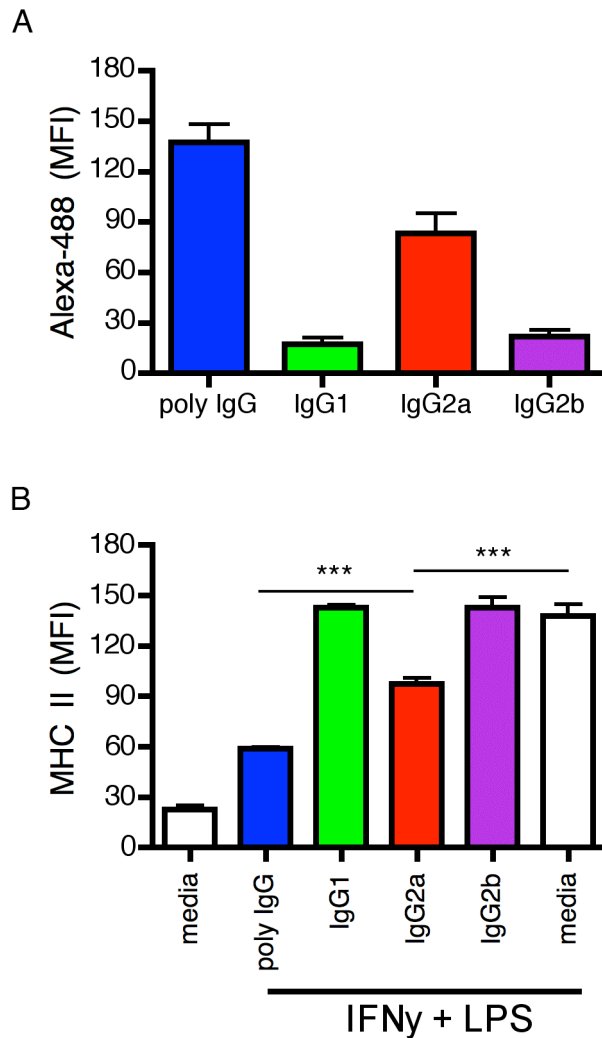


Figure 3.12. SIC that has been preformed with purified IgG2a but not IgG1 or IgG2b can induce the down-regulation of MHC II levels on BMDM.

BMDM were seeded on day 6 at 5×10^5 /ml per well and treated with 100U/ml IFN γ overnight. On day 7, macrophages were stimulated with or without LPS in the presence or absence of SIC that has been pre-formed with polyclonal IgG, purified IgG1, IgG2a or IgG2b for 6h before supernatants were removed and cells stained for flow cytometric analysis. This experiment was carried out on three separate occasions in single or duplicate and data for MHC II MFI pooled together for statistical analysis purposes. This was not however possible for Alexa-488 MFI and the graph is a representative of the three experiments. Statistical analysis was conducted using one-way ANOVA to compare the differences in MHC II expression when stimulated with LPS+IFN γ . Significant differences between groups were identified using a post-hoc Bonferroni test, which compared all groups to each other, *** = $P < 0.001$ (A) The mean \pm SD MFI values for Alexa-488. (B) The mean \pm SD MFI values for MHC II ($F_{5,17} = 147.4$, $P < 0.0001$).

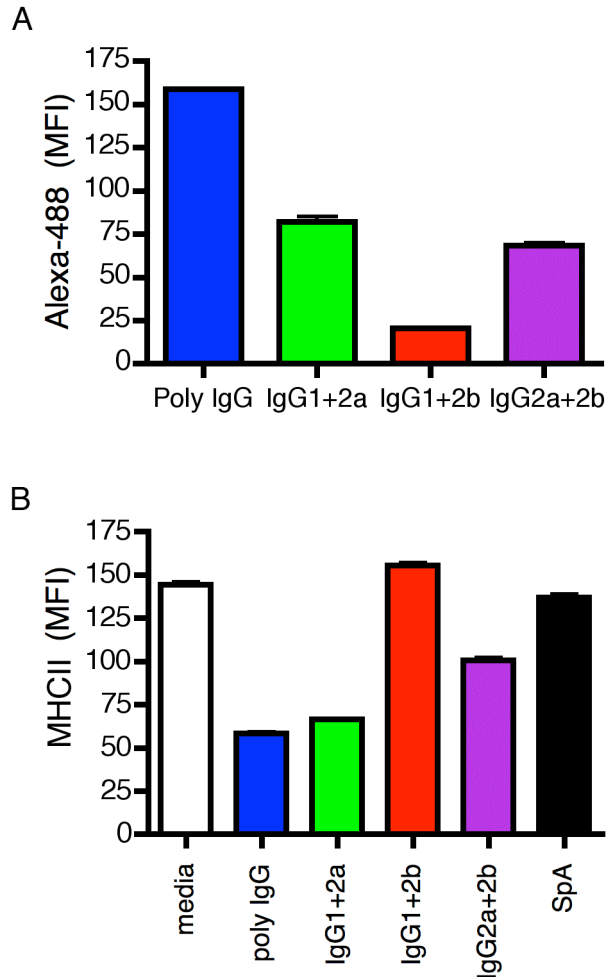


Figure 3.13. SIC that has been preformed with a mixture of purified IgG2a and IgG1 can induce macrophages to a regulatory phenotype.

BMDM were seeded on day 6 at 5×10^5 /ml per well and treated with 100U/ml IFN γ overnight. On day 7, macrophages were stimulated with or without LPS in the presence or absence of SIC that has been pre-formed with polyclonal IgG or a 1:1 mixture of purified IgG1, IgG2a or IgG2b for 6h before supernatants were removed and cells stained for flow cytometric analysis. (A) The mean \pm SD MFI values for Alexa-488. (B) The mean \pm SD MFI values for MHC II. This experiment was carried out on two separate occasions and data has been combined, however, due to too small an N, no statistical analysis was performed.

3.3 Discussion

SpA has been previously demonstrated to have immune-modulating activities as it was already classified as a B cell superantigen. It has the ability to interact with V_H3-encoded BCR and induce Bim-mediated apoptosis²⁶⁴ via a FcγRIII mechanism, which is dependent on the presence of IgG (unpublished data). SpA has also been shown to bind to macrophages when it is in complex with IgG via FcγR²⁶¹. Furthermore, it is known that when SpA is in the presence of excess IgG it will always form a specific immune complex made up of four IgG molecules and two SpA molecules²¹⁷. Macrophages have been shown to become polarized to an anti-inflammatory phenotype by the binding of many different types of immune complexes when in the presence of an inflammatory stimuli^{253 219 252}. Therefore, the ability of SpA, when in the presence of IgG (SIC), to polarize macrophages to an anti-inflammatory phenotype was investigated. The results demonstrate that when SpA is in complex with IgG it can induce macrophages stimulated with LPS to significantly up-regulate their production of IL-10 and inhibit their production of IL-12, which are key phenotypic features of anti-inflammatory macrophages. It was also discovered that SIC can down-regulate MHC II expression when macrophages were stimulated with SIC in conjunction with LPS after IFNγ priming, which did not have an effect on the ability of T cells to become activated. The anti-inflammatory phenotype that was induced when macrophages were treated with SIC was regulated through the binding of SIC to FcγRI. Interestingly, complexes composed of a mix of IgG1/2a induced the same anti-inflammatory phenotype as those made up with polyclonal IgG.

The ability of SIC to induce macrophages to an anti-inflammatory phenotype is intriguing as SpA is the active component of an (FDA) approved apheresis therapy (Prosorba column) for inflammatory and autoimmune diseases²⁶⁵. However, there has been longstanding controversy over the mechanism of action and the unpredicted beneficial effects of this therapy, especially where conventional plasmapheresis has failed (the Prosorba column could only remove IgG from roughly 60ml of plasma where traditional methods can remove IgG from 500-600ml of plasma).

It was discovered that a small quantity of SpA was released from the column via proteolytic cleavage and would enter the patient's circulation. Several

hypotheses have been proposed for the mode of action of the therapy, including removal of immunoglobulin and/or immune complex and depletion of B cells²¹⁶. However, the SpA that leaches from the column into the patient's circulation could lead to the generation of anti-inflammatory macrophages that produce high levels of IL-10, leading to the resolution of inflammation.

SpA can form homogeneous immune complexes with IgG when it is in excess and it has also been well documented that macrophages can be induced to a regulatory phenotype when they interact with immune complexes in an inflammatory setting^{77 151}. Interestingly, the majority of previous studies have utilized xenogeneic immunoglobulin, primarily rabbit or rat IgG, for the generation of immune complexes to examine their potential to polarize macrophages to an anti-inflammatory phenotype. The interaction of rabbit IgG with murine Fc receptors has never been specifically examined; though, results suggest that rabbit IgG has an order-of-magnitude lower affinity for mouse Fc receptors compared to mouse IgG^{220 221}. In this study, immune complexes were formed with the use of SpA and mouse IgG - as rabbit IgG-formed immune complexes could have altered binding activity to mouse Fc receptors, and could have produced dramatically different outcomes when compared to mouse IgG immune complexes. This was found to be true when the binding affinity of SIC and OIC, which were formed using rabbit anti-OVA IgG, to macrophages were tested and OIC were shown to have lower affinity to murine BMDM than SIC, which was formed with autologous murine IgG.

SIC's ability to polarize macrophages to an anti-inflammatory phenotype was examined. When macrophages were treated with SIC in the absence of any inflammatory stimuli, SIC induced a significant increase in IL-10 production. Importantly, this attribute has never previously been seen with immune-complexes²⁵². In the presence of LPS, SIC induced macrophages to produce significantly lower levels of IL-12 and significantly higher levels of IL-10 in comparison to LPS-treated macrophages. This cytokine profile is one of the key features of anti-inflammatory macrophages. In accordance with work previously published²⁶¹, it was demonstrated that SpA - when in complex with IgG - can bind to macrophages via an FcγR-dependent mechanism. However, the authors of the previous work did not define which FcγR was specifically involved in the binding of the complexed SpA to macrophages. Interestingly, it was discovered

that the high affinity IgG receptor, FcγRI, was essential for SIC to bind to macrophages. This was a slightly unexpected result as FcγRIIb is the inhibitory FcγR (as it has an ITIM) and has been shown to be involved in the resolution of inflammation^{176,266}; whereas FcγRI is normally an activatory receptor¹⁶⁵. CD64 was not only shown to be essential for SIC to bind to macrophages but, in its absence, the ability of SIC to impart an anti-inflammatory phenotype was also abrogated. Furthermore, and in support of the former finding, it had been previously demonstrated that anti-inflammatory macrophages production of IL-10 - which have been polarized by immune complexes (opsonized sheep erythrocytes) plus LPS - are dependent on CD64 expression²⁵². Notably, ERK activation, following FcγRI ligation, leads to a remodeling of the chromatin at the *il-10* locus, making it more accessible to transcription factors²⁶⁷. The exact signaling mechanism of SIC-induced polarization of macrophages to an anti-inflammatory phenotype via CD64 signaling has not been fully elucidated, but ERK may be a molecule of interest for future investigation.

To try to categorise further the phenotype of the macrophage SIC was inducing, supernatants from SIC-treated macrophages were screened for other cytokines such as NO and IL-6, which were still secreted at high levels in the SIC-treated macrophages. This secretion at high levels was not expected as NO is a component produced normally by inflammatory macrophages. However, IL-6 can be produced by both pro-inflammatory classical macrophages and anti-inflammatory macrophages that are induced by immune complexes - and can play a beneficial role in CNS injury by protecting neurons from death due to excitotoxicity²⁶⁰.

Another interesting feature of anti-inflammatory macrophages is that in the majority of cases they show up-regulated MHC II on their surface²⁵³; however, macrophages that have been treated with LPS or IFNγ in the presence of SIC show significantly lower expression of MHC II in comparison to LPS and IFNγ-only treated macrophages. It is known that if macrophages are polarized to an anti-inflammatory phenotype via exposure to IL-10, they show reduced levels of MHC II²⁵⁸. An example of this *in vivo*, is the ability of the cytomegalovirus to induce infected cells to produce IL-10, which leads to the down-regulation of MHC II on macrophages²⁶⁸. As it has been shown that SIC-stimulated macrophages produce large amounts of IL-10, an IL-10-dependent autocrine mechanism of reduced

MHC II expression was investigated. This was carried out with the blockade of IL-10R on macrophages using a blocking antibody. When the IL-10R was blocked on macrophages it did not alter the MHC II down-regulation induced by SIC, showing that this is not an IL-10-dependent mechanism and is most likely to be post-translational modification of MHC II as IFN γ alone increases the expression of MHC II before the addition of SIC and LPS - demonstrating that MHC II is down-regulated rather than inhibited by SIC.

Some very early work on immune complexes, and their ability to alter macrophage function, showed that immune complexes had the ability to down-regulate macrophage MHC II expression after IFN γ stimulation. However, this work showed that this was only possible when the complexes were plate-bound and had been cultured for up to a week to see immune complex-mediated down-regulation of MHC II, which was not reproducible with soluble immune complexes or over short culture periods. The conclusion to be drawn suggests that SIC does not exert its effects in the same manner. Interestingly, the authors showed that immune complexes, made with either IgG1, 2a, 2b or IgE, could induce this down-regulation of MHC II. However, no other immune-regulatory features of these macrophages were characterized²⁶⁹. SIC-induced MHC II down-regulation was only discovered to be dependent on complexes being generated with polyclonal IgG and/or a mix of IgG1/2a - and to a lesser extent IgG2a by itself. The only other work on immune complex-mediated down-regulation of MHC II involved the use of heat-aggregated human IgG. In these studies, incubation of PBMC with heat-aggregated IgG, before or after IFN γ stimulation, resulted in a reduction in MHC II compared to IFN γ -only treated PBMCs. This down-regulation of MHC II was reversible when immune complexes were removed. The data also implied that complexes induced metalloproteases and aspartic proteases, which subsequently down-regulated MHC II via cell-surface cleavage. It is therefore possible that SIC is down-regulating MHC II expression via this mechanism, but future experiments will need to address this. It should be appreciated, however, that in the heat-aggregated IgG study the authors looked at total MHC II expression in PBMCs and did not pre-gate on monocytes. They incorrectly attributed this phenomenon totally to monocytes and did not take into consideration B cells that are a component of PBMCs (and also express MHC II and Fc γ R). Therefore, this phenomenon cannot be attributed to a unique

monocyte-immune complex association - as they have not specifically isolated monocytes from the PBMCs, or looked at MHC II on these cells in isolation with immune complexes²⁷⁰.

As SIC leads to the down-regulation of MHC II on macrophages treated with LPS and IFN γ , it was therefore considered whether this abrogation of MHC II would have an effect on the ability of macrophages to activate CD4⁺ T cells after SIC treatment. This was performed by examining the expression of the activation marker CD69 on T cells after co-culture with macrophages which had been previously incubated with OVA and activated with LPS and IFN γ in the presence or absence of SIC. It was found that SIC had no effect on CD69 expression (and therefore early T cell activation after co-culture with macrophages).

Nevertheless, under normal physiological conditions *in vivo*, macrophages do not activate naïve T cells as they do not traffic to draining lymph nodes and therefore cannot take part in the initiation of the primary adaptive immune response. This task is performed by dendritic cells; no investigation into the effects SIC would have on dendritic cells have been carried out. However, we speculate that SIC would not have an effect on the activation phenotype of dendritic cells as they do not express CD64, which is the receptor shown to be essential for SIC's ability to bind to and polarize macrophages to an anti-inflammatory phenotype²⁷¹.

Although macrophage are not pivotal in the initiation of an immune response, they are essential for the perpetuation of the primary and secondary phases of the adaptive immune response via T cell clonal expansion at the site of infection. SIC-induced down-regulation of MHC II may help with the resolution of an immune response as the reduced levels of MHC II available to re-stimulate T cells could inhibit subsequent activation and expansion.

An alternative avenue of investigation in the future could be to examine the ability of SIC-treated macrophages to induce Treg cells. Inducible Tregs have also been shown to express CD69 and can be generated in the tissues if they are surrounded by cells that produce high levels of IL-10^{272 273}. Further work is needed to answer these questions.

In conclusion, it has been demonstrated in this chapter that SIC in conjunction with LPS can polarize macrophages to an anti-inflammatory phenotype with significantly increased IL-10 production, significantly reduced IL-12 production, and unaltered NO and IL-6 production when compared to LPS-only treated macrophages. SIC and LPS also exhibited the ability to down-regulate MHC II expression after macrophages had been treated with IFN γ . The fact that SIC can induce anti-inflammatory macrophages in the presence of inflammatory stimuli shows potential for this as a therapeutic agent in overt inflammatory conditions and merits further investigation into its exact mode of action through Fc γ RI.

4 SPA has the ability to induce maturation of Ly6C^{hi} monocytes into Ly6C^{low} monocytes under steady-state or inflammatory conditions

4.1 Introduction

The MPS is composed of monocytes, Langerhans cells, Kupffer cells, microglia, alveolar macrophages, dendritic cells and neutrophils, amongst others^{3 4}. It is known that the MPS is in a constant state of flux with a high turnover of cells under both steady-state and inflammation. Much debate surrounded the exact process by which cells of the MPS are replaced. In an inflammatory setting there is both renewal of differentiated cells resident in tissues and infiltration of bone marrow precursors such as monocytes⁴⁰; and these two processes most likely work synergistically. Interestingly, it has recently been demonstrated that microglia along with some other tissue-resident macrophages (Langerhans cells of the skin and pulmonary macrophages of the lung) do not derive from HSC as previously thought. They are actually derived from an early embryonic progenitor, which originates in the yolk sac at embryonic day 8, whereas monocyte/macrophages derived from HSC are not seen until embryonic day 12 in the foetal liver^{38 39}. Microglia have been shown to be self-renewing under steady-state conditions but when inflammation is present in the CNS, monocytes from the bone marrow can extravasate through the BBB and differentiate into microglia under these specialised circumstances^{35,36}.

Monocytes can remain in the circulation from 2 days up to 2 weeks before migrating into tissue and differentiating into macrophages/DCs or homing back to the bone marrow. When monocytes are in the circulation they exhibit no ability to proliferate. However, it is unknown what proliferative potential they possess when in the bone marrow or newly arrived in tissue before they differentiate into macrophages²⁷⁴. Studies by Geissmann et al have demonstrated that there are two monocyte subsets in mice (this concept has been covered in great detail in section 1.3.3; however, it will also be reviewed briefly here too). These subsets have been distinguished on the basis of their expression of Ly6C and CX₃CR1⁴⁰. The monocyte subset that expresses high levels of Ly6C and low-intermediate levels of CX₃CR1, also expresses the chemokine receptor CCR2 and the adhesion molecule L- selectin. These Ly6C^{hi}

monocytes are classified as the 'inflammatory' subset due to their tendency to migrate to sites of inflammation where they produce pro-inflammatory cytokines. This has been shown in numerous models of infection, inflammation and tissue-damage models, such as *L. major*, *T. gondii*, atherosclerosis, acute peritoneal inflammation and post ischemic brain injury^{51 275 58 276 46}. The second monocyte subset in mice is defined by low expression of Ly6C, high levels of CX₃CR1, but no expression of CCR2 or L-selectin. Ly6C^{low} monocytes have been deemed 'patrolling' or 'anti-inflammatory' monocytes as they are found to crawl along blood vessels and have the potential to migrate into tissue in the steady-state to replace tissue-resident macrophages/DC populations. Furthermore, they have the ability to participate in the resolution/tissue repair phase of an immune response in inflamed tissues^{53 277 278}. Monocytes are conserved across many species and it has more recently been demonstrated that the sub-populations of monocytes that were first demonstrated in humans (see section 1.3.4) and more recently in mice, have also been discovered in rats, pigs and cows, further demonstrating the importance and differing roles these two subsets of monocytes must play in maintaining a competent immune system in both health and disease^{279 280 281}.

The previous chapter of this thesis has demonstrated that SIC has the ability to skew macrophages to a regulatory phenotype *in vitro*. Hence, it was hypothesized that SIC would also have an effect on their myeloid precursors in tipping the balance from Ly6C^{hi} inflammatory monocytes to Ly6C^{low} anti-inflammatory monocytes, which could differentiate into regulatory macrophages under inflammatory conditions, leading to the resolution of inflammation and the initiation of the tissue repair process.

Inflammation is associated with a number of auto-immune diseases or traumatic conditions. To evaluate the ability of SIC to interact with the innate immune system in the absence of an overt auto-reactive adaptive immune response a contusion model of spinal cord injury was used, which is driven by a traumatic event resulting in significant inflammation at the site of injury.

The vast majority of SCI results in paralysis of the victim; the extent of paralysis depends on the level that the injury to the spinal cord occurs at. The reason paralysis is such a common outcome rate for SCI victims is due to two distinct

events: the primary event is the initial trauma from the injury itself; the secondary event is the so-called “secondary death” that occurs days to weeks after the initial trauma. The pathogenesis of secondary death was a major contributing factor in the choice of which murine model of inflammation to use to evaluate SIC’s ability to skew members of the myeloid lineage to a regulatory/anti-inflammatory phenotype. As described in section 1.7.1.2, the phenomenon of secondary death describes the aberrant inflammatory immune response that occurs after SCI with the infiltration and activation of microglia and leukocytes at the site of injury - where they release pro-inflammatory mediators such as cytokines, reactive oxygen species and matrix metalloproteinases, which lead to additional neuronal death after the initial injury^{94 282}.

Monocytes play a major role in the perpetuation of the inflammatory immune response after SCI (diagram 4.1) as they have been shown to differentiate into activated inflammatory macrophages once they have trafficked to the site of injury. These cells are one of the main culprits in the production of the vast amount of inflammatory mediators responsible for death of healthy neurones not killed in the initial trauma¹³³.

This chapter aims to:

- Characterize the binding profile of SpA within the myeloid compartment in steady-state and after SCI
- Assess any phenotypic changes that SpA induces in this compartment
- Determine whether or not SpA can modulate the vast amount of inflammation that is perpetuated by monocytes and macrophages in the secondary death phase of SCI.

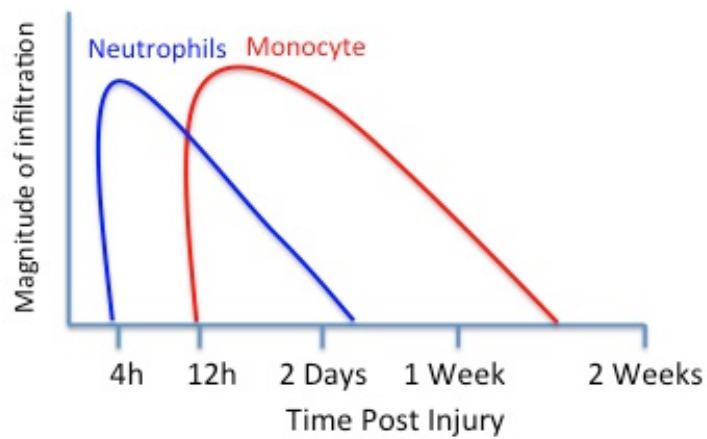


Figure 4.1: Time course of innate immune cell infiltration into the damaged spinal cord after injury.

Neutrophils arrive in the damaged spinal cord 4h after injury and can be seen at the site of injury until post injury day 2. Monocytes infiltrate into the damaged cord 12h after injury where they differentiate into macrophages and are present for up to two weeks after injury. Adapted from ⁷⁸

4.2 Results

4.2.1 SpA binding to Monocytes and Neutrophils

To examine the ability of SpA to bind to cells of the myeloid lineage in an *in vivo* setting, 500 μ g of fluorochrome-labelled SpA or OVA was injected i.p. into C57BL/6 mice. Two hours later mice were culled and blood (figure 4.2), spleen (data not shown) and bone marrow (figure 4.3) were harvested for flow cytometric analysis. In the blood, the negative control (OVA-488) did not interact with CD11b⁺ GR1^{low} Ly6C⁺ monocytes; however, SpA-488 showed significant binding to CD11b⁺ GR1^{low} Ly6C⁺ monocytes with a mean \pm SD MFI of 2759 \pm 450 (Figure 4.2A). Examination of the circulating neutrophil compartment, CD11b⁺ Gr1^{hi} Ly6C⁻, demonstrated that SpA-488, when compared to control (OVA-488), was able to bind to circulating neutrophils with a mean \pm SD MFI of 193 \pm 18. Nevertheless, it is important to note that the binding of SpA-488 to neutrophils was 10-fold lower than to monocytes. The difference in binding between the two cell populations can most likely be attributed to the differential expression of Fc γ receptors on the cell surface.

The substantial binding of SpA to the monocyte compartment led to a further interrogation of this population. As discussed in the introduction to this chapter, the circulating monocyte population can be divided into Ly6C^{hi} and Ly6C^{low} monocyte subsets that can define their functional outcomes in both steady-state and inflammation. Analysis of SpA-488 binding illustrates that both populations of monocytes significantly interact with SpA-488 when compared to control protein (OVA-488) (Figure 4.2B). Although not a significant difference, it should still be noted that Ly6C^{hi} monocytes have increased binding (mean \pm SD MFI, 2907 \pm 490) compared to Ly6C^{low} monocytes (mean \pm SD MFI, 2086 \pm 335).

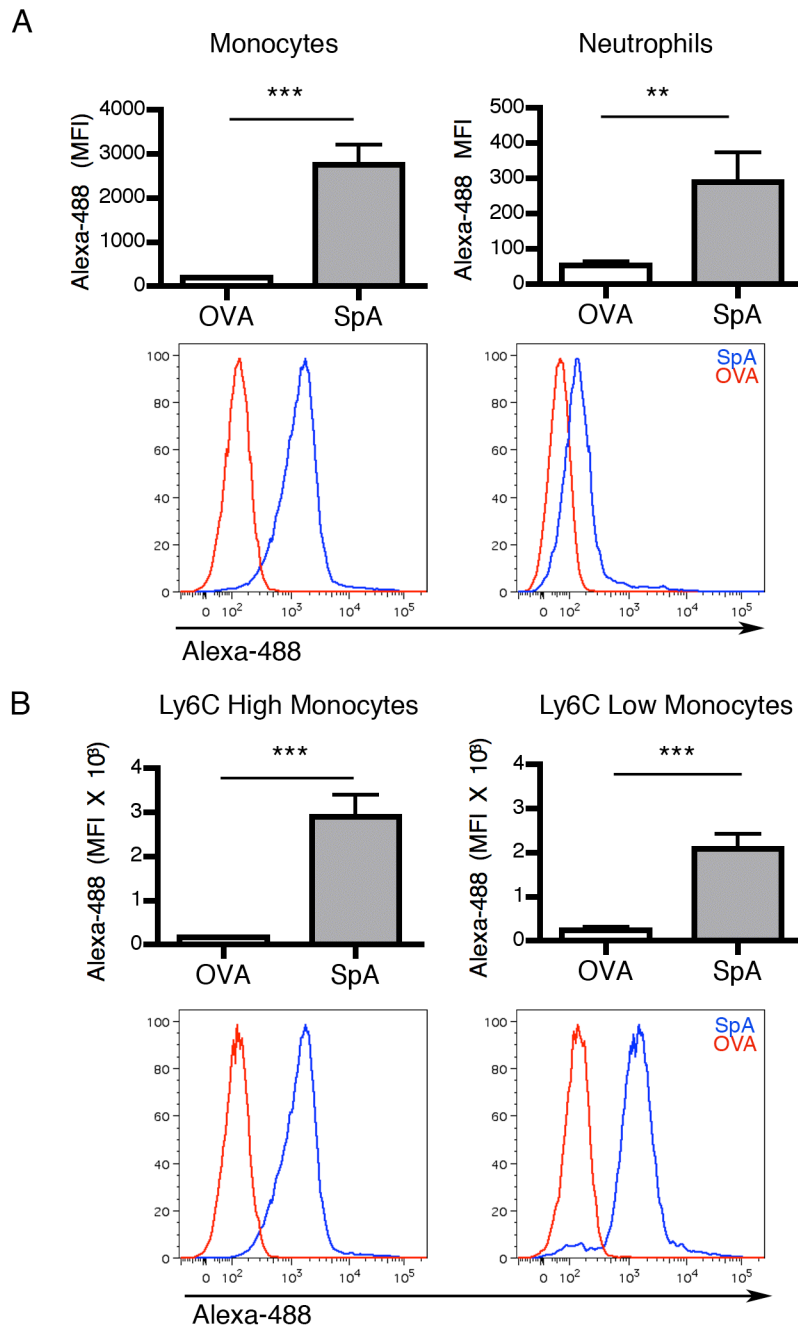


Figure 4.2 SpA-488 binding in monocytes and neutrophils in blood.

C57BL/6 mice received either 500 μ g of SpA-488 or OVA-488 i.p. After 2h mice were culled and blood was harvested and prepared for flow cytometric analysis on the MACS Quant. Data were analysed by a two-tailed, unpaired *t*-test, ** = $P < 0.01$; *** = $P < 0.001$. (A) The mean \pm SD MFI values for SpA-488 and OVA-488 binding for blood monocytes $T_{15} = 6.07$, $P < 0.0001$ (left panels) and neutrophils $T_{15} = 2.98$, $P < 0.01$ (right panels) with representative histogram plots below; SpA – blue line, OVA – red line. (B) The mean \pm SD MFI values for Ly6C^{hi} $T_{15} = 5.93$, $P < 0.0001$ (right panels) and Ly6C^{low} $T_{15} = 5.71$, $P < 0.0001$ (left panels) monocyte populations, binding with representative histogram plots below; SpA – blue line, OVA – red line. This experiment was carried out on three separate occasions; the data were then pooled together for purposes of statistical analysis. The three experiments had a total N of; SpA N=8 and OVA N=9.

The binding of SpA-488 to myeloid cells within the bone marrow was also examined 2h after injection. The control protein (OVA-488) did not interact with monocytes - as it had a mean MFI of 181 ± 11 ; however, SpA exhibited significantly higher binding to monocytes with a mean \pm SD MFI of 678 ± 129 (figure 4.3A). When comparing monocyte binding levels from the blood to the bone marrow, a dramatic decrease in binding of SpA can be seen - with a dramatic decrease in the mean \pm SD MFI value 2759 ± 450 to 678 ± 129 , respectively. It was also noted that in the bone marrow, but not in the blood, monocytes binding was bimodal. The bone marrow is the major site of haematopoiesis, thus there will be an array of monocytes at different developmental stages, exhibiting different surface receptor expression. This could explain the difference in SpA-488 binding between blood and bone marrow compartments, since in the bone marrow a wide spectrum of Fc receptor expression exists, whereas in the blood, Fc receptors are expressed at higher defined levels. Also, SpA-488 binding to neutrophils was assessed in the bone marrow where no binding was noted.

Although SpA-488 binding to monocytes was lower in the BM compared to blood, the interaction of SpA-488 with monocyte subsets was investigated due to the bimodal distribution of binding seen in the total monocyte population (Figure 4.3A), and because the bone marrow is an important site of monocyte maturation and differentiation (figure 4.3B). Furthermore, when Ly6C^{hi} monocytes do not encounter an inflammatory signal in the blood stream they are believed to home back to the bone marrow and differentiate into Ly6C^{low} monocytes, which are then released into the blood stream to either patrol the vasculature or replace tissue-specific DC and macrophages in the steady-state. In accordance with the blood, SpA-488 showed significantly increased binding to the Ly6C^{hi} monocyte subset in comparison to the control protein. However, unlike the blood, only a minor population of the Ly6C^{low} monocyte subset bound to SpA-488.

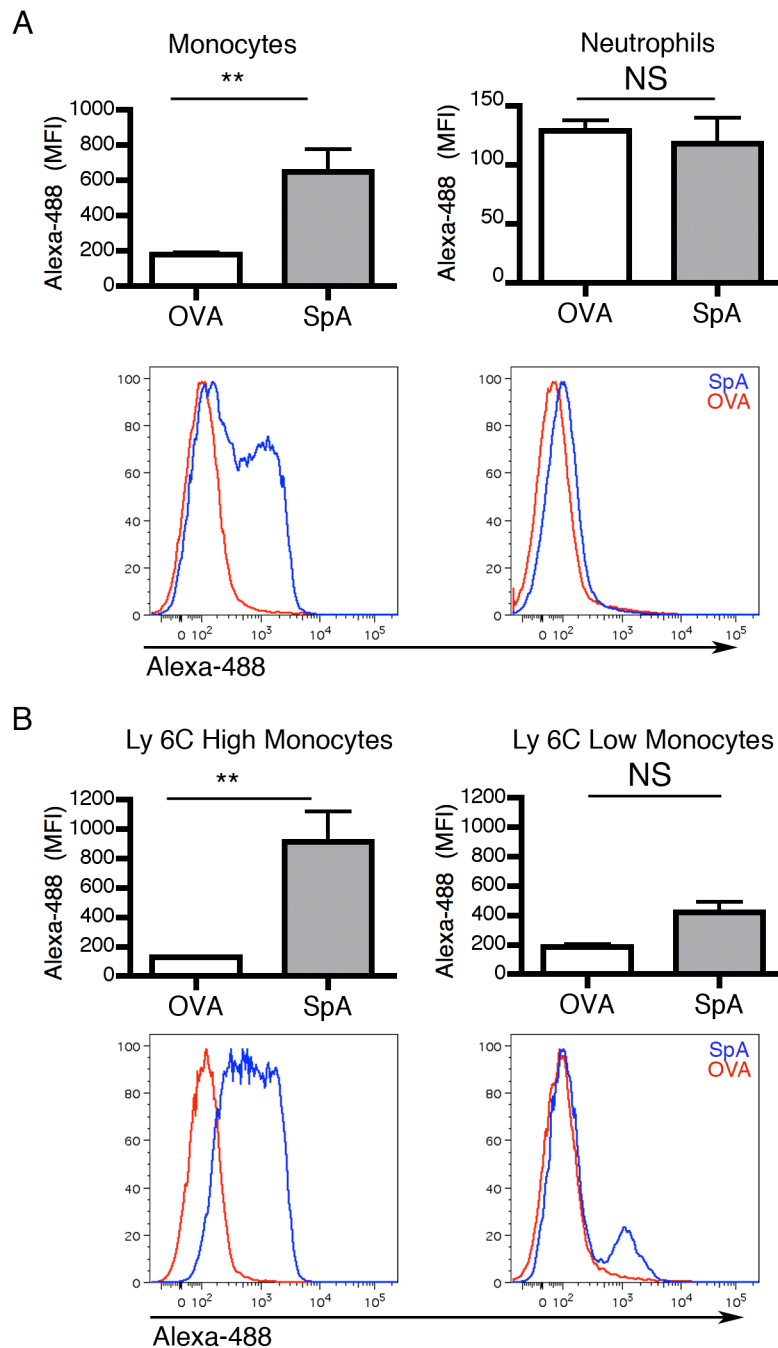


Figure 4.3 SpA-488 binding in monocytes and neutrophils in bone marrow.

C57BL/6 mice received either 500 μ g of SpA-488 or OVA-488 i.p. After 2h mice were culled and bone marrow was harvested and prepared for flow cytometric analysis on the MACS Quant. Data were analysed by a two-tailed, unpaired *t*-test, ** = $P < 0.01$; *** = $P < 0.001$. (A) The mean \pm SD MFI values for SpA-488 and OVA-488 binding for bone marrow monocytes $T_5 = 4.30$, $P < 0.0077$ (left panels) and neutrophils $T_5 = 0.52$, $P < 0.620$ (right panels) with representative histogram plots below; SpA – blue line, OVA – red line. (B) The mean \pm SD MFI values for Ly6C^{hi} $T_5 = 4.54$, $P < 0.0062$ (right panels) and Ly6C^{low} $T_5 = 2.39$, $P < 0.0621$ (left panels) monocyte populations, binding with representative histogram plots below; SpA – blue line, OVA – red line. This experiment was carried out on two separate occasions; the data were then pooled together for purposes of statistical analysis. The two experiments had a total N of; SpA N=3 and OVA N=4.

4.2.2 SpA requires IgG to interact with myeloid cells *in vivo*

It has been previously shown *in vitro* that SpA must be in complex with IgG at a 2:4 ratio (two SpA molecules and four IgG molecules for one complex) for it to exert its immuno-modulatory effects²²⁵. The inability of SpA to interact with monocytes in the absence of IgG *in vivo* was examined using μ MT mice - as they lack mature B cells. This defect is due to a mutation in their μ C gene, which leads to a loss of membrane-bound heavy chain. Failure to express the heavy chain with the surrogate light chain results in arrestment of the cell at the large pre-B cell stage of development²⁸³. μ MT mice have no immunoglobulin due to their lack of mature B cells, making the μ MT mice the perfect host to test the hypothesis that SpA must be bound to IgG to facilitate monocyte interaction.

Mice were injected i.v. with either 6mg of purified murine IgG or PBS and left for 40min to equilibrate. The same mice were subsequently injected with either 500 μ g of SpA-488 or OVA-488 i.p. and left for a further 2h before being culled and blood harvested. The control protein, OVA-488, did not interact with the monocyte population in the presence or absence of IgG (figure 4.4). Compared to controls, minimal binding of SpA-488 to monocytes was observed. However, this marginal binding could possibly be attributed to SpA's ability to interact with TNFR1 and von Willebrand factor^{284 285}. Importantly, SpA-488 in the presence of IgG binds the majority of the monocyte population to a far greater extent than SpA-488 in the absence of IgG (figure 4.4A). The dramatic difference in SpA's ability to bind to the monocyte population in the presence or absence of IgG can be demonstrated further when looking at MFI values (figure 4.4B): SpA-488 plus PBS has a mean \pm SD MFI of 1540 \pm 590, but SpA-488 plus IgG has a mean \pm SD MFI of 7952 \pm 1202, over 5 times higher when IgG is present.

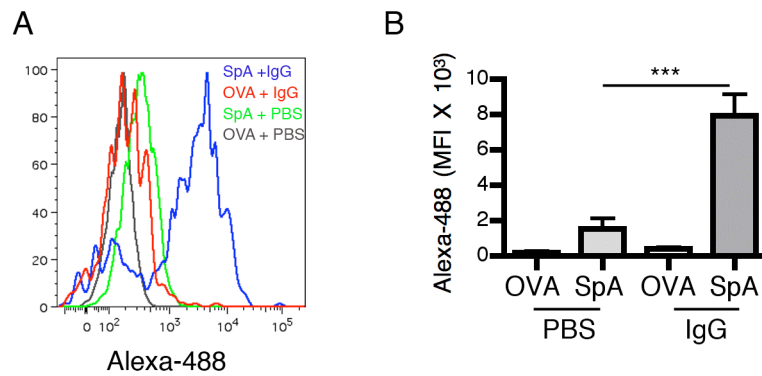


Figure 4.4. SpA requires IgG to interact with monocytes in vivo.

μ MT mice received either 500 μ g of SpA-488 or OVA-488 i.p and 6mg of IgG or PBS i.v. After 2h mice were culled and blood was harvested and prepared for flow cytometric analysis. (A) Histograms illustrate SpA-488 and OVA-488 binding in the presence and absence of IgG binding profiles to monocytes in the blood. (B) The mean \pm SD MFI values for SpA-488 and OVA-488 binding in the presence and absence of IgG binding profiles to monocytes in the blood. This experiment was carried out on two separate occasions; the data were pooled together for purposes of statistical analysis (SpA N=6, OVA N=6). *** = $P < 0.001$, by *one-way anova and post hoc Bonferroni*.

4.2.3 SpA treatment for 24hrs under non-inflammatory conditions leads to a shift in the blood monocyte population

Having established that SpA binds to monocytes in the blood and bone marrow in the presence of IgG, the next step was to examine if there was any effect on the monocyte population *in vivo* under steady-state conditions. C57BL/6 mice were treated with 600 μ g of SpA or OVA for 24h before they were euthanized, and blood (figure 4.5) and bone marrow (data not shown) harvested and prepared for flow cytometric analysis.

Monocytes were defined as CD11b⁺, Gr1^{low/-}, Ly6C⁺ and then sub-divided into CD11b⁺, Gr1^{low}, Ly6C^{hi} or CD11b⁺, Gr1⁺, Ly6C^{low} populations; and the two populations can be seen clearly in the representative histogram and FACS plots (figure 4.5A). It was observed that in comparison to the control group (OVA), SpA treatment resulted in a significant decrease in the Ly6C^{hi} population with a concurrent increase in the Ly6C^{low} population (figure 4.5B). This suggests that SpA treatment could be promoting the differentiation of Ly6C^{hi} monocytes into Ly6C^{low} monocytes. As discussed in the introduction to this chapter and in section 1.3.3, Ly6C^{hi} monocytes are termed the inflammatory sub-set and have a short half-life in the blood. If they do not migrate to a site of inflammation where they can differentiate into a macrophage or DC, Ly6C^{hi} monocytes will mature into Ly6C^{low} monocytes. The previous data would suggest that SpA accelerates this natural process.

In addition to looking at the expression of Ly6C, other relevant cell surface markers were also investigated e.g. Fc γ RI, which is essential for SIC binding in BMDM (Section 3.2.6). Evaluation of CD64 (Fc γ RI) expression after SpA treatment demonstrated that it was significantly down-regulated on both monocyte subsets (figure 4.5C). Furthermore, Gr1 was also significantly down-regulated in the Ly6C^{hi} SpA treatment group when compared to the OVA control group (figure 4.5D). It is of interest to note that the Ly6C^{hi} monocyte population starts to down-regulate its Gr1 expression in the presence of SpA - leading to the assumption that SpA is inducing the Ly6C^{hi} monocyte to mature into a Ly6C^{low}-like population - as Gr1 is not expressed on the latter population.

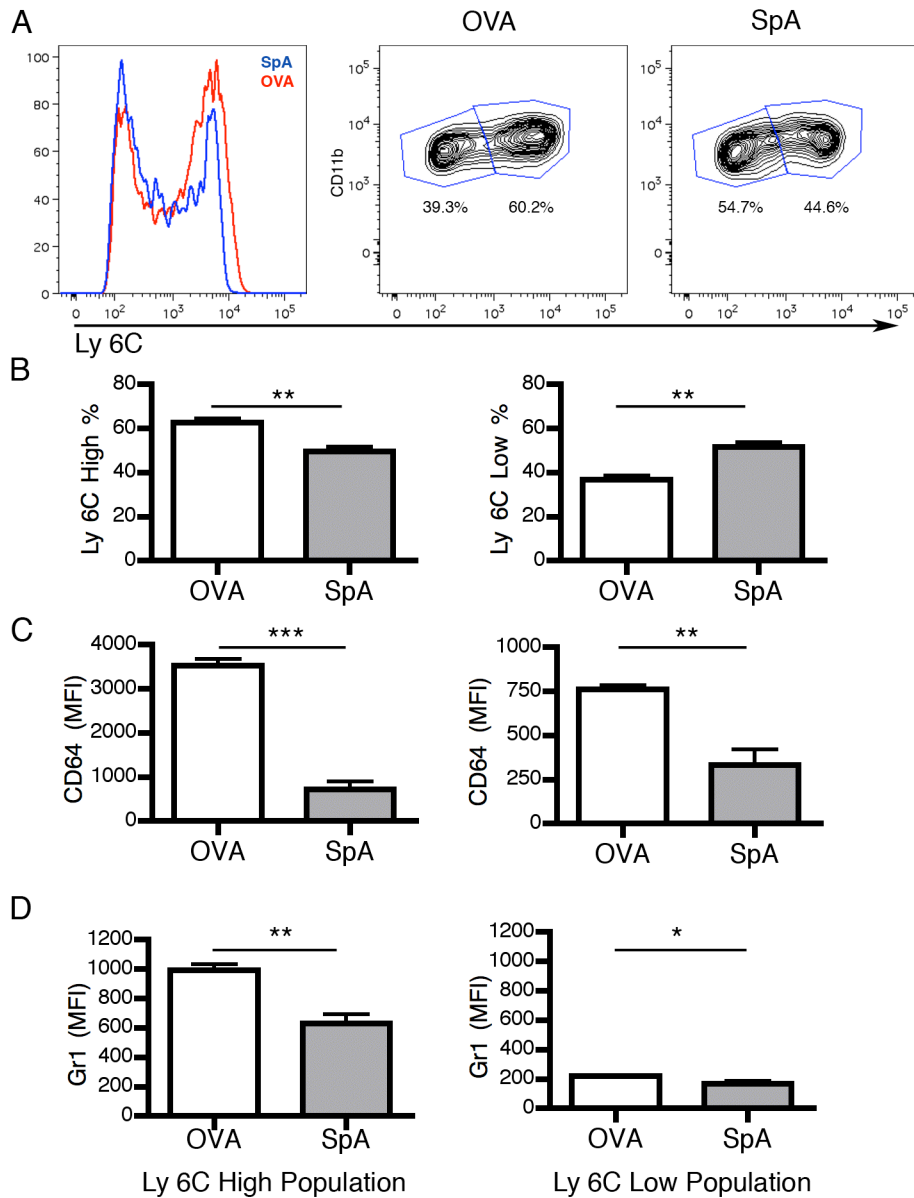


Figure 4.5. SpA treatment for 24h under non-inflammatory conditions leads to a shift in the blood monocyte population.

C57BL/6 mice received either 600 μ g of SpA or OVA i.p. After 24h mice were culled and blood was harvested and prepared for flow cytometric analysis. Data were analysed by a two-tailed, unpaired *t*-test, * = $P < 0.05$; ** = $P < 0.01$; *** = $P < 0.001$. (A) A representative histogram (OVA - red line, SpA - blue line) and FACS plots of the Ly6C^{hi} and Ly6C^{low} monocyte subsets in the blood from each treatment group. (B) The mean \pm SD % for Ly6C^{hi} $T_{10} = 4.69$, $P < 0.0015$ (left panels) and Ly6C^{low} $T_{10} = 4.53$, $P < 0.0019$ (right panels) monocyte populations in the blood. (C) The mean \pm SD MFI values of CD64 for Ly6C^{hi} $T_{10} = 12.39$, $P < 0.0002$ (left panels) and Ly6C^{low} $T_{10} = 4.76$, $P < 0.01$ (right panels) monocyte. (D) The mean \pm SD MFI values for Gr1 for Ly6C^{hi} $T_{10} = 2.98$, $P < 0.041$ (left panels) and Ly6C^{low} (right panels) monocyte populations. This experiment was carried out on two separate occasions; the data were then pooled together for purposes of statistical analysis. The two experiments had a total N of; SpA N=6 and OVA N=6.

4.2.4 FcγRIII and SpA

The binding studies performed in chapter three showed that SIC interacts with and operates via FcγRs - predominantly FcγRI - polarizing bone marrow-derived macrophages to an IL-10-producing anti-inflammatory phenotype. Unfortunately, FcγRI^{-/-} mice could not be obtained to investigate SpAs interaction with FcγRI in an *in vivo* setting. However, FcγRIII^{-/-} mice were available and these were used instead. Studies have shown that FcγRIII plays a role in the anti-inflammatory properties of IVIg in the resolution of inflammation. Bone marrow-derived macrophages exhibited reduced ROS production, endocytosis and phagocytosis via ITAMi activity, which is the inhibitory signalling component of the Fcγ receptor²⁰³. Since FcγRIII has been implicated in the mechanism of IVIg, it was decided to investigate whether FcγRIII is one of the receptors responsible for the change in phenotype of the monocyte population after treatment with SpA.

FcγRIII^{-/-} mice were injected with 600μg of SpA or OVA for 24h before the mice were culled; blood was then harvested and prepared for flow cytometric analysis. The two-monocyte sub-populations were gated as described in section 4.2.3. The same phenotypes present in blood monocytes of C57BL/6 mice (figure 4.5) after SpA treatment for 24h were seen in the FcγRIII^{-/-} with a shift in the Ly6C^{hi} to Ly6C^{low} monocyte population (figure 4.6A&B). CD64 (figure 4.6C) and Gr1 (figure 4.6D) were also down-regulated in the FcγRIII^{-/-} blood monocyte populations. This led to the conclusion that FcγRIII is not vital to the mechanism by which SpA regulates the change of Ly6C^{hi} monocytes in the blood.

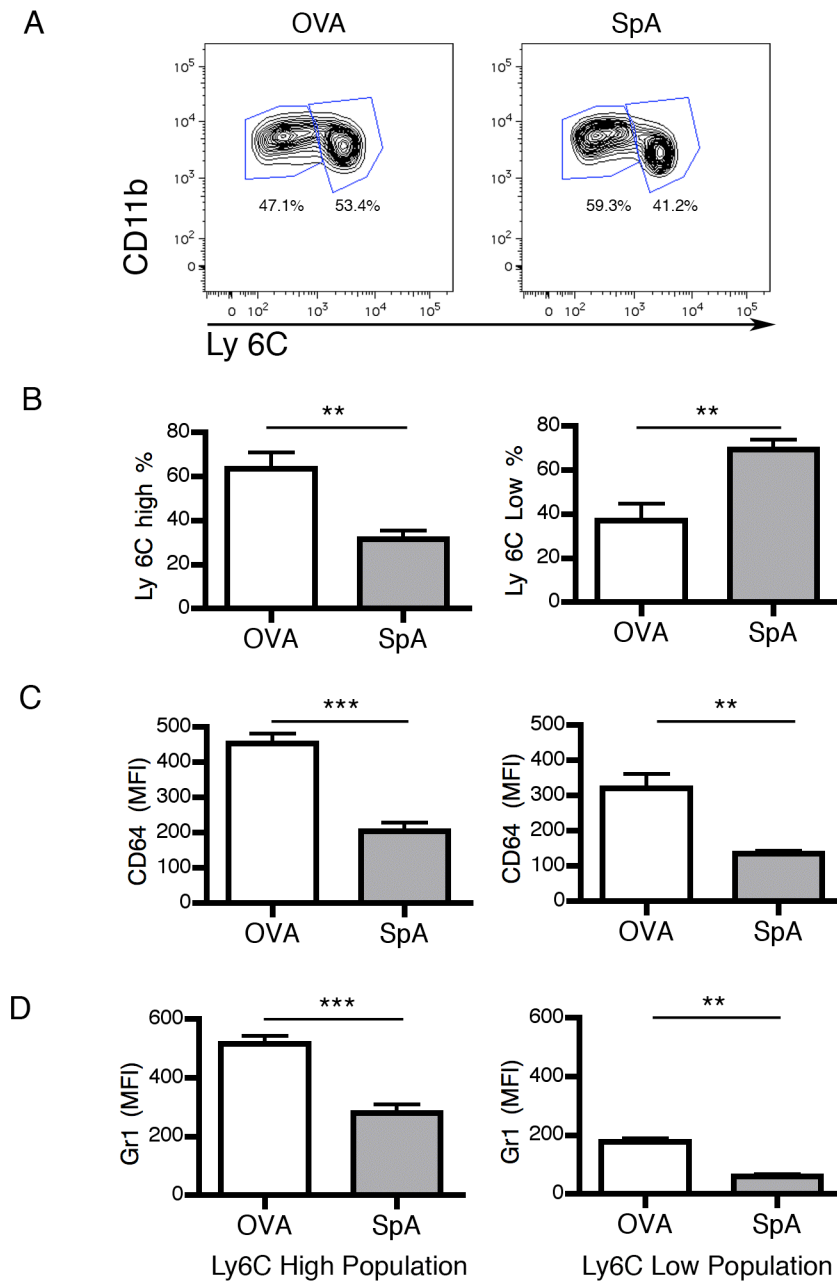


Figure 4.6. Fc γ RIII is not involved in SpAs ability to induce Ly6C^{hi} monocytes maturation to Ly6C^{low} monocytes in the blood.

Fc γ RIII^{-/-} mice received either 600 μ g of SpA or OVA i.p. After 24h mice were culled and blood was harvested and prepared for flow cytometric analysis on the LSR II. Data were analysed by a two-tailed, unpaired *t*-test, ** = *P*<0.01; *** = *P*<0.001. (A) Representative FACS plots of the Ly6C^{hi} and Ly6C^{low} monocyte subsets in the blood from each treatment group. (B) The mean \pm SD % for Ly6C^{hi} (T_5 = 4.18, *P*<0.0086, left panels) and Ly6C^{low} (T_5 = 4.04, *P*<0.0099, right panels) monocyte populations in the blood. (C) The mean \pm SD MFI values of CD64 for Ly6C^{hi} (T_5 = 6.97, *P*<0.0009 (left panels) and Ly6C^{low} (T_5 = 5.35, *P*<0.0031, right panels) monocytes. (D) The mean \pm SD MFI values of Gr1 for Ly6C^{hi} (T_5 = 8.94, *P*<0.0003, left panels) and Ly6C^{low} (T_5 = 6.01, *P*<0.0018 (right panels) monocyte populations. This experiment was carried out on two separate occasions that showed the same results: the data shown is a representative figure of one of these experiments. The experiment shown has an N of; SpA N=5 and OVA N=6. The two experiments had a combined total N of; SpA N=10 and OVA N=11.

4.2.5 SpA-488 cannot penetrate the blood-brain barrier and interact with cells in the undamaged spinal cord

The data thus far suggest that SpA induces the differentiation of the Ly6C^{hi} inflammatory monocyte subset to the Ly6C^{low} patrolling/anti-inflammatory subset in the steady-state. The ability of SpA to modulate cells of the myeloid lineage in an inflammatory environment was now investigated. To do this, the impact of SpA-mediated monocyte modulation in SCI was examined - as high levels of infiltration by monocytes are seen in the early stages of SCI. It was hypothesized that if the balance of inflammatory monocytes could be shifted to a regulatory phenotype this might reduce the amount of neuronal death that is attributed to the secondary death phenomenon seen after SCI.

The first questions to be addressed was whether SpA could pass-through the blood-brain barrier in an undamaged spinal cord and thereafter interact with cells in this microenvironment. To examine this, the same technique used in section 4.2.1 was employed here. In brief, 500 μ g of SpA-488 or OVA-488 were injected i.p into C57BL/6 mice and left for 2h; mice were culled, exsanguinated and perfused with PBS. This method was employed to make sure minimal blood cell contamination occurred in the spinal cord. The spinal cords were then harvested and prepared for flow cytometric analysis.

DAPI was used to gate out dead cells (not shown), and CD45 used to locate the leukocyte population in the spinal cord (figure 4.7A). The majority of the CD45⁺ cells present in the un-damaged cord were microglia (92.5% \pm 1.4) - defined as CD45^{int} CD11b⁺. When the CD45^{hi} and CD45^{int} population were gated, in both the control and SpA-488 group, there were only background levels of fluorescent binding (figure 4.6B). Thus, it can be concluded that SpA-488 cannot enter an un-damaged spinal cord due to the presence of the blood-brain barrier.

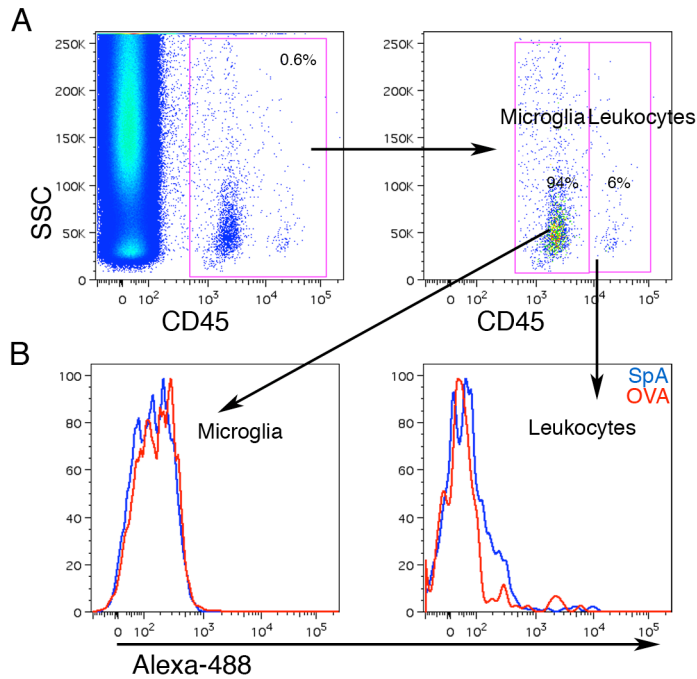


Figure 4.7. SpA cannot cross the intact blood-brain barrier to interact with cells within the spinal cord.

C57BL/6 mice received either 500 μ g of SpA-488 or OVA-488 i.p. After a further 2h mice were culled and spinal cord was harvested and prepared for flow cytometric analysis. (A) Gating strategy for un-damaged spinal cord, live/dead cell exclusion is performed first on samples (not shown), followed by CD45⁺ selection. Microglia are then distinguished as CD45^{int} and all other leukocytes are gated as CD45^{hi}. (B) Representative leukocyte and microglia histograms of SpA-488 (blue line) and OVA-488 (red line) binding. This experiment was carried out on three separate occasions. The total N number for all three experiments is; SpA N=8, OVA N=9.

4.2.6 SpA-488 interactions in the damaged spinal cord

When the blood-brain barrier is intact, SpA is unable to bind to cells within the spinal cord (Figure 4.7). However, physical disruption to the barrier should facilitate entry of SpA and allow interaction with myeloid cells in the spinal cord microenvironment. To generate SCI, mice received a contusion injury of 100Kdyn to the C5/C6 border of the spinal cord (see methods section 2.10); 24h later mice were injected i.p with 500µg of SpA-488 or OVA-488 and left for a further 2h. Mice were euthanized and the damaged spinal cord sections (figure 4.8) were then harvested along with blood (figure 4.9) and prepared for flow cytometric analysis to look at the SpA-488 binding profile in comparison to the binding profile of SpA-488 in the non-injured mice (figure 4.7).

Gating of the damaged spinal cord cells was carried out as described in the undamaged spinal cord (section 4.2.5). The proportion of the CD45⁺ population found in the damaged spinal cord was vastly different from the undamaged spinal cord with 58.4% ± 6.8 being CD45^{hi} cells- in comparison to the undamaged cord of only 7.4% ± 1.4 cells, which is a very statistically significant change ($P < 0.0001$). The CD45^{hi} cell population was analysed further to determine composition (figure 4.8A). This revealed that, as expected, both neutrophils (CD11b^{hi}, Gr1⁺ and Ly6C⁻) and monocytes (CD11b^{hi}, Gr1⁺ and Ly 6C⁺) were present in the spinal cord.

Evaluation of SpA-488 binding in the monocyte, neutrophil and microglial populations (CD45^{int}, CD11b^{int} and Ly6C⁻) were determined (Figure 4.8B&C) - concluding that monocytes and microglia showed significantly higher binding of SpA-488 than the control protein OVA-488. In the microglia population, MFI values demonstrated that SpA-488 had a mean ±SD of 670 ±81 compared to just 231 ±22 in the OVA-488 group. Microglia are a branch of the myeloid cell lineage and as such are said to be the “macrophages of the CNS”, so it was to be expected that these cells would interact with SpA-488. Monocyte MFI mean ± SD for SpA-488 binding was 1547 ± 341 in comparison to that of the control protein of 256 ± 48. With regard to the neutrophils, although we saw significant binding of SpA-488 in comparison with the OVA-488 control (Figure 4.8C), as can be seen in the histogram (Figure 4.8B), this represented a small population skewing the

MFI value. It is possible that this was due to a very small proportion of monocytes being present in the neutrophil gate.

The SpA-488 binding profile in blood of the injured mice was also examined (figure 4.9) and interestingly, this confirmed previous findings shown in the blood of the uninjured mice (figure 4.2). SpA-488 binds significantly more than control protein (OVA-488) to the total monocyte population as well as to the two sub-populations (Figure 4.9B) and the neutrophil population (Figure 4.9B). In the neutrophil population, the mean \pm SD MFI of SpA-488 is 280 ± 27 , which is a 10-fold decrease in comparison to monocytes' ability to bind to SpA-488, which have an mean \pm SD MFI of 3574 ± 609 . A detailed analysis of SpA-488 binding (mean \pm SD MFI) to a variety of myeloid cells within the damaged portion of the spinal cord, blood and bone marrow after SCI is presented in Appendix 3. It can be concluded therefore that SpA-488 can bind to microglia and monocytes in the spinal cord but only when the blood-brain barrier has been compromised.

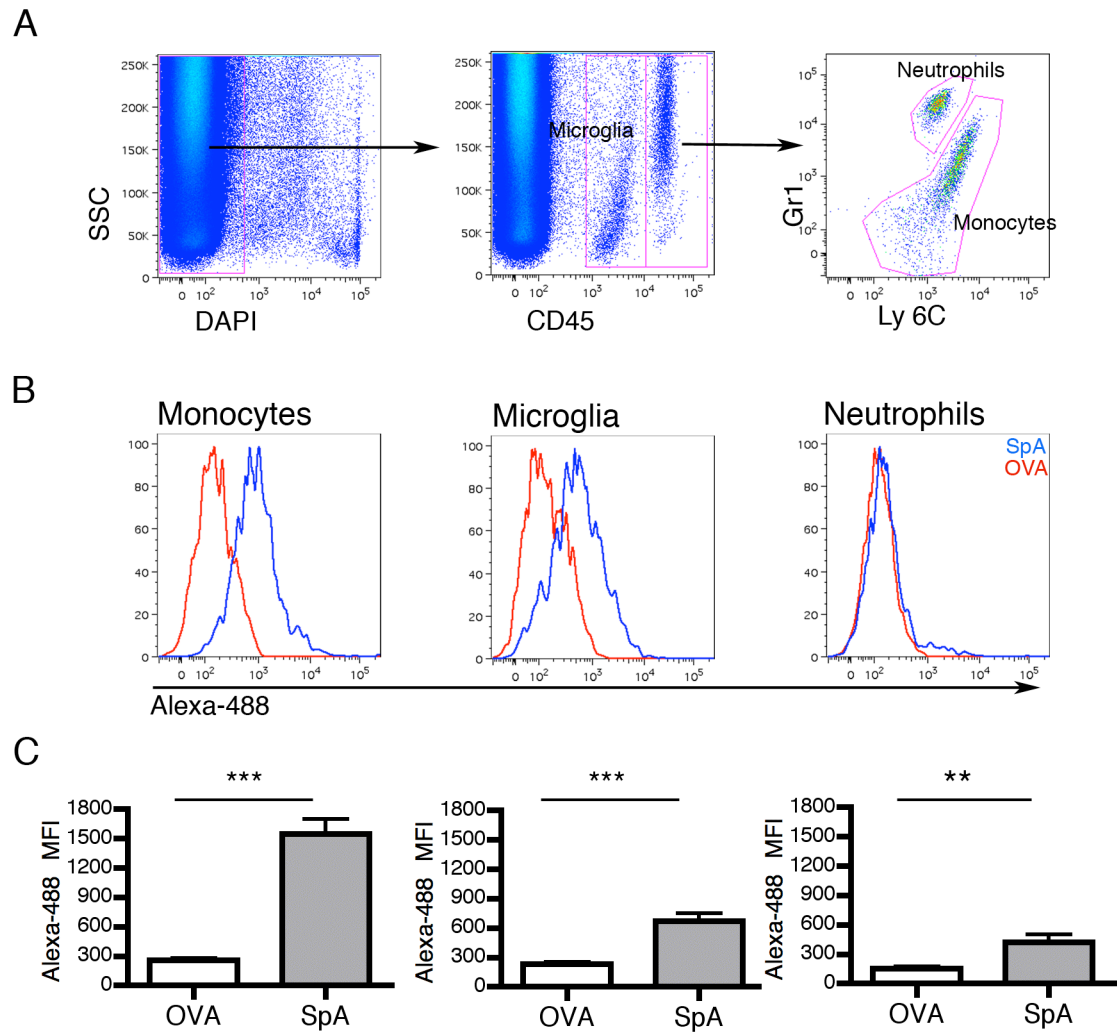


Figure 4.8. SpA-488 can bind to cells within a damaged spinal cord.

C57BL/6 mice received SCI at the C5/6 border. 24h after injury mice received either 500 μ g of SpA-488 or OVA-488 i.p. After a further 2h mice were culled and spinal cords were harvested and prepared for flow cytometric analysis. Data were analysed by a two-tailed, unpaired *t*-test, ** = $P < 0.01$; *** = $P < 0.001$. (A) Gating strategy for the damaged spinal cord. (B) Representative histograms depicting SpA-488 (blue) and OVA-488 (red) binding to monocytes, microglia and neutrophils. (C) The mean \pm SD MFI values for SpA-488 and OVA-488 binding to monocytes ($T_8 = 3.41$, $P < 0.01$), microglia ($T_8 = 5.24$, $P < 0.0008$) and neutrophils ($T_8 = 8.94$, $P < 0.0003$). This experiment was carried out on two separate occasions; the data were then pooled together for purposes of statistical analysis. The two experiments had a total N of; SpA N=5 and OVA N=5.

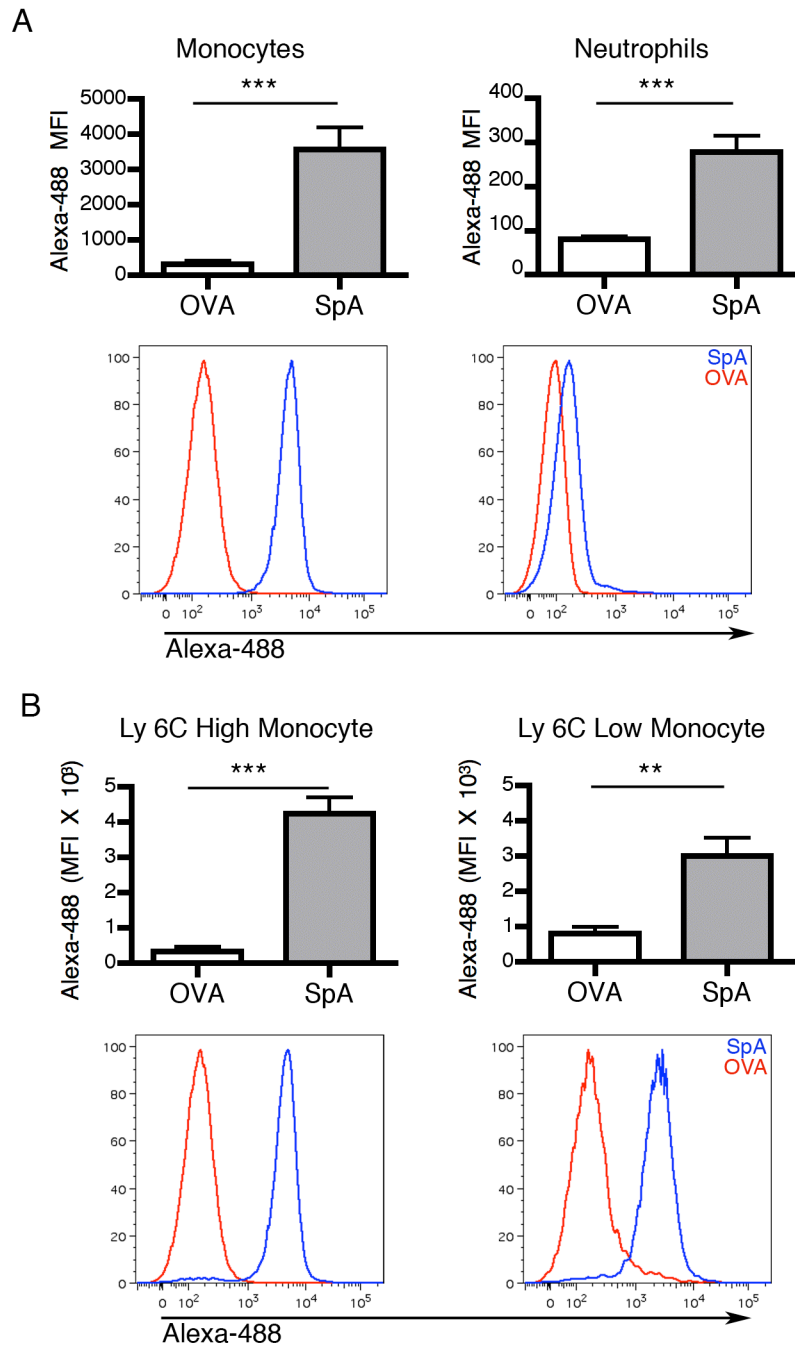


Figure 4.9. SpA-488 binding profile in blood monocytes and neutrophils after SCI.

C57BL/6 mice received SCI at the C5/6 border. 24h after injury mice received either 500 μ g of SpA-488 or OVA-488 i.p. After a further 2h mice were culled and blood was harvested and prepared for flow cytometric analysis on the MACS Quant. Data were analysed by a two-tailed, unpaired *t*-test, ** = $P < 0.01$; *** = $P < 0.001$. (A) The mean \pm SD MFI values for SpA-488 and OVA-488 binding for blood monocytes ($T_8 = 5.27$, $P < 0.0008$, left panels) and neutrophils ($T_8 = 7.13$, $P < 0.0001$, right panels) with representative histogram plots below; SpA – blue line, OVA – red line. (B) The mean \pm SD MFI values for Ly6C^{hi} ($T_8 = 8.24$, $P < 0.0001$, right panels) and Ly6C^{low} ($T_8 = 4.08$, $P < 0.0035$, left panels) monocyte populations, binding with representative histogram plots below; SpA – blue line, OVA – red line. This experiment was carried out on two separate occasions; the data were then pooled together for purposes of statistical analysis. The two experiments had a total N of; SpA N=5 and OVA N=5.

4.2.7 24hr treatment with SpA has an effect on the infiltrating monocyte populations after SCI

It has already been established that SpA can bind to cells in the damaged spinal cord. The next task was to examine if SpA treatment had an effect on the myeloid cell populations found in the damaged spinal cord after treatment. To do this, mice received 100Kdyn contusion injuries at the C5/6 border of the spinal cord. After a recovery period of 24h, mice then received 600µg of either SpA or OVA by i.p injection. After a further 24h, mice were euthanized and blood (figure 4.11), bone marrow (data not shown) and the damaged portion of the spinal cord (figure 4.10) were harvested and prepared for flow cytometric analysis.

The monocyte population showed an altered phenotype after 24h treatment with SpA, and this included changes in the sub-populations Ly6C^{hi} and Ly6C^{low}, which make up the total monocyte population. Analysis demonstrated that the Ly6C^{hi} inflammatory monocyte subset was significantly decreased after SpA treatment (figure 4.10A&B) - whereas, the Ly 6C^{low} monocyte subset was significantly increased (figure 4.10A&B). Further investigation of CD64 (figure 4.10C) and Gr1 (figure 4.10D), in a subsequent experiment, showed a substantial down-regulation of both markers after SpA treatment. It should be appreciated, however, that due to fatalities in surgery and time restraints, only 2 mice pre-group were evaluated and therefore statistical tests could not be performed. In support of this finding, the results showed a similar phenotype to those exhibited in the blood of uninjured mice that were treated with SpA for 24h (figure 4.5). However, the microglial and neutrophil populations within the damaged spinal cord exhibited no observable phenotypic variations after 24h treatment with SpA - in comparison to the control treated group (data not shown).

Furthermore, evaluation of the circulating monocytes in the blood of SCI mice (Figure 4.11) confirmed the altered phenotype in the myeloid compartment. SpA treatment significantly decreased the Ly6C^{hi} monocyte population while significantly increasing the Ly6C^{low} monocytes (figure 4.11 A&B). This outcome was also associated with the down-regulation of CD64 (figure 4.11C) and Gr1

(figure 4.11D). Once again, statistical analysis could not be performed on CD64 and Gr1 levels because, as previously described, only two mice could be evaluated. These data therefore suggest that SpA treatment 24h after SCI is inducing the maturation of the Ly6C^{hi} inflammatory monocytes to the Ly6C^{low} monocytes, which are assumed to be of an anti-inflammatory or regulatory nature.

4.2.8 IL-10, SCI and SpA

SpA treatment for 24h has been shown in section 4.2.7 to modify the monocyte population within the damaged spinal cord to a predominately Ly6C^{low} monocytes population. This is an interesting finding as Ly6C^{low} monocytes are said to differentiate into regulatory or tissue-repair macrophages within an inflammatory environment. SpA has also been shown to promote bone marrow-derived macrophages to an anti-inflammatory phenotype when stimulated in conjunction with LPS, with significantly higher IL-10 (one of the main immunomodulatory cytokines of the immune system) and significantly decreased IL-12 (pro-inflammatory cytokine) production when compared to controls. Hence, it was of interest to examine if SpA treatment after SCI would induce the infiltrating monocyte population to produce IL-10 and be truly polarized to a regulatory or tissue-repair phenotype after SpA treatment - as well as having decreased Ly6C surface expression.

Vert-X mice are IL-10 reporter mice, and have a GFP (green fluorescent protein) reporter gene linked to the IL-10 promoter - leading to the production of GFP when the cell is induced to produce IL-10. This allows the quantification of IL-10 production at an individual cell level by the correlation of the amount of fluorescence each cell exhibits. SCI was induced in the Vert-X mice and after 24h of recovery, mice were i.p. injected with SpA or OVA. Twenty-four hours later mice were euthanized and blood and the damaged portion of the SC were removed and prepared for flow cytometric analysis.

The same monocyte phenotype that was noted previously in the damaged SC (figure 4.10A) after SpA treatment was also seen in the Vert-X mice, with the consequential reduction of Ly6C^{hi} monocyte population and an increase in the Ly6C^{low} monocyte subset (figure 4.12A).

In the OVA treatment group, 49.7% of the population of monocytes in the damaged spinal cord produced IL-10, which concurs with recent literature that there will be 50% of inflammatory and regulatory macrophages/monocytes present 3-4 days post-injury¹³³; after this point the authors saw an exponential increase in inflammatory macrophages. In the SpA treatment group, 68.5% of the population expressed IL-10. The Ly6C^{hi} monocytes population predominantly seen in the control group did not produce any IL-10, corroborating their status as being the inflammatory subset of monocytes. The entire population of Ly6C^{low} monocytes, which were the predominant population in the damaged spinal cord of the SpA treatment group, produced IL-10, confirming their status as the regulatory subset. It is interesting to note that monocytes in the blood in both treatment groups did not express any IL-10. This finding is most likely due to a lack of tissue-specific signal to induce the production of IL-10.

Again, due to technical issues with the contusion surgery there was only N=1 per group for this experiment. Furthermore, there was an outbreak of pseudomonas in the facility that breeds the Vert-X mice colonies, resulting in the colony having to be culled. The Vert-X mouse line has not yet been re-derived, therefore, as a consequence this experiment has not been repeated. The above result has been added here only as an interesting observation, and will have to be repeated before statistical analysis can be performed and any conclusions drawn.

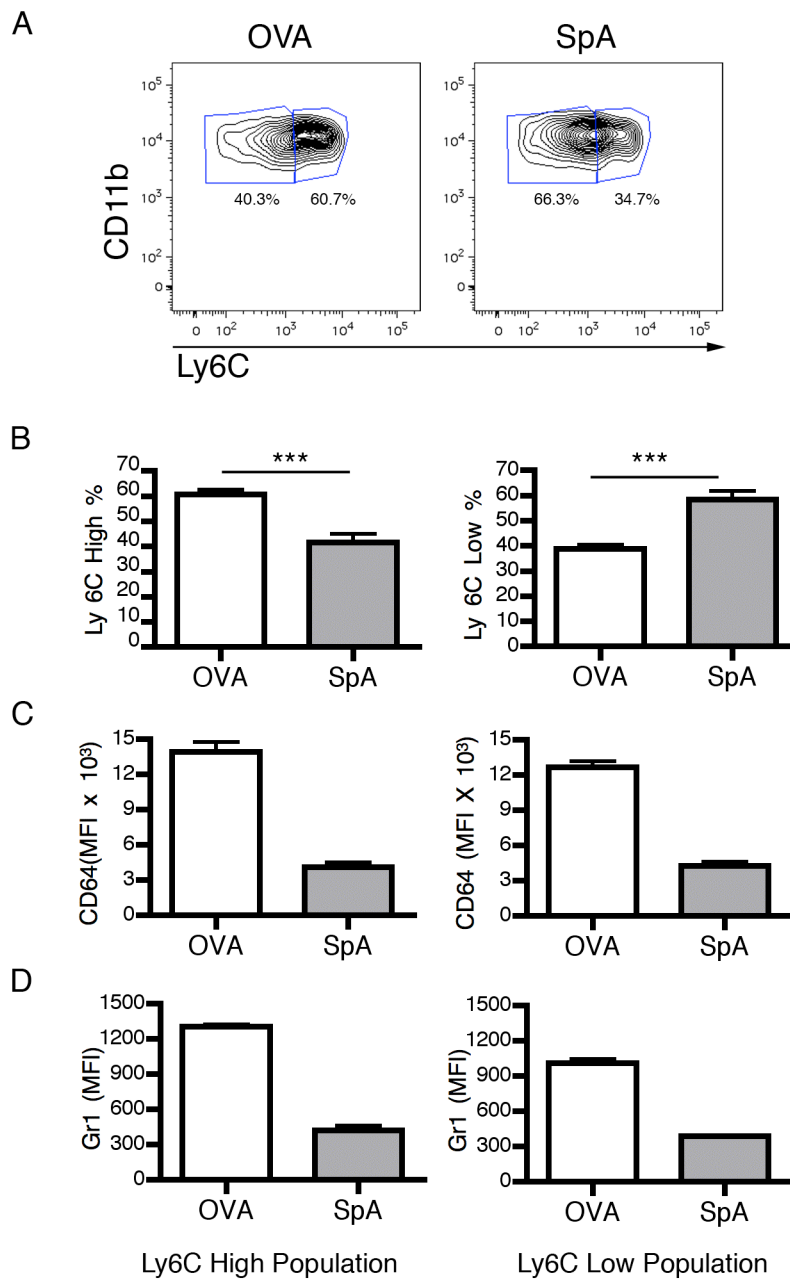


Figure 4.10, 24h treatment with SpA alters the infiltrating monocyte populations after SCI.

C57BL/6 mice received contusion at the C5/6 border. 24h post-injury mice received either 600 μ g of SpA or OVA i.p. After a further 24h mice were culled and spinal cords were harvested and prepared for flow cytometric analysis. Data were analysed by a two-tailed, unpaired *t*-test, *** = $P < 0.001$. (A) Representative image of the monocyte population within the damaged spinal cord of a SpA and control group. (B) The mean \pm SD % for Ly6C^{hi} ($T_{10} = 5.29$, $P < 0.0004$, left panels) and Ly6C^{low} ($T_{10} = 5.33$, $P < 0.0003$, right panels) monocyte populations in the damaged spinal cord. (C) The mean \pm SD MFI values of CD64 for Ly6C^{hi} (left panels) and Ly6C^{low} (right panels) monocyte. (D) The mean \pm SD MFI values of Gr1 for Ly6C^{hi} (left panels) and Ly6C^{low} (right panels) monocyte populations. This experiment was carried out on two separate occasions; the data were then pooled together for purposes of statistical analysis. The two experiments had a total N of; SpA N=6 and OVA N=6. CD64 & Gr1 were not introduced until the second experiment; due to fatalities in surgery sample size was too small to perform statistical analysis (SpA N=2, OVA N=2).

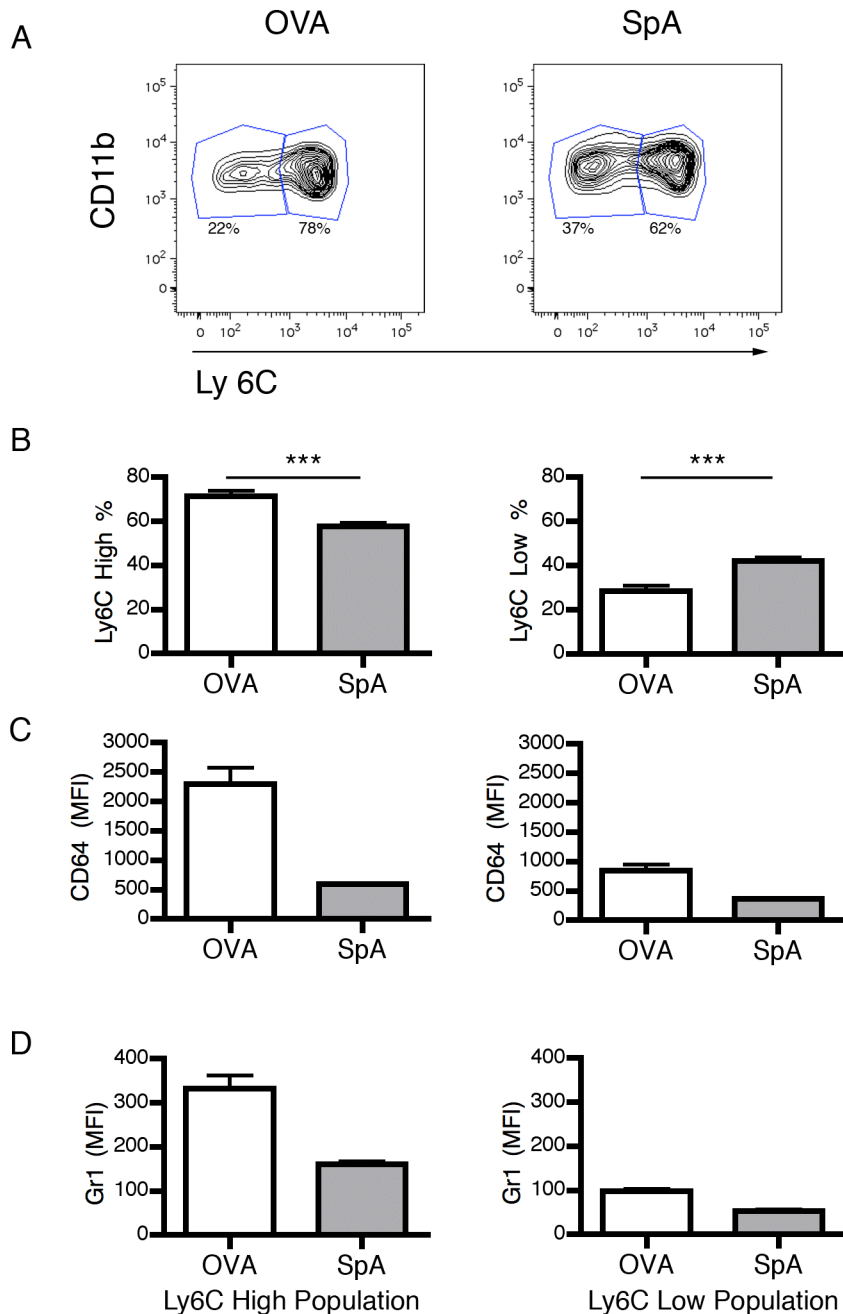


Figure 4.11, 24h treatment with SpA alters the blood monocyte populations after SCI.

C57BL/6 mice received a contusion injury at the C5/6 border. 24h post-injury mice received either 600 μ g of SpA or OVA i.p. After a further 24h, mice were culled and spinal cords were harvested and prepared for flow cytometric analysis. Data were analysed by a two-tailed, unpaired *t*-test, *** = $P < 0.001$. (A) Representative FACS plots of the Ly6C^{hi} and Ly6C^{low} monocyte subsets in the blood from each treatment group. (B) The mean \pm SD % for Ly6C^{hi} ($T_{10} = 4.71$, $P < 0.0008$, left panels) and Ly6C^{low} ($T_{10} = 4.66$, $P < 0.0009$, right panels) monocyte populations in the blood after SCI. (C) The mean \pm SD MFI values of CD64 for Ly6C^{hi} (left panels) and Ly6C^{low} (right panels) monocyte. (D) The mean \pm SD MFI values of Gr1 for Ly6C^{hi} (left panels) and Ly6C^{low} (right panels) monocyte populations. This experiment was carried out on two separate occasions; the data were then pooled together for purposes of statistical analysis. The two experiments had a total N of; SpA N=6 and OVA N=6. CD64 & Gr1 were not introduced until the second experiment; due to fatalities in surgery sample size was too small to perform statistical analysis (SpA N=2, OVA N=2).

To validate if SpA was in fact inducing IL-10 production in these mice, BMDM were generated from Vert-X mice (as described in section 2.2). On day 6, the BMDM were plated out at a concentration of 1.5×10^6 cells in 3ml of complete media in 6 well plates and left overnight to adhere. On day 7, the macrophages were treated with SIC or IgG at $25 \mu\text{g}/\text{ml}$ with or without $100 \text{ng}/\text{ml}$ of LPS for 6h. Only enough cells were generated to have 1 well per condition. Medium was removed and cells scraped off the plates; flow cytometric analysis was carried out to look at GFP expression, which correlates to IL-10 production in the cells.

The treatment of SIC and LPS in combination leads to superior IL-10 production from the Vert-X macrophages in comparison to the controls (figure 4.13A), which was also shown in chapter 3 by IL-10 ELISA when this experiment was performed with C57BL/6 mice. CD64, another marker that has been shown in previous experiments to be down-regulated with SpA treatment *in vivo*, was also down-regulated with SIC treatment. Unlike IL-10, this occurred in the presence or absence of LPS. In chapter 3 it was demonstrated that CD64, also known as Fc γ RI, was essential for SIC's ability to polarize BMDM to an anti-inflammatory phenotype. The observations made in figures 4.12 and 4.13 are extremely interesting and indicate that SpA is inducing monocytes to differentiate and mature into a regulatory or anti-inflammatory macrophage population that has the ability to produce IL-10. However, the results are only of an observational nature due to the small 'n' and must be repeated so statistical analysis can be performed before any definitive conclusions are drawn from this data set.

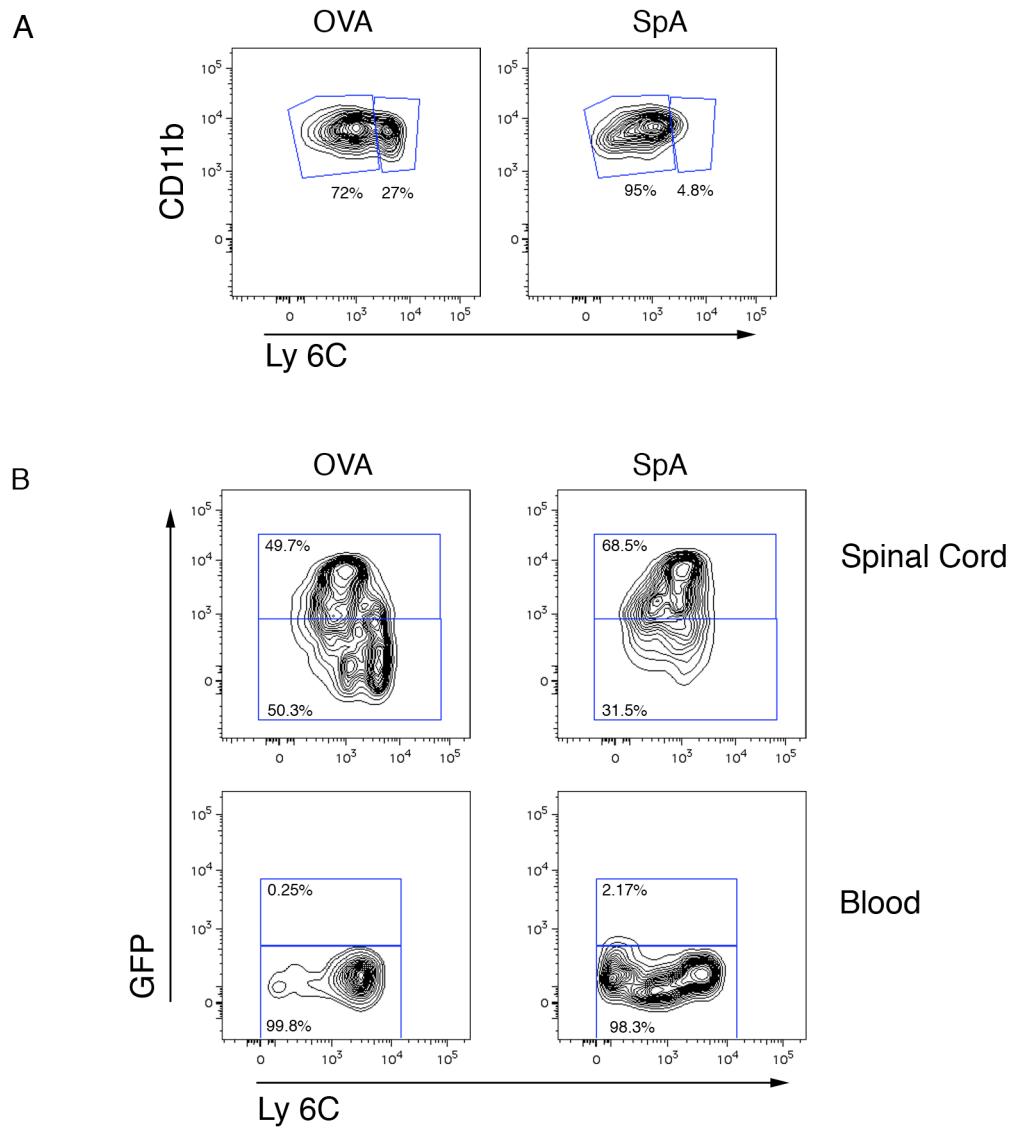


Figure 4.12, Does SpA treatment induce monocytes to become polarized to an IL-10 producing phenotype in the context of SCI?

Vert-X mice received SCI at the C5/6 border; 24h later mice received either 600 μ g of SpA or OVA i.p. After a further 24h mice were culled and blood and spinal cord were harvested and prepared for FACS analysis. (A) Shows Ly6C^{high} and Ly6C^{low} monocyte subsets in the damaged spinal cords of an OVA and a SpA treated mouse. (B) Shows the total spinal cord and blood monocyte populations and their expression of IL-10 after OVA or SpA treatment. (SpA N=1, OVA N=1).

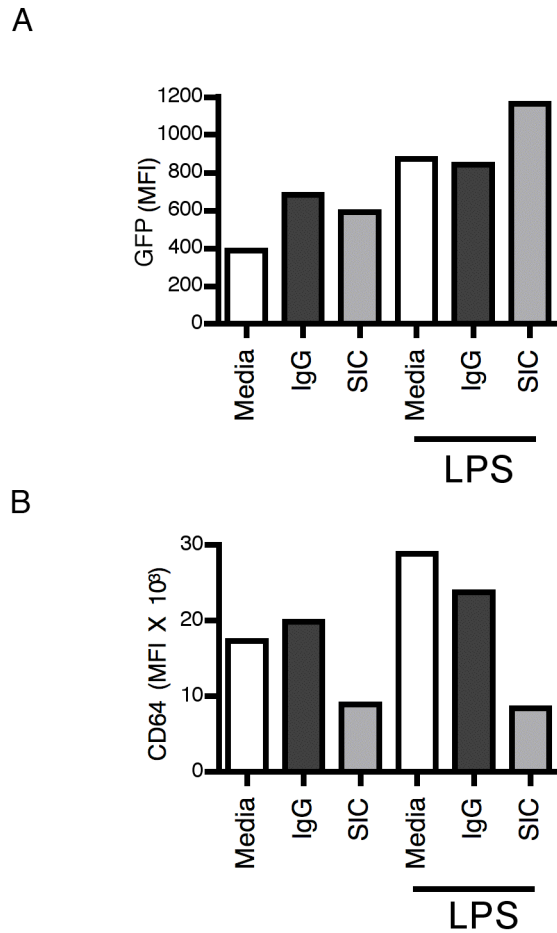


Figure 4.13, Does SIC have the ability to induce BMDM from Vert-X mice to produce IL-10 in vitro?

Bone marrow was taken from Vert-X mouse and BMDM were generated using L929 supernatant containing M-CSF. On day 6, BMDM were re-seeded in 3ml in 6 well plates at a concentration of $0.5 \times 10^6/1\text{ml}$ and left to adhere overnight. On day 7, cells were treated with SIC or IgG, with or without LPS (100ng/ml) for 6hrs. BMDM were then scraped off the plate and stained for FACS analysis. (A) Shows IL-10 GFP MFI and (B) Shows CD64 MFI. This experiment was only carried out once. (N=1 for all conditions)

4.2.9 SpA is inducing Ly6C^{hi} monocytes to differentiate into Ly6C^{low} monocytes

SpA treatment for 24h under steady-state or inflammatory conditions leads to a shift in the circulating monocyte population - whereby a decrease in the Ly6C^{hi} subset and an increase in the Ly6C^{low} subset is observed. It has been hypothesised that this shift is due to the Ly6C^{hi} monocyte population down-regulating its Ly6C expression. The differentiation of Ly6C^{hi} monocytes into Ly6C^{low} monocytes has been previously described and involves the homing of circulating Ly6C^{hi} monocytes back to the bone marrow, due to a lack of encounter with an inflammatory signal in the periphery. The newly-differentiated Ly6C^{low} monocytes are then released back into the circulation as patrolling monocytes⁴⁸.

In this model of SpA treatment, the ratio of Ly6C^{hi} monocytes to Ly6C^{low} monocytes was altered in the blood and in the damaged spinal cord (which is a highly inflammatory site). The hypothesis is that this is due to monocyte differentiation but an alternative possibility is that the change in monocyte subsets after SpA treatment is due to the trafficking of Ly6C^{hi} cells into other compartments, which artificially increases the Ly6C^{low} population in the blood and the damaged spinal cord. The aim of this series of studies was to test the hypothesis that SpA treatment induces the differentiation of Ly6C^{hi} monocytes into Ly6C^{low} monocytes.

CX₃CR1 is the membrane-bound receptor of the chemokine Fractalkine; it is one of the key markers for defining the monocyte population subsets (along with Ly6C). Ly6C^{hi} monocytes express intermediate levels of CX₃CR1, whereas Ly6C^{low} monocytes express high levels of CX₃CR1. CX₃CR1^{GFP} transgenic mice have already been generated. In these mice, one allele of the Fractalkine receptor was removed and replaced with the gene for GFP⁴⁰. To test the above-mentioned hypothesis, an adoptive transfer system was employed with the use of the CX₃CR1^{GFP} mice. 20 of these mice were euthanized. The hind legs were removed and bone marrow cells were flushed out. Bone marrow cells were then filtered through nitex and stained with the phenotypic markers Ly6C, Gr1, CD11b and C-kit. This combination of antibodies allows the isolation of Ly6C^{hi} monocytes by flow cytometric cell sorting (figure 4.14).

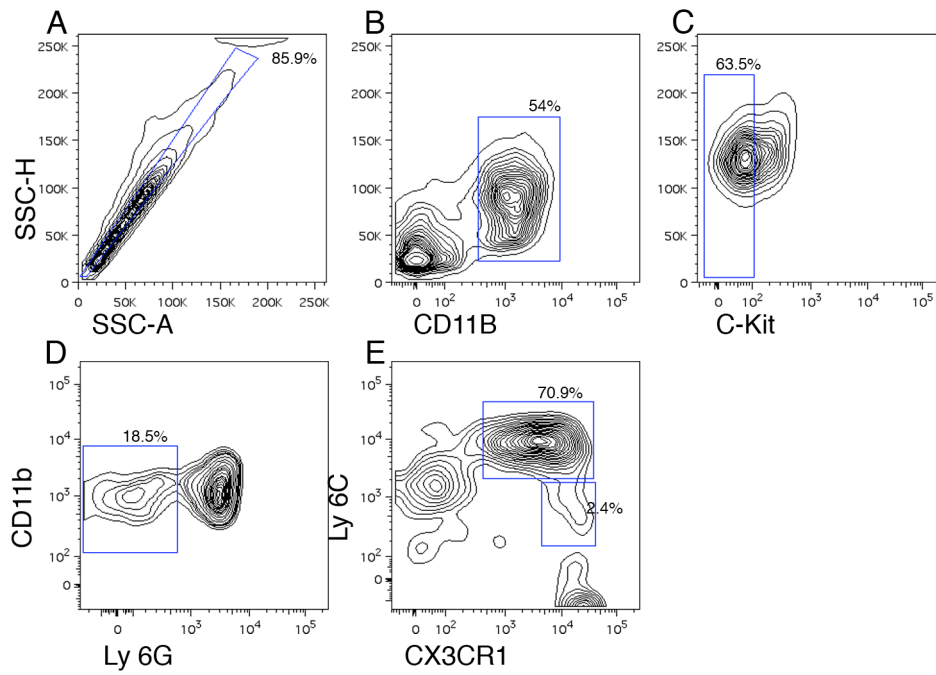


Figure 4.14, Gating strategy for isolation of Ly6C^{hi} GFP^{int} monocytes from the bone marrow cells of CX₃CR1 mice.

To obtain Ly6C^{hi} GFP^{int} monocytes, cells were sorted based on (A) Single doublet exclusion, (B) CD11b⁺ cells, (C) C-Kit⁻ (to exclude precursor of monocytes), (D) Ly6G^{low} (to exclude neutrophils) and (E) Ly 6C and GFP expression to split the monocytes into two populations of Ly6C^{hi} or Ly6C^{low} monocytes subsets. The Ly6C^{hi} populations were collected and adoptively transferred by i.v. injection into C57BL/6 mice.

1.5 million purified Ly6C^{hi} monocytes were injected i.v into C57BL/6 mice, and 600 μ g of SpA or OVA was subsequently injected i.p. Twenty-two hours later the mice were culled and blood, spleen and bone marrow harvested for flow cytometric analysis. However, on the first occasion, due to technical limitations with sorting of cells, only enough cells were collected for an N=4 experiment. The experiment was repeated a second time with N=5.

It was seen that GFP⁺ cells were present in the blood and peripheral organs, such as the bone marrow and the spleen, 24h after their injection (figure 4.15). This demonstrates that GFP monocytes are surviving after the adoptive transfer procedure and are trafficking into other organs as well as circulating within the blood. When absolute numbers of GFP⁺ monocytes were examined within the blood, bone marrow and spleen, there were a greater number of GFP⁺ monocytes found in the SpA-treated mice in both experiments in comparison to the control group (figure 4.16). This suggests that SpA may provide a survival signal to monocytes after adoptive transfer, but further experiments are needed to test this theory.

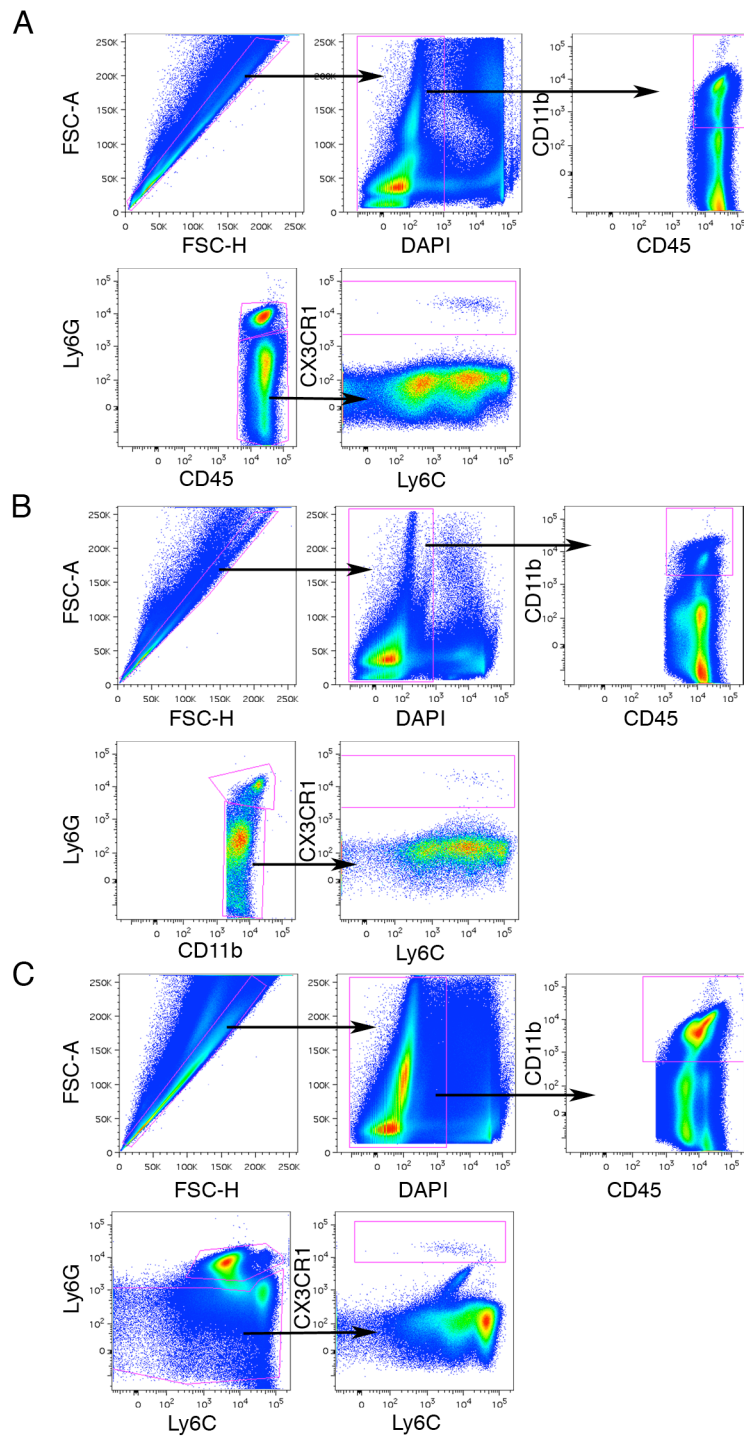


Figure 4.15, GFP⁺ monocytes were present 22h after adoptive transfer.

1.5×10^6 GFP⁺ Ly6C^{hi} monocytes were adoptively transferred by iv injection into C57BL/6 mice. 600 μ g of either SpA or OVA were administered i.p at the same time as the GFP⁺ cells. 22h later mice were euthanized and blood, bone marrow and spleen were harvested and analysed by flow cytometry. (A) Gating strategy for locating the GFP monocytes in the blood. (B) Gating strategy for locating the GFP monocytes in the spleen. (C) Gating strategy for locating the GFP monocytes in the bone marrow.

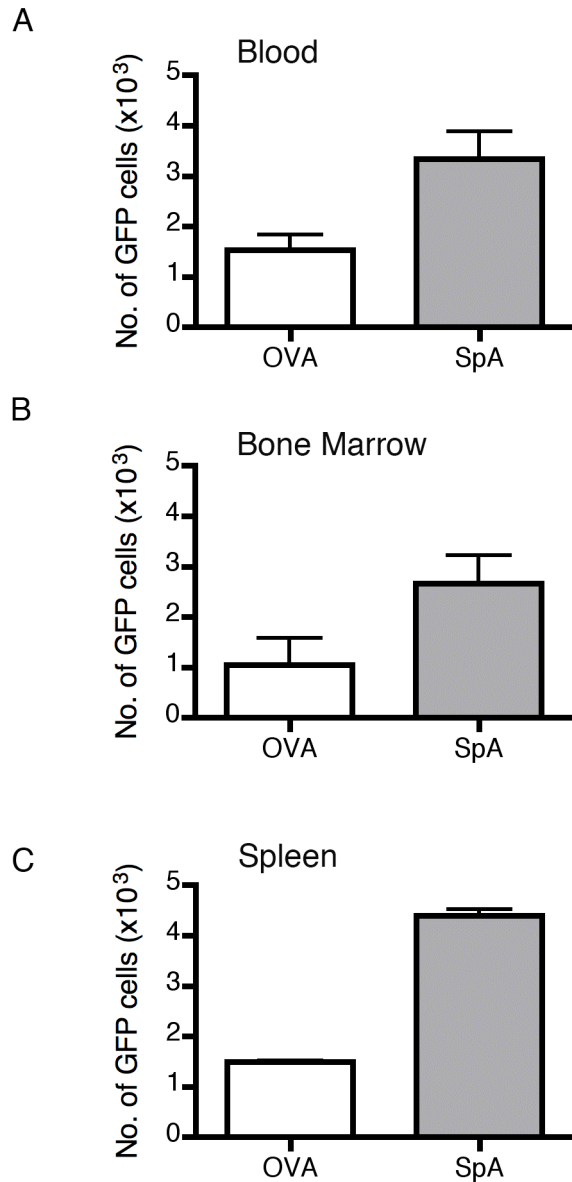


Figure 4.16, SpA-treated mice have a higher number of GFP+ cells present 22h after adoptive transfer.

1.5×10^6 GFP⁺ Ly6C^{hi} monocytes were adoptively transferred by iv injection into C57BL/6 mice. 600 μ g of either SpA or OVA was administered i.p at the same time as the GFP⁺ cells. 22h later mice were euthanized and blood, bone marrow and spleen were harvested and analysed by flow cytometry. (A) Absolute number of GFP+ monocytes in the blood. (B) Absolute number of GFP+ monocytes in the bone marrow. (C) Absolute number of GFP+ monocytes in the spleen. This experiment was carried out on two separate occasions (SpA N=2, OVA N=2 for the first experiment and SpA N=3, OVA N=2 for the second experiment) that showed the same results: the data presented is a representative figure of one of these experiments.

The Ly6C^{hi} GFP⁺ monocyte population found in the blood of adoptively-transferred mice that were treated with SpA for 24h, showed a down-regulation of their Ly6C marker in comparison to the controls (figure 4.17A). A representative histogram and contour plots of the GFP⁺ monocyte population within the blood of OVA and SpA treatment groups demonstrate the down-regulation of Ly6C that the monocyte population underwent when it was treated with SpA. When the total GFP⁺ monocyte population was sub-divided into two populations of Ly6C^{hi} and Ly6C^{low} the difference in percentage of each population seen between the two treatment groups showed a significant increase in the percentage of GFP⁺ Ly6C^{low} monocytes in the SpA-treated group in comparison to the control group (figure 4.17B). Importantly, the GFP⁺ Ly6C^{low} monocytes could only have differentiated from the adoptively-transferred GFP⁺ Ly6C^{hi} monocytes.

Furthermore, examination of CD64 expression (figure 4.17C) demonstrated that it was significantly down-regulated in both monocyte subset populations in the SpA treatment group in comparison to the OVA group. This is consistent with all previous experiments. CX₃CR1 MFI was looked at in the two monocyte populations; unfortunately, due to a difference in the MFI values seen across the two experiments, the two sets of results could not be pooled together to allow statistical analysis. However, in both experiments the Ly6C^{hi} monocytes had increased expression (MFI mean \pm SD 20000 \pm 1000) of CX₃CR1 after SpA treatment when compared to the control group (MFI mean \pm SD 14500 \pm 500) (figure 4.17D). It was noted that Ly6C^{low} monocytes express higher levels of CX₃CR1 than Ly6C^{hi} monocytes. Therefore, it is reasonable to speculate that this increase may be due to the Ly6C^{hi} monocyte population readying themselves to differentiate into Ly6C^{low} monocytes, which express a MFI mean \pm SD of 21500 \pm 500. There was only a very minimal change detected in CX₃CR1 expression in the Ly6C^{low} population between the SpA-treated group and the OVA treated group.

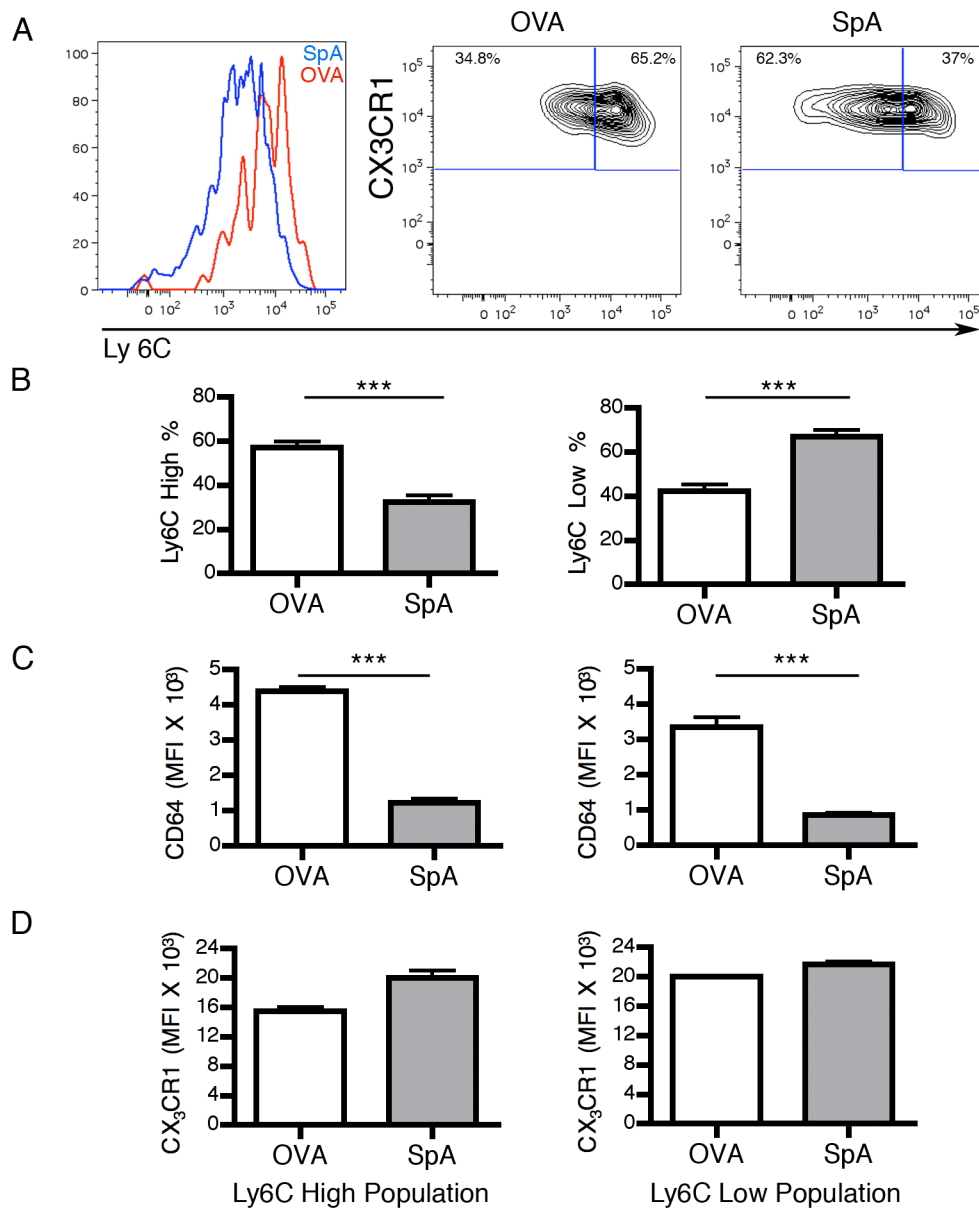


Figure 4.17. SpA treatment for 22h leads Ly6C^{hi} monocytes to differentiate into Ly6C^{low} monocytes in the blood.

1.5×10^6 GFP⁺ Ly6C^{hi} monocytes were adoptively transferred by i.v. injection into C57BL/6 mice. 600 μ g of SpA or OVA was administered i.p. at the same time as the GFP⁺ cells. 22h later mice were euthanized and blood, bone marrow and spleen were harvested and analysed by flow cytometry. Data were analysed by a two-tailed, unpaired *t*-test, *** = $P < 0.001$. (A) Representative histogram and contour plot showing the division of the total monocyte population into Ly6C^{hi} and Ly6C^{low} GFP⁺ monocytes sub-populations in the blood. (B) The mean \pm SD % for Ly6C^{hi} GFP⁺ ($T_7 = 6.01$, $P < 0.0005$, left panels) and Ly6C^{low} GFP⁺ ($T_7 = 6.16$, $P < 0.0005$, right panels) monocyte populations in the blood. (C) The mean \pm SD MFI values of CD64 for Ly6C^{hi} ($T_7 = 17.87$, $P < 0.0001$, left panels) and Ly6C^{low} ($T_7 = 10.15$, $P < 0.0001$, right panels) monocyte. (D) The mean \pm SD MFI values of CX₃CR1 for Ly6C^{hi} (left panels) and Ly6C^{low} (right panels) monocyte. This experiment was carried out on two separate occasions; the data were then pooled together for the purposes of statistical analysis. The two experiments had a total N of; SpA N=5 and OVA N=4. Due to differences in voltage, CX₃CR1 values could not be pooled together for statistical purposes.

Monocytes migrate into the peripheral organs, such as the spleen, where they can differentiate into macrophages. For this reason, the spleen was examined for GFP⁺ cells (figure 4.15B); and it was found that GFP⁺ cells were present 22h after adoptive transfer. Furthermore, the GFP⁺ cells present in the spleen showed a significant increase in the macrophage lineage marker F4/80. Nevertheless, the population of GFP⁺ cells still expressed high levels of Ly6C and have the same FSC and SSC characteristics as blood monocytes. Therefore, the GFP⁺ cells present in the spleen will be defined as “monocytes/macrophages” as they could not be defined to any greater extent with the panel of antibodies used in this experiment. The representative histogram of the total GFP⁺ monocyte/macrophage population within the spleen shows the SpA-treated group (Blue line) and the control group (red line); the decrease in Ly6C expression can be seen clearly on the histogram within the SpA treatment group compared to the OVA group (figure 4.18A). The contour-plots show the gates that have been drawn to divide up the two Ly6C monocyte populations. The percentage of Ly6C^{hi} population that is found in the spleen is significantly reduced in the SpA-treated group, along with a significant increase in the Ly6C^{low} monocyte population - compared to the OVA treatment group (figure 4.18B).

The same significant down-regulation of CD64 that was seen in the peripheral blood was seen again in both of the monocyte subsets in the spleen (figure 4.18C). Also, in the SpA treated group CX₃CR1 was up-regulated on the Ly6C^{hi} monocyte subset isolated from the spleen (figure 4.18D); as with the peripheral blood, no statistical analysis could be performed as the values between the experiments were too different (figure 4.17D). It is interesting to note that adoptively-transferred Ly6C^{hi} monocytes traffic to the spleen and are differentiating to Ly6C^{low} monocytes in this compartment when, in point of fact, the literature states that they must traffic back to the bone marrow before differentiation can occur.

Therefore, further analysis of the bone marrow would be beneficial after monocyte adoptive transfer. As mentioned above, this is the compartment that the literature states Ly6C^{hi} monocytes must traffic back to in order to differentiate into Ly6C^{low} monocytes prior to subsequent release back into the circulation²⁸⁶. The bone marrow findings were consistent with what was seen within the blood and spleen examinations. SpA treatment for 22h induces the

differentiation of the adoptively-transferred Ly6C^{hi} GFP⁺ monocytes to Ly6C^{low} GFP⁺ monocytes in the bone marrow (figure 4.19). This can be observed when gates are drawn to divide up the monocyte population into two separate groups (figure 4.19A); there is a significant down-regulation of the percentage of Ly6C^{hi} monocyte population and a significant increase in the percentage of the Ly6C^{low} population resulting from this (figure 4.19B). There was also a significant down-regulation in CD64 expression (figure 4.19C) in both the Ly 6C^{high} and Ly 6C^{low} populations. CX₃CR1 also appeared to have increased in both of these populations but, as previously stated, statistical tests could not be performed due to differences in values between the two experiments (figure 4.19D).

These data demonstrate that GFP⁺ Ly6C^{hi} monocytes can be adoptively-transferred and isolated 22h later in the blood, spleen and bone marrow. Interestingly, when these mice are treated with a control protein, OVA, a small proportion of the adoptively-transferred Ly6C^{hi} monocytes differentiate into Ly6C^{low} monocytes. However, when the mice were treated with SpA for 22h there was a significantly higher rate of differentiation of the GFP⁺ Ly6C^{hi} monocytes in the peripheral blood (and the two tissues that were also examined). SpA not only increased the rate of Ly6C down-regulation, but also caused the down-regulation of CD64 and an up-regulation of CX₃CR1.

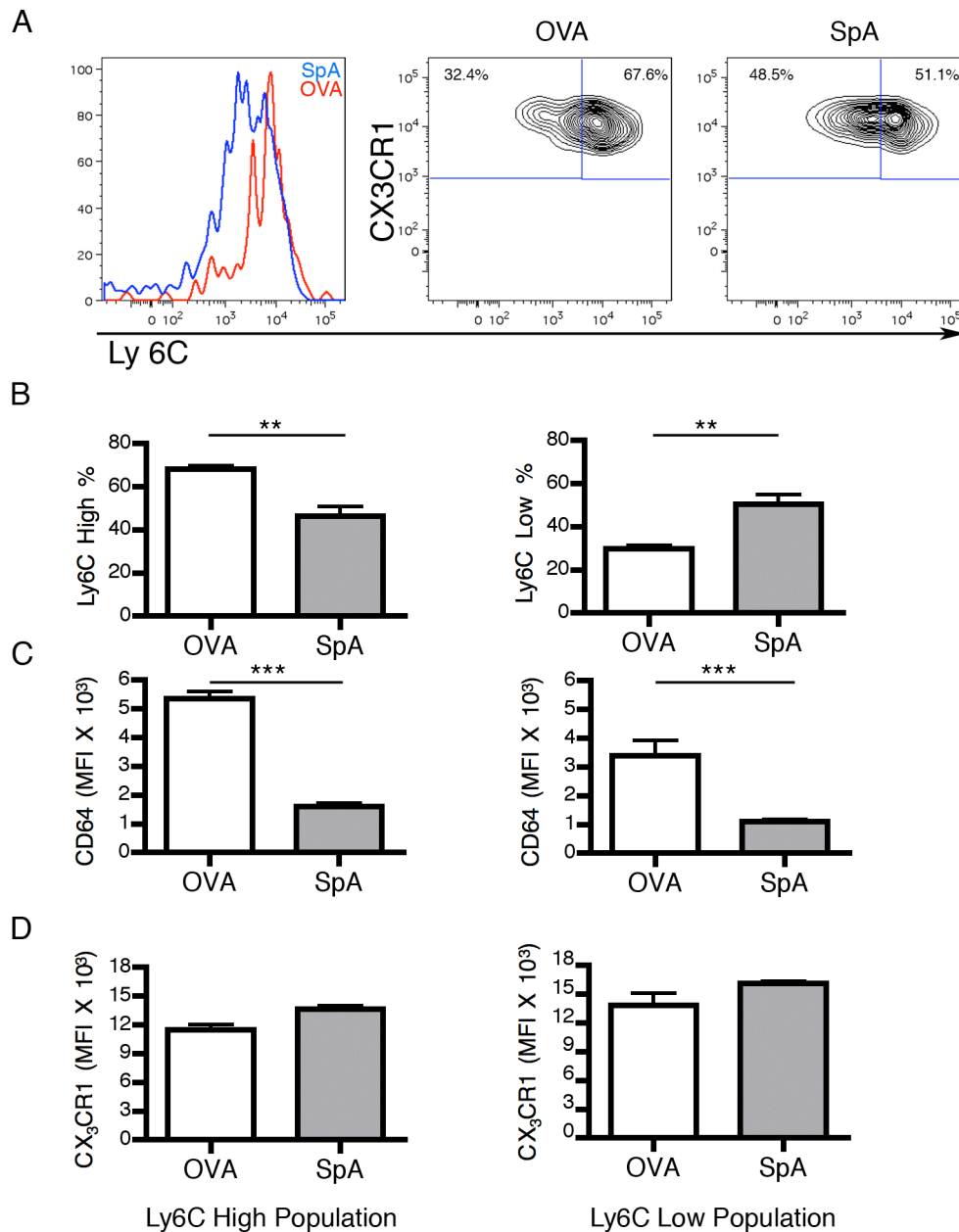


Figure 4.18. SpA treatment for 22h leads Ly6C^{hi} monocytes to differentiate into Ly6C^{low} monocytes in the spleen.

1.5×10^6 GFP⁺ Ly6C^{hi} monocytes were adoptively transferred by i.v. injection into C57BL/6 mice. 600 μ g of SpA or OVA was administered i.p. at the same time as the GFP⁺ cells. 22h later mice were euthanized and the spleen was harvested and analysed by flow cytometry. Data were analysed by a two-tailed, unpaired *t*-test, **= $P < 0.01$; *** = $P < 0.001$. (A) Representative histogram and contour plot showing the arbitrary division of the total monocyte population into Ly6C^{hi} and Ly6C^{low} GFP⁺ monocyte sub-populations in the spleen. (B) The mean \pm SD % for Ly6C^{hi} GFP⁺ ($T_7 = 4.26$, $P < 0.0036$, left panels) and Ly6C^{low} GFP⁺ ($T_7 = 3.93$, $P < 0.0057$, right panels) monocyte populations in the spleen. (C) The mean \pm SD MFI values of CD64 for Ly6C^{hi} ($T_7 = 15.01$, $P < 0.0001$, left panels) and Ly6C^{low} ($T_7 = 4.85$, $P < 0.0019$, right panels) monocyte. (D) The mean \pm SD MFI values of CX₃CR1 for Ly6C^{hi} (left panels) and Ly6C^{low} (right panels) monocyte. This experiment was carried out on two separate occasions; the data were then pooled together for purposes of statistical analysis. The two experiments had a total N of; SpA N=5 and OVA N=4. Due to differences in voltage, CX₃CR1 values could not be pooled together for statistical purposes.

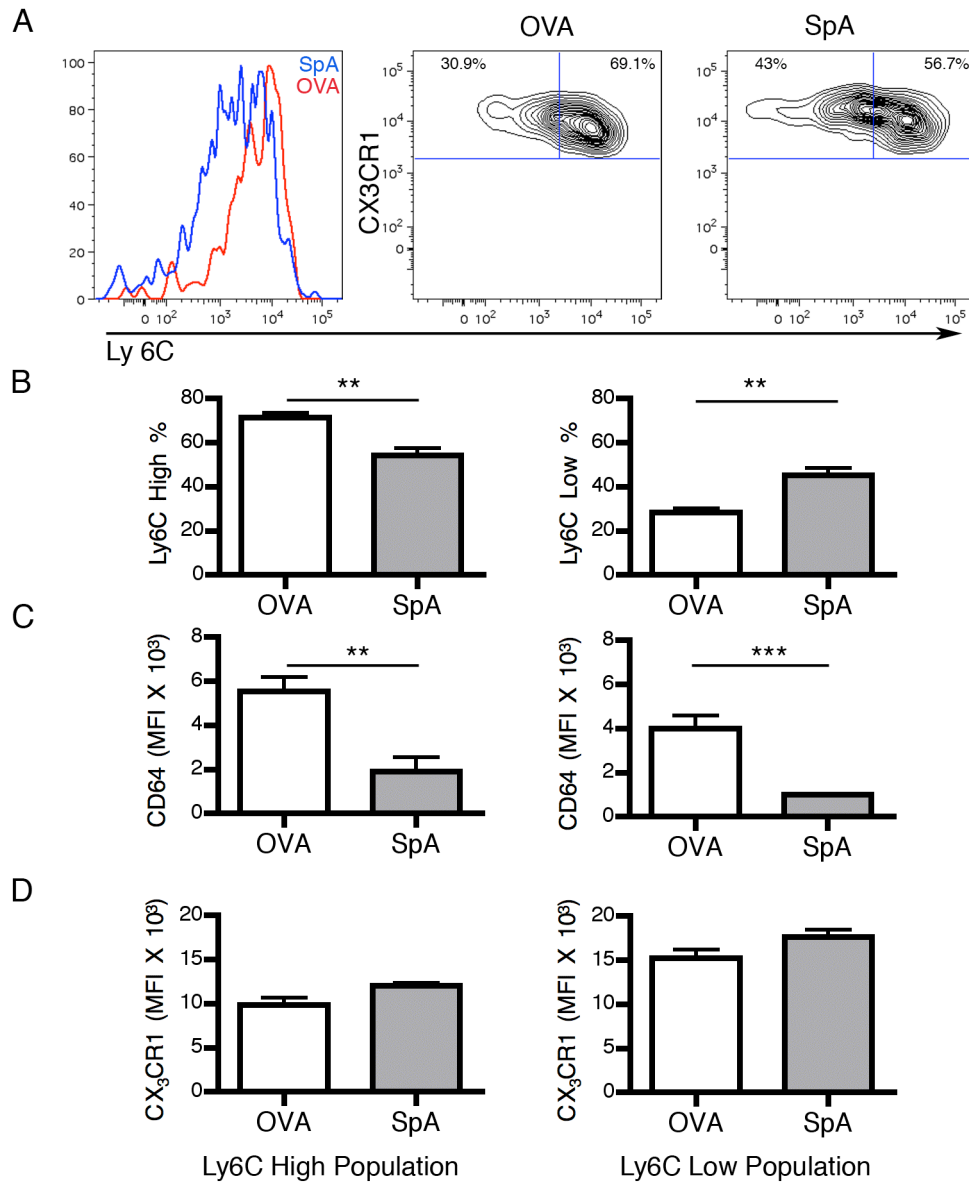


Figure 4.19. SpA treatment for 22h leads Ly6C^{hi} monocytes to differentiate into Ly6C^{low} monocytes in the bone marrow.

1.5×10^6 GFP⁺ Ly6C^{hi} monocytes were adoptively transferred by i.v. injection into C57BL/6 mice. 600 μ g of SpA or OVA was administered i.p. at the same time as the GFP⁺ cells. 22h later mice were euthanized and the bone marrow was harvested and analysed by flow cytometry. Data were analysed by a two-tailed, unpaired *t*-test, **= $P < 0.01$; *** = $P < 0.001$. (A) Representative histogram and contour plot showing the arbitrary division of the total monocyte population into Ly6C^{hi} and Ly6C^{low} GFP⁺ monocytes sub-populations in the bone marrow. (B) The mean \pm SD % for Ly6C^{hi} GFP⁺ ($T_7 = 4.24$, $P < 0.0038$, left panels) and Ly6C^{low} GFP⁺ ($T_7 = 4.32$, $P < 0.0035$, right panels) monocyte populations in the bone marrow. (C) The mean \pm SD MFI values of CD64 for Ly6C^{hi} ($T_7 = 3.94$, $P < 0.0056$, left panels) and Ly6C^{low} ($T_7 = 6.01$, $P < 0.0005$, right panels) monocyte. (D) The mean \pm SD MFI values of CX₃CR1 for Ly6C^{hi} (left panels) and Ly6C^{low} (right panels) monocyte. This experiment was carried out on two separate occasions; the data were then pooled together for purposes of statistical analysis. The two experiments had a total N of; SpA N=5 and OVA N=4. Due to differences in voltage, CX₃CR1 values could not be pooled together for statistical purposes.

4.3 Discussion

In this chapter it has been demonstrated that SpA can interact with monocytes in the blood and bone marrow of mice under steady-state conditions, inducing the maturation of Ly6C^{hi} monocytes to Ly6C^{low} monocytes. Moreover, in the inflammatory setting of SCI, SpA treatment can interact with monocytes in the blood and the damaged spinal cord. Furthermore, SpA can also interact with the resident microglial population. Consistent with homeostatic conditions, SpA treatment induced a maturation of the spinal cord infiltrating Ly6C^{hi} monocyte subset into Ly6C^{low} monocytes. It was further demonstrated that treatment with SpA after SCI induced the Ly6C^{low} monocyte population to increase its production of IL-10. The ability of SpA to induce the maturation of the inflammatory Ly6C^{hi} monocyte population into an IL-10-producing Ly6C^{low} anti-inflammatory monocyte in the vastly inflammatory environment of SCI is an intriguing prospect for a therapeutic approach for a cells-specific modification of the inflammatory environment to a far less inflammatory setting, which would possibly result in increased functional recovery for patients.

One of the primary aims of this chapter was to assess the *in vivo* binding capacity of SpA to cells of the myeloid lineage. Under steady-state, SpA interacted with monocytes in the blood and bone marrow. Moreover, it was also able to interact with neutrophils; however, the level of binding was 10-fold lower than that observed with monocytes. In explanation, neutrophils and monocytes express different Fcγ receptors. In the blood under steady-state conditions, neutrophils are known to express FcγRIII and FcγRIV, but only very low levels of FcγRI or FcγRIIb, while monocytes express all four FcγRs at higher levels than neutrophils²⁸⁷. The reduced level of FcγR expression on the cell surface of neutrophils is responsible for the decreased levels of SpA binding. In support of this it has been shown in chapter 3 that FcγRI is responsible for SIC's ability to bind to and polarize BMDMs to an anti-inflammatory phenotype. Neutrophils express FcγRI only very weakly²⁸⁸, whereas monocytes and macrophages express high levels of FcγRI constitutively. Interestingly, when considering circulating monocytes, it is important to note that Ly6C^{hi} monocytes express higher levels of FcγRI than the Ly6C^{low} subset²⁸⁷. This in part explains why SpA has an increased degree of interaction with Ly6C^{hi} monocytes (Figure 4.2).

It has been demonstrated in the literature that the two different monocyte subsets have different roles in homeostasis and inflammation. As discussed in the introduction to this chapter, Ly6C^{hi} monocytes are the inflammatory subset and have a short half-life in blood. Ly6C^{low} monocytes, patrol the blood vessels and are involved in the resolution of inflammation and the initiation of wound-healing processes when they migrate into tissue^{274 48 46}. When the effects of SpA binding on the monocyte population in steady-state was investigated further, a curious skewing of the monocyte compartment to an increased presence of the Ly6C^{low} monocyte subset was revealed, even though it had been shown that SpA preferentially binds to the Ly6C^{hi} subset of monocytes. The mechanism by which this anomaly could be explained is that if Ly6C^{hi} monocytes do not migrate from the blood to a site of inflammation, where they differentiate into a macrophage or a DC, Ly6C^{hi} monocytes will traffic back to the bone marrow and mature into Ly6C^{low} monocytes⁴⁷. The data present suggests that SpA accelerates the differentiation of Ly6C^{hi} into Ly6C^{low} monocytes. Importantly, it also suggests that the Ly6C^{hi} monocytes do not need to home back to the bone marrow to undergo this transformation.

Another indicator showing that SpA is inducing the maturation of Ly6C^{hi} monocytes is that the SpA-treated Ly6C^{hi} monocytes have decreased Gr1 (Ly6G) expression -conventionally used as a neutrophil marker. However, this has recently been shown to be expressed at low levels on the Ly6C^{hi} subset (but is not expressed on the Ly6C^{low} monocyte subset²⁸⁹), indicating that the SpA-treated Ly6C^{hi} population is down-regulating this marker in preparation for maturing into a Ly6C^{low} monocyte. The SpA-treated Ly6C^{hi} population additionally down-regulated their CD64 (FcγRI) expression in comparison to the Ly6C^{hi} monocytes of the control group, suggesting further changes in their maturation state are taking place as CD64 is expressed at decreased levels on Ly6C^{low} monocyte population compared to Ly6C^{hi} monocytes²⁸⁷.

On the other hand, the change in the balance of the monocyte compartment after SpA treatment could be attributed to the Ly6C^{hi} population dying off or migrating to another site and/or more Ly6C^{low} cells migrating into the blood, and may not in fact be a change in maturation status of the Ly6C^{hi} monocytes at all. An adoptive transfer experiment was set up to address the following question: is SpA inducing Ly6C^{hi} monocytes to mature into Ly6C^{low} monocytes?

To answer this, Ly6C^{hi} GFP⁺ monocytes were adoptively-transferred into WT mice, which were then treated with SpA or the control protein OVA, and 22h later the GFP⁺ cells' phenotype was interrogated. The results showed that GFP⁺ monocytes in the SpA-treated group, compared to the control group, had significantly lower surface expression of Ly6C. This demonstrates that SpA is inducing Ly6C^{hi} monocytes to differentiate into Ly6C^{low} cells and that this is at a higher rate than exhibited in homeostasis. As was seen in previous experiments (figure 4.5), Ly6C was not the only surface phenotype that was changed on the Ly6C^{hi} SpA-treated group; CD64 and Gr1 were also significantly down-regulated.

Another monocyte subset-specific marker that was examined after SpA treatment was CX₃CR1, which is expressed at higher levels on the Ly6C^{low} monocyte sub-set compared to the Ly6C^{hi} monocyte sub-set⁴⁰. The Ly6C^{hi} monocytes of the SpA-treated group had higher levels of CX₃CR1, further suggesting they are readying themselves for differentiation into Ly6C^{low} monocytes.

After adoptive transfer, GFP⁺ cells were not only discovered in the blood, but were also detected in the spleen and the bone marrow. GFP⁺ monocytes in these tissues exhibited the same phenotype after SpA treatment as the blood monocytes. It is interesting to note that although it has previously been reported that Ly6C^{hi} monocytes must migrate back to the bone marrow before differentiation can occur^{47,67}, it was also found that adoptively-transferred Ly6C^{hi} monocytes trafficked to the spleen and differentiated to Ly6C^{low} monocytes. Another interesting and somewhat unexpected observation was that SpA not only altered the phenotype of Ly6C^{hi} monocytes to Ly6C^{low} monocytes, but there was also a higher number of GFP monocytes recovered in the SpA-treated group after both adoptive transfer experiments. No statistical analysis could be performed on this phenomenon, as recovery of cells was different in both experiments. The question that needs to be addressed in future work is: Can SpA induce monocytes to proliferate, even though literature states otherwise, and is this outcome specific to a certain sub-set, or alternatively is SpA acting as a survival agent for the monocytes?

The ability of SpA to induce maturation of Ly6C^{hi} monocytes to Ly6C^{low} monocytes was recognised to be a very promising therapeutic approach to the

amelioration of inflammation and therefore secondary death after SCI; Ly6C^{low} monocytes have been shown in many inflammation models to induce the resolution of inflammation and play a vital role in tissue remodelling^{58 55 290}. To evaluate the ability of SpA to modulate the inflammatory monocyte compartment in the absence of an overt auto-reactive adaptive immune response, a contusion model of spinal cord injury was used - driven by a traumatic event - resulting in significant inflammation at the site of injury^{132 291 292}. Ly6C^{hi} monocytes have already been targeted as a method for the modulation of CNS inflammation in neurodegenerative diseases such as Amyotrophic Lateral Sclerosis (ALS). ALS results from progressive muscle weakness associated with degeneration of motor neurons in the brain and spinal cord²⁹³. The disease pathology is perpetrated by activated microglia and infiltrating pro-inflammatory Ly6C^{hi} monocytes in the spinal cord, an outcome that is very similar to the pathogenesis of secondary death in SCI. Interestingly, the administration of an anti-Ly6C monoclonal antibody to mice prone to ALS, significantly increased survival and neurological scoring in the treatment group compared to the control group (which received an isotype control antibody). This result was due to decreased recruitment of Ly6C^{hi} monocytes into the spinal cord, which correlated with an increase in neuronal survival and a decrease of pro-inflammatory cytokine production²⁹⁴. Although this is not SCI, it is nevertheless a neuro-inflammatory disease - which illustrates that inflammation is decreased by minimizing the presence of Ly6C^{hi} monocytes in the spinal cord, resulting in a decreased neuronal death and an increased level of survival.

The depletion of monocytes/macrophages has been previously investigated in the experimental treatment of SCI. Scientists have used clodronate liposomes when seeking to deplete monocytes or macrophages from a model system²⁹⁵. However, this is not a very specific or elegant method as it also depletes any cells that can phagocytose the toxic liposomes. When clodronate has been used to “selectively” deplete monocytes/macrophages in SCI studies, varying results were noted, prompting much debate in the past as to whether macrophages/monocytes played a protective or determinate role in SCI^{296 94}.

It has become much clearer in recent years that macrophages and monocytes are heterogeneous populations, and the sub-sets within these cell types play both beneficial and detrimental roles in the recovery from diseases or tissue injuries.

A new and more sophisticated experimental strategy designed to specifically modulate the inflammatory Ly6C^{hi} component of the monocyte population uses siRNA against CCR2. CCR2 is the chemokine receptor that the inflammatory Ly6C^{hi} monocytes utilise to egress from the bone marrow and travel to sites of inflammation⁶⁹. Firstly, Leuschner et al demonstrated that Ly6C^{hi} monocytes take up the highest level of the CCR2 siRNA, showing a significant decrease in the amount of CCR2 mRNA that these Ly6C^{hi} cells were producing. Leuschner et al went on to demonstrate that in several models of inflammation (myocardial infarction, pancreatic islet transplantation and atherosclerosis), which are all characterized by large infiltrates of inflammatory monocytes, reduced Ly6C^{hi} monocytes were recruited to the site of inflammation, correlating with improved recovery after CCR2 siRNA treatment.¹

The use of siRNA or Ly6C blocking antibodies are two methods that have been shown to reduce the infiltration of Ly6C^{hi} monocytes into sites of inflammation, correlating with better outcomes. However, the potential benefit of using SpA instead of either of these two strategies is evidenced by the fact that SpA treatment has been shown to induce the maturation of Ly6C^{hi} inflammatory monocyte into Ly6C^{low} anti-inflammatory monocytes. The increase in Ly6C^{low} monocytes at the site of inflammation theoretically could have an additional benefit by resolving inflammation over just blocking the inflammatory subsets infiltration. It is also noteworthy to mention that previous studies have shown that CNS regeneration after SCI is greatly increased when the overt inflammatory immune response is down-regulated with the modulation of residual monocyte/macrophages^{297 133} and results from chapter 3 demonstrated the ability of SpA to polarize macrophages to an anti-inflammatory phenotype when it is in complex with IgG. Taking into consideration the evidence that (a) anti-inflammatory macrophages are less toxic to neurons and can induce growth of axon¹³³, and (b) that reducing the Ly6C^{hi} infiltrating monocyte population results in increased recovery in numerous models of inflammatory conditions, justifies SpA's potential as a molecule that can modulate monocyte populations.

To further investigate SpA's potential for use as a therapeutic in SCI, it was vital to prove that SpA could not only bind to myeloid populations in the blood and bone marrow, but could also bind to myeloid cells in the spinal cord. To substantiate this, it was important to examine SpA's binding potential in the

spinal cord of injured and non-injured states. In the non-injured spinal cord, microglia dominated the CD45+ population and did not bind any SpA (figure 4.7). Conversely, the injured spinal cord had a vastly different cellular profile after injury; there was a massive increase in the inflammatory infiltrate of monocyte/macrophages and neutrophils, in conjunction with the resident microglia adopting an activated phenotype (figure 4.8). The monocyte/macrophage population found in the injured spinal cord bound SpA-488 at a significantly higher level than the control protein. Microglia showed the ability to bind to SpA, though this was at a reduced level compared to the level of monocyte/macrophage population. However, it is noteworthy to mention that a recent discovery has established that microglia do not develop from HSC-like monocyte-derived macrophages but derive from a primitive yolk sac progenitor cell at embryonic day 8^{39 38}. This is possibly the reason why there is reduced binding in the microglial population in comparison to the monocyte/macrophage population. The discovery therefore highlights a major caveat to the collective term “CNS macrophages” used regularly in SCI literature to refer to monocytes/macrophages and microglia as the same population. And because of the fact that microglia are not derived from HSC, the umbrella term “CNS macrophage” will not be used to define these two separate populations in this body of work.

Now that it has been shown that SpA can interact with cells in the damaged spinal cord, SpA's ability to induce the maturation of Ly6C^{hi} monocytes to a Ly6C^{low} phenotype was examined in the inflammatory setting of SCI.

It was found that SpA exhibited the ability to alter the phenotype of the infiltrating Ly6C^{hi} monocyte population, leading to a preferential Ly6C^{low} monocyte population in the damaged spinal cord of the SpA treated group compared to the control group. The skewing of the monocyte population was also noted in the peripheral blood of the SpA-treated SCI group. This result further supports the potential of SpA as a cell-specific therapeutic strategy to combat the aberrant inflammatory immune response displayed after SCI.

Contrary to current literature, Shechter et al published a paper in 2009 which states that the Ly6C^{hi} monocytes are important for recovery after SCI as they localise to the lesion margin and are induced to produce IL-10, which they

suggest leads to a small recovery in hind limb function, assessed via the Basso mouse score (BMS) ²⁹⁸. However, it should be noted that the authors immunised the mice a week before injury with a MOG peptide T cell vaccine, which they stated boosts the monocyte population that infiltrates into the spinal cord after injury, and justify the use of the vaccination strategy by inferring that the monocyte population would be otherwise undetectable in the damaged spinal cord after injury, which is quite contradictory to literature ¹⁰¹ and the finding in this body of work. Moreover, the authors did not address how this vaccination strategy affected the phenotype of the infiltrating monocytes. It is highly likely that vaccination polarized the infiltrating monocytes to an anti-inflammatory phenotype prior to their entry into the spinal cord. This phenomenon did not occur in the un-vaccinated SCI model.

In light of the Shechter et al paper ²⁹⁸, it was vital to show that the Ly6C^{low} population of monocytes within the spinal cord does have the ability to produce IL-10 and be anti-inflammatory given the right stimuli. The ability of both the Ly6C^{hi} and Ly6C^{low} monocyte subsets were, therefore, examined for their potential to produce IL-10 after SCI with and without SpA treatment.

SCI was performed in Vert-X mice, which are GFP IL-10 reporter mice; unfortunately, due to technical issues in surgery only an N=1 for each condition could be performed in this experiment, and it must therefore be repeated to statistically significant levels to validate the finding. However, the findings that were gathered showed that the SpA-treated mouse had a higher percentage of monocytes that were producing IL-10 in the damaged spinal cord than the OVA control mouse did. In the control mouse, 49% of cells expressed IL-10, which is consistent with findings from a study that revealed there was a 50:50 ratio in mRNA levels of M1 (pro-inflammatory macrophages) and M2 (regulatory/anti-inflammatory) macrophages present in the damaged spinal cord until day 3 post-injury¹³³. Furthermore, in the spinal cord of the control mouse, there was a distinct Ly6C^{hi} population that was IL-10 negative, contrary to the Shechter et al findings. The SpA-treated mouse had a reduced Ly6C^{hi} monocyte compartment within the damaged spinal cord, with a corresponding increase in the Ly6C^{low} monocyte (69%) population, which were all positive for IL-10 production. The blood of the SCI mice was examined to determine whether SpA also induced the production of IL-10 in the Ly6C^{low} monocyte population in this compartment.

However, no production of IL-10 was exhibited in either of the two treatment groups. This was an interesting observation as Ly6C^{low} monocytes produced IL-10 at the site of inflammation (damaged spinal cord) but did not produce it systemically, leading to the assumption that there must be tissue-specific signals that govern the production of IL-10 in the Ly6C^{low} population. The tissue-specific regulation of IL-10 permits the regulation of inflammation in one compartment of the body but still allows the immune system to stay primed in case of secondary infection at another site. The ability to combat secondary infections is a major concern in the design of a therapeutic for SCI patients given the potentially long recovery period spent in hospital.

To elucidate the mode of action that SpA was working through to induce the maturation of Ly6C^{hi} monocytes to Ly6C^{low} monocytes *in vivo*, the function of SpA was investigated in FcγRIII knock-out mice. The rationale for a role of FcγRIII in the process was based on the fact that its expression on accessory cells was required for SpA-induced apoptosis of B cells *in vivo*, via V_H3 BCR engagement (unpublished data, Goodyear). FcγRIII has furthermore been shown to be involved in the anti-inflammatory mechanism of IVIg, via ITAMi signalling that leads to the up-regulation of FcγRIIb on macrophages²⁰³.

From this investigation, data presented conclusively demonstrated that the ability of SpA to modulate the Ly6C^{hi} monocyte population to the Ly6C^{low} monocyte population was not dependent on the expression of FcγRIII. Taken together with the findings in Chapter 3, this indicates that the most likely candidate is FcγRI.

In summary, the data so far support the concept that SpA treatment after SCI (or in steady-state) can induce the maturation of the Ly6C^{hi} inflammatory monocyte to the Ly6C^{low} anti-inflammatory IL-10 producing phenotype. This finding is of particular interest in the setting of SCI, as SpA could in the future be used as a cell-specific method for modulating the massive inflammatory response contributing to the secondary death of neurons days to possibly months after the initial trauma; a detrimental response that, without modulation, results in substantially impaired functional recovery for SCI patients.

5 Optimisation of behavioural testing for murine spinal cord injury

5.1 Introduction

The spinal cord comprises only 2% of the total human central nervous system however, if damaged, it can result in disruption to essential functions such as the replay of sensory, motor and autonomic signals. There are many types of injury that can occur to the spinal cord, some of which are lacerations, contusions and compression injuries; the most common of these is a contusion injury. This form of injury occurs when a substantial force comes into contact with the spinal cord vertebra causing movement of the vertebra, injuring the normally protected spinal cord, which can lead to haemorrhaging and bruising.

Almost half of all spinal cord injuries occur at the cervical level in humans, the level that controls both the upper and lower extremities. Injury at this area can therefore leave patients as quadriplegics. Due to its prevalence, this level of contusion was chosen as the injury site for the optimisation of murine spinal cord injury. It should be appreciated that in order to recreate a spinal cord contusion injury model in mice, the device used for measurement had to be reliable and produce consistent injury severities throughout the experimental run.

5.1.1 Experimental methods for SCI induction

The first experimental system for spinal cord injury was the weight drop technique of Allen ²⁹⁹. This was used to create contusion injuries in rats and it relied on distance, weight and any resistance experienced as the weight fell, to determine the severity of the injury. However, this method showed huge variations in data and had a lack of consistency between specimens; therefore the technique underwent modifications to become the contemporary basis of techniques now used today to create spinal cord contusion injury.

Contusion injuries are now typically produced by using one of three devices; the New York University impactor (NYUi), the Ohio State University device (OSUd) or the Infinite Horizon device (IH). All of these devices provide measurements of

biomechanical parameters, including force on the spinal cord, impact displacement, and velocity of the impact tip. The first of these devices involves releasing its impactor tip at a set height onto an exposed spinal cord. The severity of the injury can be adjusted by changing the height at which the impactor tip is dropped. The NYUi can measure such force feedback parameters as velocity and tissue compression depth³⁰⁰. The OSUd uses a computer-driven probe to measure displacement from the dura to the cord. Different injury severities were created by changing the distance of displacement³⁰¹. This device is yet to be produced commercially but has been used in a variety of studies³⁰². The commercially-available IH device is a standardised means of replicating contusion injuries, reliably producing contusion injuries of a user-defined force that displaces the exposed spinal cord of the specimen by means of a computer-driven steel impounder tip with a force sensor attached. The sensor measures the force applied to the spinal cord in kilodynes (Kdyn)³⁰³. The IH device allows a more controlled and repeatable method of creating contusion injuries and minimises the variability of severity between specimens. As the force can be defined it can be used to produce graded severities of these injuries. This was one of the main reasons the IH was the device of choice for this project. Although each of three devices was originally created for injuring rats, they have all been adapted for experiments on mice.

Once a reliable and reproducible model of injury induction can be guaranteed it was realised that when evaluating a therapeutic, such as SpAs, potential to reduce inflammation at the site of trauma in SCI and hopefully improve recovery outcome, it was clear that a functional read out as well as cellular analysis would have to be employed to determine this goal.

5.1.2 Behavioural testing methods for SCI assessment

There are four main types of categories of behavioural assessments: locomotor, sensory, motor or sensory-motor. The behavioural assessments that have been used in this study were motor-based.

5.1.2.1 Baso mouse scale

The Basso, Beattie and Bresnahan (BBB) Scale for rats is a modified open-field-gait test designed to standardise locomotor testing³⁰⁴. It grades hind limb movement on a scale of 0-21. Zero represents no spontaneous locomotor activity while 21 denotes normal locomotory movement with co-ordinated gait. The Basso Mouse Scale (BMS) test was adapted from the BBB Scale as it was thought that the rat-scoring system was not applicable or sensitive enough for mice - it being a 9-point scale for testing hind limb function of mice³⁰⁵. BMS works on the same principles as the BBB scale in that the animals are allowed to roam freely in a pen for 4 minutes, and two examiners grade hind limb locomotor function.

Three key features that had to be modified between the BBB and the BMS were: joint movement during periods of paresis, frequency of coordination and toe clearance. There was great difficulty in discerning movements of the hip and knee joint from each other in the mice compared to the rats, since in the mice these movements were very slight and they were quite often obscured by the fur or folds of the skin. Ankle movement was easily observed in the mice and this is what is focused on in the BMS score.

Mouse locomotion follows a repetitive pattern of fore-limb-stepping coinciding with a stepping of the contralateral hind limb - unlike with larger quadrupeds such as rats. Mice also move more rapidly than rats, and it was shown to be too difficult to discriminate whether mice were walking with co-ordination in three consistent body lengths at the same pace, therefore, in the BMS there is only one category for 'if the mouse is walking with co-ordination' unlike in the BBB where there are four categories of co-ordination.

Due to the small size of mice it was not possible to see whether toe clearance was occurring. If this could not be seen with rats when conducting the BBB scale the examiner would listen out for dragging of the toe, but this could not be reliably heard over ambient noise on a consistent basis due to the small size of mice so this category was removed from the BMS scale. Table 5.1 shows the scoring characteristics used in the BMS.

5.1.2.2 Grip strength test

Another motor assessment technique that was employed in this study to evaluate long-term recovery after SCI in mice was the grip-strength test. This is where the maximal peak force development by a mouse is determined when an operator tries to pull the rodent off of a specifically designed bar attached to a force meter. The amount of force a mouse uses, gripping with its front paws, is measured before and periodically after SCI to see if the injury has led to changes in gripping potential and, if so, whether the grip spontaneously recover or not.

5.1.2.3 Digital Gait analysis techniques

Gait analysis is an invaluable tool for assessing SCI as it can be used to assess recovery progression. By understanding a normal gait it can then be used to compare any subtle changes seen after SCI or in other neurological defects. There are several methods that have been employed to look at gait analysis: one such method is the 'Footprint Analysis' test. This consists of rodents walking along a papered runway with painted paws. Using different colours for the individual paws allows different parameters of gait to be evaluated such as paw angle, stance width and stride length. This technique is laborious and can lack sensitivity as the speed of walking cannot be controlled, which can affect gait read outs.

Another technique used widely to evaluate gait is the 'Catwalk', it was developed to increase the number of gait indices that could be measured³⁰⁶. Essentially, it works by having a transparent conveyor belt with a chamber over it that restricts the movement of a mouse, resulting in a consistent forward motion. The bottom of the chamber has a glass plate, the catwalk, with an LED light emitting from inside it. The light is completely internally reflected, except from the area the mouse had stepped on, which is captured by the high-speed camera underneath the glass plate. This footage is then analysed by specific software that scrutinizes paw angle, swing stride and has the ability to tell how heavily an animal is bearing on one or more of its paws. This is achieved by the correlation of intensity from the fluorescent footprint captured by the camera.

Score	Description
0	No ankle movement
1	Slight ankle movement
2	Extensive ankle movement
3	Plantar placing of the paw with or without weight support - Or - Occasional, frequent or consistent dorsal stepping but no plantar stepping
4	Occasional plantar stepping
5	Frequent or consistent plantar stepping with no coordination or some coordination and paws rotated at initial contact and lift off
6	Frequent or consistent plantar stepping, some coordination, paws parallel at initial contact and lift off or mostly coordinated, paws rotated at initial contact and lift off
7	Frequent or consistent plantar stepping, mostly coordinated, paws parallel at initial contact and lift off - or - all of the stated plus severe trunk instability
8	Frequent or consistent plantar stepping, mostly coordinated, paws parallel at contact and lift off and mild trunk instability or normal trunk stability and tail down or up and down
9	Frequent or consistent plantar stepping, mostly coordinated, paws parallel at initial contact and lift off, and normal trunk stability and tail always up

Table 5.1: BMS scoring definitions.

Adapted from ³⁰⁵

Another gait analysis system is the 'DigiGait'. This was the favoured method of video-gait analysis due to the vast number of parameters it can assess, and was the system employed in the present study. This method involves videoing sequential images of the animal walking for a defined length of time on a transparent treadmill. Once the data have been collected it is input into DigiGait analysis software, which examines individual paw-steps from each run. The DigiGait imaging system generates 20 different indices of gait dynamics and posture, some of which can be seen in table 5.2. Indices generated by the DigiGait system convey information about sensory and motor outputs of gait and gait variability before and after injury or disease in rodents. Figure 5.1 shows a typical paw contact with the belt - along with the different phases of walking that could be expected in a healthy rodent.

The DigiGait imaging system has been used in a number of injury and disease models such as CIA (Collagen Induced Arthritis)³⁰⁷; Parkinson's³⁰⁸ and Huntington's³⁰⁹ disease. It has never before been used as a measure of SCI-outcome in mice, although it has been successfully used to evaluate SCI in rats, where it has been shown to be sensitive enough to determine drug efficacy in the treatment of SCI³¹⁰. Neu2000, which is a derivative of Acetylsalicylic acid and salicylic acid, has been shown indirectly to prevent excitotoxicity, which is a major contributor in the pathogenesis of secondary death in SCI. The authors showed that parameters such as stride-duration spent in swing-phase and stance-phase, swing-to-stance ratio and hind-limb-paw-angle, all significantly changed in comparison to the vehicle-group-treated group. The high number of parameters that DigiGait can assess in conjunction with the successful application in a drug regime in SCI analysis with rats is why the DigiGait was used in this study instead of other gait-analysis systems.

Index	Units	Definition
Swing Duration	ms	Time duration of the swing phase of the stride. This is when the paw is not in contact with the belt
Swing Stride	%	% of the total swing that the paw is in the air
Brake Stance	%	Braking+Propulsion = stance. % of the stance phase (when the paw is in contact with the belt) that the paw is in the braking phase
Propel Stance	%	Braking+Propulsion = stance. % of the stance phase that the paw is in the propulsion phase (when the paw is coming off the belt)
Stride Duration	ms	Time duration of one complete stride for one paw
Stride Frequency	strides per sec	The number of times each second that a paw takes a complete stride
Stride Length	cm	The spatial length that a paw traverses through a given stride
Paw Angle	deg	Sometimes known as "degree of external rotation of the paw"
Stance Width	cm	The distance between a set of axial paws during peak stance
Step Angle	deg	The angle made between the left and right paws as a function of stride length and stance width
Gait Symmetry	Real*	Ratio of forelimb stepping frequency to hind limb stepping frequency
Brake Stride	%	% of the total duration that the paw is in braking phase
Propel stride	%	% of the stance phase the paw is in the propulsion phase
Stance Stride	%	% of the total stride duration that the paw is in any contact with the belt
Step Number	No.	Number of steps taken in a given time period
Stance Swing	Real*	The ratio of swing phase time to stance phase time

Table 5.2: Parameters measured by the DigiGait Imaging System.
Table adapted from Mouse Inc data sheet on DigiGait Imaging System ³¹¹

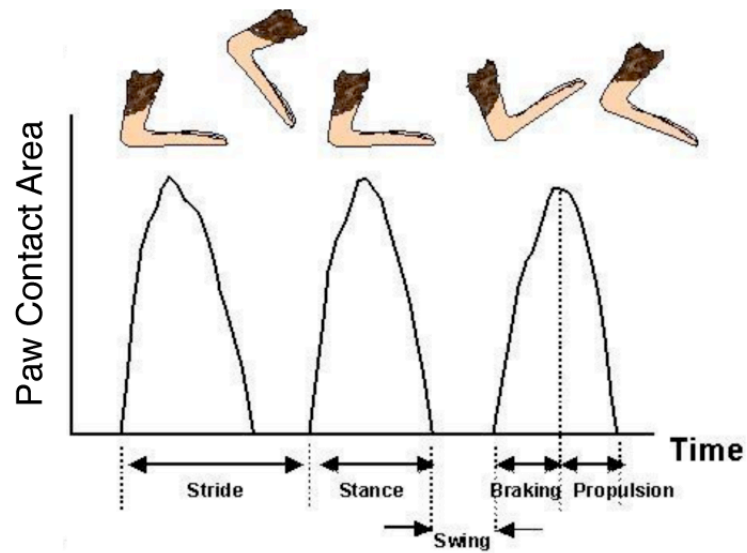


Figure 5.1. Healthy paw placement on the DigiGait in a healthy rodent and the different phases of walking they go through.

Diagram adapted from Mouse Inc data sheet on DigiGait Imaging System. ³¹¹

5.2 Aims

The object of the research carried out within this chapter was to identify and critically assess different methods of behavioural testing and histological staining after murine SCI that could be used in the future to evaluate the potential outcome of a therapeutic strategy, such as SpA. This was carried out by:

- Assessing the potential of BMS, grip strength and DigiGait for use as appropriate behavioural tests after contusive cervical SCI with the IH device.
- The first objective was to identify if any of the parameters measured by the behavioural tests showed changes that did not recover over the 6 weeks of post-injury testing
- Four different injury severities of 50Kdyn, 80Kdyn, 100Kdyn and 120Kdyn were trialled to evaluate the sensitivity of each of the behavioural tests. This was done by examining the limit of detection of each parameter within each of the tests measured to see which, if any, of the behaviour tests were sensitive enough to show differences between the injury groups. This was important, as the test used must be sensitive enough to identify subtle changes in recovery after therapeutic intervention.
- Tract tracing of the cortico-spinal tract was also evaluated as an alternative method to evaluate improvement in outcome after SCI.

5.3 Results

5.3.1 BMS

Twenty C57BL/6 mice underwent SCI contusion surgeries with the Infinite Horizon (IH) device. Four different severities were performed, with 5 mice per group. The impactor tip of the IH delivered a force of 50Kdyn, 80Kdyn, 100Kdyn or 120Kdyn. The 4 different injury groups were tested for hind limb function using the BMS for 6 weeks post-operatively. Mice were allowed to run around a meter pen for four minutes once a day for 5 days prior to the surgery. This acclimatised the mice to the test/apparatus prior to surgery. After surgery the mice were left for a week to recover before the testing commenced. Mice were placed in the same pen and allowed to roam freely while two investigators observed and scored each of the animals back legs separately using the BMS 9 point-scoring system (Table 5.1).

Pre-operatively it was assumed that all mice started with a score of 9 for both limb functions. At the end of testing, mice in the 50Kdyn injury group had recovered full left hind limb function with a score of 9 (figure 5.2A) and almost completely recovered right hind limb function with a score of 7.7 ± 1.2 (figure 5.2B). The 80Kdyn injury group had an average score of 8.2 ± 1.1 for both hind limbs by completion of testing. The 100Kdyn injury group had an average score of 7 ± 0 for both limbs, which meant that they had frequent or occasional planter stepping that is mostly coordinated, and did not show any change from post-operatively 1 to the final testing session.

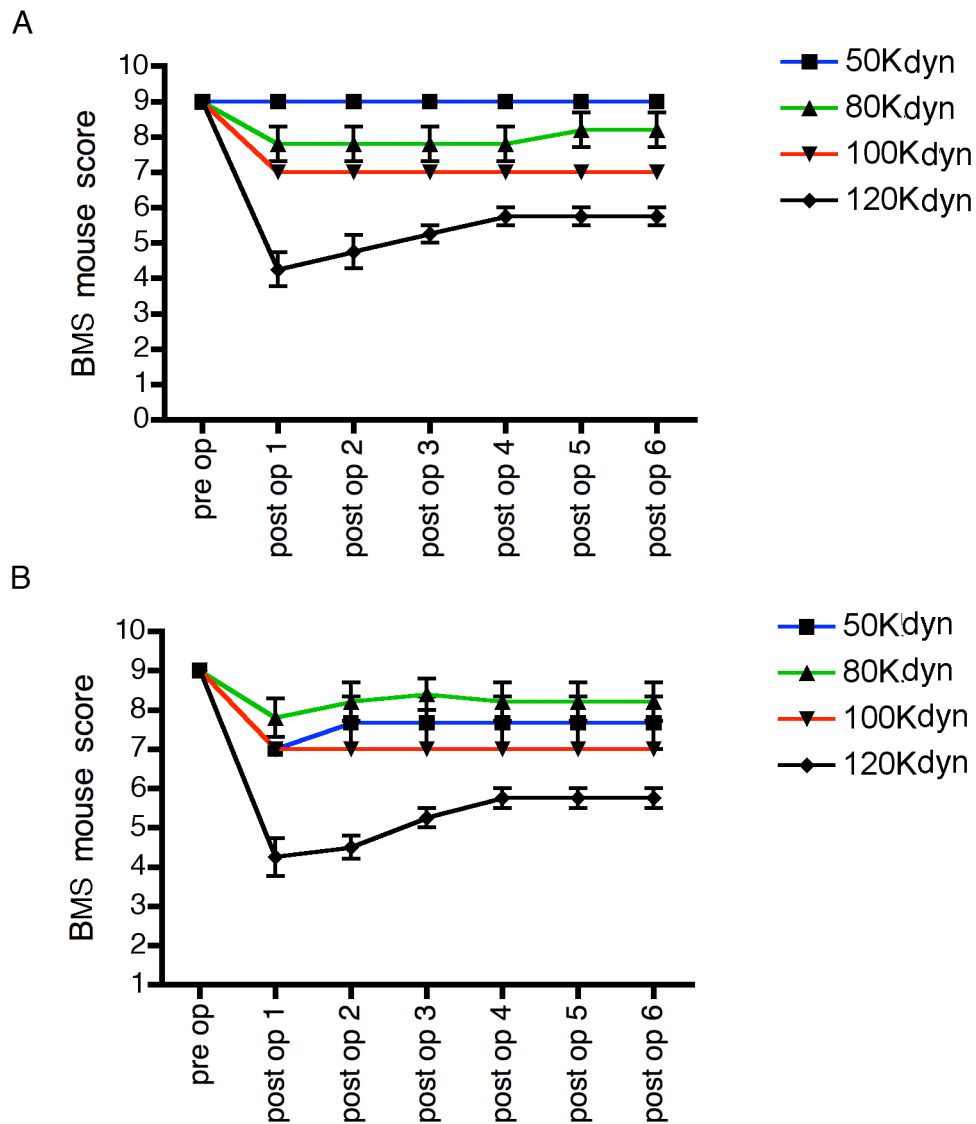
The 50Kdyn, 80Kdyn and 100Kdyn injury group showed a predominately fore limb phenotype and almost normal movement of hind limbs, whereas, the 120Kdyn injury group scored 4, which correlates to only occasional planter stepping, at post-operatively week 1. These mice exhibited a small steady recovery of hind limb function until plateauing at post-operatively week 4 with a final score of 5.8 ± 0.5 for both hind limbs (figure 5.2). From the data collected for the period of BMS testing and the observed phenotype that the animals exhibited, it was concluded that the BMS was not the most suitable test for a mild to medium cervical contusion injury as it solely focused on the hind limbs function and the mice predominately exhibited fore limb ataxia with little impairment to their

hind limbs. With the most severe injury group, this test was deemed to be applicable as this group displayed ataxia in both fore and hind limbs.

5.3.2 Grip Strength

The BMS locomotor test predominantly detects defects in hind limb function. The SCI model, as discussed above, primarily affects fore limbs and not hind limbs. Therefore an alternative test, the grip strength test, was utilized. Importantly, the grip strength test was thought to be a more suitable behavioural test for the injury phenotype induced in this model because it specifically measures fore limb function.

Mice were allowed to acclimatize to the force meter for a week prior to surgery. At the end of this week, baseline data were taken, which consists of allowing the mouse to grab the bar that protrudes from the end of the force meter and then pulling the mouse back by its tail until it releases the bar; the corresponding value is registered on the force meter. This was performed five times per session with each mouse. Mice received an 80Kdyn, 100Kdyn injury or no injury. One-week post-surgery data were collected as described for the acquisition of baseline data. Data were collected once per week from the animals for 6 weeks post surgery.



When the raw data from the 3 groups of animals were examined, there was a clear difference in the maximal muscle strength of injured and non-injured mice (figure 5.3). Following further examination of the data, a similar pattern was seen in all three groups: the amount of grip strength would increase and decrease in harmony until the end of testing (Figure 5.3A). This was true for the uninjured animals as well, which leads to the conclusion that an external factor was influencing the amount of force the animals were able to pull from week to week as the same pattern was displayed in the uninjured group as well as the injured groups. Animals that undergo behavioural testing are very sensitive to external factors such as heat, draught, light and one of these factors could easily account for the difference in the level of force being registered.

For the above reason, the data for the injured animals were normalised against the uninjured animals' scores to show a reduction in the force of the injured mice in comparison to non-injured controls to eliminate external variation (figure 5.3B). When the data were normalised it gave a much clearer picture of the effect of injury. Essentially, animals that are injured dramatically lose maximal muscle strength by comparison with those in the non-injured group. One week after injury the 80Kdyn injury group displayed a significant decrease ($P<0.001$) in grip strength of $42.7\text{g}\pm 12.4\text{g}$. They showed a steady rate of recovery until post-operation week 5, where they had a reduction in normal force of $23.5\text{g}\pm 5.2\text{g}$ in comparison to the non-injured animals. By post-operative week 6 they still showed a significant decrease ($P<0.001$) in the amount of force they could pull ($32.5\text{g}\pm 7.4\text{g}$) (figure 5.3C). When the 80Kdyn injury group's reduction in the amount of force the animals could pull was compared to the non-injured group, there was a statistically significant reduction ($P<0.001$) at every time point (figure 5.3C).

The 100Kdyn injury group showed an initial drop of $54.5\text{g}\pm 6.7\text{g}$ and also exhibited a steady recovery patterns, and by post-operative week 5, the group's decrease of gripping force had increased to $40.3\text{g}\pm 10.1\text{g}$ less than the uninjured group. By the completion of testing, the 100Kdyn showed a grip strength reduction to post-operative week 1 levels of $54.4\text{g}\pm 10.7\text{g}$ (figure 5.3D). When the 100Kdyn injury group's reduction in the amount of force the animals could pull was compared to the non-injured group, there was a statistically significant reduction ($P<0.001$) at every time point (figure 5.3D). The 100Kdyn injury group

displayed the same dip in performance at post-operative week 6 as the 80Kdyn injury group leading to the conclusion that the mice could have become habituated to the test and 6 weeks may be too long for this particular behavioural test. Nevertheless, the grip strength test has shown promising results, which makes it a very good candidate for studies in the future as it is specifically tailored to the fore limb injury phenotype. There were no statistically significant differences between the two injury severities when comparing their reduction in maximal muscle strength after injury at any of the time points (figure 5.3E). This suggests that the grip strength test is not sensitive enough to show subtle differences between the injury groups; however this could be an artefact of too small a sample size and warrants further investigation to see if this issue could be resolved with a bigger sample group to reduce variation within the groups.

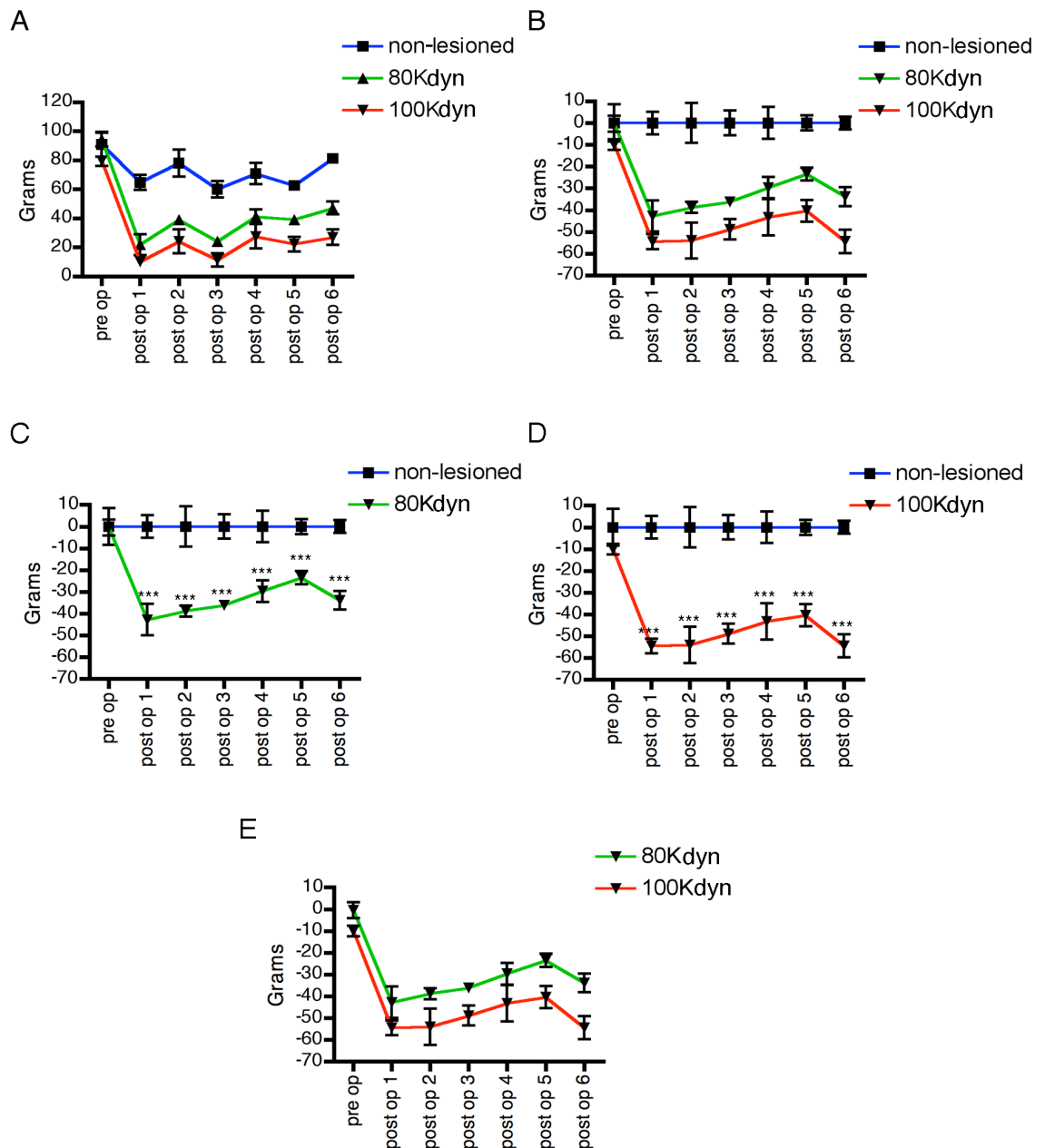


Figure 5.3. Assessment of grip strength in the fore-paws pre-operatively and for 6 weeks post-operatively, following SCI surgery.

Thirteen male C57BL/6 mice were acclimatized to the grip-strength meter and then pre-operative data were recorded. Mice received SCI at differing forces (80Kdyn: n=3 and 100Kdyn: n=4), and three were left as uninjured controls. Mice were left for 1 week to recover and then data collection followed for 6 weeks post-operatively. (A) Raw data from non-lesioned, 80Kdyn and 100Kdyn groups $F_{2,60}=42.18$, $P<0.0001$. (B) The 80Kdyn and 100Kdyn injury groups were normalised against the uninjured group so that the graph shows the reduction in grip strength of the injury group in comparison to non-injured animals $F_{2,60}=42.05$, $P<0.0001$. Statistical analysis was conducted on figure A and B using a repeated measures *two-way ANOVA*, significant differences between groups were determined using a post-hoc Bonferroni test, which compared all groups to each other. For illustrative purposes figure C, D and E were generated from figure B and statistical annotation was added. *** = $P<0.001$

5.3.3 DigiGait

The grip-strength test has been shown to be a potentially useful assessment of fore limb recovery after SCI but it is only 1 parameter. In comparison, DigiGait examines 20 different indices of gait in both the fore and hind limbs and was therefore employed as an additional test to give a more complete measure of recovery from SCI.

Pre-operatively, mice were acclimatised to the DigiGait for one week before data were collected. This consisted of mice being taken one at a time and placed inside the DigiGait perspex box, which surrounds a portion of the transparent treadmill, and trained to walk. When the treadmill is activated electronic “footprints” of the mouse that is ambulating are collected by a high-speed video camera mounted underneath the treadmill shown in figure 5.4. Data were collected during ambulation at two different speeds of 15 and 20 cm/sec. Three runs of 4 sec were collected per speed pre-operatively and then for 6 weeks post-operatively. The segments of data that were collected provided enough strides to determine characteristic gait parameters (e.g. stride length, width and angle) of the mouse for each time-point and speed.

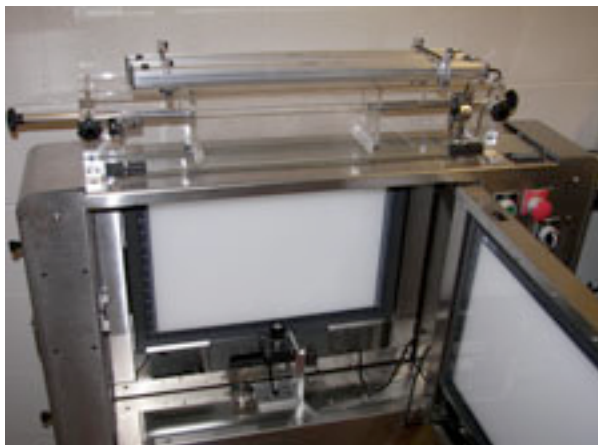


Figure 5.4. DigiGait apparatus.

This consists of a high-speed camera mounted underneath a transparent treadmill. A perspex box covers a segment of the treadmill where the animal is confined.

Of an initial 50 mice that were tested on the DigiGait, only 34 of these mice could be trained to walk on the apparatus and pre-operative data were only gathered for these mice. Of the 34 mice which underwent surgery, only 14 would walk on the DigiGait post-operatively at the speed of 15cm/sec (50Kdyn: n=3, 80Kdyn: n=6 and 100Kdyn: n=5) and 8 mice would run at 20cm/sec (50Kdyn: n=3, 80Kdyn: n=4 and 100Kdyn: n=1) for the entirety of the experiment. Due to the small sample number of mice that would run at the higher speed of 20cm/sec, the results have not been shown. After injury the 50Kdyn mice had no issues in participating in testing from post-operatively week 1; the 80Kdyn mice could participate in testing from post-operatively week 2 and the 100Kdyn could start participating from post-operatively week 4. However, the 120Kdyn mice were too severely injured to take part in this method of behavioural assessment.

Some of the parameters that were analysed by the DigiGait after injury did not change, examples being swing stride % (figure 5.5), brake stride % and propel stride (data not shown). These three parameters are all interlinked as they make up the complete movement of the stride, defined as the time the foot takes from leaving the belt to touching it again. Propel is the point at which the foot is leaving the belt; swing is where it is off the belt entirely and brake is where it makes contact with the belt until it is completely flat. As such, these parameters are of limited utility for further analysis.

Some of the parameters the DigiGait analysed showed initial change from the baseline pre-operative data but returned to normal by the end of the testing period. This was most evident with the 50Kdyn injury group as it was noted that they had only a very transient injury phenotype and by post-operatively week 4 appeared to be fully recovered. An example of this is in the brake stance (figure 5.6A) where the fore-limb shows initial change, reaches a significant change at post-operatively week 3, but has returned to baseline by post-operative week 4. The parameter brake stance also showed inherent fluctuations and variability within each of the groups - having very large variations throughout all of the injury groups. This is most evident in the 80Kdyn and 100Kdyn groups where it looks as if there is a change in this parameter compared to pre-operative testing, however, the spread of data is so wide it is not statistically relevant.

The DigiGait analysis did reveal some parameters that changed from the baseline to the end of post-operatively week 6. The parameter 'stride frequency', which measures the number of strides a mouse takes per second, was statistically significant at post-operatively week 6 in comparison to pre-operative data within fore (figure 5.7) and hind limbs (data not shown) in all three of the injury severities. Nonetheless, when the data from each of the injury severities was combined together to examine if the DigiGait was sensitive enough to be able to show significant differences in the injury severities at individual time points (figure 5.7D), it revealed that the most statistically significant time-point between the 50Kdyn and 80Kdyn was in fact the pre-operative data (figure 5.7E). This was also seen between the 50Kdyn and the 100Kdyn injury groups (figure 5.7E). The result reveals the high variability and inherent insensitivity of using this method for behavioural testing, as these are genetically inbred mice, which you would expect to have the same pre-operative levels of stride frequency. The 80Kdyn and 100Kdyn groups showed no significant difference at any time points.

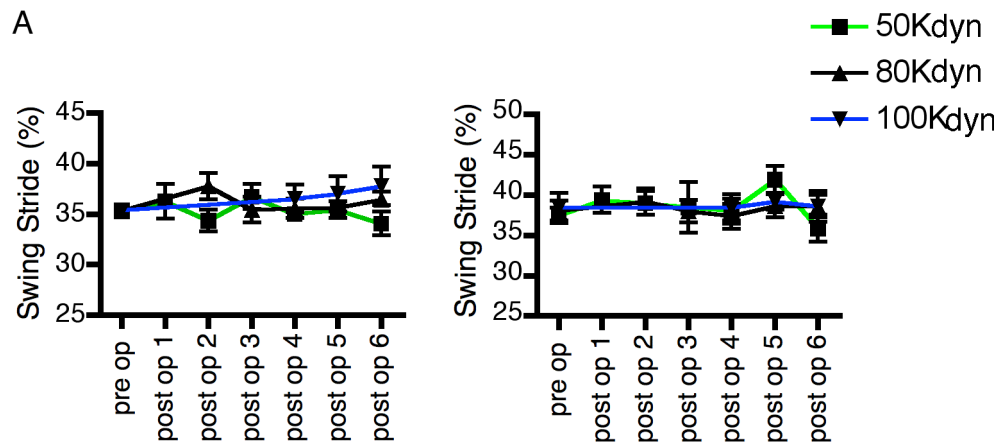


Figure 5.5. Assessment of swing stride percentage in the fore and hind limbs pre-operatively and 6 weeks post-operatively, following SCI surgery.

14 C57BL/6 mice were trained on the DigiGait to walk and then pre-operative data were recorded. Mice received SCI at differing forces (50Kdyn: n=3, 80Kdyn: n=6 and 100Kdyn: n=5). The mice were left for 1 week to recover and then data collection followed for 6 weeks post-operatively. Data were analysed on the DigiGait software. (A) Fore-limb swing stride. (B) Hind-limb swing stride data

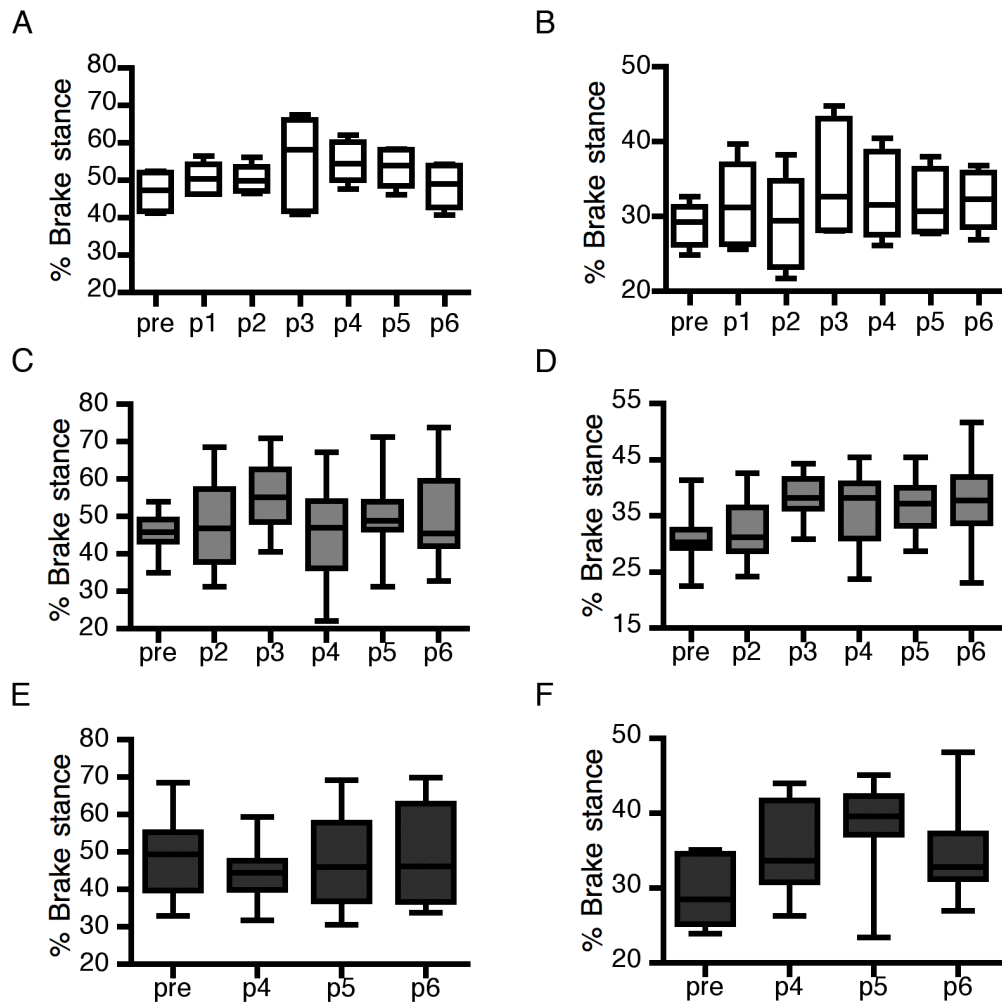


Figure 5.6. Assessment of percentage brake stance in the fore and hind limbs pre-operatively and 6 weeks post-operatively, following SCI surgery.

14 C57BL/6 mice were trained on the DigiGait to walk and then pre-operative data were recorded. Mice received SCI at differing forces (50Kdyn: n=3, 80Kdyn: n=6 and 100Kdyn: n=5). Mice were left for 1 week to recover and then data collection followed for 6 weeks post-operatively. Data were analysed on the DigiGait 'mouse-specific' computer programme. (A) Fore-limb 50Kdyn. (B) Hind-limb 50Kdyn. (C) Fore-limb 80Kdyn. (D) Hind-limb 80Kdyn. (E) Fore-limb 100Kdyn. (F) Hind-limb 100Kdyn.

Two parameters that are also examined in the DigiGait system and are intertwined with stride frequency are steps per second (figure 5.8) and stride length (figure 5.9). Both of these parameters show significant differences in their pre-operative levels in comparison to post-operative week 6, which fulfils one of the aims of this chapter. Nevertheless, when the sensitivity of these parameters was examined further the same level of inconsistency in pre-operative test data was demonstrated in both steps per second (figure 5.8E) and stride length (figure 5.9E). The data-spread within each of the post-operative weeks is extremely wide for the parameter 'steps per second' and again demonstrates the substantial levels of variability within the system.

Another limitation of this behavioural test was that due to the fore-paws of the 100Kdyn injury group exhibiting spastic clenching, fore-paw angle could not be looked at. Hind-paw angle showed no significant change in 50Kdyn (figure 5.10A) and 100Kdyn (figure 5.10C) injury groups at the end of testing. This was due to massive amounts of variation in the data recorded for each of the time points. The 80Kdyn groups did show a statistically significant difference in paw angle (figure 5.10B), showing a decrease in rotation by the end of testing. When the data from the three injury groups were combined together no statistical difference was seen amongst the pre-operative injury groups. The 80Kdyn group showed a statistical difference in paw rotation from the 50Kdyn injury group at the end of testing - but not compared to the 100Kdyn injury (figure 5.10D). However, due to the massive variation within each of the injury group's data-sets, at each time point, it made the finding somewhat irrelevant. Thus the data suggests that the DigiGait is not sensitive or reliable enough for use in the testing of therapeutic intervention in mice. However, it has given us a small insight into the phenotype of the injury that the contusion injury induces. This insight reveals that the mice decrease the number and frequency of steps and strides they take per second, but that they compensate by increasing the length of the strides that they do take.

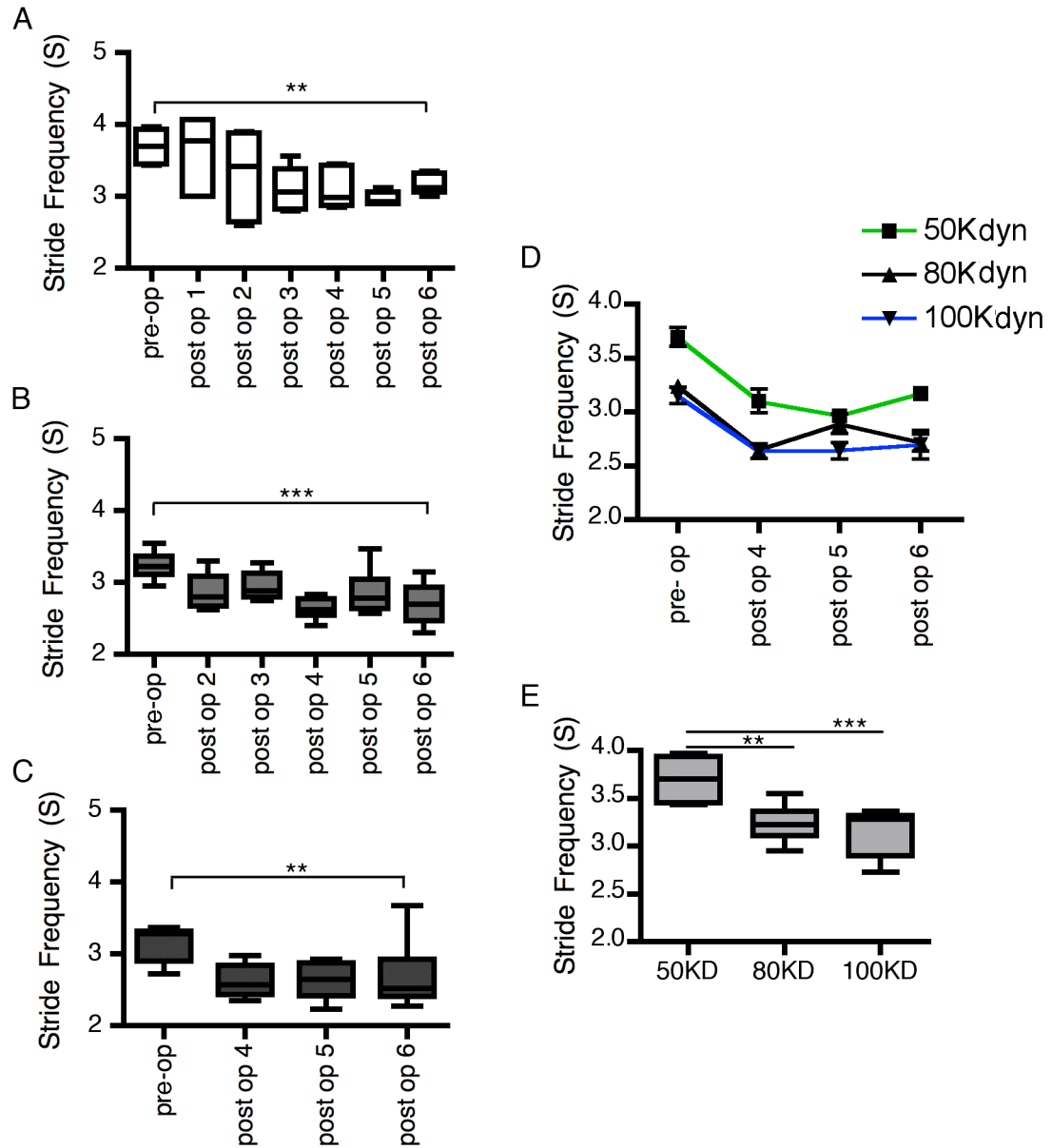


Figure 5.7. Assessment of stride frequency per second in the fore limbs pre-operatively and 6 weeks post-operatively, following SCI surgery.

14 C57BL/6 mice were trained on the DigiGait to walk and then pre-operative data were recorded. Mice received SCI at differing forces (50Kdyn: n=3, 80Kdyn: n=6 and 100Kdyn: n=5). Mice were left for 1 week to recover and then data collection followed for 6 weeks post-operatively. Data were analysed on the DigiGait 'mouse specific' computer programme. Statistical analysis was conducted using a repeated measures *one-way ANOVA*, significant differences between groups were determined using a post-hoc Bonferroni test, which compared all post-operative week 6 data to pre-operative data, apart from in figure E which used a Bonferroni post-hoc test that compared all groups to each other. * = $P < 0.05$, ** = $P < 0.01$, *** = $P < 0.001$. (A) Fore limb 50Kdyn $F_{6,41} = 5.656$, $P < 0.0005$. (B) Fore limb 80Kdyn $F_{5,71} = 10.41$, $P < 0.0001$. (C) Fore limb 100Kdyn $F_{3,39} = 7.14$, $P < 0.0011$. (D) Combined 50Kdyn, 80Kdyn and 100Kdyn fore limb data. (E) Pre-operative combined data $F_{2,27} = 13.32$, $P < 0.0001$

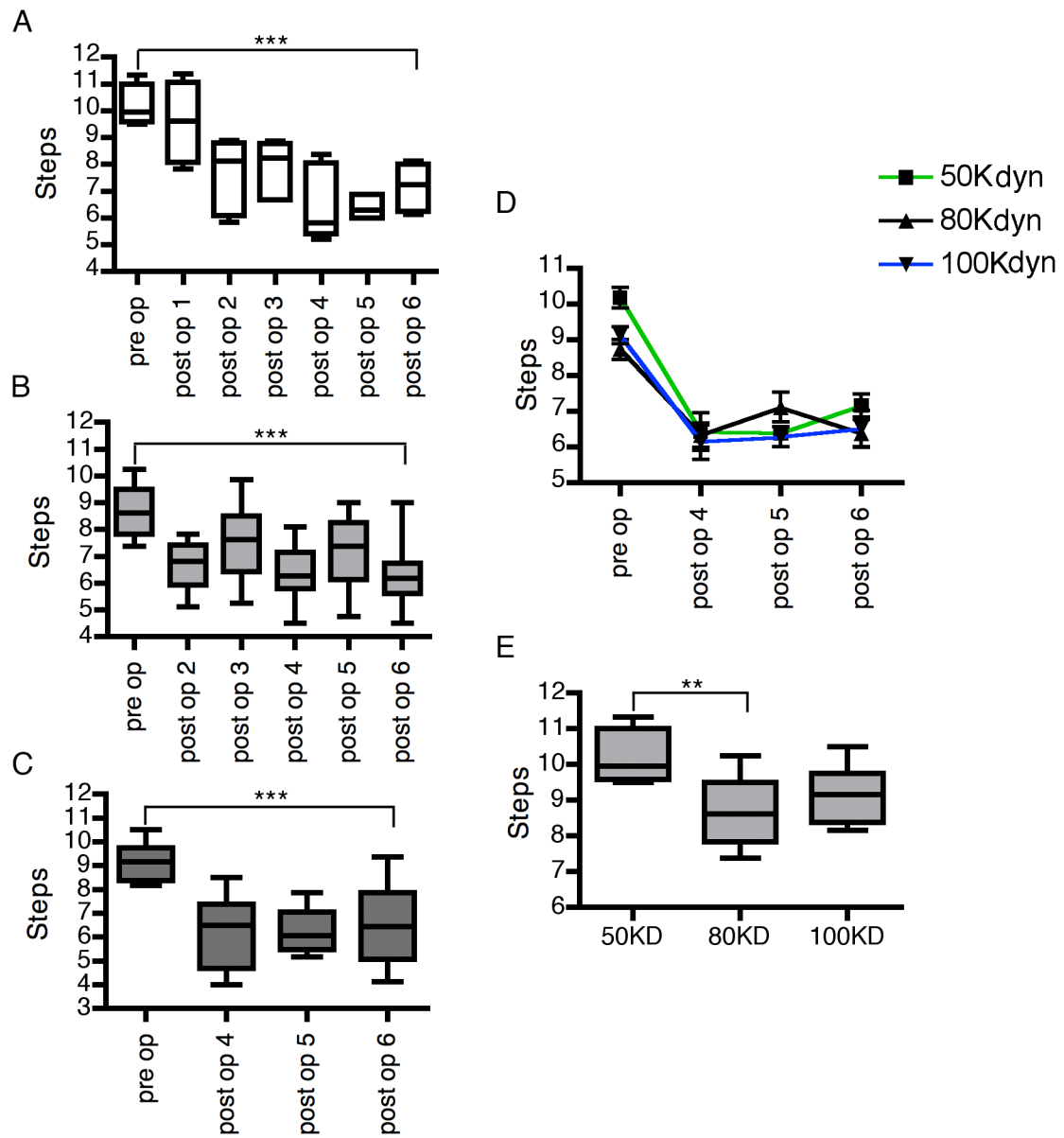


Figure 5.8. Assessment of the number of steps taken within a second in the fore limbs pre-operatively and 6 weeks post-operatively, following SCI surgery.

14 C57BL/6 mice were trained on the DigiGait to walk and then pre-operative data were recorded. Mice received SCI at differing forces (50Kdyn: n=3, 80Kdyn: n=6 and 100Kdyn: n=5), and were left for 1 week to recover; then data collection followed for 6 weeks post-operatively. Data were analysed on the DigiGait 'mouse specific' computer programme. Statistical analysis was conducted using a repeated measures *one-way ANOVA*, significant differences between groups were determined using a post-hoc Bonferroni test, which compared all post-operative week 6 data to pre-operative data, apart from in figure E which used a Bonferroni post-hoc test that compared all groups to each other. **= $P < 0.01$, *** = $P < 0.001$. (A) Fore limb 50Kdyn $F_{6,41} = 11.72$, $P < 0.0001$. (B) Fore limb 80Kdyn $F_{5,71} = 7.46$, $P < 0.0001$. (C) Fore limb 100Kdyn $F_{3,39} = 12.36$, $P < 0.0001$. (D) Combined 50Kdyn, 80Kdyn and 100Kdyn fore limb data. (E) Pre-operative combined data $F_{2,27} = 5.73$, $P < 0.0089$

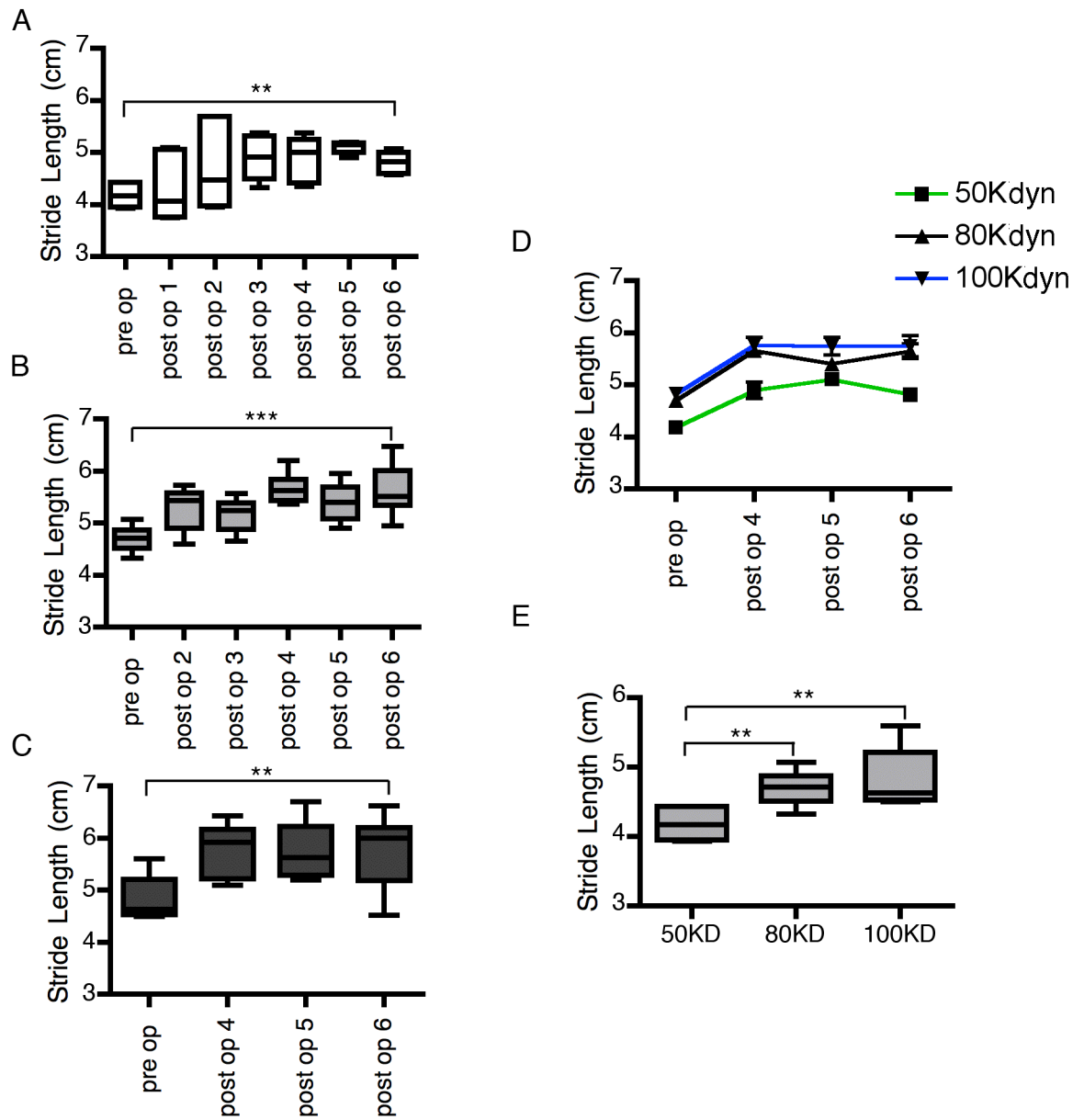


Figure 5.9. Assessment of stride length in the fore limbs pre-operatively and 6 weeks post-operatively, following SCI surgery.

14 C57BL/6 mice were trained to walk on the DigiGait, and then pre-operative data were recorded. Mice received SCI at differing forces (50Kdyn: n=3, 80Kdyn: n=6 and 100Kdyn: n=5), and were left for 1 week to recover; then data collection followed for 6 weeks post-operatively. Data were analysed on the DigiGait 'mouse specific' computer programme. Statistical analysis was conducted using a repeated measures *one-way ANOVA*, significant differences between groups were determined using a post-hoc Bonferroni test, which compared all post-operative week 6 to pre-operative data, apart from in figure E which used a Bonferroni post-hoc test that compared all groups to each other. * = $P < 0.05$, ** = $P < 0.01$, *** = $P < 0.001$. (A) Fore limb 50Kdyn $F_{6,41} = 4.771$, $P < 0.0016$. (B) Fore limb 80Kdyn $F_{5,71} = 14.19$, $P < 0.0001$. (C) Fore limb 100Kdyn $F_{3,39} = 7.88$, $P < 0.0006$. (D) Combined 50Kdyn, 80Kdyn and 100Kdyn fore limb data. (E) Pre-operative combined data $F_{2,27} = 8.496$, $P < 0.0015$

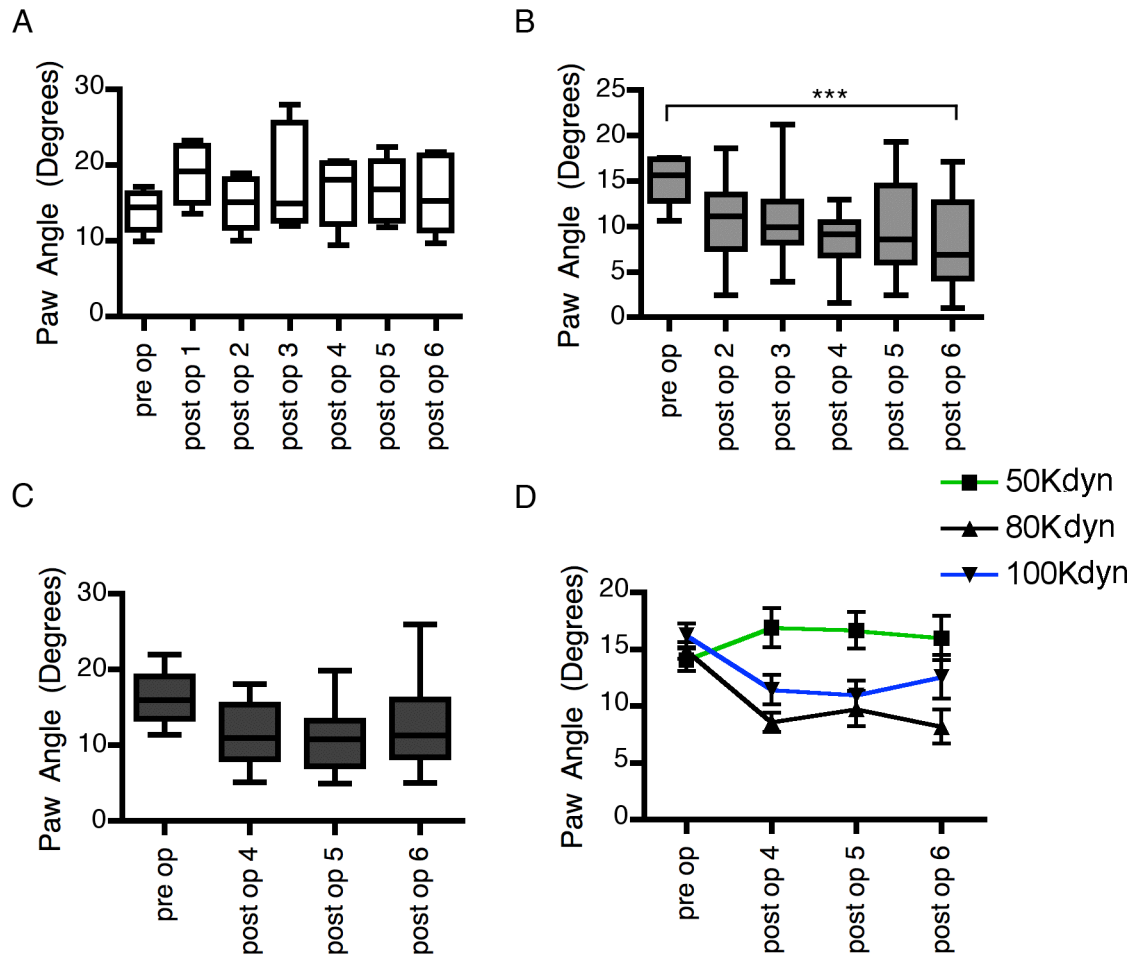


Figure 5.10. Assessment of paw angle in the hind limbs pre-operatively and 6 weeks post-operatively, following SCI surgery.

14 C57BL/6 mice were trained to walk on the DigiGait and then pre-operative data were recorded. Mice received SCI at differing forces (50Kdyn: n=3, 80Kdyn: n=6 and 100Kdyn: n=5), and were left for 1 week to recover; then data collection followed for 6 weeks post-operatively. Data were analysed on the DigiGait 'mouse specific' computer programme. Statistical analysis was conducted using a repeated measures *one-way ANOVA*, significant differences between groups were determined using a post-hoc Bonferroni test, which compared all post-operative week 6 to pre-operative data. *** = $P < 0.001$. (A) Hind limb 50Kdyn. (B) Hind limb 80Kdyn $F_{5,71} = 6.099$, $P < 0.0001$. (C) Hind limb 100Kdyn. (D) Combined 50Kdyn, 80Kdyn and 100Kdyn hind limb data.

5.3.4 BDA tract tracing

Another avenue with which to investigate SCI and therapeutic efficacy is BDA tract tracing of axonal tracks. BDA track tracing labels axons of a given neuronal track. This is relevant for the assessment of therapeutic efficacy as damage to individual neural pathways can be quantified with the amount of BDA tracer present rostral and caudal of the lesion. BDA track tracing of the cortico-spinal tract is already an established technique for assessing axonal regeneration, and examining levels of Wallerian degeneration. It has also been used recently to test the efficacy of a T-cell based therapy in a rat SCI model - showing that when treated rats had a decrease in the level of 'die back' of axons from the lesion site compared to the control treated group¹⁴⁶. The cortico-spinal tract was chosen for BDA tracing because it is a tract that contains mostly motor neurons - which underlie our voluntary movements - and runs from the brain along the spinal cord. In humans the tract controls fine, complex movements such as hand and finger dexterity.

Twenty mice from a range of injury severities underwent the BDA tract tracing procedure. However, a full investigation could not be performed due to both time constraints and access to the microscope. In brief, mice were allowed a week to recover from SCI surgery before they underwent surgery for BDA tract tracing (performed by Dr John Riddell and assisted by Andrew Toft). This was performed by making a small incision in the scalp of the mouse with a subsequent small window being drilled into the skull over the left sensorimotor cortex. Using the bregma as an anatomical reference point, injections of BDA were made at four sites. The scalp incision was sutured closed; the mice were allowed to recover for 14 days before being perfused, and the damaged section of the cord being removed. Sections were cut on a freezing microtome, first in a horizontal section caudally to the lesion to examine if the BDA track tracing targeted the correct tract. The remaining section was cut in sagittal cross-section to look at the longitudinal staining of the tract (sectioning and staining was performed by myself under the tutelage of Andrew Toft, who also supervised with the imaging of sections).

In the only sections that were imaged, it can be observed that in the horizontal sections of the spinal cord, above the injury site, staining is mainly observed in

the dorsal cortico-spinal tract (figure 5.11A). In the longitudinal section a large lesion can be seen in the centre of the picture with reactive astrocytes (GFPA: blue) forming the glial scar round the outside of the lesion epicenter. BDA (green) stained neurons can be identified rostral to the lesion site - but caudally there was no staining (figure 5.11B). This reveals that the dorsal cortico-spinal tract in 100Kdyn SCI mice is totally ablated by the injury and BDA tract tracing may be a possible technique to use to determine if there is sparing of any of the axons in this tract after treatment with a therapeutic agent.

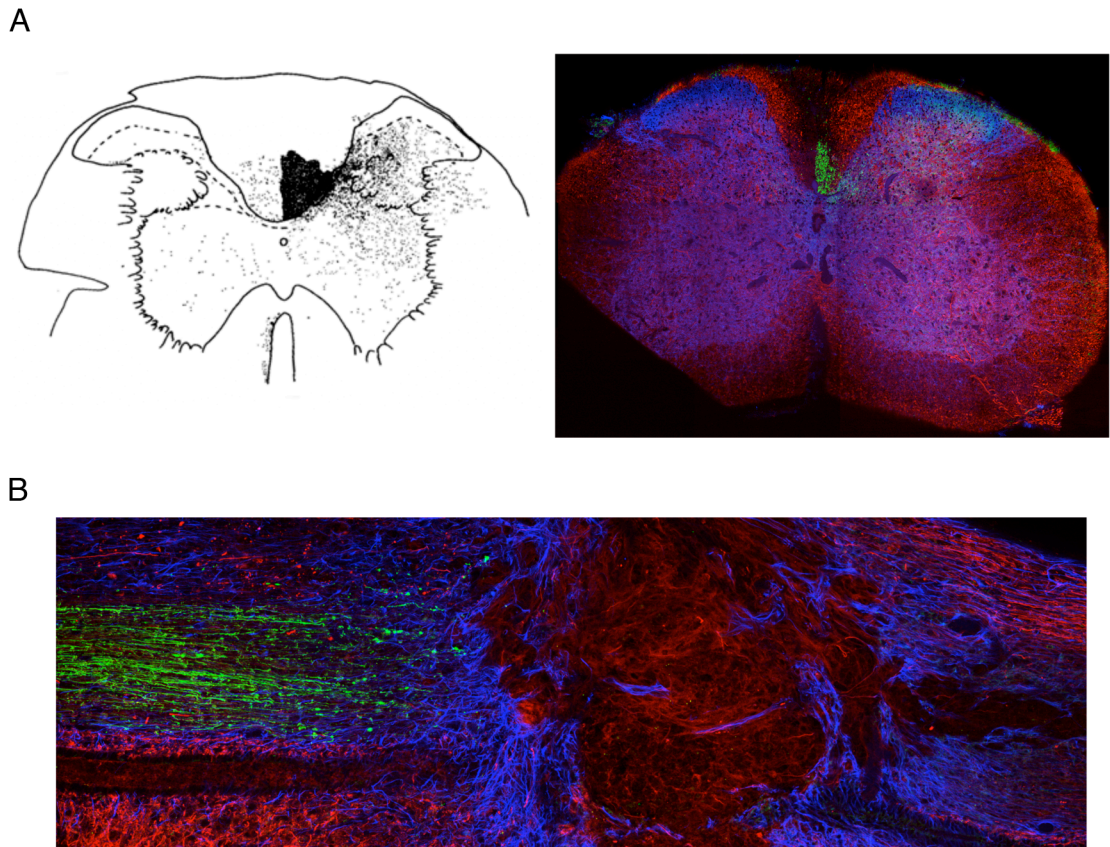


Figure 5.11. BDA staining of the cortico-spinal tract in a 100Kdyn SCI mouse.

(A) Horizontal cross sections of the damaged spinal cord rostral to the lesion and a schematic diagram of the same section of the spinal cord identifying the location of the dorsal cortico-spinal tract. (B) Sagittal sections of the damaged portion of the spinal cord. In both sections staining consists of GFPA (blue), NF200 (red) and BDA (green).

5.4 Discussion Conclusion

The aim of this chapter was to discover the most sensitive and appropriate single or multiple readouts for the possible future experimental treatment of SCI with SpA as a mode of modulating the inflammatory response seen after SCI.

At the outset, it was determined that the method of assessment must be sensitive enough to show subtle improvements in anatomical structure or functional recovery that the therapeutic might impart. BDA tract tracing of the cortico-spinal tract was inspected to determine if it was suitable for use as an indicator of anatomical change following the treatment of SpA after SCI. Three different behavioural tests were also considered when it came to assessing hind limb function, fore limb function and gait parameters. The tests not only had to identify a functional read-out/parameter that was changed after SCI - and remained changed for the length of the testing period - but also had to be sensitive enough to detect minor oscillations in these parameters after treatment of a therapeutic. This was the reason four different injury severities were used to scrutinize the sensitivity each of the tests was able to offer - and in the tests' ability to detect differences between the various injury-severity groups.

Unfortunately, a full and proper examination of the BDA tract tracing method was not possible due to time constraints operating the microscope used to generate images from sections of damaged spinal cord that had their cortico-spinal tract traced with BDA. Two complete images of 100Kdyn animals were generated and these showed the complete ablation of the cortico-spinal cord with only axons rostral, but not caudal, of the lesion being labelled with BDA. This type of tract tracing has been used in many experiments in conjunction with behavioural testing to assess therapeutic regimes^{312 146}. It is therefore a method that warrants further investigation as it has been shown to be an appropriate method of examining the damaged spinal cord as there was no spontaneous regeneration of the cortico-spinal tract in either of the sections scrutinized; however the sensitivity level of this technique must be investigated further to establish its overall suitability.

Looking at the first possible behavioural test measure, BMS, the data suggests that this is not an appropriate test for cervical contusion injury of 100Kdyn or less as the injury has a predominately fore limb phenotype and the BMS is a hind limb only locomotor gait scoring system³⁰⁵. The only injury group that this test had potential utility in was the 120Kdyn injury group as this injury severity exhibited a hind limb, as well as a fore limb, phenotype. Nevertheless, even though the BMS did recognise the hind limb phenotype in the 120Kdyn group, the group had a far more pronounced deficiency in their fore than hind limbs that this measure did not take account of. The BMS did not exhibit any notable differences between the scoring of the 50Kdyn, 80Kdyn and 100Kdyn injury phenotypes - leading to the conclusion that the BMS is not a sufficiently sensitive assessment of injury, and will thus not be used in the future.

Next to be considered was the DigiGait, which examines the gait of mice when ambulating, encompassing both hind and fore limbs, and giving a readout of over 20 different parameters for analysis. Some of the parameters such as number of steps taken per second, stride length and stride frequency did show significant statistical changes from pre-operative to post-operative week 6. Nevertheless, this test was not sensitive, stringent or reliable enough for use in the future to evaluate the ability of a therapeutic agent such as SpA.

One of the major draw-backs of using the DigiGait compared to the other two methods of behavioural testing was that not all injury groups could participate in testing from post-operative week 1 - or, indeed, at any stage in the process; the most telling reason for this being the fact that the most severe injury group (120Kdyn) were unable to walk on the DigiGait at any time-point during the whole testing period. The 100Kdyn mice did not all walk until post-operative week 4; the 80Kdyn mice walked from post-operative week 2 onwards and the 50Kdyn injury group was the only group that could take part in every week of testing.

Due to these limitations, this test did not give a good indication of the varying degrees in injury phenotypes of these mice at different injury severities. The 50Kdyn mice showed very little permanent adverse effects, and exhibited normal behaviour such as hanging upside down from the roof of their cages from post-operative week 4 onwards. This was substantially different to the 100Kdyn

mice as they showed significant injury phenotypes until the end of the study with no sign of resolution. One such phenotype was the spastic clenching of fore-paws in at least one, if not both, of the paws. The 100Kdyn mice also exhibited hair loss on the inside of their fore limbs and thorax, which was suspected by the vet to be a consequence of over grooming or rubbing of these areas due to partial or full loss of sensation as a consequence of the injury. The clenched paw and hair loss was not evident in the 80Kdyn groups.

The DigiGait results did not adequately capture the visible differences observed between the 80Kdyn and the 100Kdyn injury groups in any of the parameters that showed a significant difference after the 6 weeks of testing from the pre-operative data. This highlights the lack of sensitivity of this technique - that a distinctive set of injury phenotypes can be seen in the different groups but could not be picked up by the behavioural test. The DigiGait did show statistically significant differences in post-operative week 6 phenotypes between 50Kdyn versus 80Kdyn and 50Kdyn versus 100Kdyn in parameters of stride length and stride frequency. However, on closer examination of these results it was revealed that there was not only a statistically significant difference in post-operative data between the 50Kdyn versus 80Kdyn and 50Kdyn versus 100Kdyn, but there were also statistically significant differences in the pre-operative data. This is very concerning and identifies a worrying lack of reliability and sensitivity in the DigiGait system: the pre-operative data for the cohort of a genetically identical inbred mouse strain should *not* be significantly different.

Another problem with the DigiGait system was the very high drop-out rate: 72% of the starting cohort failed to complete. 50 mice were initially earmarked for testing with the DigiGait but only 14 finished the study. This was for the most part due to mice being unwilling to walk on the DigiGait at the time of testing; only 3 of the drop-outs were due to fatalities in surgery. Mice would simply not move when the treadmill started or they would avoid the treadmill by climbing up the walls of the Perspex box in which they were housed when testing began. At other times they would “bunny hop” with their hind legs, which was not an accurate representation of their walking ability and many runs had to be excluded based on this. If three runs could not be collected over a three-day period of the post-operative week, the mice had to be excluded from the study.

Furthermore, large variation was seen within each of the injury groups; percentage brake stride being a good example of this: results from the post-operative week 4 for the fore-paw 80Kdyn group ranged from 20% to almost 70% of a spread in values for what was the same group. This is a substantial degree of fluctuation and may be due to limitations/deficiencies within the analysis software (DigiGait systems). It was noted that mice would become habituated to running on the DigiGate and “bunny hop”, as discussed above. These runs were excluded from the test if they were noticed; however, it is possible that not all of these types of movement were caught before the raw data were analysed and therefore it is possible that a true representation of the animals’ gait was not always portrayed.

Another source of variability that could have been introduced at the analysis level is in relation to the ‘snout and tail blocker’. In this test, there must be a snout and tail blocker manually added by the investigator within the analysis software. The reason for this requirement is that as the software tracks the footprints of the mouse by their pink colour, it can therefore inadvertently mistake a nose or tail for a paw if these have not been blocked out completely. This normally causes a problem if the mouse runs in a side-to-side motion on the treadmill resulting in the blockers being ineffective. Thus, the DigiGait may not be sensitive, suitable or reliable enough as a test for use in the future for examining the benefits of therapeutic strategies in mice.

The most suitable form of behaviour testing was the grip strength test. This was due to the predominant fore limb injury phenotype that was induced by the SCI contusion model used in this study, and the grip strength being a behavioural test that is specifically designed to test for deficiencies in forelimb function⁸⁷. The grip strength is also a well-established behavioural test that has been used by many other groups to assess recovery after SCI in both mice and rats^{313 302}.

The grip strength test showed a statistically significant decrease in the maximal muscle force the injured animal could grip with their fore-paws throughout the test period, and showed a significant difference at all time points between the non-injured group versus the 80Kdyn and 100Kdyn injury groups. A trend was observed in the data, showing that the 100Kdyn injury group lost a greater degree of maximal muscle strength than the 80Kdyn injury group. Nevertheless,

there was no significant difference between the two injury groups, indicating that the test lacks a finer level of sensitivity. However, it should be appreciated that this aspect of the study was only carried out with N=3 for the 80Kdyn and N=4 for the 100Kdyn injury group, which may be too small a sample size. Statistical significance may be achieved if the sample size is increased.

Two major advantages of the grip strength over the DigiGait test emerged: there were no drop-outs from the grip strength over the testing period and all animals could take part in the testing from week 1; unlike the DigiGait, where 100Kdyn animals could not take part in testing until post-operative week 4 and 72% of the initial 50 animals designated to take part in the DigiGait study failed to complete the testing period. Secondly, whilst the DigiGait does examine fore limb function like the grip strength test, it is very dependent on the training and cooperation of the animals taking part in the study, whereas the grip strength takes advantage of the inherent trait that mice will grab onto the closest object to them when held by the tail - and little training is therefore needed.

Thus, in conclusion, future studies will be needed to evaluate the potential of the grip strength test and BDA tracing of the cortico-spinal tract to determine if they are sensitive enough methods of assessment in detecting subtle improvements in recovery in the setting of SCI after treatment with an experimental therapeutic, such as SpA.

6 Discussion, conclusion and future experiments

6.1 Discussion

In this thesis, it has been shown that SpA in the presence of IgG (SIC) has the ability to polarize macrophages to an anti-inflammatory phenotype *in vitro* in conjunction with LPS. The phenotype of SIC-treated macrophage is characterized by the induction of IL-10 and inhibition of IL-12 cytokine production. The macrophages also show MHC II down-regulated via an IL-10-independent pathway. However, SIC-treated macrophages show no alteration in their ability to produce NO and IL-6 compared to LPS-only treated macrophages. This phenotype was dependent on the formation of SIC with polyclonal IgG or complexes generated with a 1:1 ratio of IgG1/2a and to a lesser extent with IgG2a and their ability to signal through FcγRI.

When SpA's ability to interact with and polarize the myeloid compartment to an anti-inflammatory phenotype was examined *in vivo*, it was demonstrated that SpA can bind to monocytes, and preferentially to the Ly6C^{hi} monocyte sub-population. It was also revealed that SpA induced the maturation of the Ly6C^{hi} (pro-inflammatory) monocyte population into a Ly6C^{low} (anti-inflammatory) monocyte in steady-state conditions in the blood. It should be appreciated, however, that monocyte phenotype is a controversial issue. Studies have stated that Ly6C^{low} cells are anti-inflammatory/patrolling and Ly6C^{hi} cells are pro-inflammatory⁴⁰; while others have provided evidence that Ly6C^{low} monocytes can induce inflammatory responses and Ly6C^{hi} cells can be anti-inflammatory⁶². In the steady-state, it would seem that the classification of Ly6C^{hi} and Ly6C^{low} specific subsets by Geissman et.al. is the evolutionarily conserved default phenotype. Nevertheless, there is growing recognition that monocyte and macrophage function can be modified by their local environment to become either pro or anti-inflammatory no matter what they were pre-disposed to do before they entered the tissue⁶³. A good example of an environment that induces phenotypic modifications in monocytes is the intestine, where newly-arrived inflammatory monocytes (Ly6C^{hi}) differentiate into IL10-producing anti-inflammatory CX₃CR1^{hi} tissue macrophages⁶⁴.

To examine the ability of SpA to induce the maturation of Ly6C^{hi} monocytes into Ly6C^{low} monocytes in inflammation without the complication of environmental modification (for example, what happens in the intestine), SCI was chosen as a model because of its large inflammatory infiltrate, which is predominantly myeloid in nature. One caveat that has recently been discovered is that the glial scar may have some immune-modulating properties. Fourteen days after SCI, it was shown that microglia and infiltrating blood monocytes co-localized in the margins of the lesion where copious amounts of CSPG are produced. This results in the production of high levels of IGF-1, which has been shown to be a neuronal survival factor ¹¹⁰. Inhibition of CSPG via Xyloside (a pharmacological inhibitor of CSPG) treatment attenuates IGF-1 production and increases TNF α production via the monocyte and microglial populations that surround the margins of the lesion. This leads to an increase in lesion size and decrease in functional recovery ¹¹¹. More interestingly, at 7 days post-injury, IL-10-producing macrophages were seen at the site of the margin where CSPG was present; the macrophages were also shown to have up-regulated MMP-13, which in turn leads to the degradation of the glial scar. This data suggests a unique regulatory feedback loop that not only alters the immune response but also changes glial scar degradation. However, this work was performed in the context of a T cell-specific MOG-activating vaccine, which was administered a week before injury and may have skewed the results ¹¹². Having stated this concern, it should be appreciated that it was shown that isolated CD115+ monocytes, when cultured in the presence of LPS and CSPG, produce IL-10 in an *in vitro* setting and therefore may be of physiological relevance.

This previous work shows that IL-10 is a vital mechanism for immune regeneration in the spinal cord, though it might be initiated too late to have an effect on the harmful pro-inflammatory immune response which begins within hours of injury. For this reason, the time-point of 24h post-injury was chosen to administer SpA as it was recognized that elimination of the inflammatory immune response would lead to inefficient clearing of cellular debris and would not initiate a wound-healing program. Thus 24h would allow the infiltration of neutrophils and some monocytes to initiate the clean-up and repair program. However, after the administration of SpA at 24h post injury this would allow the generation of anti-inflammatory monocytes. This, in turn, would shut off the

uncontrolled inflammatory feedback loop that is established within the spinal cord after injury.

When SpA treatment was examined in the inflammatory setting of SCI, it was seen to have the ability to increase the Ly6C^{low} monocyte population within the damaged cord and also in the peripheral blood. CD64 and Gr1 were both down-regulated on the Ly6C^{hi} monocytes after SpA treatment. These markers are expressed at lower level (CD64) or are absent (Gr1) on Ly6C^{low} monocytes when compared to the Ly6C^{hi} population. Interestingly, there was no down-regulation of MHC II on the monocyte populations found in blood after SpA treatment, which was a feature of SIC-treated BMDMs *in vitro*. However, it is known that MHC II is not constitutively expressed by all monocytes - being present on the Ly6C^{low} monocytes but not on the Ly6C^{hi} monocyte subpopulation. Therefore, this difference in monocyte and BMDM phenotypes may explain the anomaly in results. Another reason could be the cytokine milieu of the blood in homeostasis - and after SCI may not exhibit the right environmental cues to induce the up-regulation of MHC II from their constitutive baseline levels, therefore masking the effect SpA could potentially have on MHC II levels. MHC II could not be examined on the monocytes in the damaged spinal cord due to technical issues with the number of flouorochromes being available on the FACS machine being used to carry out this set of experiments. In future experiments it would be interesting to examine monocyte MHC II expression in the injured spinal cord after SpA treatment to determine if MHC II is expressed at higher levels on these infiltrating monocytes than their peripheral blood counterparts and, if so, can treatment induce the down-regulation of MHC II on monocytes found in the spinal cord after injury.

Due to some differences with SpA's effects on monocytes and BMDM, along with the findings from Shechter et al that Ly6C^{hi} monocytes were actually the subset that produced IL-10 in the damaged spinal cord²⁹⁸, it was sought to confirm *in vivo* the *in vitro* observation that SIC (in the presence of LPS - an inflammatory surrogate) could induce IL-10 up-regulation in BMDCs. To do this, we examined the ability of SpA to induce the up-regulation of IL-10 in the Ly6C^{hi} & ^{low} monocyte populations that are present in the damaged cord after injury. Vert-X mice, which are GFP IL-10 reporter mice, were used due to the technical difficulties of carrying out intracellular cytokine staining in whole spinal cord

preps. It was demonstrated that the SpA-treated group showed more IL-10 production in the damaged spinal cord compared to the control group. Of interest, in the control group, the Ly6C^{hi} monocytes in the cord were IL-10-negative, but 70% of the Ly6C^{low} cells in the SpA-treated mouse were IL-10-positive. This shows that in this model of SCI, Ly6C^{hi} monocytes do not produce IL-10 and SpA can induce the increased production of IL-10 in the monocyte population present in the spinal cord compared to the control group. The data also suggests that SpA induces the maturation of Ly6C^{hi} monocytes to Ly6C^{low} monocytes, and that there is an increased presence of these IL-10 producing cells in the damaged spinal cord of SpA-treated mouse compared to the control. However, these studies do not categorically prove that SpA is changing Ly6C^{hi} into Ly6C^{low} monocytes that are subsequently induced to produce IL-10. It is still a possibility that the Ly6C^{low} monocyte population is increased via a pre-existing circulating pool of Ly6C^{low} monocytes. The former interpretation is still an interesting and relevant finding but it would be interesting to investigate if the monocytes that SpA induced to mature into the anti-inflammatory subset were the cells producing IL-10. A way of investigating this would be to use an adoptive transfer system. Ly6C^{hi} monocytes from vert-X mice, which are CD45.1, could be adoptively transferred into a CD45.2 congenic mouse 24h after SCI and treated with SpA - 24h later the adoptively transferred cells could be examined via flow cytometry. This system would allow the tracking of Ly6C^{hi} monocytes maturation into Ly6C^{low} monocytes and their subsequent ability to produce IL-10.

Interestingly, there was no IL-10 production from any of the monocytes in the blood, even though there was an increase in the Ly6C^{low} monocyte population after SpA treatment. *In vitro* it was determined that IL-10 was up-regulated by SIC alone, however, the production of IL-10 was increased further if there was LPS also present. This *in vitro* phenomenon could be mimicking what is happening *in vivo* in the setting of SCI and SpA treatment. Monocytes infiltrating into the damaged cord are encountering danger signals; these could include heat shock proteins, dsDNA and RNA which are all recognised by TLRs, and this could be stimulating the monocytes within the damaged spinal cord to produce high levels of IL-10. Although monocytes in the blood encounter SpA, which is known to induce a phenotypic change in Ly6C^{hi} monocytes under non-inflammatory conditions, they do not receive the second TLR signal while in the peripheral

blood that would induce them to up-regulate their IL-10 production. It should be appreciated that this experiment was only carried out with one mouse per group and needs to be repeated to validate the results - but it does show a very interesting result for SpA as a modulator of inflammation in SCI.

Thus far in chapters 3 and 4 of this thesis, it has been demonstrated that SpA induces an anti-inflammatory phenotype in monocytes and macrophages under inflammatory conditions - both *in vitro* and *in vivo*. Nevertheless, a functional read-out to assess if this modulation of the inflammatory response is actually having a beneficial effect on recovery after SCI would be essential. To answer this question, BDA tract-tracing of the cortico-spinal tract was examined as a potential measure of neuronal survival and regeneration. A full study of this technique could not be undertaken because of constraints on microscope time, and therefore not all of the sections could be imaged. Two animals that were BDA tract-traced, which had received 100Kdyn injuries, showed that the cortico-spinal tract could be detected by BDA-tracking and that the cortico-spinal tract was ablated by the contusion injury.

A variety of behavioural techniques were also tested to identify a suitable method to scrutinize the potential functional recovery in mice after the use of SpA in SCI. The test chosen to produce these results had to be sensitive, reliable and reproducible. Different severities of SCI (50Kdyn, 80Kdyn, 100Kdyn and 120Kdyn) were induced to see if the behavioural tests could sufficiently detect differences between each of the injury groups and therefore would be sensitive enough to detect subtle changes in recovery between treated and non-treated groups. The BMS was deemed not to be a suitable assessment of recovery as it is a hind limb locomotor test, and the cervical contusion injury induced a fore limb injury phenotype. Using the BMS test, no differences were seen between the 50Kdyn, 80Kdyn and 100Kdyn injury groups, even though there was very noticeable differences in fore limb function. The DigiGait analyses gait, can give a read-out of over 20 parameters that are attributed to gait, and assesses both forelimb and hind-limb functions. Unfortunately, this method of behavioural testing had a very high drop-out rate, with only 25% of all animals completing the 6 weeks post-operation testing routine. Additionally, there was a very wide data spread within each of the injury groups at specific time points. More worrying still was that there was found to be an unacceptably wide, statistically

significant variation between mice groups in the pre-operative data. To avoid external factors interfering with the results and to ensure consistency of measurement, all mice in the study were ordered in from the same supplier and were all age and sex-matched. Due to these performance issues, the DigiGait was deemed to be unreliable and insufficiently sensitive for assessing the ability of SpA to improve recovery after SCI. The final behavioural testing method that was examined was the grip strength test, which showed the most promising results for future use as a functional read-out, as it is a dedicated fore limb-specific test. All mice at both the 100Kdyn and 80Kdyn injury level could take part in this form of behavioural test from post-operative week 1, with no drop-outs. The only issue that arose with the test was its level of sensitivity: there was a statistically significant difference in each of the injury severities compared to the non-injured control group at all time points. There was also a visible difference between the two injury groups - though this was not statistically significant due to variation within each of the injury groups. However, this study was carried out with only 3 mice in the 80Kdyn injury group and 4 mice in the 100Kdyn injury group and further investigation is warranted with a bigger study group to establish if SpA can cause a functionally relevant improvement in recovery after SCI by modulating the inflammatory immune response.

6.2 Conclusion

In summary, it has been demonstrated in chapter 3 of this thesis that SpA, when in complex with IgG, can polarize BMDM to an anti-inflammatory phenotype, which consists of increased IL-10 and reduced ability to produce IL-12. IFN γ -primed macrophages that are treated with SIC and LPS also show down-regulated MHC II surface expression; interestingly they still exhibited normal levels of co-stimulatory molecule CD86 compared to classically-activated macrophage. In chapter 4 it was demonstrated that SpA can bind to monocytes *in vivo* and this was preferentially to the Ly6C^{hi} monocyte sub-population. Additionally, SpA was shown to induce the maturation of the Ly6C^{hi} monocyte population into Ly6C^{low} monocytes in steady state and in the inflammatory setting of SCI. SpA treatment also induced monocytes within the damaged cord to produce increased levels of IL-10 compared to the control.

Taken together, these observations indicate that when SpA and IgG form SIC and interact with macrophages and monocytes *in vitro* or *in vivo* the cells can be polarized to an anti-inflammatory phenotype, which has the potential to down-regulate the massive inflammatory response after SCI. While several methods of functional assessment were examined for their ability to measure discernable changes in the recovery of mice after SCI, none of the behavioural tests assessed met all the requirements for a functional read-out that would be effective in the assessment of SpA's ability to induce greater recovery than controls. However, more investigation of the grip strength and the BDA track tracking techniques are warranted and did show promising potential.

In conclusion, it has been shown in this thesis that SpA has the potential to be used as a cell-specific method for modulating the massive inflammatory response that contributes to the secondary death of neurons days to weeks after the initial trauma and is responsible for reduced functional recovery in SCI victims.

7 Appendix 1

1. Buffer and solutions:

10x PBS: 80 g NaCl, 2 g KCl, 11.5g Na₂HPO₄·7H₂O and 2g KH₂PO₄ to 1 litre distilled water (pH 7.4) 10x stock.

FACS Buffer: 1% (v/v) FCS, 5mM EDTA, 0.02 Sodium azide in 1X PBS

Complete media: 1% (v/v) Pen/Strep, 1% (v/v) L-Glut, 10% (v/v) FCS in 500ml RPMI

Separation media: 2.5% (v/v) FCS 2mM EDTA 1X PBS

2. Immunohistochemistry antibodies

Primary antibody:

1) Neurofilament-200 (NF200), mouse IgG1, Sigma #N0412, dilution: 1:1000

2) Glial fibrillary acidic protein (GFAP), rabbit IgG1, DAKO #Z0334, dilution: 1:1000

Secondary antibody:

1) Donkey anti-mouse IgG, Rhodamine conjugate, Jackson ImmunoResearch #715-025-150, dilution: 1:100

2) Donkey anti-rabbit IgG, DyLight 649 conjugate, BioLegend #406406, dilution: 1:500

Streptavidin:

Streptavidin-Alexa Fluor 488 conjugate (Green), Invitrogen #S11223, concentration: 1:1000

3.Flow Cytometry Antibodies

APC

Marker	Dilution	Manufacturer	Catalogue Number
CD45	1:200	ebioscience	17-0451
CD19	1:200	BD Pharmingen	550992
CD64/FcγR I	1:200	BD Pharmingen	558539
F4/80	1:300	ebioscience	17-4801-82
MR/CD206	1:100	Biologend	123010
CD45R/B220	1:300	Biologend	103226
Streptavidin	1:400	ebioscience	17-4317-82
Gr1/Ly-6C G	1:100	BD Pharmingen	553129

APC cy7

Marker	Dilution	Manufacturer	Catalogue Number
CD11b	1:200	BD Pharmingen	557657
CD45	1:300	BD Pharmingen	557659

FITC/Alexa-488

Marker	Dilution	Manufacturer	Catalogue Number
CD11B	1:100-200	Biologend	101205
CD80	1:100 - 200	BD Pharmingen	553768
CD86	1:100 - 200	BD Pharmingen	553691
CD45	1:100	ebioscience	11-0451
MHC II I-A(B)	1:100	BD Pharmingen	553605
Streptavidin	1:100	ebioscience	11-4317-87
IgG2a (iso MHCII) FITC	1:100	BD Pharmingen	553456
IgG2a (iso Alexa-488)	1:100	Ebioscience	53-4724-80

PE cy7

Marker	Dilution	Manufacturer	Catalogue Number
MHC II I-A(B)	1:300	Biologend	116419

PE

Marker	Dilution	Manufacturer	Catalogue Number
CD3	1:300	BD Pharmingen	553064
CD11b	1:500	ebioscience	12-0112-83
CD40	1:300	BD Pharmingen	553791
CD45	1:500	Biolegend	103106
CD69	1:300	ebioscience	12-0691-82
CD86	1:300	BD Pharmingen	553692
Streptavidin	1:1000	ebioscience	12-4317-87
IgG2a (iso)	1:300	BD Pharmingen	551799
F4/80	1:400	Biolegend	123109

PerCP-cy5.5/PE cy 5.5

Marker	Dilution	Manufacturer	Catalogue Number
B220 PE cy 5.5	1:300	BD Pharmingen	551001
Ly-6C PerCP-cy5.5	1:100	BD Pharmingen	560525

Purified

Marker	Dilution	Manufacturer	Catalogue Number
IL-10R/CD210		BD Pharmingen	550012

AF700

Marker	Dilution	Manufacturer	Catalogue Number
Ly6G	1:200	ebioscience	56-5931
CD45	1:400	ebioscience	56-0451

8 Appendix 2

ARTHRITIS & RHEUMATISM
Vol. 63, No. 12, December 2011, pp 3897–3907
DOI 10.1002/art.30629
© 2011, American College of Rheumatology

Co-Opting Endogenous Immunoglobulin for the Regulation of Inflammation and Osteoclastogenesis in Humans and Mice

Lindsay M. MacLellan,¹ Jennifer Montgomery,¹ Fujimi Sugiyama,¹ Susan M. Kitson,¹
Katja Thümmeler,¹ Gregg J. Silverman,² Stephen A. Beers,³ Robert J. B. Nibbs,¹
Iain B. McInnes,¹ and Carl S. Goodyear¹

Objective. Cells of the monocytic lineage play fundamental roles in the regulation of health, ranging from the initiation and resolution of inflammation to bone homeostasis. In rheumatoid arthritis (RA), the inflamed synovium exhibits characteristic infiltration of macrophages along with local osteoclast maturation, which, together, drive chronic inflammation and downstream articular destruction. The aim of this study was to explore an entirely novel route of immunoglobulin-mediated regulation, involving simultaneous suppression of the inflammatory and erosive processes in the synovium.

Methods. Using *in vivo* and *in vitro* studies of human cells and a murine model of RA, the ability of staphylococcal protein A (SPA) to interact with and modulate cells of the monocytic lineage was tested. In

addition, the efficacy of SPA as a therapeutic agent was evaluated in murine collagen-induced arthritis (CIA).

Results. SPA showed a capacity to appropriate circulating IgG, by generating small immunoglobulin complexes that interacted with monocytes, macrophages, and preosteoclasts. Formation of these complexes resulted in Fc γ receptor type I–dependent polarization of macrophages to a regulatory phenotype, rendering them unresponsive to activators such as interferon- γ . The antiinflammatory complexes also had the capacity to directly inhibit differentiation of preosteoclasts into osteoclasts in humans. Moreover, administration of SPA in the early stages of disease substantially alleviated the clinical and histologic erosive features of CIA in mice.

Conclusion. These findings demonstrate the overarching utility of immunoglobulin complexes for the prevention and treatment of inflammatory diseases. The results shed light on the interface between immunoglobulin complex-mediated pathways, osteoclastogenesis, and associated pathologic processes. Thus, therapeutic agents designed to harness all of these properties may be an effective treatment for arthritis, by targeting both the innate inflammatory response and prodestructive pathways.

Monocytes differentiate into either macrophages or osteoclasts depending on their response to specific intra- and extracellular signals (1,2). These cells play pivotal roles in the generation of adaptive immune responses, initiation and resolution of inflammation, and bone homeostasis (3). In chronic inflammatory conditions such as rheumatoid arthritis (RA), these cells have crucial roles in perpetuating disease pathogenesis. Monocytes and macrophages are the primary source of the inflammatory cytokines and chemokines that drive the chronicity of the synovial lesion (4,5), while the increased differentiation of osteoclasts from cells pres-

Supported by funding from the University of Glasgow, Arthritis Research UK, and Medical Research Scotland (Vipiana Award) (to Dr. Goodyear) and by a Capacity Building Award in Integrative Mammalian Biology (to Ms Montgomery and Dr. Goodyear) funded by the Biotechnology and Biological Sciences Research Council, British Pharmacological Society Integrative Pharmacology Fund (donors AstraZeneca, GlaxoSmithKline, and Pfizer), Knowledge Transfer Network, the Medical Research Council, and the Scottish Further and Higher Education Funding Council. Dr. Thümmeler's work was supported by the DFG (postdoctoral fellowship TH1599/1-1). Dr. Goodyear's work was also supported by a nonclinical career development fellowship from Arthritis Research UK (grant 17653).

¹Lindsay M. MacLellan, PhD, Jennifer Montgomery, BSc (Hons), Fujimi Sugiyama, BSc, Susan M. Kitson, BSc (Hons), Katja Thümmeler, Dr. rer. nat, Robert J. B. Nibbs, PhD, Iain B. McInnes, MBChB, FRCP, PhD, Carl S. Goodyear, PhD: University of Glasgow, Glasgow, UK; ²Gregg J. Silverman, MD: University of California at San Diego, La Jolla; ³Stephen A. Beers, PhD: Southampton University, Southampton, UK.

Address correspondence to Carl S. Goodyear, PhD, Institute of Infection, Immunity and Inflammation, College of Medicine, Veterinary Medicine and Life Sciences, University of Glasgow, Sir Graeme Davies Building, 120 University Place, Glasgow G12 8TA, UK. E-mail: Carl.Goodyear@glasgow.ac.uk.

Submitted for publication October 3, 2010; accepted in revised form August 16, 2011.

ent in the joint (6,7) is considered critical for the development of the major erosive lesion.

The local environment has a dramatic influence on macrophage maturation and can drive the development of a spectrum of functionally diverse phenotypes (8). Two of the functional extremes are the antiinflammatory “regulatory” macrophages and the proinflammatory “classically” activated macrophages. The regulatory phenotype is characterized by increased expression of interleukin-10 (IL-10) but decreased expression of IL-12. In contrast, the proinflammatory phenotype is defined as Th1-driven (interferon- γ [IFN γ]-primed) and characterized by increased expression of IL-12 and inducible nitric oxide synthase (8). Therapeutic strategies with the potential to polarize macrophages to a regulatory phenotype are of intense interest in the generation of new approaches to treat patients during the chronic self-perpetuation phase of RA (5).

One potential therapeutic approach for inflammatory diseases comes from an understanding of immune complexes (ICs) and their interactions with macrophages. It has been recognized for several decades that ICs play a central role in the pathogenesis of RA (9), being responsible for driving inflammation and, indirectly, joint erosion, via Fc γ receptor (Fc γ R)-mediated interactions (10). In the right context, ICs can have antiinflammatory properties (8), and this is partly due to their ability to contribute to the generation of regulatory macrophages (11). Recent studies have demonstrated that small, preformed ICs (12), intravenous immunoglobulin (IVIG) complexes (13,14), and antibodies to soluble serum proteins (15) can be used to ameliorate arthritis in passive transfer autoimmune models such as K/BxN serum-induced inflammatory arthritis. However, such unoptimized therapies as IVIG have little clinical benefit in RA.

Staphylococcal protein A (SPA), a microbial protein widely used for therapeutic antibody purification and formerly used as a column-bound apheresis therapy for severe RA (16), has the ability to co-opt circulating IgG and exclusively form small, defined hexameric complexes, or (IgG₂SPA)₂ (17–19). Exploiting the ability of SPA to hijack endogenous IgG may facilitate a novel macrophage-targeting approach, aimed at driving Fc γ R-mediated signaling toward regulatory pathways that can modify autoimmune inflammatory diseases.

In this study, we show that SPA-IgG immune complexes (SICs) have the ability to ameliorate antigen-induced arthritis, by inhibiting both the clinical and pathologic aspects of murine collagen-induced arthritis (CIA). Mechanistically, SICs modulate macrophage responsiveness to proinflammatory cytokines via Fc γ R,

and thus alter the phenotype of these cells. Furthermore, we show, for the first time, that specific ICs can interact with preosteoclasts, can dramatically inhibit osteoclastogenesis, and can substantially reduce osteoclast abundance in the joint. We conclude that co-opting endogenous IgG into ICs may provide an alternative therapy for RA and other autoimmune/inflammatory diseases, by targeting both inflammatory and erosive aspects of the disease process.

MATERIALS AND METHODS

Mice. DBA/1J and C57BL/6 mice (ages 7–10 weeks) were purchased from Charles River. Mice of the μ MT strain were bred and maintained at the University of Glasgow, UK. FcR $\gamma^{-/-}$, Fc γ RI $^{-/-}$, and Fc γ RII $^{-/-}$ mice (C57BL/6 background) were bred and maintained at the University of Southampton, UK. The Ethical Review Process Committee and the UK Home Office approved all experimental procedures.

In vivo tracking of SPA. Recombinant SPA (rSPA; Repligen), or ovalbumin (OVA) as a control, was conjugated to Alexa Fluor 488-labeled *N*-hydroxysuccinimide (Molecular Probes), as previously described (20). In μ MT mice, 6 mg of mouse IgG (Jackson Immunochemicals) in phosphate buffered saline (PBS) was injected intravenously. Labeled protein (300–500 μ g of SPA-488 or OVA-488) was then injected intraperitoneally (IP), and 2 hours later, the blood and spleens were harvested and erythrocyte-free single cell suspensions were prepared.

Flow cytometry. Cells were preincubated with or without Fc Block and stained with specific antibodies or isotype controls. Data were acquired on a FACSCaliber LSRII (Becton-Dickinson) or MACSQuant (Miltenyi) flow cytometer, and results were analyzed with FlowJo software (Tree Star).

Generation of immune complexes. To generate the SICs, rSPA (SPA-488) at a concentration of 37.5 μ M was mixed with 150 μ M human or mouse IgG in PBS at 37°C for 1 hour. To generate the OVA plus polyclonal IgG (OpIg) control, 37.5 μ M of OVA (OVA-488) was mixed with 150 μ M of mouse IgG in PBS at 37°C for 1 hour. Prior to being used in these experiments, the IgG was centrifuged at 13,000 revolutions per minute for 5 minutes, to remove large IgG complexes.

Generation and stimulation of murine bone marrow-derived macrophages (BMMs) and preosteoclasts. Cells were flushed from the mouse femurs and tibiae. In some studies, monocytes were enriched by magnetic negative selection (StemCell Technologies). Bone marrow monocytes or enriched monocytes were cultured in complete RPMI with 20% L929-conditioned medium or 30 ng/ml recombinant macrophage colony-stimulating factor (M-CSF) for 5–6 days to generate BMMs, or with 30 ng/ml M-CSF and 50 ng/ml RANKL for 5 days to generate preosteoclasts. On days 5–6, the BMMs and preosteoclasts were removed and either used directly in flow cytometry or washed, reseeded, and left to adhere overnight prior to stimulation.

BMMs were stimulated for 6–24 hours with lipopolysaccharide (LPS) (100 ng/ml *Escherichia coli* O127:B8; Sigma-Aldrich) in the presence or absence of SICs, SPA, or IgG. In some instances, BMMs were prestimulated overnight with

IFN γ (100 units/ml) prior to these other treatments. To analyze the macrophage response to OVA ICs (designated M Φ -II in Figure 3), after prestimulation of the BMMs with IFN γ , the cells were treated with LPS and 150 μ g/ml ICs consisting of OVA and rabbit anti-OVA IgG, as previously described (21).

Enzyme-linked immunosorbent assay (ELISA). Cytokine and anticollagen antibody levels were assayed by ELISA, using appropriately diluted sera or culture supernatants. Mouse IL-10 and IL-12p40 (BD Biosciences), and human IL-10, IL-12, and tumor necrosis factor α (TNF α ; Biosource) were assayed in accordance with the manufacturers' instructions. Anti-type II collagen (anti-CII) antibody titers in individual sera were evaluated using ELISA-grade collagen (Chondrex) and detected with horseradish peroxidase (HRP)-conjugated anti-mouse IgG1 or IgG2a (Southern Biotechnology). Total IgG was determined using an unlabeled anti-mouse IgG capture antibody and detected with HRP-conjugated anti-mouse IgG1 or IgG2a. Antibody ELISAs were developed using OPD substrate (Sigma).

Induction and assessment of arthritis. CIA was induced in DBA/1J mice with 100 μ g of bovine CII emulsified in Freund's complete adjuvant (MD Biosciences) on day 0, and boosted on day 21 with an IP injection of CII in PBS (22). Starting on day 21, mice were scored by a treatment-blinded researcher (LMM) for clinical signs of arthritis, as previously described (23). On day 25, mice were randomized to receive an IP injection of 100 μ g rSPA or vehicle control (pyrogen-free PBS). Treatment was continued every other day.

The hind paws were histologically scored by treatment-blinded researchers (LMM and CSG) for inflammation and joint damage (24), in which 0 = healthy, 1 = mild, 2 = moderate, and 3 = severe. The researchers scored 3 sections per knee, and the mean score per treatment group was calculated.

In addition, the hind paws were assessed by immunohistochemistry for the presence of osteoclasts. Sections were deparaffinized, and antigen retrieval was performed. Slides were blocked in 3% horse serum/Tris buffered saline and stained with a rabbit polyclonal IgG against cathepsin K (ProteinTech Group) or normal rabbit IgG. Slides were developed using the ImmPRESS Anti-Rabbit Ig (peroxidase) substrate kit (Vector), and counterstained with hematoxylin. The bone surface area and the numbers of cathepsin K-positive cells per section were determined for each knee joint, and the number of cells per mm² of bone was calculated.

Restimulation of lymph node (LN) cells. Single cell suspensions were prepared from inguinal LNs. Cells were cultured in triplicate in 96-well plates at 6×10^5 cells/well in complete RPMI. Cells were restimulated with medium, 30 μ g/ml CB11 peptide (optimal concentration; Chondrex), or 30 μ g/ml of the irrelevant peptide MOG₃₅₋₅₅. Proliferation was analyzed 88 hours thereafter by assessing ³H-thymidine incorporation (GE Healthcare) for the last 16 hours of culture.

Real-time quantitative polymerase chain reaction (PCR). Cell and tissue RNA was isolated using Qiagen Mini and Micro kits in accordance with the manufacturer's instructions. Tissue samples were disrupted in liquid nitrogen using a pestle and mortar. To quantify RNA transcripts, complementary DNA (cDNA) was prepared using the Stratagene Affinity Script Multiple Temperature cDNA Synthesis Kit. Real-time quantitative PCR using SYBR Green (Applied Biosystems)

was carried out using the Applied Biosystems 7900HT Fast Real-Time PCR System. Specific transcript levels were normalized to those for GAPDH, and the $\Delta\Delta C_t$ calculation method was used to determine gene expression, as previously described (25).

Generation and stimulation of human peripheral blood monocyte-derived macrophages. Buffy coats of healthy human blood were obtained from the Scottish Blood Transfusion Service, and their use was approved by the Glasgow East Ethics Committee. Peripheral blood mononuclear cells were separated on Histopaque (Sigma-Aldrich), and monocytes were purified using the CD14-positive selection EasySep kit (StemCell Technologies). The monocytes were cultured in complete RPMI with 10 ng/ml human M-CSF (PeproTech) for 7 days in the presence or absence of SICs, SPA, or IgG. On day 7, cultures were stimulated with LPS (100 ng/ml) and supernatants were harvested for analysis of cytokine content. For the investigation of IFN γ -mediated signaling, monocytes were cultured for 6 days with M-CSF, washed, and treated with either SICs, SPA, or IgG for 48 hours. These cultures were then stimulated with 10 units/ml of IFN γ (PeproTech) for 10 minutes and immediately used for immunoblotting or imaging.

Immunoblotting. Whole cell extracts were obtained by lysing cells in radioimmunoprecipitation assay extraction buffer with protease and phosphatase inhibitors. Protein amounts were quantified with the BCA Protein Assay (Pierce), according to the manufacturer's instructions. Twenty micrograms of cell lysate was fractionated on 4–12% Bis-Tris Gels, transferred to PVDF membranes (Invitrogen), and incubated with antibodies specific for phosphorylated STAT-1 tyrosine 701, total STAT-1, or β -actin (Abcam). Membranes were washed and incubated with HRP-labeled anti-IgG antibodies and developed with SuperSignal West Pico substrate (Pierce).

Immunofluorescence imaging. Chamber slide cultures were fixed with 4% paraformaldehyde for 10 minutes at room temperature. Phosphorylated STAT-1 was visualized in cells by permeabilizing with 90% ethanol in PBS and staining with a biotinylated anti-phosphorylated STAT-1 antibody. This was followed by staining with streptavidin–HRP, biotinylated tyramide (Invitrogen), and, finally, streptavidin–Alexa Fluor 647. The sections were also stained with DAPI and mounted in Vectashield (Vector). Fluorescence imaging was conducted using an LSC fluorescence microscope (Compucyte) with a Hamamatsu Orca ER digital camera and Openlab digital imaging program (Improvision).

Generation of human peripheral blood monocyte-derived osteoclasts. Monocytes (1×10^6) were cultured in α -minimum essential medium (10% fetal bovine serum, 2 mM L-glutamine, 100 μ g/ml penicillin, 100 μ g/ml streptomycin) with 30 ng/ml M-CSF and 100 ng/ml RANKL (PeproTech) in the presence or absence of SICs, SPA, OpIg, or IgG. The medium was changed every 3 days, and on day 7, the cultures were evaluated for osteoclast differentiation. Slides were stained for tartrate-resistant acid phosphatase (TRAP) using a leukocyte acid phosphatase kit (Sigma-Aldrich). Osteoclasts were identified under light microscopy by the presence of ≥ 3 nuclei (identified as purple staining); osteoclast precursor cells were identified as TRAP-positive cells with 1 or 2 nuclei.

Statistical analysis. GraphPad Prism was used for all statistical analyses: *t*-tests, Mann-Whitney U tests, one-way analysis of variance (ANOVA) with post hoc tests, or two-way ANOVA with repeated measures, as appropriate. Data are

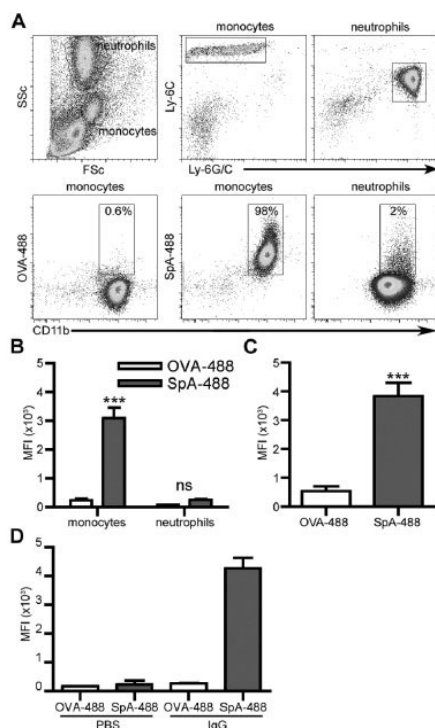


Figure 1. Staphylococcal protein A (SPA) binds to circulating monocytes and tissue macrophages in mice with collagen-induced arthritis. Mice were injected with 500 μ g of Alexa Fluor 488–labeled SPA (SPA-488) or ovalbumin (OVA-488), and 2 hours later, the blood and spleens were harvested for cell analyses. **A**, Representative results of flow cytometry are shown. Monocytes and neutrophils from the blood were initially gated based on their forward light-scatter (FSc) versus side light-scatter (SSc) patterns (top left panel), and then gated by lymphocyte antigen (Ly-6C versus Ly-6G/C) expression (top right panels). The lower panels show binding of OVA-488 or SPA-488 to CD11b+ monocytes and neutrophils. Values in the boxed areas (same as boxed areas in the top panels) are the percentage of positive cells in each population. **B** and **C**, The extent of OVA-488 or SPA-488 binding was determined in monocytes and neutrophils (**B**) and in splenic CD11b+ macrophages (**C**). Bars show the mean \pm SD representative results from 1 of 3 independent experiments, expressed as the mean fluorescence intensity (MFI) in 3 mice per group. *** = $P < 0.001$ versus OVA-488, by *t*-test. NS = not significant. **D**, Mice of the μ MT strain were injected intravenously with phosphate buffered saline (PBS) or mouse polyclonal IgG. Mice were then injected intraperitoneally with 300 μ g SPA-488 or OVA-488, and 2 hours later, the blood was collected to determine the extent of binding of OVA-488 or SpA-488 to monocytes. Bars show the mean \pm SD representative results from 1 of 2 independent experiments, expressed as the MFI in 2 mice per group.

expressed as the mean \pm SD, except for clinical scores of CIA, which are given as the mean \pm SEM. P values less than or equal to 0.05 were considered significant, and all tests were 2-sided.

RESULTS

Binding of SPA-IgG complexes to monocytes, macrophages, and preosteoclasts via Fc γ RI. SPA binds to B cells in a B cell receptor (BCR)–dependent manner. However, it can also interact with non-B cell and non-T cell populations in vivo (20). We analyzed the non-B cell binding of fluorescently labeled SPA in vivo. In the blood of mice injected with SPA-488, we observed considerable binding to monocytes but minimal binding to neutrophils (Figures 1A and B). SPA-488 also interacted with differentiated monocytes, i.e., CD11b+ macrophages, in the spleen (Figure 1C).

In B cell/immunoglobulin–deficient μ MT mice, SPA was able to interact with circulating monocytes only if the mice had been reconstituted with IgG (Figure 1D). To further investigate the interaction of SPA and IgG

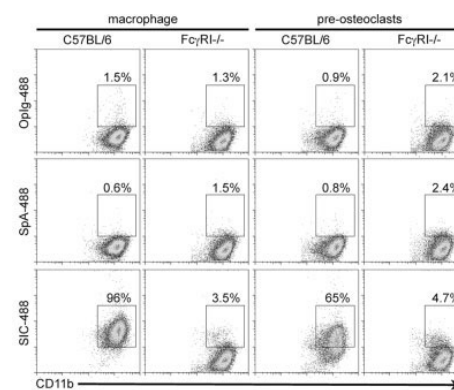


Figure 2. Formation of staphylococcal protein A (SPA)–IgG immune complexes (SICs) and the presence of Fc γ receptor type I (Fc γ RI) are required for binding to macrophages and preosteoclasts. Bone marrow cells from C57BL/6 and Fc γ RI^{-/-} mice were enriched for monocytes and cultured with recombinant macrophage colony-stimulating factor (M-CSF) or M-CSF plus RANKL for 5 days to generate bone marrow–derived macrophages (BMMs) or preosteoclasts, respectively. These cells were incubated with Alexa Fluor 488–labeled ICs (ovalbumin plus polyclonal IgG [Oplg-488], SPA-488, SIC-488, or ovalbumin-488 [not shown]) to evaluate binding. Representative images show the binding of each complex to CD11b+ BMMs and preosteoclasts. Values over the boxed populations are the percentage of positive cells. The data shown are representative flow cytometry results, tested in duplicate, from 1 of 3 independent experiments.

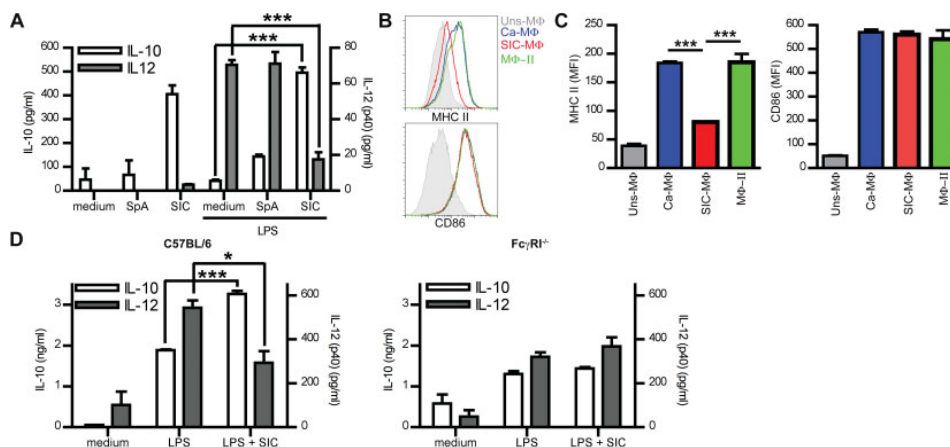


Figure 3. Treatment of mice with staphylococcal protein A (SPA)-IgG immune complexes (SICs) alters the cytokine profile and activation state of macrophages in a $Fc\gamma$ receptor type 1 ($Fc\gamma$ RI)-dependent manner. **A**, Bone marrow-derived macrophages (BMMs) from DBA1/J mice were stimulated for 6 hours without or with lipopolysaccharide (LPS) in the absence or presence of SICs, and levels of interleukin-10 (IL-10) and IL-12p40 were determined. Stimulation with IgG did not yield results significantly different from those with either medium alone or SPA, and therefore IgG is not shown. **B** and **C**, BMMs from C57BL/6 mice were primed with interferon- γ , and 16 hours later, the cells were stimulated with LPS (Ca-M Φ), SICs + LPS (SIC-M Φ), or ovalbumin ICs (M Φ -II) (21) or left unstimulated (Uns-M Φ). Six hours later, the BMMs were analyzed by flow cytometry for the expression of class II major histocompatibility complex (MHC II) and CD86, as shown in representative histograms (**B**) and shown as the mean fluorescence intensity (MFI) (**C**). Incubations over 24 hours (not shown) resulted in the same expression profiles. **D**, BMMs from C57BL/6 and $Fc\gamma$ RI^{-/-} mice were stimulated for 6 hours with LPS in the absence or presence of SICs. Results with IgG + LPS and SPA + LPS did not differ significantly from those with LPS alone, and therefore these are not shown. Bars show the mean \pm SD representative results from 1 of 3 independent experiments, determined in samples from triplicate wells, measured in triplicate. * = $P < 0.05$; *** = $P < 0.001$, by analysis of variance with post hoc test.

with monocytes, macrophages, or preosteoclasts, we generated SPA-488-IgG immune complexes (SIC-488) (data not shown) at a molar ratio that is consistent with what would be formed in the circulation when excess IgG, or (IgG₂SPA)₂ (17–19), is present. SIC-488 showed significant binding both to BMMs and to preosteoclasts, while SPA-488, OVA-488 (data not shown), or OpIg-488 were unable to bind to these cells (Figure 2).

As was indicated in Figure 1, SPA-488 showed substantial binding only to monocytes. Importantly, whereas both monocytes and neutrophils express $Fc\gamma$ RIIb, $Fc\gamma$ RIII, and $Fc\gamma$ RIV, only monocytes express $Fc\gamma$ RI (26) (data not shown). Thus, as anticipated, SIC-488 was unable to bind to BMMs or to preosteoclasts that were deficient in their expression of $Fc\gamma$ RI (Figure 2).

Skewing of macrophages to a regulatory phenotype by SICs. The aforementioned findings and those from previous studies using experimental ICs (refs. 21, 27, and data not shown) raised the possibility that SICs

would interact with, and polarize, macrophages toward a regulatory phenotype. The addition of SICs, and not SPA or IgG alone, in the absence of a Toll-like receptor 4 agonist (LPS) was able to induce significant production of IL-10 (Figure 3A and data not shown), a phenomenon not noted previously with other experimental ICs (21,27). Moreover, the addition of SICs along with stimulation with LPS resulted in a significant inhibition of IL-12 secretion (Figure 3A). Levels of TNF α and nitric oxide were unchanged, and transforming growth factor β was not detectable (data not shown). The induction of IL-10 was also confirmed at a transcriptional level, in which SICs induced an 8-fold increase in IL-10 transcripts (data not shown). Crucially, mannose receptor expression did not change (data not shown), suggesting that SPA does not induce a formal regulatory phenotype.

To further define this apparently novel regulatory macrophage lineage, BMMs from DBA1/J and C57BL/6 mice were primed with IFN γ , and 16 hours

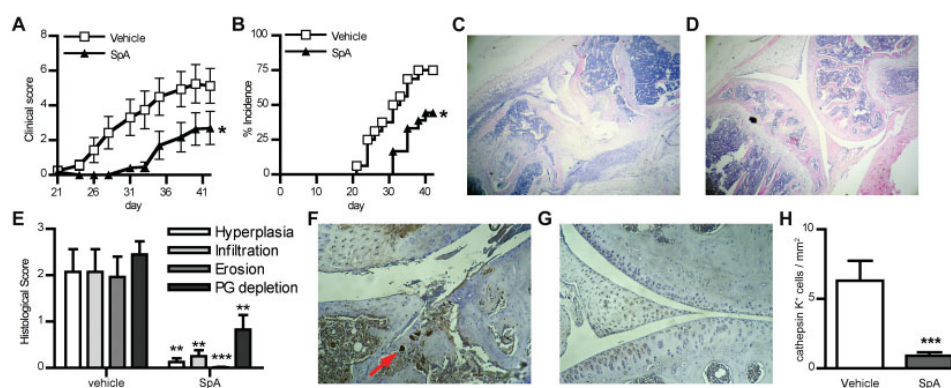


Figure 4. Treatment of mice with staphylococcal protein A (SPA) at disease onset inhibits the development of arthritis. Mice with collagen-induced arthritis were treated on day 25 after induction of arthritis and every other day thereafter with either vehicle or SPA. **A** and **B**, The severity (**A**) and incidence (**B**) of arthritis were assessed in each group. Bars in **A** and **B** show the mean \pm SEM results (pooled from 2 experiments) in 16–17 mice per group. * = $P = 0.02$ versus vehicle, by two-way repeated-measures analysis of variance (ANOVA) in **A** or by log-rank test in **B**. **C** and **D**, Representative histologic images of hematoxylin and eosin (H&E)-stained knees from vehicle-treated (**C**) and SPA-treated (**D**) mice on day 42 after arthritis induction are shown. **E**, Histologic features of arthritis (assessed as hyperplasia, infiltration, and erosion in H&E-stained knees, and cartilage destruction, as measured by proteoglycan [PG] depletion, in Safranin O-stained sections) were scored in a blinded manner. Bars show the mean \pm SD of 9 mice per group. ** = $P < 0.01$; *** = $P < 0.001$ versus vehicle, by ANOVA with post hoc test. **F** and **G**, Knees from vehicle-treated (**F**) and SPA-treated (**G**) mice were stained for cathepsin K-positive cells (osteoclasts) (indicated by the red arrow) on day 42 after arthritis induction. Representative images are shown. **H**, Sections stained for cathepsin K were measured for bone area and the number of osteoclasts (cathepsin K-positive cells) per mm^2 of bone was determined. Bars show the mean \pm SD of 5–8 mice per group. *** = $P < 0.001$ versus vehicle, by *t*-test.

later, the cells were stimulated with LPS in the presence or absence of SICs. As a result, upon stimulation of the cells with SICs and LPS, the levels of CD86 were up-regulated, which was also observed with SICs alone (data not shown), whereas there was an abrogation of the up-regulated expression of class II major histocompatibility complex (MHC) (Figures 3B and C and data not shown). This is distinct from the observations made with other experimental ICs, which, in general, up-regulated class II MHC and CD86 (Figures 3B and C) (21,27). In addition, neither LIGHT nor CCL-1 transcript levels, both of which are known to be associated with the regulatory phenotype, were altered by stimulation with SICs plus LPS when compared to LPS alone (data not shown).

Polarization of macrophages by SICs via Fc γ RI interactions. Studies on the mechanisms of experimental ICs have demonstrated that these complexes impart their effects through ligation of Fc γ RI (11). Based on these studies and our own findings (as shown in Figure 2), we hypothesized that SICs would interact with macrophages in a similar way. To determine whether Fc γ RI or an alternative Fc receptor was the main mechanism of

interaction, we generated BMMs from C57BL/6, Fc γ R1 $^{-/-}$, Fc γ RII $^{-/-}$, and Fc γ RIII $^{-/-}$ mice. When BMMs from C57BL/6 mice were treated with SICs, regulatory macrophages were generated (Figure 3D). However, in the absence of either the Fc γ chain, i.e., lack of the Fc receptors Fc γ RI, Fc γ RIII, and Fc γ RIV (data not shown), or in the absence of Fc γ RI alone (Figure 3D), SICs were unable to modify the effect of LPS and skew BMMs toward a regulatory phenotype. Interestingly, SICs were still effective at inducing regulatory macrophages in the absence of Fc γ RII (data not shown).

Amelioration of murine arthritis by treatment with SPA. Given the ability of SICs to interact with monocytes, macrophages, preosteoclasts, and B cells, and, more specifically, their ability to polarize macrophages to a regulatory phenotype, we investigated the potential of treatment with SPA to ameliorate disease in the early phase of inflammatory arthritis. Treatment of mice with SPA significantly decreased the severity and incidence of disease (Figures 4A and B). Histomorphometric evaluation revealed that, compared with vehicle-treated mice, SPA-treated mice had significantly fewer features of inflammatory disease and displayed

markedly less hyperplasia, infiltration, and cartilage and bone erosion (Figures 4C–E).

In addition, the evaluation of osteoclast numbers in the joints illustrated that SPA-treated mice had substantially fewer osteoclasts present in the joints (Figures 4F–H). This latter finding could arise from a suppression of macrophages or a reduction in inflammation, which thus would decrease RANKL, IL-1, or M-CSF release, or alternatively could reflect a direct, and unidentified, effect of SPA/SICs upon preosteoclasts and the resulting osteoclastogenesis.

Skewed anti-CII antibody response and increased serum IL-10 levels following SPA treatment. In vivo administration of SPA results in the depletion of V_H3 BCR-encoded B cells (28). In the murine CIA model, this depletion occurs (data not shown); however, susceptible B cells only represent ~3% of the repertoire. Total B cell depletion late in CIA has no effect on clinical disease (29), and although we cannot conclusively rule out the impact of this small level of depletion, it is unlikely to be the main contributing factor to such a dramatic clinical effect.

To identify alternative factors for the clinical effect of SPA, we investigated the established adaptive immune response. Surprisingly, treatment with SPA resulted in increased ex vivo lymphocyte proliferative responses to collagen peptide (Figure 5A). Moreover, the levels of CII-specific IgG2a antibodies were unaffected, whereas anti-CII IgG1 titers were elevated by SPA treatment (Figures 5B and C), thus demonstrating that in SPA-treated mice, the capacity to generate and maintain a class-switched antibody response with T cell help, albeit skewed to the IgG1 subclass, is retained. In addition, we also observed a significant increase in serum IL-10 levels with SPA treatment (Figure 5D).

Activation of macrophages with skewing to a regulatory phenotype can lead to an increase in IgG1 antibodies and an increase in the secretion of IL-10 (30), and SPA, in the form of SICs, can lead to a regulatory macrophage phenotype (Figure 3). Therefore, we considered the possibility that SPA-mediated disease suppression may occur via the modulation of macrophage function.

Alteration of macrophage responsiveness to $IFN\gamma$ by SPA. Although $IFN\gamma^{-/-}$ mice have exacerbated disease in the CIA model, treatment with $IFN\gamma$ in the early stages of disease can exacerbate the clinical features even further (31). To address the capacity of SPA to alter macrophages in vivo, mice with CIA were treated with SPA or vehicle control, and on day 42, the mice received an IP injection of $IFN\gamma$. Three hours later, peritoneal macrophages were harvested and RNA was extracted for gene expression analyses. As expected, the

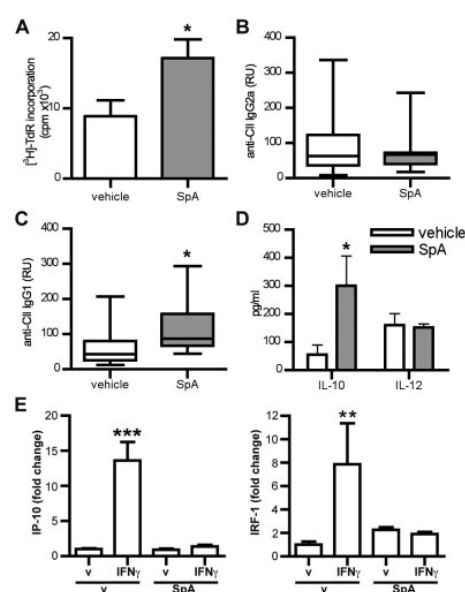


Figure 5. Treatment of mice with staphylococcal protein A (SPA) enhances the proliferative responses to CB11 peptide, increases collagen-specific IgG1 antibodies, and renders macrophages unresponsive to interferon- γ ($IFN\gamma$). Mice with established collagen-induced arthritis (CIA) were treated on day 25 with intraperitoneal (IP) injections of either vehicle alone or 0.1 mg of SPA every other day. **A**, Inguinal lymph nodes collected on day 42 were cultured in medium alone or with 30 μ g/ml CB11 peptide. The recall response to CB11 peptide was calculated as the counts per minute of 3H -thymidine (3H -TdR) incorporation in medium alone subtracted from the peptide-specific counts. Bars show the mean \pm SEM of 7 mice per group. **B–D**, Serum levels of anticollagen (anti-CII) mouse IgG2a (**B**) and IgG1 (**C**), expressed as relative units (RU), and serum levels of interleukin-10 (IL-10) and IL-12 (**D**) were determined on the day of harvest (day 42). There were no significant differences in the total levels of IgG (data not shown). In **B** and **C**, results are shown as box plots, where the boxes represent the 25th to 75th percentiles, the lines within the boxes represent the median, and the lines outside the boxes represent the 10th and 90th percentiles, for 9–10 mice per group. In **D**, results are the mean \pm SD of 5 mice per group. **E**, Mice with established CIA in each treatment group were treated on day 42 with an IP injection of $IFN\gamma$ or vehicle (v). Peritoneal macrophages were harvested 3 hours later, RNA was extracted, and quantitative polymerase chain reaction was performed to determine the expression of IP10 and IRF1. Values for the target genes were normalized to those for GAPDH, with results expressed as the mean \pm SD fold change in gene expression compared to vehicle in 7–9 mice per group. * = $P < 0.05$ versus vehicle, by t -test; ** = $P < 0.01$ and *** = $P < 0.001$ versus vehicle, by analysis of variance with post hoc test.

addition of $IFN\gamma$ in the vehicle treatment group resulted in a significant increase in the expression of the $IFN\gamma$ -

inducible genes IP10 and IRF1. In contrast, macrophages from the SPA-treated mice were completely unresponsive to IFN γ (Figure 5E).

Inhibition of inflammatory cytokine production and reduction in responsiveness to IFN γ by SICs in human macrophages. To confirm that SIC modulation was not a species-specific phenomenon, we investigated whether human monocyte polarization could be affected by SIC treatment. Human blood monocyte-derived macrophages were treated with SICs and stimulated with LPS. The addition of SICs resulted in a 46% decrease in the secretion of IL-12 ($P < 0.05$), and the levels of IL-10 were undetectable in the cultures (data not shown). Unlike in mouse BMMs (data not shown), SICs were able to decrease the production of TNF α in human macrophages by 76% ($P < 0.001$) (Figure 6A).

To extend our studies to demonstrate that SICs can also impair the capacity of proinflammatory cytokines to “classically” activate human macrophages, we cultured human blood-derived macrophages with SPA, IgG, or SICs for 48 hours prior to stimulation with IFN γ . The addition of either SPA or IgG alone was unable to inhibit the ability of IFN γ to activate STAT-1 (Figures 6B and C). The presence of SICs, however, considerably inhibited the phosphorylation of STAT-1 in response to IFN γ (Figures 6B–D).

Inhibition of osteoclastogenesis by SICs. SICs can interact with preosteoclasts (as shown in Figure 2) and these cells express Fc γ RI (data not shown). Furthermore, in vivo treatment is associated with a decrease in osteoclast abundance in the mouse joint (Figures 4F and H). To investigate whether SICs can alter the differentiation of preosteoclasts, human CD14 $^{+}$ monocytes were cultured in the presence of RANKL and M-CSF. The addition of SICs on day 1 resulted in the downregulation of CD115 (c-Fms), the M-CSF receptor, 6 hours posttreatment (Figure 6E).

To investigate whether this decrease in the level of CD115 was associated with a decrease in the subsequent ability of preosteoclasts to differentiate into osteoclasts, the number of multinucleated (≥ 3 nuclei) TRAP $^{+}$ cells was assessed on day 7 (Figures 6F and G). We observed a near complete inhibition of human osteoclast differentiation. Commensurate with this, there was no significant difference in the total number of viable cells in the cultures on day 7 (data not shown). Crucially, delaying the addition of SICs until day 5 (a time firmly associated with the initiation of osteoclast differentiation and emergence of cells capable of bone resorption [32,33]), led to the suppression of cell maturation (data not shown).

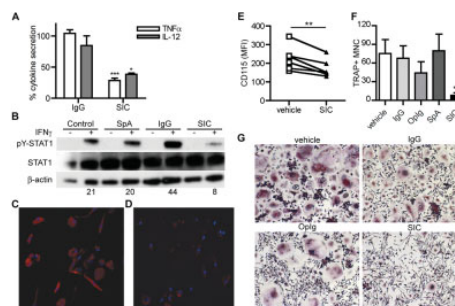


Figure 6. Staphylococcal protein A (SPA)–IgG immune complexes (SICs) alter the activation state of human macrophages and inhibit human preosteoclast differentiation into osteoclasts. **A**, Human CD14 $^{+}$ monocytes were cultured with macrophage colony-stimulating factor (M-CSF) without or with SICs, and on day 7, the cells were stimulated with lipopolysaccharide (LPS). Levels of tumor necrosis factor α (TNF α) and interleukin-12 (IL-12) were determined at 6 hours and 24 hours, respectively. The level of secretion with LPS alone (medium) was defined as 100%. The results in cultures with SPA were not significantly different from those with IgG or medium alone, and therefore SPA is not shown. Bars show the mean \pm SD results from triplicate wells ($n = 4$ per group). * = $P < 0.05$; *** = $P < 0.001$ versus IgG, by analysis of variance with post hoc test. **B**, Differentiated human macrophages were treated on day 6 with either medium, SPA, IgG, or SICs at 25 μ g/ml for 48 hours. Cultures were left unstimulated or stimulated with 10 units/ml of interferon- γ (IFN γ) 10 minutes prior to lysis. Relative values of phosphorylated STAT-1 (pY-STAT-1) were normalized to those for the total STAT-1 signal by densitometric quantitation (non-IFN γ treated = 1); normalized values are shown below the blots. β -actin was used as a control. **C** and **D**, Human macrophages were incubated with either medium (**C**) or SICs (**D**) for 48 hours, followed by 10 units/ml of IFN γ 10 minutes prior to fixation, and the cells were stained for phosphorylated STAT-1 (pY-STAT-1) (in red) and nuclei (in blue). No pY-STAT-1 staining was observable in cells that did not receive IFN γ . Images show representative results from 1 of 3 separate experiments. **E**, Human CD14 $^{+}$ monocytes ($n = 6$) were cultured with RANKL and M-CSF overnight and treated with SICs for 6 hours. Expression of CD115 was assessed as the mean fluorescence intensity (MFI). ** = $P < 0.01$ by paired t -test. **F**, Human CD14 $^{+}$ monocytes ($n = 7$) were cultured with RANKL and M-CSF in the presence of medium, IgG, ovalbumin plus polyclonal IgG (OpIg), SPA, or SICs starting on day 1. On day 7, cells were counted to determine the number of tartrate-resistant acid phosphatase-positive multinucleated cells (TRAP $^{+}$ MNC) (defined as ≥ 3 nuclei). Bars show the mean \pm SD. ** = $P < 0.01$ versus vehicle, by Mann-Whitney U test. **G**, Representative images of osteoclast cultures on day 7 after treatment with medium, IgG, OpIg, or SIC are shown.

DISCUSSION

In this study, we evaluated the ability of SPA to ameliorate inflammatory arthritis in the early stages of disease and investigated the underlying mechanism of action. Although it remains to be determined whether

this form of therapy is efficacious in established disease, the results of our study show that SPA is a strong inhibitor of the inflammatory and erosive aspects of CIA. We show that these effects are due to the formation of immunoglobulin complexes, which are able to engage Fc γ RI, polarizing macrophages to a regulatory phenotype. We further demonstrate that SICs are a potent inhibitor of IFN γ -mediated macrophage activation, and we predict that this occurs via Fc γ RIII-mediated suppression of IFN γ RII expression (13). Furthermore, SICs can interact with preosteoclasts and inhibit their differentiation into mature osteoclasts.

SPA binds the Fc and variable heavy chains (V_H3) of immunoglobulin (28). These interactions do not inhibit the ability of IgG to engage Fc receptors (34). The ability of SPA to interact with the V_H3 BCR expressed on B cells leads to the induction of apoptosis (20,35–38) via an Fc γ RIII-dependent mechanism (Goodyear CS and Silverman GJ: unpublished data). In addition, SPA was the active component of a discontinued US Food and Drug Administration–approved apheresis therapy for inflammatory and autoimmune diseases, including severe RA (39). There has been longstanding controversy over the mechanism of action and unpredictable efficacy of the therapy for inflammatory and autoimmune diseases. Several hypotheses have been proposed, including removal of immunoglobulin and/or ICs, modification of small circulating ICs, and B cell depletion (40). A salient finding was that during each treatment, SPA could be proteolytically cleaved and enter the patient's circulation (41). The quantity of SPA entering was significantly less than the amount of circulating immunoglobulin, and Hanson and colleagues demonstrated that, when excess immunoglobulin is present, SPA will form only one type of immunoglobulin complex (17,42). Our findings (as shown in Figures 1 and 2) show that these homogeneous complexes can interact with monocytes, macrophages, and preosteoclasts via an Fc γ RI-mediated interaction. It is interesting to speculate that the administration of SPA would be of greater benefit than the suboptimal administration via uncontrollable proteolytic cleavage.

To put the potential of SICs in some perspective, several studies have shown that ICs present in IVIG (13,14) or generated in alternative ways (12,15) have the ability to inhibit inflammatory responses. Unlike our findings with SPA (Figure 4), these ICs have never been shown to be efficacious in active-immunization murine models of RA or in patients with RA. The formation of ICs in IVIG is a heterogeneous process, due to the diverse binding interactions, and is therefore nonstandardized for size and content, suggesting that IVIG is far

from an optimized therapy. An alternative way to emulate IVIG ICs is the use of antibodies to immunologically inert serum protein, which can ameliorate arthritis in passive transfer autoimmune models. Unlike the findings in the present study (Figure 3), these complexes are dependent on the presence of Fc γ RIIb (15).

It is interesting to speculate that these differences may be attributable to the nature of the immunoglobulin used. The majority of previous studies have utilized xenogenic immunoglobulin, primarily rabbit IgG, to generate ICs (15,43). The interaction of rabbit IgG with murine Fc receptors has never been specifically investigated; however, results would suggest that rabbit IgG has a certain order-of-magnitude lower affinity for mouse Fc receptors compared to mouse IgG (44–47). It is feasible to envisage that rabbit IgG ICs will have altered binding activity to mouse Fc receptors that could result in dramatically different outcomes when compared to mouse IgG ICs. In this study, with the use of SPA, we were able to directly overcome any xenogenic-mediated differences and generate optimal homogeneous complexes with endogenous IgG, and it is this entity that contains immunomodulatory potential.

The alteration of monocytes and macrophages by ICs has been studied intensively, demonstrating that macrophages stimulated with ICs can be polarized to a regulatory phenotype (21). Macrophage plasticity, a recently described phenomenon (8), would suggest that phenotypes are not definitive but part of a spectrum. Our data suggest that SIC-stimulated macrophages are in the regulatory area of the spectrum and may have the capacity to regulate the inflammatory response by being unresponsive to inflammatory cytokines (Figures 5 and 6), producing antiinflammatory cytokines (i.e., IL-10 in Figure 3) and by altered antigen presentation via class II MHC (Figure 3 and currently under investigation). We postulate that the difference with our SICs when compared to experimental ICs in previous studies is based on the affinity of autogenic IgG to Fc receptors compared to that of xenogenic IgG.

Monocyte-derived osteoclastogenesis is considered critical to the erosive RA process (48), and it has been suggested that in RA, circulating monocytes are primed prior to their arrival in the joint. Maturation of these monocytes is driven by M-CSF, via CD115, and RANKL (2). In juxtaposition to earlier studies illustrating the induction of bone loss and osteoclast accumulation via heat-aggregated IgG (49), our findings demonstrate that SICs not only are capable of directly interacting with monocytes and preosteoclasts via an Fc γ RI-mediated interaction (Figure 2), but also have the ability to down-regulate CD115 and inhibit osteo-

clastogenesis (Figure 6). The mechanisms underlying this SIC-mediated inhibition of osteoclastogenesis remain to be determined (currently under investigation). However, it is interesting to speculate that the interaction of SICs with Fc receptors on circulating monocytes, or even those that have entered the joint, might alter the threshold for initiation of M-CSF and RANKL signaling, thereby inhibiting the ability of monocytes and preosteoclasts to mature into fully functional osteoclasts.

In conclusion, monocyte/macrophage-targeting therapeutic approaches offer a rich potential for the treatment of human inflammatory diseases. We herein provide a novel approach that utilizes the ability of SPA to co-opt endogenous IgG, forming highly regulated complexes with defined size and shape (17,18). SPA, which presumably arose in *Staphylococcus aureus* to interfere with the host inflammatory responses required for immunogenicity of microbial antigens, can also serve as a potent inhibitor of autoimmune inflammatory disease. The antiinflammatory mode of action appears to operate via the modification of macrophage responsiveness to inflammatory signals and the generation of a regulatory macrophage that is characterized by IL-10 production but without the conventional regulatory phenotype. Finally, we provide a hitherto unrecognized effect of ICs on osteoclastogenesis, providing a second potent pathway whereby defined ICs could mediate therapeutic benefit.

ACKNOWLEDGMENTS

We thank J. Reilly for technical assistance and Drs. M. J. Glennie, S. Milling, H. J. Willison, and C. Linington for helpful comments on the manuscript.

AUTHOR CONTRIBUTIONS

All authors were involved in drafting the article or revising it critically for important intellectual content, and all authors approved the final version to be published. Dr. Goodyear had full access to all of the data in the study and takes responsibility for the integrity of the data and the accuracy of the data analysis.

Study conception and design. Silverman, McInnes, Goodyear.

Acquisition of data. MacLellan, Montgomery, Sugiyama, Kitson, Thümmel, Beers.

Analysis and interpretation of data. MacLellan, Montgomery, Nibbs, Goodyear.

REFERENCES

- Geissmann F, Manz M, Jung S, Sieweke M, Merad M, Ley K. Development of monocytes, macrophages, and dendritic cells. *Science* 2010;327:656–61.
- Takayanagi H. Osteoimmunology: shared mechanisms and cross-talk between the immune and bone systems. *Nat Rev Immunol* 2007;7:292–304.
- Hume DA. Differentiation and heterogeneity in the mononuclear phagocyte system. *Mucosal Immunol* 2008;1:432–41.
- Firestein GS. Evolving concepts of rheumatoid arthritis. *Nature* 2003;423:356–61.
- Kinne RW, Stuhlmueller B, Burmester GR. Cells of the synovium in rheumatoid arthritis: macrophages. *Arthritis Res Ther* 2007;9:224–39.
- Herman S, Muller RB, Kronke G, Zwerina J, Redlich K, Hueber AJ, et al. Induction of osteoclast-associated receptor, a key osteoclast costimulation molecule, in rheumatoid arthritis. *Arthritis Rheum* 2008;58:3041–50.
- Schett G. Cells of the synovium in rheumatoid arthritis: osteoclasts. *Arthritis Res Ther* 2007;9:203.
- Mosser DM, Edwards JP. Exploring the full spectrum of macrophage activation. *Nat Rev Immunol* 2008;8:958–69.
- Zvaifler NJ. The immunopathology of joint inflammation in rheumatoid arthritis. *Adv Immunol* 1973;16:265–336.
- Van Lent PL, Grevers L, Lubberts E, de Vries TJ, Nabbe KC, Verbeek S, et al. Fcγ receptors directly mediate cartilage, but not bone, destruction in murine antigen-induced arthritis: uncoupling of cartilage damage from bone erosion and joint inflammation. *Arthritis Rheum* 2006;54:3868–77.
- Sutterwala FS, Noel GJ, Salgame P, Mosser DM. Reversal of proinflammatory responses by ligating the macrophage Fcγ receptor type I. *J Exp Med* 1998;188:217–22.
- Bazin R, Lemieux R, Tremblay T, St-Amour I. Tetramolecular immune complexes are more efficient than IVIg to prevent antibody-dependent in vitro and in vivo phagocytosis of blood cells. *Br J Haematol* 2004;127:90–6.
- Park-Min KH, Serbina NV, Yang W, Ma X, Krystal G, Neel BG, et al. FcγRIII-dependent inhibition of interferon-γ responses mediates suppressive effects of intravenous immune globulin. *Immunity* 2007;26:67–78.
- Siragam V, Crow AR, Brinc D, Song S, Freedman J, Lazarus AH. Intravenous immunoglobulin ameliorates ITP via activating Fcγ receptors on dendritic cells. *Nat Med* 2006;12:688–92.
- Siragam V, Brinc D, Crow AR, Song S, Freedman J, Lazarus AH. Can antibodies with specificity for soluble antigens mimic the therapeutic effects of intravenous IgG in the treatment of autoimmune disease? *J Clin Invest* 2005;115:155–60.
- Silverman GJ, Goodyear CS, Siegel DL. On the mechanism of staphylococcal protein A immunomodulation. *Transfusion* 2005;45:274–80.
- Hanson DC, Schumaker VN. A model for the formation and interconversion of protein A-immunoglobulin G soluble complexes. *J Immunol* 1984;132:1397–409.
- Langone J, Das C, Mainwaring R, Shearer W. Complexes prepared from protein A and human serum, IgG, or Fcγ fragments: characterization by immunochemical analysis of ultracentrifugation fractions and studies on their interconversion. *Mol Cell Biochem* 1985;65:159–70.
- Das C, Langone J. Correlation between antitumor activity of protein A and in vivo formation of defined high molecular weight complexes with immunoglobulin G in BALB/c mice. *Cancer Res* 1987;47:2002–7.
- Goodyear CS, Silverman GJ. Staphylococcal toxin induced preferential and prolonged in vivo deletion of innate-like B lymphocytes. *Proc Natl Acad Sci U S A* 2004;101:11392–7.
- Edwards JP, Zhang X, Frauwirth KA, Mosser DM. Biochemical and functional characterization of three activated macrophage populations. *J Leukoc Biol* 2006; 80:1298–307.
- Leung BP, McInnes IB, Esfandiari E, Wei XO, Liew FY. Combined effects of IL-12 and IL-18 on the induction of collagen-induced arthritis. *J Immunol* 2000;164:6495–502.
- Simelyte E, Rosengren S, Boyle DL, Corr M, Green DR, Firestein GS. Regulation of arthritis by p53: critical role of adaptive immunity. *Arthritis Rheum* 2005;52:1876–84.
- Joosten LA, Lubberts E, Durez P, Helsen MM, Jacobs MJ, Goldman M, et al. Role of interleukin-4 and interleukin-10 in

- murine collagen-induced arthritis: protective effect of interleukin-4 and interleukin-10 treatment on cartilage destruction. *Arthritis Rheum* 1997;40:249–60.
25. Schmittgen TD, Livak KJ. Analyzing real-time PCR data by the comparative C(T) method. *Nat Protoc* 2008;3:1101–8.
 26. Willcocks LC, Smith KG, Clatworthy MR. Low-affinity Fc γ receptors, autoimmunity and infection. *Exp Rev Mol Med* 2009;11:e24.
 27. Tierney JB, Kharkrang M, La Flamme AC. Type II-activated macrophages suppress the development of experimental autoimmune encephalomyelitis. *Immunol Cell Biol* 2009;87:235–40.
 28. Silverman GJ, Goodyear CS. Confounding B-cell defences: lessons from a staphylococcal superantigen. *Nat Rev Immunol* 2006;6:465–75.
 29. Yanaba K, Hamaguchi Y, Venturi GM, Steeber DA, St Clair EW, Tedder TF. B cell depletion delays collagen-induced arthritis in mice: arthritis induction requires synergy between humoral and cell-mediated immunity. *J Immunol* 2007;179:1369–80.
 30. Anderson CF, Mosser DM. Cutting edge: biasing immune responses by directing antigen to macrophage Fc γ receptors. *J Immunol* 2002;168:3697–701.
 31. Boissier MC, Chiochia G, Bessis N, Hajnal J, Garotta G, Nicoletti F, et al. Biphasic effect of interferon- γ in murine collagen-induced arthritis. *Eur J Immunol* 1995;25:1184–90.
 32. Massey HM, Flanagan AM. Human osteoclasts derive from CD14-positive monocytes. *Br J Haematol* 1999;106:167–70.
 33. Lader CS, Scopes J, Horton MA, Flanagan AM. Generation of human osteoclasts in stromal cell-free and stromal cell-rich cultures: differences in osteoclast CD11c/CD18 integrin expression. *Br J Haematol* 2001;112:430–7.
 34. Sulica A, Medesan C, Laky M, Onica D, Sjoquist J, Ghetie V. Effect of protein A of *Staphylococcus aureus* on the binding of monomeric and polymeric IgG to Fc receptor-bearing cells. *Immunology* 1979;38:173–9.
 35. Silverman GJ, Nayak JV, Warnatz K, Hajjar FF, Cary S, Tighe H, et al. The dual phases of the response to neonatal exposure to a VH family-restricted staphylococcal B cell superantigen. *J Immunol* 1998;161:5720–32.
 36. Goodyear CS, Sugiyama F, Silverman GJ. Temporal and dose-dependent relationships between in vivo B cell receptor-targeted proliferation and deletion-induced by a microbial B cell toxin. *J Immunol* 2006;176:2262–71.
 37. Goodyear CS, Silverman GJ. Death by a B cell superantigen: in vivo VH-targeted apoptotic supraclonal B cell deletion by a Staphylococcal toxin. *J Exp Med* 2003;197:1125–39.
 38. Goodyear CS, Corr M, Sugiyama F, Boyle DL, Silverman GJ. Cutting edge: Bim is required for superantigen-mediated B cell death. *J Immunol* 2007;178:2636–40.
 39. Poullin P, Announ N, Mugnier B, Guis S, Roudier J, Lefevre P. Protein A-immunoabsorption (ProSORBA column) in the treatment of rheumatoid arthritis. *Joint Bone Spine* 2005;72:101–3.
 40. Brunner J, Kern P, Gaipf U, Munoz L, Voll R, Kalden J, et al. The low-throughput protein A adsorber: an immune modulatory device. Hypothesis for the mechanism of action in the treatment of rheumatoid arthritis. *Mod Rheumatol* 2005;15:9–18.
 41. Sasso EH, Merrill C, Furst DT. Is release of staphylococcal protein A (SPA) during immunoabsorption therapy of rheumatoid arthritis related to clinical response? [abstract]. *Arthritis Rheum* 2000;43 Suppl:S290.
 42. Hanson DC, Phillips ML, Schumaker VN. Electron microscopic and hydrodynamic studies of protein A-immunoglobulin G soluble complexes. *J Immunol* 1984;132:1386–96.
 43. Gerber JS, Mosser DM. Reversing lipopolysaccharide toxicity by ligating the macrophage Fc γ receptors. *J Immunol* 2001;166:6861–8.
 44. Bernstein KE, Alexander CB, Mage RG. Nucleotide sequence of a rabbit IgG heavy chain from the recombinant F-I haplotype. *Immunogenetics* 1983;18:387–97.
 45. Johansson PJ, Myhre EB, Blomberg J. Specificity of Fc receptors induced by herpes simplex virus type 1: comparison of immunoglobulin G from different animal species. *J Virol* 1985;56:489–94.
 46. Antonsson A, Johansson P. Binding of human and animal immunoglobulins to the IgG Fc receptor induced by human cytomegalovirus. *J Gen Virol* 2001;82:1137–45.
 47. Ravetch JV, Nimmerjahn F. Fc receptors. In: Paul WE, editor. *Fundamental immunology*. 5th ed. Philadelphia: Lippincott-Raven; 2008. p. 684–705.
 48. Gravalles EM, Harada Y, Wang JT, Gorn AH, Thornhill TS, Goldring SR. Identification of cell types responsible for bone resorption in rheumatoid arthritis and juvenile rheumatoid arthritis. *Am J Pathol* 1998;152:943–51.
 49. Torbinezad M, Clagett J, Engel D. A cat model for the evaluation of mechanisms of bone resorption: induction of bone loss by simulated immune complexes and inhibition by indomethacin. *Calcif Tissue Int* 1979;29:207–14.

9 Appendix 3

	Blood	Damaged spinal cord	Bone marrow
Ly6C high monocytes	4248 ± 459	1704 ± 416	913 ± 206
Ly6C low monocytes	3013 ± 508	978 ± 293	352 ± 80
Total monocytes	3574 ± 609	1547 ± 341	678 ± 129
Neutrophils	280 ± 27	424 ± 77	118 ± 22
Microglia		670 ± 81	

Table 9.1 Comparison of SpA-488 ability to bind cells of the myeloid lineage in the blood, damaged spinal cord and bone marrow after SCI. In C57BL/6 mice SCI was induced at the C5/6 border. 24h after injury mice received either 500 μ g of SpA-488 i.p. After a further 2h mice were culled and the damaged portion of the spinal cord, blood and bone marrow were harvested and prepared for flow cytometric analysis on the MACS Quant. The mean \pm SD MFI values for SpA-488 binding in the damaged portion of the spinal cord, blood and bone marrow were determined. This experiment was carried out on two separate occasions; the data were then pooled together for purposes of statistical analysis. The two experiments had a total N=5.

List of references

1. Medzhitov, R. *et al.* Innate immunity. *N. Engl. J. Med.* **343**, 338-344 (2000).
2. Parkin, J. *et al.* An overview of the immune system. *Lancet* **357**, 1777-1789 (2001).
3. Hume, D. A. *et al.* The mononuclear phagocyte system revisited. *J Leukoc Biol* **72**, 621-627 (2002).
4. Wiktor-Jedrzejczak, W. *et al.* Cytokine regulation of the macrophage (M phi) system studied using the colony stimulating factor-1-deficient op/op mouse. *Physiol. Rev.* **76**, 927-947 (1996).
5. van Furth, R. *et al.* The origin and kinetics of mononuclear phagocytes. *J. Exp. Med.* **128**, 415-435 (1968).
6. Cumano, A. *et al.* Ontogeny of the hematopoietic system. *Annu. Rev. Immunol.* (2007).
7. Kondo, M. *et al.* Identification of Clonogenic Common Lymphoid Progenitors in Mouse Bone Marrow. *Cell* (1997).
8. Akashi, K. *et al.* A clonogenic common myeloid progenitor that gives rise to all myeloid lineages. *Nature* (2000).
9. Akashi, K. *et al.* Bcl-2 rescues T lymphopoiesis in interleukin-7 receptor-deficient mice. *Cell* **89**, 1033-1041 (1997).
10. Corcoran, A. E. *et al.* Impaired immunoglobulin gene rearrangement in mice lacking the IL-7 receptor. *Nature* **391**, 904-907 (1998).
11. Iwasaki, H. *et al.* Myeloid Lineage Commitment from the Hematopoietic Stem Cell. *Immunity* **26**, 726-740 (2007).
12. Auffray, C. *et al.* Blood monocytes: development, heterogeneity, and relationship with dendritic cells. *Annu Rev Immunol* **27**, 669-692 (2009).
13. Reid, A. *et al.* Leukemia translocation gene, PLZF, is expressed with a speckled nuclear pattern in early hematopoietic progenitors. *Blood* **86**, 4544-4552 (1995).
14. Klemsz, M. J. *et al.* The macrophage and B cell-specific transcription factor PU.1 is related to the ets oncogene. *Cell* **61**, 113-124 (1990).
15. Goebel, M. K. *et al.* The PU.1 transcription factor is the product of the putative oncogene Spi-1. *Cell* **61**, 1165-1166 (1990).
16. Chen, H. *et al.* Neutrophils and monocytes express high levels of PU.1 (Spi-1) but not Spi-B. *Blood*. **10**, 2918-28 (1995).

17. Hromas, R. *et al.* Hematopoietic lineage- and stage-restricted expression of the ETS oncogene family member PU.1. *Blood*. **10**, 2998-3004. (1993).
18. Scott, E. W. *et al.* Requirement of transcription factor PU.1 in the development of multiple hematopoietic lineages. *Science* **265**, 1573-1577 (1994).
19. Olson, M. *et al.* PU.1 is not essential for early myeloid gene expression but is required for terminal myeloid differentiation. *Immunity* (1995).
20. Henkel, G. *et al.* PU.1 but not ets-2 is essential for macrophage development from embryonic stem cells. *Blood*. **8**, 2917-26. (1996).
21. Kawasaki, E. S. *et al.* Molecular cloning of a complementary DNA encoding human macrophage-specific colony-stimulating factor (CSF-1). *Science* **230**, 291-296 (1985).
22. Dai, X.-M. *et al.* Targeted disruption of the mouse colony-stimulating factor 1 receptor gene results in osteopetrosis, mononuclear phagocyte deficiency, increased primitive progenitor cell frequencies, and reproductive defects. *Blood* **99**, 111-120 (2002).
23. Lin, H. *et al.* Discovery of a cytokine and its receptor by functional screening of the extracellular proteome. *Science* **320**, 807-811 (2008).
24. Scott, L. M. *et al.* A novel temporal expression pattern of three C/EBP family members in differentiating myelomonocytic cells. *Blood* **80**, 1725-1735 (1992).
25. Dahl, R. *et al.* Regulation of macrophage and neutrophil cell fates by the PU.1:C/EBP α ratio and granulocyte colony-stimulating factor. *Nat Immunol* **4**, 1029-1036 (2003).
26. Hohaus, S. *et al.* PU.1 (Spi-1) and C/EBP alpha regulate expression of the granulocyte-macrophage colony-stimulating factor receptor alpha gene. *Mol Cell Biol*. **10**, 5830-45 (1995).
27. Lee, S. L. *et al.* Unimpaired macrophage differentiation and activation in mice lacking the zinc finger transcription factor NGFI-A (EGR1). *Mol. Cell. Biol.* **16**, 4566-4572 (1996).
28. Laslo, P. *et al.* Multilineage transcriptional priming and determination of alternate hematopoietic cell fates. *Cell* **126**, 755-766 (2006).
29. Zhang, D. E. *et al.* Identification of a region which directs the monocytic activity of the colony-stimulating factor 1 (macrophage colony-stimulating factor) receptor promoter and binds PEBP2/CBF (AML1). *Mol.*

- Cell. Biol.* **14**, 8085-8095 (1994).
30. Nakajima, K. *et al.* A central role for Stat3 in IL-6-induced regulation of growth and differentiation in M1 leukemia cells. *EMBO J.* **15**, 3651-3658 (1996).
 31. Hanna, R. N. *et al.* The transcription factor NR4A1 (Nur77) controls bone marrow differentiation and the survival of Ly6C⁻ monocytes. *Nature* **12**, 778-785 (2011).
 32. Alder, J. K. *et al.* Kruppel-like factor 4 is essential for inflammatory monocyte differentiation in vivo. *J Immunol* **180**, 5645-5652 (2008).
 33. Hanisch, U.K. *et al.* Microglia: active sensor and versatile effector cells in the normal and pathologic brain. *Nat. Neurosci.* **10**, 1387-1394 (2007).
 34. Ajami, B. *et al.* Local self-renewal can sustain CNS microglia maintenance and function throughout adult life. *Nat. Neurosci.* **10**, 1538-1543 (2007).
 35. Djukic, M. *et al.* Circulating monocytes engraft in the brain, differentiate into microglia and contribute to the pathology following meningitis in mice. *Brain* **129**, 2394-2403 (2006).
 36. Mildner, A. *et al.* Microglia in the adult brain arise from Ly-6ChiCCR2⁺ monocytes only under defined host conditions. *Nature Neuroscience* **10**, 1544-1553 (2007).
 37. Ginhoux, F. *et al.* Fate mapping analysis reveals that adult microglia derive from primitive macrophages. *Science* **330**, 841-845 (2010).
 38. Schulz, C. *et al.* A Lineage of Myeloid Cells Independent of Myb and Hematopoietic Stem Cells. *Science* **336**, 86-90 (2012).
 39. Gomez Perdiguero, E. *et al.* Development and homeostasis of “resident” myeloid cells: The case of the microglia. *Glia* (2012).
doi:10.1002/glia.22393
 40. Geissmann, F. *et al.* Blood Monocytes Consist of Two Principal Subsets with Distinct Migratory Properties. *Immunity* **19**, 71-82 (2003).
 41. Chow, A. *et al.* Studying the mononuclear phagocyte system in the molecular age. *Nat Rev Immunol* **11**, 788-798 (2011).
 42. Bothwell, A. *et al.* Isolation and expression of an IFN-responsive Ly-6C chromosomal gene. *J Immunol* **140**, 2815-2820 (1988).
 43. Mallya, M. *et al.* Transcriptional analysis of a novel cluster of LY-6 family members in the human and mouse major histocompatibility complex: five

- genes with many splice forms. *Genomics* **80**, 113-123 (2002).
44. Fleming, T. J. *et al.* Characterization of two novel Ly-6 genes. Protein sequence and potential structural similarity to alpha-bungarotoxin and other neurotoxins. *J Immunol* **150**, 5379-5390 (1993).
 45. Jaakkola, I. A. *et al.* Ly6C induces clustering of LFA-1 (CD11a/CD18) and is involved in subtype-specific adhesion of CD8 T cells. *J Immunol* **170**, 1283-1290 (2003).
 46. Sunderkötter, C. *et al.* Subpopulations of mouse blood monocytes differ in maturation stage and inflammatory response. *J Immunol* **172**, 4410-4417 (2004).
 47. Varol, C. *et al.* Monocytes give rise to mucosal, but not splenic, conventional dendritic cells. (2007).
<<http://jem.rupress.org/content/204/1/171.short>>
 48. Geissmann, F. *et al.* Blood monocytes: distinct subsets, how they relate to dendritic cells, and their possible roles in the regulation of T-cell responses. *Immunol Cell Biol* **86**, 398-408 (2008).
 49. Peters, W. *et al.* CCR2-Dependent Trafficking of F4/80dim Macrophages and CD11cdim/intermediate Dendritic Cells Is Crucial for T Cell Recruitment to Lungs Infected with Mycobacterium tuberculosis. *J Immunol*. **12**, 7647-53 (2004).
 50. Peters, W. *et al.* Chemokine receptor 2 serves an early and essential role in resistance to Mycobacterium tuberculosis. *Proc. Natl. Acad. Sci. U.S.A.* **98**, 7958-7963 (2001).
 51. Robben, P. M. *et al.* Recruitment of Gr-1+ monocytes is essential for control of acute toxoplasmosis. *J. Exp. Med.* **201**, 1761-1769 (2005).
 52. Ling, Y. M. *et al.* Vacuolar and plasma membrane stripping and autophagic elimination of Toxoplasma gondii in primed effector macrophages. *J. Exp. Med.* **203**, 2063-2071 (2006).
 53. Auffray, C. *et al.* Monitoring of Blood Vessels and Tissues by a Population of Monocytes with Patrolling Behavior. *Science* **317**, 666-670 (2007).
 54. Serbina, N. V. *et al.* Monocyte emigration from bone marrow during bacterial infection requires signals mediated by chemokine receptor CCR2. *Nat Immunol* **7**, 311-317 (2006).
 55. Nahrendorf, M. *et al.* Monocytes: protagonists of infarct inflammation and repair after myocardial infarction. *Circulation* **121**, 2437-2445

- (2010).
56. Panizzi, P. *et al.* Impaired Infarct Healing in Atherosclerotic Mice With Ly-6Chi Monocytosis. *JAC* **55**, 1629-1638 (2010).
 57. Murphy, A. J. *et al.* ApoE regulates hematopoietic stem cell proliferation, monocytosis, and monocyte accumulation in atherosclerotic lesions in mice. *J Clin Invest* **121**, 4138-4149 (2011).
 58. Swirski, F. K. *et al.* Ly-6Chi monocytes dominate hypercholesterolemia-associated monocytosis and give rise to macrophages in atheromata. *J Clin Invest* **117**, 195-205 (2007).
 59. Tacke, F. *et al.* Monocyte subsets differentially employ CCR2, CCR5, and CX3CR1 to accumulate within atherosclerotic plaques. *J Clin Invest* **117**, 185-194 (2007).
 60. Hanna, R. N. *et al.* NR4A1 (Nur77) deletion polarizes macrophages toward an inflammatory phenotype and increases atherosclerosis. *Circ. Res.* **110**, 416-427 (2012).
 61. Hamers, A. A. J. *et al.* Bone marrow-specific deficiency of nuclear receptor Nur77 enhances atherosclerosis. *Circ. Res.* **110**, 428-438 (2012).
 62. Arnold, L. *et al.* Inflammatory monocytes recruited after skeletal muscle injury switch into antiinflammatory macrophages to support myogenesis. *Journal of Experimental Medicine* **204**, 1057-1069 (2007).
 63. Nguyen, H.H. *et al.* IL-10 Acts As a Developmental Switch Guiding Monocyte Differentiation to Macrophages during a Murine Peritoneal Infection. *The Journal of Immunology* **189**, 3112-3120 (2012).
 64. Bain, C. C. *et al.* Resident and pro-inflammatory macrophages in the colon represent alternative context-dependent fates of the same Ly6Chi monocyte precursors. *Mucosal Immunol* 1-13 (2012).
doi:10.1038/mi.2012.89
 65. Ziegler-Heitbrock, L. *et al.* The CD14+ CD16+ blood monocytes: their role in infection and inflammation. *J Leukoc Biol* **81**, 584-592 (2006).
 66. Ziegler-Heitbrock, L. *et al.* Nomenclature of monocytes and dendritic cells in blood. *Blood* **116**, e74-e80 (2010).
 67. Geissmann, F. *et al.* Development of Monocytes, Macrophages, and Dendritic Cells. *Science* **327**, 656-661 (2010).
 68. Boring, L. *et al.* Impaired monocyte migration and reduced type 1 (Th1) cytokine responses in C-C chemokine receptor 2 knockout mice. *J Clin*

- Invest* **100**, 2552-2561 (1997).
69. Tsou, C.-L. *et al.* Critical roles for CCR2 and MCP-3 in monocyte mobilization from bone marrow and recruitment to inflammatory sites. *J Clin Invest* **117**, 902-909 (2007).
 70. Jia, T. *et al.* Additive Roles for MCP-1 and MCP-3 in CCR2-Mediated Recruitment of Inflammatory Monocytes during *Listeria monocytogenes* Infection. *J Immunol.* **10**, 6846-53 (2008).
 71. Landsman, L. *et al.* CX3CR1 is required for monocyte homeostasis and atherogenesis by promoting cell survival. *Blood* **113**, 963-972 (2009).
 72. Galli, S. J. *et al.* Phenotypic and functional plasticity of cells of innate immunity: macrophages, mast cells and neutrophils. *Nature* **12**, 1035-1044 (2011).
 73. Gordon, S. *et al.* Monocyte and macrophage heterogeneity. *Nat Rev Immunol* **5**, 953-964 (2005).
 74. Porcheray, F. *et al.* Macrophage activation switching: an asset for the resolution of inflammation. *Clinical & Experimental Immunology* **142**, 481-489 (2005).
 75. Qin, H. *et al.* SOCS3 Deficiency Promotes M1 Macrophage Polarization and Inflammation. *The Journal of Immunology* (2012).doi:10.4049/jimmunol.1201168
 76. Mantovani, A. *et al.* Orchestration of macrophage polarization. *Blood* **114**, 3135-3136 (2009).
 77. Sutterwala, F. S. *et al.* Selective suppression of interleukin-12 induction after macrophage receptor ligation. *J. Exp. Med.* **185**, 1977-1985 (1997).
 78. Mantovani, A. *et al.* The chemokine system in diverse forms of macrophage activation and polarization. *Trends Immunol* **25**, 677-686 (2004).
 79. Todd, R. B. *et al.* *The descriptive and physiological anatomy of the brain, spinal cord and ganglions*. Boston Library Consortium Member Libraries (1845).
 80. Watson, C. *et al.* *The Spinal Cord*. 408 (Academic Press: 2009).
 81. Windle, W. F. *et al.* *The Spinal cord and its reaction to traumatic injury*. *Journal of neurosurgery* **384** (1980).
 82. Engelhardt, B. *et al.* Development of the blood-brain barrier. *Cell and Tissue Research* **314**, 119-129 (2003).

83. Brightman, M. W. *et al.* Junctions between intimately apposed cell membranes in the vertebrate brain. *J Cell Biol* **40**, 648-677 (1969).
84. Cserr, H. F. *et al.* Cervical lymphatics, the blood-brain barrier and the immunoreactivity of the brain: a new view. *Immunol Today* **13**, 507-512 (1992).
85. Trivedi, A. *et al.* Inflammation and Spinal Cord Injury: Infiltrating Leukocytes as Determinants of Injury and Repair Processes. *Clinical neuroscience research* **6**, 283-292 (2006).
86. Cayrol, R. *et al.* Activated leukocyte cell adhesion molecule promotes leukocyte trafficking into the central nervous system. *Nature* **9**, 137-145 (2008).
87. Anderson, K. D. *et al.* Quantitative assessment of deficits and recovery of forelimb motor function after cervical spinal cord injury in mice. *Exp Neurol* **190**, 184-191 (2004).
88. Freund, P. *et al.* Disability, atrophy and cortical reorganization following spinal cord injury. *Brain* **134**, 1610-1622 (2011).
89. Eftekharpour, E. *et al.* Current status of experimental cell replacement approaches to spinal cord injury. *Neurosurgical FOCUS* **24**, E19 (2008).
90. Tator, C. H. *et al.* Review of the secondary injury theory of acute spinal cord trauma with emphasis on vascular mechanisms. *J. Neurosurg.* **75**, 15-26 (1991).
91. Stirling, D. P. *et al.* Dynamics of the inflammatory response after murine spinal cord injury revealed by flow cytometry. *J. Neurosci. Res.* **86**, 1944-1958 (2008).
92. Blight, A. R. *et al.* Effects of silica on the outcome from experimental spinal cord injury: implication of macrophages in secondary tissue damage. *Neuroscience* **60**, 263-273 (1994).
93. Ghirnikar, R. S. *et al.* Chemokine antagonist infusion attenuates cellular infiltration following spinal cord contusion injury in rat. *J. Neurosci. Res.* **59**, 63-73 (2000).
94. Popovich, P. G. *et al.* Depletion of hematogenous macrophages promotes partial hindlimb recovery and neuroanatomical repair after experimental spinal cord injury. *Exp Neurol* **158**, 351-365 (1999).
95. Nishio, Y. *et al.* Deletion of macrophage migration inhibitory factor attenuates neuronal death and promotes functional recovery after

- compression-induced spinal cord injury in mice. *Acta Neuropathol* **117**, 321-328 (2009).
96. Kerr, B. J. *et al.* Potent pro-inflammatory actions of leukemia inhibitory factor in the spinal cord of the adult mouse. *Exp Neurol* **188**, 391-407 (2004).
 97. Okada, S. *et al.* Blockade of interleukin-6 receptor suppresses reactive astrogliosis and ameliorates functional recovery in experimental spinal cord injury. *J. Neurosci. Res.* **76**, 265-276 (2004).
 98. Gris, P. *et al.* Transcriptional regulation of scar gene expression in primary astrocytes. *Glia* **55**, 1145-1155 (2007).
 99. Gensel, J. C. *et al.* Achieving CNS axon regeneration by manipulating convergent neuro-immune signaling. *Cell and Tissue Research* **349**, 201-213 (2012).
 100. Donnelly, D. J. *et al.* Inflammation and its role in neuroprotection, axonal regeneration and functional recovery after spinal cord injury. *Exp Neurol* **209**, 378-388 (2008).
 101. Hawthorne, A. L. *et al.* Emerging concepts in myeloid cell biology after spinal cord injury. *Neurotherapeutics* **8**, 252-261 (2011).
 102. Neumann, H. *et al.* Debris clearance by microglia: an essential link between degeneration and regeneration. *Brain* **132**, 288-295 (2009).
 103. Ransohoff, R. M. *et al.* Microglial physiology: unique stimuli, specialized responses. *Annu Rev Immunol* **27**, 119-145 (2009).
 104. Yiu, G. *et al.* Glial inhibition of CNS axon regeneration. *Nat Rev Neurosci* **7**, 617-627 (2006).
 105. Tester, N. J. *et al.* Chondroitinase ABC improves basic and skilled locomotion in spinal cord injured cats. *Exp Neurol* **209**, 483-496 (2008).
 106. Bradbury, E. J. *et al.* Chondroitinase ABC promotes functional recovery after spinal cord injury. *Nature* **416**, 636-640 (2002).
 107. Tan, A. M. *et al.* Antibodies against the NG2 proteoglycan promote the regeneration of sensory axons within the dorsal columns of the spinal cord. *Journal of Neuroscience* **26**, 4729-4739 (2006).
 108. Rolls, A. *et al.* The bright side of the glial scar in CNS repair. *Nat Rev Neurosci* **10**, 235-241 (2009).
 109. Wei, C. *et al.* Inducible Ablation of Astrocytes Shows That These Cells Are Required for Neuronal Survival in the Adult Brain. *Glia*. **4**, 272-82 (2001).

110. Carro, E. *et al.* Brain repair and neuroprotection by serum insulin-like growth factor I. *Mol. Neurobiol.* **27**, 153-162 (2003).
111. Rolls, A. *et al.* Two faces of chondroitin sulfate proteoglycan in spinal cord repair: a role in microglia/macrophage activation. *PLoS Med* **5**, e171 (2008).
112. Shechter, R. *et al.* The Glial Scar-Monocyte Interplay: A Pivotal Resolution Phase in Spinal Cord Repair. *PLoS ONE* **6**, e27969 (2011).
113. Popovich, P. G. *et al.* The neuropathological and behavioral consequences of intraspinal microglial/macrophage activation. *J Neuropathol Exp Neurol* **61**, 623-633 (2002).
114. Horn, K. P. *et al.* Another barrier to regeneration in the CNS: activated macrophages induce extensive retraction of dystrophic axons through direct physical interactions. *Journal of Neuroscience* **28**, 9330-9341 (2008).
115. Gensel, J. C. *et al.* Macrophages promote axon regeneration with concurrent neurotoxicity. *Journal of Neuroscience* **29**, 3956-3968 (2009).
116. Ma, Y. *et al.* TLR8: an innate immune receptor in brain, neurons and axons. *Cell Cycle* **6**, 2859-2868 (2007).
117. Kigerl, K. A. *et al.* Toll-like receptor (TLR)-2 and TLR-4 regulate inflammation, gliosis, and myelin sparing after spinal cord injury. *J Neurochem* **102**, 37-50 (2007).
118. Reddy, S. J. *et al.* The role of heat shock proteins in spinal cord injury. *Neurosurgical FOCUS* **25**, E4 (2008).
119. Michelucci, A. *et al.* Characterization of the microglial phenotype under specific pro-inflammatory and anti-inflammatory conditions: Effects of oligomeric and fibrillar amyloid-beta. *J Neuroimmunol* **210**, 3-12 (2009).
120. Boivin, A. *et al.* Toll-like receptor signaling is critical for Wallerian degeneration and functional recovery after peripheral nerve injury. *Journal of Neuroscience* **27**, 12565-12576 (2007).
121. Bessis, A. *et al.* Microglial control of neuronal death and synaptic properties. *Glia* **55**, 233-238 (2007).
122. Beattie, M. S. *et al.* Inflammation and apoptosis: linked therapeutic targets in spinal cord injury. *Trends in molecular medicine* **10**, 580-583 (2004).
123. Schori, H. *et al.* Genetic manipulation of CD74 in mouse strains of

- different backgrounds can result in opposite responses to central nervous system injury. *J Immunol* **178**, 163-171 (2007).
124. McTigue, D. M. *et al.* Localization of transforming growth factor-beta1 and receptor mRNA after experimental spinal cord injury. *Exp Neurol* **163**, 220-230 (2000).
 125. Kerschensteiner, M. *et al.* Activated human T cells, B cells, and monocytes produce brain-derived neurotrophic factor in vitro and in inflammatory brain lesions: a neuroprotective role of inflammation? *J. Exp. Med.* **189**, 865-870 (1999).
 126. Nakajima, K. *et al.* Neurotrophin secretion from cultured microglia. *J. Neurosci. Res.* **65**, 322-331 (2001).
 127. Rimaniol, A. C. *et al.* Na⁺-dependent high-affinity glutamate transport in macrophages. *J Immunol* **164**, 5430-5438 (2000).
 128. Nakamura, M. *et al.* Role of IL-6 in spinal cord injury in a mouse model. *Clin Rev Allergy Immunol* **28**, 197-204 (2005).
 129. Hakkoum, D. *et al.* Interleukin-6 promotes sprouting and functional recovery in lesioned organotypic hippocampal slice cultures. *J Neurochem* **100**, 747-757 (2007).
 130. Lozoff, B. *et al.* Iron Deficiency and Brain Development. *Seminars in Pediatric Neurology* **13**, 158-165 (2006).
 131. Schonberg, D. L. *et al.* Ferritin stimulates oligodendrocyte genesis in the adult spinal cord and can be transferred from macrophages to NG2 cells in vivo. *Journal of Neuroscience* **32**, 5374-5384 (2012).
 132. Popovich, P. G. *et al.* Can the immune system be harnessed to repair the CNS? *Nat Rev Neurosci* **9**, 481-493 (2008).
 133. Kigerl, K. A. *et al.* Identification of Two Distinct Macrophage Subsets with Divergent Effects Causing either Neurotoxicity or Regeneration in the Injured Mouse Spinal Cord. *Journal of Neuroscience* **29**, 13435-13444 (2009).
 134. BETHEA, J. R. *et al.* Systemically Administered Interleukin-10 Reduces Tumor Necrosis Factor-Alpha Production and Significantly Improves Functional Recovery Following Traumatic Spinal Cord Injury in Rats. *Journal of Neurotrauma* **16**, 851-863 (1999).
 135. Zhou, Z. *et al.* IL-10 promotes neuronal survival following spinal cord injury. *Exp Neurol* **220**, 183-190 (2009).

136. Rapalino, O. *et al.* Implantation of stimulated homologous macrophages results in partial recovery of paraplegic rats. *Nat Med* **4**, 814-821 (1998).
137. Bomstein, Y. *et al.* Features of skin-coincubated macrophages that promote recovery from spinal cord injury. *J Neuroimmunol* **142**, 10-16 (2003).
138. Mosser, D. M. *et al.* The many faces of macrophage activation. *J Leukoc Biol* **73**, 209-212 (2003).
139. LU, P. *et al.* BDNF-expressing marrow stromal cells support extensive axonal growth at sites of spinal cord injury. *Exp Neurol* **191**, 344-360 (2005).
140. Rössignol, S. *et al.* Spinal cord injury: time to move? *Journal of Neuroscience* **27**, 11782-11792 (2007).
141. Mikami, Y. *et al.* Implantation of dendritic cells in injured adult spinal cord results in activation of endogenous neural stem/progenitor cells leading to de novo neurogenesis and functional recovery. *J. Neurosci. Res.* **76**, 453-465 (2004).
142. Yaguchi, M. *et al.* Transplantation of dendritic cells promotes functional recovery from spinal cord injury in common marmoset. *Neurosci. Res.* **65**, 384-392 (2009).
143. Kipnis, J. *et al.* Neuronal survival after CNS insult is determined by a genetically encoded autoimmune response. *Journal of Neuroscience* **21**, 4564-4571 (2001).
144. Sicotte, M. *et al.* Immunization with myelin or recombinant Nogo-66/MAG in alum promotes axon regeneration and sprouting after corticospinal tract lesions in the spinal cord. *Molecular and Cellular Neuroscience* **23**, 251-263 (2003).
145. Hauben, E. *et al.* Passive or Active Immunization with Myelin Basic Protein Promotes Recovery from Spinal Cord Contusion. (2000).
146. Wang, H.-J. *et al.* Passive immunization with myelin basic protein activated T cells suppresses axonal dieback but does not promote axonal regeneration following spinal cord hemisection in adult rats. *Int. J. Neurosci.* **122**, 458-465 (2012).
147. Imbach, P. *et al.* Treatment of immune thrombocytopenia with intravenous immunoglobulin and insights for other diseases. A historical review. *Swiss Med Wkly* **142**, w13593 (2012).

148. Gok, B. *et al.* Immunomodulation of acute experimental spinal cord injury with human immunoglobulin G. *Journal of Clinical Neuroscience* **16**, 549-553 (2009).
149. Fehlings, M. G. *et al.* Immunoglobulin G: A Potential Treatment to Attenuate Neuroinflammation Following Spinal Cord Injury. *J Clin Immunol* **30**, 109-112 (2010).
150. Silverman, G. *et al.* Roles of B cells in rheumatoid arthritis. *Arthritis Res. Ther.* (2003).
151. Mosser, D. M. *et al.* Exploring the full spectrum of macrophage activation. *Nat Rev Immunol* **8**, 958-969 (2008).
152. Grundbacher, F. J. *et al.* Behring's discovery of diphtheria and tetanus antitoxins. *Immunol. Today* **13**, 188-190 (1992).
153. Paul, W. E. *et al.* Elvin A. Kabat (1914-2000). *Nature* **407**, 316 (2000).
154. Harry W Schroeder Jr MD, *et al.* Structure and function of immunoglobulins. *Journal of Allergy and Clinical Immunology* **125**, S41-S52 (2010).
155. Williams, A. F. *et al.* The immunoglobulin superfamily--domains for cell surface recognition. *Annu Rev Immunol* **6**, 381-405 (1988).
156. Andersen, J. T. *et al.* A strategy for bacterial production of a soluble functional human neonatal Fc receptor. *Journal of Immunological Methods* **331**, 39-49 (2008).
157. Antohe, F. *et al.* Expression of functionally active FcRn and the differentiated bidirectional transport of IgG in human placental endothelial cells. *Hum. Immunol.* **62**, 93-105 (2001).
158. Woof, J. M. *et al.* Human antibody-Fc receptor interactions illuminated by crystal structures. *Nat Rev Immunol* **4**, 89-99 (2004).
159. Raju, T. S. *et al.* Species-specific variation in glycosylation of IgG: evidence for the species-specific sialylation and branch-specific galactosylation and importance for engineering recombinant glycoprotein therapeutics. *Glycobiology* **10**, 477-486 (2000).
160. Kobata, A. *et al.* The N-linked sugar chains of human immunoglobulin G: their unique pattern, and their functional roles. *Biochim. Biophys. Acta* **1780**, 472-478 (2008).
161. Nimmerjahn, F. *et al.* Impact of differential glycosylation on IgG activity. *Adv. Exp. Med. Biol.* **780**, 113-124 (2011).

162. Routier, F. H. *et al.* Quantitation of the oligosaccharides of human serum IgG from patients with rheumatoid arthritis: a critical evaluation of different methods. *Journal of Immunological Methods* **213**, 113-130 (1998).
163. Kaneko, Y. *et al.* Anti-inflammatory activity of immunoglobulin G resulting from Fc sialylation. *Science* **313**, 670-673 (2006).
164. Nimmerjahn, F. *et al.* Fc γ Receptors: Old Friends and New Family Members. *Immunity* **24**, 19-28 (2006).
165. Nimmerjahn, F. *et al.* Fc γ receptors as regulators of immune responses. *Nat Rev Immunol* **8**, 34-47 (2008).
166. Kato, K. *et al.* A conformational change in the Fc precludes the binding of two Fc γ receptor molecules to one IgG. *Immunol Today* **21**, 310-312 (2000).
167. Sondermann, P, *et al.* The 3.2-Å crystal structure of the human IgG1 Fc fragment Fc γ RIII complex. *Nature*. 6793, 267-73 (2000).
168. Radaev, S. *et al.* The structure of a human type III Fc γ receptor in complex with Fc. *J. Biol. Chem.* **276**, 16469-16477 (2001).
169. Allen, J. M. *et al.* Isolation and expression of functional high-affinity Fc receptor complementary DNAs. *Science* **243**, 378-381 (1989).
170. Hulet, M. D. *et al.* Chimeric Fc receptors identify functional domains of the murine high affinity receptor for IgG. (1991).
171. Nimmerjahn, F. *et al.* Divergent immunoglobulin g subclass activity through selective Fc receptor binding. *Science* **310**, 1510-1512 (2005).
172. Amigorena, S. *et al.* Cytoplasmic domain heterogeneity and functions of IgG Fc receptors in B lymphocytes. *Science* **256**, 1808-1812 (1992).
173. Bruhns, P. *et al.* Properties of mouse and human IgG receptors and their contribution to disease models. *Blood* **119**, 5640-5649 (2012).
174. Nimmerjahn, F. *et al.* Antibody-mediated modulation of immune responses. *Immunol. Rev.* **236**, 265-275 (2010).
175. Bolland, S. *et al.* Spontaneous autoimmune disease in Fc(γ)RIIB-deficient mice results from strain-specific epistasis. *Immunity* **13**, 277-285 (2000).
176. McGaha, T. L. *et al.* Restoration of tolerance in lupus by targeted inhibitory receptor expression. *Science* **307**, 590-593 (2005).
177. Mendez-Fernandez, Y. V. *et al.* The inhibitory Fc γ RIIb modulates the

- inflammatory response and influences atherosclerosis in male apoE^{-/-} mice. *Atherosclerosis* **214**, 73-80 (2011).
178. Raghavan, M. *et al.* Fc receptors and their interactions with immunoglobulins. *Annu. Rev. Cell Dev. Biol.* **12**, 181-220 (1996).
 179. Ji, H. *et al.* Arthritis critically dependent on innate immune system players. *Immunity* **16**, 157-168 (2002).
 180. Lee, D. M. *et al.* Mast Cells: A Cellular Link Between Autoantibodies and Inflammatory Arthritis. *Science* **297**, 1689-1692 (2002).
 181. Nimmerjahn, F. *et al.* FcγRIV deletion reveals its central role for IgG2a and IgG2b activity in vivo. *Proceedings of the National Academy of Sciences* **107**, 19396-19401 (2010).
 182. Giorgini, A. *et al.* FcγRIII and FcγRIV Are Indispensable for Acute Glomerular Inflammation Induced by Switch Variant Monoclonal Antibodies. *J Immunol.* **12**, 8745-8752.(2008).
 183. Seeling, M. *et al.* Inflammatory monocytes and Fcγ receptor IV on osteoclasts are critical for bone destruction during inflammatory arthritis in mice. *Proceedings of the National Academy of Sciences* **110**, 10729-10734 (2013).
 184. Rodewald, R. *et al.* Distribution of immunoglobulin G receptors in the small intestine of the young rat. *J Cell Biol* **85**, 18-32 (1980).
 185. Dijstelbloem, H. M. *et al.* Inflammation in autoimmunity: receptors for IgG revisited. *Trends Immunol* **22**, 510-516 (2001).
 186. Abram, C. L. *et al.* The expanding role for ITAM-based signaling pathways in immune cells. *Sci. STKE* **2**, (2007).
 187. Daëron, M. *et al.* Fc RECEPTOR BIOLOGY. *Annu Rev Immunol* **15**, 203-234 (1997).
 188. Boross, P. *et al.* *Encyclopedia of Life Sciences.* (John Wiley & Sons, Ltd: Chichester, UK, 2001).doi:10.1002/9780470015902.a0000916.pub2
 189. Ivashkiv, L. B. *et al.* Cross-regulation of signaling by ITAM-associated receptors. *Nature Publishing Group* **10**, 340-347 (2009).
 190. Ravetch, J. V. *et al.* Immune inhibitory receptors. *Science* **290**, 84-89 (2000).
 191. Vély, F. *et al.* Conservation of structural features reveals the existence of a large family of inhibitory cell surface receptors and noninhibitory/activatory counterparts. *J Immunol.* **5**, 2075-7. (1997).

192. Ivashkiv, L. B. *et al.* How ITAMs inhibit signaling. *Sci Signal* **4**, pe20 (2011).
193. Durandy, A. *et al.* Intravenous immunoglobulins - understanding properties and mechanisms. *Clinical & Experimental Immunology* **158**, 2-13 (2009).
194. Anthony, R. M. *et al.* A novel role for the IgG Fc glycan: the anti-inflammatory activity of sialylated IgG Fcs. *J Clin Immunol* **30 Suppl 1**, S9-14 (2010).
195. Anthony, R. M. *et al.* Recapitulation of IVIG Anti-Inflammatory Activity with a Recombinant IgG Fc. *Science* **320**, 373-376 (2008).
196. Anthony, R. M. *et al.* Intravenous gammaglobulin suppresses inflammation through a novel TH2 pathway. *Nature* 1-5 (2011).
197. Vassilev, T. L. *et al.* Variable region-connected, dimeric fraction of intravenous immunoglobulin enriched in natural autoantibodies. *J. Autoimmun.* **8**, 405-413 (1995).
198. Peng, W. *et al.* Intravenous immunoglobulin treatment on anti-GM1 antibodies associated neuropathies inhibits cholera toxin and galectin-1 binding to ganglioside GM1. *Immunology letters* **143**, 146-151 (2012).
199. Crow, A. *et al.* IVIg inhibits reticuloendothelial system function and ameliorates murine passive-immune thrombocytopenia independent of anti-idiotypic reactivity. *British Journal of Haematology*, **3**, 679-686 (2001).
200. Yu, Z. *et al.* Mechanism of intravenous immune globulin therapy in antibody-mediated autoimmune diseases. *N. Engl. J. Med.* **340**, 227-228 (1999).
201. Crow, A. R. *et al.* The neonatal Fc receptor (FcRn) is not required for IVIg or anti-CD44 monoclonal antibody-mediated amelioration of murine immune thrombocytopenia. *Blood* **118**, 6403-6406 (2011).
202. Blank, U. *et al.* Inhibitory ITAMs as novel regulators of immunity. *Immunol. Rev.* **232**, 59-71 (2009).
203. Aloulou, M. *et al.* IgG1 and IVIg induce inhibitory ITAM signaling through Fc RIII controlling inflammatory responses. *Blood* (2012).
doi:10.1182/blood-2011-08-376046
204. Xu, C. *et al.* Modulation of endothelial cell function by normal polyspecific human intravenous immunoglobulins: a possible mechanism

- of action in vascular diseases. *Am J Pathol* **153**, 1257-1266 (1998).
205. Bayry, J. *et al.* Inhibition of maturation and function of dendritic cells by intravenous immunoglobulin. *Blood* **101**, 758-765 (2003).
206. Rhoades, *et al.* Monocyte-macrophage system as targets for immunomodulation by intravenous immunoglobulin. *Blood Rev.* **14**, 14-30 (2000).
207. Teeling, J. L. *et al.* Therapeutic efficacy of intravenous immunoglobulin preparations depends on the immunoglobulin G dimers: studies in experimental immune thrombocytopenia. *Blood* **98**, 1095-1099 (2001).
208. Stangel, M. *et al.* Side effects of intravenous immunoglobulins in neurological autoimmune disorders. *Journal of neurology* **250**, 818-821 (2003).
209. Kanik, K. S. *et al.* Failure of low-dose intravenous immunoglobulin therapy to suppress disease activity in patients with treatment-refractory rheumatoid arthritis. *Arthritis & Rheumatism* **39**, 1027-1029 (1996).
210. Pyne, D. *et al.* The therapeutic uses of intravenous immunoglobulins in autoimmune rheumatic diseases. *Rheumatology* **41**, 367-374 (2002).
211. Hjelm, H. *et al.* Protein a from *Staphylococcus aureus*. Its isolation by affinity chromatography and its use as an immunosorbent for isolation of immunoglobulins. *FEBS letters* (1972).
212. Graille, M. *et al.* Crystal structure of a *Staphylococcus aureus* protein A domain complexed with the Fab fragment of a human IgM antibody: structural basis for recognition of B-cell receptors and superantigen activity. *Proc. Natl. Acad. Sci. U.S.A.* **97**, 5399-5404 (2000).
213. Hillson, J. L. *et al.* The structural basis of germline-encoded VH3 immunoglobulin binding to staphylococcal protein A. *Journal of Experimental Medicine* **178**, 331-336 (1993).
214. Page, M. *et al.* *The Protein Protocols Handbook*. 733-734 (Humana Press: Totowa, NJ, 1996). doi:10.1007/978-1-60327-259-9_130
215. Notani, G. W. *et al.* Versatility of *Staphylococcus aureus* protein A in immunocytochemistry. Use in unlabeled antibody enzyme system and fluorescent methods. *J Histochem Cytochem.* **27**, 1438-44 (1979).
216. Silverman, G. J. *et al.* On the mechanism of staphylococcal protein A immunomodulation. *Transfusion* **45**, 274-280 (2005).
217. Hanson, D. C. *et al.* A model for the formation and interconversion of

- protein A-immunoglobulin G soluble complexes. *J Immunol* **132**, 1397-1409 (1984).
218. Siragam, V. *et al.* Can antibodies with specificity for soluble antigens mimic the therapeutic effects of intravenous IgG in the treatment of autoimmune disease? *J Clin Invest* **115**, 155-160 (2005).
219. Edwards, J. P. *et al.* Biochemical and functional characterization of three activated macrophage populations. *J Leukoc Biol* **80**, 1298-1307 (2006).
220. Johansson, P. J. *et al.* Specificity of Fc receptors induced by herpes simplex virus type 1: comparison of immunoglobulin G from different animal species. *J Virol.* **56**, 489-494 (1985).
221. Antonsson, A. *et al.* Binding of human and animal immunoglobulins to the IgG Fc receptor induced by human cytomegalovirus. *J Gen Virol.* **82**, 1137-45 (2001).
222. Gerber, J. S. *et al.* Reversing Lipopolysaccharide Toxicity by Ligating the Macrophage Fcγ Receptors. *J Immunol.* **166**, 6861-8 (2001).
223. Silverman, G. J. *et al.* A model B-cell superantigen and the immunobiology of B lymphocytes. *Clin. Immunol.* **102**, 117-134 (2002).
224. Goodyear, C. S. *et al.* Death by a B cell superantigen: In vivo VH-targeted apoptotic supraclonal B cell deletion by a Staphylococcal Toxin. *J. Exp. Med.* **197**, 1125-1139 (2003).
225. MacLellan, L. M. *et al.* Co-opting endogenous immunoglobulin for the regulation of inflammation and osteoclastogenesis in humans and mice. *Arthritis & Rheumatism* **63**, 3897-3907 (2011).
226. Weischenfeldt, J. *et al.* Bone Marrow-Derived Macrophages (BMM): Isolation and Applications. *CSH Protoc* **2008**, pdb.prot5080 (2008).
227. Kaufmann, S. H. E. *et al.* Immunology's foundation: the 100-year anniversary of the Nobel Prize to Paul Ehrlich and Elie Metchnikoff. *Nat Immunol* **9**, 705-712 (2008).
228. Anderson, D. *et al.* Leukocyte Adhesion Deficiency: An Inherited Defect in the Mac-1, LFA-1, and p150,95 Glycoproteins - Annual Review of Medicine, 38(1):175. *Annual review of medicine* (1987).
229. Segal, B. H. *et al.* Genetic, biochemical, and clinical features of chronic granulomatous disease. *Medicine (Baltimore)* **79**, 170-200 (2000).
230. Taylor, P. *et al.* MACROPHAGE RECEPTORS AND IMMUNE RECOGNITION -

- Annual Review of Immunology, 23(1):901. *Annu Rev ...* (2005).
231. Poltorak, A. *et al.* Defective LPS Signaling in C3H/HeJ and C57BL/10ScCr Mice: Mutations in Tlr4 Gene. *Science* **282**, 2085-2088 (1998).
 232. Nomura, F. *et al.* Cutting Edge: Endotoxin Tolerance in Mouse Peritoneal Macrophages Correlates with Down-Regulation of Surface Toll-Like Receptor 4 Expression. *J Immunol.* **164**, 3476-9 (2000).
 233. Mège, J. L. *et al.* Macrophage polarization and bacterial infections. *Curr. Opin. Infect. Dis.* **24**, 230-234 (2011).
 234. Martinez, F. O. *et al.* Macrophage activation and polarization. *Front. Biosci.* **13**, 453-461 (2008).
 235. Herberman, R. B. *et al.* Natural killer cells: their roles in defenses against disease. *Science* **214**, 24-30 (1981).
 236. Borden, E. C. *et al.* Interferons at age 50: past, current and future impact on biomedicine. *Nat Rev Drug Discov* **6**, 975-990 (2007).
 237. Stout, R. D. *et al.* Macrophages sequentially change their functional phenotype in response to changes in microenvironmental influences. *J Immunol* **175**, 342-349 (2005).
 238. Janeway, C. A. *et al.* Immunobiology. New York: Garland Science, (2001).
 239. Kovacsovics-Bankowski, M. *et al.* Presentation of exogenous antigens by macrophages: analysis of major histocompatibility complex class I and II presentation and regulation by cytokines. *Eur. J. Immunol.* **24**, 2421-2428 (1994).
 240. Maloy, K. J. *et al.* Intestinal homeostasis and its breakdown in inflammatory bowel disease. *Nature* **474**, 298-306 (2011).
 241. McGaha, T. L. *et al.* Marginal zone macrophages suppress innate and adaptive immunity to apoptotic cells in the spleen. *Blood* **117**, 5403-5412 (2011).
 242. Brandt, E. *et al.* IL-4 production by human polymorphonuclear neutrophils. *J Leukoc Biol* **68**, 125-130 (2000).
 243. Gratchev, A. *et al.* Alternatively activated macrophages differentially express fibronectin and its splice variants and the extracellular matrix protein beta1G-H3. *Scand. J. Immunol.* **53**, 386-392 (2001).
 244. Hesse, M. *et al.* Differential regulation of nitric oxide synthase-2 and arginase-1 by type 1/type 2 cytokines in vivo: granulomatous pathology is shaped by the pattern of L-arginine metabolism. *J Immunol* **167**, 6533-

- 6544 (2001).
245. Sunderkötter, C. *et al.* Macrophages and angiogenesis. *J Leukoc Biol* **55**, 410-422 (1994).
 246. Roberts, A. B. *et al.* Transforming growth factor type beta: rapid induction of fibrosis and angiogenesis in vivo and stimulation of collagen formation in vitro. *Proc. Natl. Acad. Sci. U.S.A.* **83**, 4167-4171 (1986).
 247. Kurowska-Stolarska, M. *et al.* IL-33 amplifies the polarization of alternatively activated macrophages that contribute to airway inflammation. *The Journal of Immunology* **183**, 6469-6477 (2009).
 248. Wynn, T. *et al.* Macrophages: Master Regulators of Inflammation and Fibrosis. *Semin Liver Dis* **30**, 245-257 (2010).
 249. Raes, G. *et al.* Differential expression of FIZZ1 and Ym1 in alternatively versus classically activated macrophages. *J Leukoc Biol* **71**, 597-602 (2002).
 250. Stein, M. *et al.* Interleukin 4 potently enhances murine macrophage mannose receptor activity: a marker of alternative immunologic macrophage activation. *J. Exp. Med.* **176**, 287-292 (1992).
 251. Fadok, V. A. *et al.* Macrophages that have ingested apoptotic cells in vitro inhibit proinflammatory cytokine production through autocrine/paracrine mechanisms involving TGF-beta, PGE2, and PAF. *J Clin Invest* **101**, 890-898 (1998).
 252. Sutterwala, F. S. *et al.* Reversal of proinflammatory responses by ligating the macrophage Fcγ receptor type I. *J. Exp. Med.* **188**, 217-222 (1998).
 253. Tierney, J. *et al.* Type II-activated macrophages suppress the development of experimental autoimmune encephalomyelitis. *Immunol Cell Biol* (2008).doi:10.1038/icb.2008.99
 254. Elenkov, I. J. *et al.* Glucocorticoids and the Th1/Th2 balance. *Ann. N. Y. Acad. Sci.* **1024**, 138-146 (2004).
 255. Haskó, G. *et al.* Shaping of monocyte and macrophage function by adenosine receptors. *Pharmacol. Ther.* **113**, 264-275 (2007).
 256. Delgado, M. *et al.* Vasoactive intestinal peptide and pituitary adenylate cyclase-activating polypeptide enhance IL-10 production by murine macrophages: in vitro and in vivo studies. *J Immunol* **162**, 1707-1716 (1999).
 257. Ando, M. *et al.* Siglec-9 enhances IL-10 production in macrophages via

- tyrosine-based motifs. *Biochem. Biophys. Res. Commun.* **369**, 878-883 (2008).
258. De Waal Malefyt, R. *et al.* Interleukin 10(IL-10) inhibits cytokine synthesis by human monocytes: an autoregulatory role of IL-10 produced by monocytes. *J. Exp. Med.* **174**, 1209-1220 (1991).
259. Ramos, R. N. *et al.* Monocyte-derived dendritic cells from breast cancer patients are biased to induce CD4+CD25+Foxp3+ regulatory T cells. *J Leukoc Biol* **92**, 673-682 (2012).
260. Gadiant, R. *et al.* Progress in Neurobiology - Interleukin-6 (IL-6)—A molecule with both beneficial and destructive potentials. *Progress in neurobiology* (1997).
261. Sulica, A. *et al.* Effect of protein A of *Staphylococcus aureus* on the binding of monomeric and polymeric IgG to Fc receptor-bearing cells. *Immunology* **38**, 173-179 (1979).
262. Bashyam, H. *et al.* *Ralph Steinman: dendritic cells bring home the Lasker.* *J. Exp. Med.* **204**, 2245-2248 (2007).
263. Mancardi, D. A. *et al.* FcγR4 is a mouse IgE receptor that resembles macrophage FcεR1 in humans and promotes IgE-induced lung inflammation. *J Clin Invest* **118**, 3738-3750 (2008).
264. Goodyear, C. S. *et al.* Cutting Edge: Bim is required for superantigen-mediated B cell death. *J Immunol* **178**, 2636-2640 (2007).
265. Poullin, P. *et al.* Protein A-immunoabsorption (Prosorba column) in the treatment of rheumatoid arthritis. *Joint Bone Spine* **72**, 101-103 (2005).
266. Boross, P. *et al.* The Inhibiting Fc Receptor for IgG, FcγRIIB, Is a Modifier of Autoimmune Susceptibility. *The Journal of Immunology* **187**, 1304-1313 (2011).
267. Lucas, M. *et al.* ERK activation following macrophage FcγR4 ligation leads to chromatin modifications at the IL-10 locus. *J Immunol* **175**, 469-477 (2005).
268. Redpath, S. *et al.* Murine Cytomegalovirus Infection Down-Regulates MHC Class II Expression on Macrophages by Induction of IL-10. *J Immunol.* **162**, 6701-7 (1999).
269. Virgin, H. W. *et al.* Immune complex effects on murine macrophages. I. Immune complexes suppress interferon-gamma induction of Ia expression. *J Immunol.* **135**, 3735-43 (1985).

270. Barrionuevo, P. *et al.* Immune complexes (IC) down-regulate the basal and interferon-gamma-induced expression of MHC class II on human monocytes. *Clinical & Experimental Immunology* **125**, 251-257 (2001).
271. Tamoutounour, S. *et al.* CD64 distinguishes macrophages from dendritic cells in the gut and reveals the Th1-inducing role of mesenteric lymph node macrophages during colitis. *Eur. J. Immunol.* (2012).
doi:10.1002/eji.201242847
272. Lu, S. Y. *et al.* High frequency of CD4⁺ CD25⁻ CD69⁺ T cells is correlated with a low risk of acute graft-versus-host disease in allotransplants. *Clin Transplant* **26**, E158-67 (2012).
273. Vignali, D. A. A. *et al.* How regulatory T cells work. *Nat Rev Immunol* **8**, 523-532 (2008).
274. Yona, S. *et al.* Monocytes: subsets, origins, fates and functions. *Curr. Opin. Hematol.* **17**, 53-59 (2010).
275. Bao, Y. *et al.* A role for spleen monocytes in post-ischemic brain inflammation and injury. *J Neuroinflammation* **7**, 92 (2010).
276. Parihar, A. *et al.* Monocytes and macrophages regulate immunity through dynamic networks of survival and cell death. *Journal of Innate Immunity* **2**, 204-215 (2010).
277. Kampfrath, T. *et al.* A mouse model of yellow fluorescent protein (YFP) expression in hematopoietic cells to assess leukocyte-endothelial interactions in the microcirculation. *Microvasc. Res.* **78**, 294-300 (2009).
278. Landsman, L. *et al.* Distinct differentiation potential of blood monocyte subsets in the lung. *J Immunol* **178**, 2000-2007 (2007).
279. Goff, W. L. *et al.* Assessment of bovine mononuclear phagocytes and neutrophils for induced L-arginine-dependent nitric oxide production. *Vet. Immunol. Immunopathol.* **55**, 45-62 (1996).
280. Chamorro, S. *et al.* Phenotypic characterization of monocyte subpopulations in the pig. *Immunobiology* **202**, 82-93 (2000).
281. Ahuja, V. *et al.* Identification of two subpopulations of rat monocytes expressing disparate molecular forms and quantities of CD43. *Cell. Immunol.* **163**, 59-69 (1995).
282. Silver, J. *et al.* Regeneration beyond the glial scar. *Nat Rev Neurosci* **5**, 146-156 (2004).
283. Kitamura, D. *et al.* A B cell-deficient mouse by targeted disruption of the

- membrane exon of the immunoglobulin mu chain gene. *Nature* **350**, 423-426 (1991).
284. Gómez, M. I. *et al.* Staphylococcus aureus protein A activates TNFR1 signaling through conserved IgG binding domains. *J. Biol. Chem.* **281**, 20190-20196 (2006).
285. O'Seaghdha, M. *et al.* Staphylococcus aureus protein A binding to von Willebrand factor A1 domain is mediated by conserved IgG binding regions. *FEBS J.* **273**, 4831-4841 (2006).
286. Saha, P. *et al.* Toward a functional characterization of blood monocytes. *Immunol Cell Biol* **89**, 0-0 (2010).
287. Biburger, M. *et al.* Monocyte Subsets Responsible for Immunoglobulin G-Dependent Effector Functions In Vivo. *Immunity* **35**, 932-944 (2011).
288. Soni, S. *et al.* Evaluation of CD64 Expression on Neutrophils as an Early Indicator of Neonatal Sepsis. *Pediatr. Infect. Dis. J.* (2012).
doi:10.1097/INF.0b013e31826faede
289. Nagendra, S. *et al.* Absence of cross-reactivity between murine Ly-6C and Ly-6G - Nagendra - 2004 - Cytometry Part A - *Cytometry* (2004).
290. Shi, C. *et al.* Monocyte recruitment during infection and inflammation. *Nat Rev Immunol* **11**, 762-774 (2011).
291. Benowitz, L. I. *et al.* Inflammation and axon regeneration. *Curr. Opin. Neurol.* **24**, 577-583 (2011).
292. Hausmann, O. N. *et al.* Post-traumatic inflammation following spinal cord injury. *Spinal Cord* **41**, 369-378 (2003).
293. Rosen, D. R. *et al.* Mutations in Cu/Zn superoxide dismutase gene are associated with familial amyotrophic lateral sclerosis. *Nature* **362**, 59-62 (1993).
294. Butovsky, O. *et al.* Modulating inflammatory monocytes with a unique microRNA gene signature ameliorates murine ALS. *J Clin Invest* **122**, 3063-3087 (2012).
295. van Rooijen, N. *et al.* Elimination, blocking, and activation of macrophages: three of a kind? *J Leukoc Biol* **62**, 702-709 (1997).
296. Salegio, E. A. A. *et al.* Macrophage presence is essential for the regeneration of ascending afferent fibres following a conditioning sciatic nerve lesion in adult rats. *BMC Neurosci* **12**, 11 (2011).

297. Ditor, D. S. *et al.* A therapeutic time window for anti-CD11d monoclonal antibody treatment yielding reduced secondary tissue damage and enhanced behavioral recovery following severe spinal cord injury. *J Neurosurg Spine*. 5:343-52 (2006).
298. Shechter, R. *et al.* Infiltrating blood-derived macrophages are vital cells playing an anti-inflammatory role in recovery from spinal cord injury in mice. *PLoS Med* 6, e1000113 (2009).
299. Allen, A. R. *et al.* Surgery of experimental lesion of spinal cord equivalent to crush injury of fracture dislocation of spinal column a preliminary report. *Journal of the American Medical Association* 57, 878-880 (1911).
300. Young, W. *et al.* Glucocorticoid therapy of spinal cord injury. *Ann. N. Y. Acad. Sci.* 743, 241-63; discussion 263-5 (1994).
301. Stokes, B. T. *et al.* Experimental spinal cord injury: a dynamic and verifiable injury device. *Journal of Neurotrauma* 9, 129-31; discussion 131-4 (1992).
302. Pearse, D. D. *et al.* Histopathological and behavioral characterization of a novel cervical spinal cord displacement contusion injury in the rat. *Journal of Neurotrauma* 22, 680-702 (2005).
303. Scheff, S. W. *et al.* Experimental modeling of spinal cord injury: characterization of a force-defined injury device. *Journal of Neurotrauma* 20, 179-193 (2003).
304. Basso, D. M. *et al.* A sensitive and reliable locomotor rating scale for open field testing in rats. *Journal of Neurotrauma* 12, 1-21 (1995).
305. Basso, D. M. *et al.* Basso Mouse Scale for locomotion detects differences in recovery after spinal cord injury in five common mouse strains. *Journal of Neurotrauma* 23, 635-659 (2006).
306. Hamers, F. P. *et al.* Automated quantitative gait analysis during overground locomotion in the rat: its application to spinal cord contusion and transection injuries. *Journal of Neurotrauma* 18, 187-201 (2001).
307. Berryman, E. R. *et al.* Digigait quantitation of gait dynamics in rat rheumatoid arthritis model. *J Musculoskelet Neuronal Interact* 9, 89-98 (2009).
308. Glajch, K. E. *et al.* Sensorimotor assessment of the unilateral 6-hydroxydopamine mouse model of Parkinson's disease. *Behav. Brain Res.*

- 230, 309-316 (2012).
309. Pallier, P. N. *et al.* The detection and measurement of locomotor deficits in a transgenic mouse model of Huntington's disease are task- and protocol-dependent: influence of non-motor factors on locomotor function. *Brain Res. Bull.* **78**, 347-355 (2009).
 310. Springer, J. E. *et al.* The functional and neuroprotective actions of Neu2000, a dual-acting pharmacological agent, in the treatment of acute spinal cord injury. *Journal of Neurotrauma* **27**, 139-149 (2010).
 311. Mouse Imaging System - Digigait Indices. 1-11 (2013).
 312. Boato, F. *et al.* C3 peptide enhances recovery from spinal cord injury by improved regenerative growth of descending fiber tracts. *J. Cell. Sci.* **123**, 1652-1662 (2010).
 313. Aguilar, R. & Steward, O. A bilateral cervical contusion injury model in mice: Assessment of gripping strength as a measure of forelimb motor function. *Exp Neurol* (2009). doi:10.1016/j.expneurol.2009.09.028